Thèse de doctorat

NNT : 2021UPASG035

Modeling and control of discrete-time and sampled-data port-Hamiltonian systems

Thèse de doctorat de l'université Paris-Saclay et de Sapienza Università di Roma

École doctorale n°580: sciences et technologies de l'information et de la communication (STIC)
Spécialité de doctorat: Automatique

Unité de recherche : Université Paris-Saclay, CNRS, CentraleSupélec, Laboratoire des Signaux et Systèmes, 91190, Gif-sur-Yvette, France
Sapienza Università di Roma, Dipartimento di Ingegneria Informatica, Automatica e Gestionale «Antonio Ruberti», 00185, Rome, Italy

Référent : Faculté des sciences d'Orsay

Thèse présentée et soutenue à Paris-Saclay, le 20/05/2021, par

Alessio MORESCHINI

COMPOSITION DU JURY

Stefano BATTILOTTI Professeur, Sapienza Università di Roma (Italy)	Président
Jean-Pierre BARBOT Professeur, ENSEA, Cergy-Pontoise, Quartz Laboratory (France)	Rapporteur & Examinateur
Stefano DI GENNARO Professeur associé, Università degli Studi di L'Aquila (Italy)	Rapporteur & Examinateur
Stefano BATTILOTTI Professeur, Università degli Studi di Roma La Sapienza (Italy)	Examinateur
Bernhard MASCHKE Professeur, Université de Lyon (France)	Examinateur
Elena PANTELEY Directrice de recherche, L2S, CNRS - université Paris-Saclay (France)	Examinatrice
Stefano PANZIERI Professeur, Università degli Studi Roma Tre (Italy)	Examinateur

DIRECTION DE LA THESE

Salvatore MONACO Professeur, Sapienza Università di Roma (Italy)	Directeur de thèse
Dorothée NORMAND-CYROT Directeur de recherche, L2S, CNRS - université Paris-Saclay (France)	Directeur de thèse
Mattia MATTIONI Professeur assistant, Sapienza Università di Roma (Italy)	Membre invité

SAPIENZA
UNIVERSITÀ DI ROMA

Modeling and control of discrete-time and sampled-data port-Hamiltonian systems

Dottorato in Automatica, Bioingegneria e Ricerca Operativa (ABRO)

Dottorato di Ricerca in Automatica – XXXIII Ciclo

Alessio Moreschini

Advisors

Prof. Salvatore Monaco

Dr. Dorothée Normand-Cyrot

Thesis defended on 20 May 2021
in front of a Board composed by:

Prof. Stefano Battilotti (chairman)
Prof. Jean-Pierre Barbot (reviewer and examiner)
Prof. Stefano Di Gennaro (reviewer and examiner)
Prof. Bernhard Maschke (examiner)
Dr. Elena Panteley (examiner)
Prof. Stefano Panzieri (examiner)
Prof. Salvatore Monaco (advisor)
Dr. Dorothée Normand-Cyrot (advisor)
Dr. Mattia Mattioni (invited member)

Modeling and control of discrete-time and sampled-data port-Hamiltonian systems
Ph.D. thesis. Sapienza University of Rome and université Paris-Saclay
NNT: 2021UPASG035

Author's email: alessio.moreschini@uniroma1.it

Acknowledgments

I want to express my deepest gratitude to my supervisors Professors Salvatore Monaco and Dorothée Normand-Cyrot. Their supervision these past three and a half year made it possible for me to learn and grow as a scholar and as an individual. Their passion and generosity in sharing with me their extensive knowledge have inspired me to always strive for the best. Through their guidance and contribution to the field of discrete-time and sample-data systems, they have fostered many generations of researchers of which I feel honored to be part.

I would like to thank the committee members Professors Jean-Pierre Barbot, Stefano Di Gennaro, Stefano Battilotti, Bernhard Maschke, Elena Panteley, and Stefano Panzieri for their constructive feedback and generosity during the defence. I am especially grateful to Professor Maschke for sharing additional insights on the topic of this thesis.

I am grateful to Dr Mattia Mattioni for always keeping my spirits up, giving me unvaluable advice, and helping me navigate tough situations. He has been far more than a colleague in these years.

I thank my fantastic colleagues at DIAG and L2S for welcoming me into a stimulating environment. Their intellectual generosity and kindness had a profound impact on my PhD experience. Special thanks go to Bowen, Dongjun, Gökhan, Massimiliano, and Mohammed for their friendship and support in and outside the labs.

I wish to thank my parents for their unwavering encouragement and for providing me with moral support at all times.

Last but not least, I would like to thank Caterina, who has been by my side every step of the way. Her faith in my ability kept me going even when things got rough: *God only knows what I'd be without you.*

Abstract

Modeling and control of port-Hamiltonian systems are extensively studied in the continuous-time literature as powerful tools for network modeling and control of complex physical systems. Since controllers are unavoidably implemented through digital devices, accurate sampled-data models and control strategies are highly recommended to prevent a negative impact on the closed-loop performances under digital control. This thesis contributes to the description of new port-Hamiltonian structures both in a purely discrete-time and sampled-data framework. Then, on these bases, stabilizing and energy-based digital feedback strategies are developed. Regarding modeling, the proposed state-space forms make use of the concepts of Difference/Differential Representation (DDR) of discrete-time dynamics and the discrete gradient function. The proposed models exhibit a Dirac structure that properly defines the storing, resistive and external elements of the concerned port-Hamiltonian system. For stabilization purposes, the u-average passivity property has been essential for properly discussing passivity-based-control (PBC) strategies such as damping output feedback and Interconnection and Damping Assignment (IDA-PBC) both in discrete time and under sampling. Three case studies from different physical domains aim to illustrate the computational aspects related to the modeling and control design and further we validate their performances by means of simulations.

Keywords : port-Hamiltonian Systems, sampled-data systems, passivity-based control.

Abstract

I sistemi port-Hamiltoniani sono stati ampiamente studiati nella letteratura a tempo continuo come strutture essenziali per la modellazione di sistemi fisici complessi e sistemi di reti. Dal momento che le leggi di controllo sono inevitabilmente implementate per mezzo di dispositivi digitali, è essenziale avere appropriati modelli e strategie di controllo a dati campionati al fine di prevenire un impatto negativo della discretizzazione sulle prestazioni dell'azione di controllo. Questa tesi è incentrata sulla descrizione di nuove strutture port-Hamiltoniane sia in un contesto tempo discreto puro che in un contesto a dati campionati. A partire da queste forme, sono state sviluppate strategie di stabilizzazione basate sulla gestione dell'energia sia nel tempo discreto che sotto campionamento. Per quanto riguarda la modellazione, la rappresentazione nello spazio di stato proposta si basa sul concetto di Rappresentazione Differenziale e alle Differenze (DDR) della dinamica discreta e sulla nozione di Gradiente discreto. I modelli proposti ammettono una struttura di Dirac associata e definiscono opportunamente i diversi elementi di conservazione, resistenza ed esterni che costituiscono il sistema port-Hamiltoniano. Per quanto riguarda la stabilizzazione, la nozione di passività u-media è essenziale per descrivere in maniera opportuna le strategie di controllo basate sulla passività (PBC) come il controllo calcolato sull'uscita passiva del sistema e l'assegnazione dell'interconnessione e dello smorzamento (IDA-PBC), sia nel contesto tempo continuo che sotto campionamento. Sono stati considerati tre casi di studio, basati su diversi modelli fisici, al fine di illustrare gli aspetti computazionali relativi alla modellistica e al controllo dei sistemi port-Hamiltoniani introdotti.

Parole chiave : sistemi port-Hamiltoniani, sistemi a dati campionati, controllo basato sulla passività.

Résumé

Les systèmes Hamiltoniens ont été largement étudiés dans la littérature en temps continu comme des éléments essentiels pour la modélisation de systèmes physiques complexes et en réseaux. Les schémas de commande étant nécessairement implantés au moyen de dispositifs numériques, il est primordial de disposer de modèles et de stratégies de commande échantillonnés afin de s'affranchir d'un impact négatif de la discrétisation sur les performances de contrôle. Cette thèse s'intéresse à la description de nouvelles structures Hamiltoniennes à la fois en temps discret pur et dans le contexte échantillonné. A partir de ces formes, des stratégies de stabilisation basées sur la gestion de l'énergie sont développées en temps discret et sous échantillonnage. Concernant la modélisation, la représentation par espace d'état proposée fait référence au concept de representation Différentielle et aux Différences (DDR) de dynamiques discrètes et à la notion de fonction gradient en temps discret. Les modèles proposés admettent une représentation sous forme de structure de Dirac définissant ainsi précisément les différents éléments de stockage, resistance et interaction avec l'extérieur qui constituent le système Hamiltonien. Concernant la stabilisation, la notion de passivité en u-moyenne est essentielle pour décrire des stratégies de commande par bouclage exploitant cette passivité au service d'approches de type amortissement (PBC) ou affectation de structures cibles (IDA-PBC), ceci en temps discret et sous échantillonnage. Trois examples classiques issus des domaines physiques sont développés afin d'illustrer les aspects de calcul liés à la modélisation et à la commande et valider les nouvelles stratégies proposées en illustrant leurs performances par des simulations.

Mots clés : systèmes Hamiltoniens à ports, systèmes échantillonnés, commande basée sur la passivité.

Sommario della tesi

I sistemi port-Hamiltoniani sono stati ampiamente studiati nella letteratura a tempo continuo come strutture essenziali per la modellazione di sistemi complessi. Dal momento che le leggi di controllo sono inevitabilmente implementate attraverso dispositivi digitali, è essenziale definire appropriati modelli e strategie di controllo a dati campionati al fine di prevenire un effetto negativo della discretizzazione sulle prestazioni dell'azione di controllo. A tal fine, la tesi mira alla definizione di nuove strutture port-Hamiltoniane e alla loro stabilizzazione sia in un contesto tempo discreto che a dati campionati. Riassumiamo qui i principali risultati raggiunti nella tesi distinguendo i contributi a tempo discreto da quelli a dati campionati.

Per quanto riguarda lo studio a tempo discreto:

1. Abbiamo dato una nuova definizione di struttura port-Hamiltoniana a tempo discreto sfruttando i concetti di Rappresentazione Differenziale e alle Differenze (DDR) e di Gradiente Discreto. Questa nuova rappresentazione è originale in quanto divide in maniera naturale il contributo dell'evoluzione libera del sistema port-Hamiltoniano dalla parte controllata dando vita ad una nuova uscita passiva, in termini di gradiente discreto, ottenuta sfruttando la nozione di passività u-media. Attraverso queste proprietà, per la prima volta in letteratura abbiamo proposto una equazione di bilancio energetico a tempo discreto avente una parte dissipativa non dipendente dalla variabile di controllo, fornendo così un vantaggio alla progettazione dei controllori basati sulla passività. Infatti, attraverso tale uscita abbiamo proposto un controllore di smorzamento per stabilizzare il punto di equilibrio del sistema.

2. Abbiamo validato la struttura port-Hamiltoniana proposta costruendo una associata struttura di Dirac che definisce i diversi elementi di conservazione, resistenza ed esterni che costituiscono il sistema port-Hamiltoniano discreto. A differenza dalle rappresentazioni in letteratura, l'originalità della struttura di

Dirac introdotta è che essa è definita su uno spazio aumentato dovuto dalla forma DDR. Essenzialmente abbiamo definito in maniera opportuna la coppia di flussi e sforzi associati alla componente di storage che non dipendono dal controllo, introducendo una nuova coppia di flussi e sforzi che modellano l'effetto del controllo nella struttura. Questa rappresentazione è originale e permette di definire in maniera strutturale il contributo del controllo sulla rappresentazione discreta.

3. Abbiamo dimostrato che l'interconnessione dei due sistemi port-Hamiltoniani definiti a tempo discreto è ancora un sistema port-Hamiltoniano. Il risultato è garantito in quanto la composizione di strutture di Dirac recupera l'interconnessione attraverso le uscite dei sistemi passivi u-medi. Al fine di raggiunge tale obiettivo, abbiamo mostrato preventivamente che i sistemi passivi u-medi interconnessi attraverso le loro uscite u-medie garantiscono una preservazione di potenza.

4. Infine abbiamo discusso la stabilizzazione del sistema port-Hamiltoniano ad un desiderato punto di equilibrio definendo una appropriato controllore IDA-PBC tempo discreto. La soluzione proposta nel contesto non lineare fornisce una condizione sufficiente al soddisfacimento del problema, inquanto il calcolo delle soluzioni si basa su un'equazione algebrica non lineare da risolvere. Una completa caratterizzazione della soluzione è stata proposta nel contesto lineare, fornendo una condizione necessaria e sufficiente definita dal soddisfacimento di una equazione matriciale lineare.

Per quanto riguarda il caso sotto campionamento, lo studio è stato affrontato definendo operatori formali che sfruttano le manipolazioni combinatorie dei flussi associati alle soluzioni delle equazioni differenziali. Di conseguenza, tutti i punti 1-4 sono stati rivisitati nel contesto a dati campionati e le soluzioni proposte sono state presentate fornendo i primi termini delle loro espansioni in serie. Infatti, il beneficio di questo approccio è quello di dare soluzioni algoritmicamente calcolabili e costruttive in un senso approssimativo. Tuttavia, concentriamoci sui principali risultati raggiunti.

La principale difficoltà nel contesto a dati campionati è quella di recuperare una appropriata struttura port-Hamiltoniana. Questo problema è stato risolto sia nel contesto non lineare che lineare. La soluzione proposta dice che, mentre sotto campionamento la funzione Hamiltoniana rimane la stessa, la procedura di campionamento

richiede una trasformazione delle matrici di interconnessione e smorzamento nella struttura port-Hamiltoniana. Queste nuove matrici sono parametrizzate dal periodo di campionamento e per costruzione definite intorno alle matrici del modello tempo continuo. Il risultato è originale e fornisce una rappresentazione esatta del modello port-Hamiltoniano sotto campionamento garantendo approssimazioni della struttura ad ogni ordine di approssimazione.

Per quanto riguarda la stabilizzazione ad un desiderato punto di equilibrio è possibile in questo contesto sfruttando la soluzione continua IDA-PBC per progettare, almeno in un senso approssimato, i primi termini del controllore digitale. Il controllore digitale mira a riprodurre il comportamento del controllore ideale continuo su una desiderata funzione Hamiltoniana. Tale controllore assegna, in senso approssimato, una struttura port-Hamiltoniana del secondo ordine.

Tre differenti casi di studio sono stati affrontati nella tesi (elettrico, meccanico ed elettro-meccanico) al fine di validare la modellazione e il controllo dei sistemi port-Hamiltoniani proposti. L'interesse della metodologia proposta sta nel fatto che il modello a dati campionati proposto trova applicazione in tutti i domini in cui i sistemi port-Hamiltoniani vengono solitamente utilizzati, ma dove una stabilizzazione digitale è necessaria. Inoltre, grazie alle proprietà energetiche del modello proposto a tempo discreto, la loro modellazione originale può essere una punto di partenza per migliorare problemi di ottimizzazione (e.g. riduzione del rumore nelle immagini) e per modellare dinamiche discrete (e.g. sistemi economici).

Résumé étendu de la thèse

Les systèmes Hamiltoniens à ports ont été largement étudiés dans la littérature temps continu comme des structures essentielles pour la modélisation de systèmes complexes. Étant donné que les lois de commande sont inévitablement mises en œuvre par des dispositifs numériques, il est essentiel de définir des modèles appropriés et des stratégies de commande en temps discret ou à données échantillonnées afin de s'affranchir un effet négatif de l'implantation numérique sur les performances. À cette fin, la thèse propose de nouvelles structures Hamiltoniennes à ports en temps discret et sous échantillonnage ainsi que des stratégies de commande associées. Les principaux résultats présentés dans la thèse sont résumés ci-dessous en distinguant les contributions de temps discret de celles à données échantillonnées.

Concernant le temps discret.

1. Nous avons donné une nouvelle définition d'une structure Hamiltonienne à ports pour des dynamiques linéaire et non linéaire temps discret en adoptant la représentation différentielle et de différences (DDR) de telles dynamiques et la notion de fonction gradient discret. Cette représentation permet de distinguer naturellement la dynamique en évolution libre de la partie commandée. Ceci permet de définir très naturellement une sortie passive, soit à partir de la notion de passivité en u-moyenne soit directement en termes en termes de la fonction gradient discret. A partir de cette représentation, nous avons proposé une équation bilan des échanges énergétiques en distinguant la partie dissipative indépendante de la variable de contrôle, et la partie conservative. Sur ces bases, il devient possible de définir des stratégies de commande reposant sur le bilan énergétique pour la stabilisation par amortissement.

2. La nouvelle structure Hamiltonienne à ports proposée a été validée par la définition, nouvelle dans la littérature également, d'une structure de Dirac associée. Nous avons essentiellement défini les paires de flux et efforts associées

aux différents éléments de stockage, dissipation et d'interaction avec l'extérieur, qui constituent le système discret port-Hamiltonien le définissant au moyen d'un graphe de liaison.

3. Nous avons ensuite montré la propriété fondamentale d'interconnexion. L'interconnexion de deux systèmes Hamiltoniens à ports est un système Hamiltonienne à ports dont l'hamiltonien est la somme des hamiltoniens. Le résultat repose sur le fait que la composition de deux structures de Dirac est une structure de Dirac et que l'interconnexion qui préserve la puissance de deux systèmes passifs en u-moyenne est encore un système en u-moyenne.

4. Enfin, nous avons étudié la stabilisation du système Hamiltonien à ports à un point d'équilibre souhaité en construisant une stratégie de commande à partir du bilan énergétique rappelant la commande IDA-PBC (Interconnection and Damping Assigment). La solution proposée dans le contexte non linéaire décrit une condition suffisante. Le calcul d'une solution fait appel à la résolution d'une équation algébrique non linéaire. Une caractérisation nécessaire et suffisante est exprimée en termes d'une égalité matricielle pour des dynamiques linéaires avec Hamiltonien quadratique.

Concernant les systèmes échantillonnés.

Les contributions 1 à 4 ont été revisitées pour les systèmes discrets issus de l'échantillonnage de dynamiques continues. Dans ce cas, les modèles sont décrits en termes d'opérateurs non linéaires formels et de manipulations combinatoires sur les flots associés aux solutions d'équations différentielles ordinaires. Les solutions proposées ont l'avantage d'être représentées en termes de séries asymptotiques paramétrées par la période d'échantillonnage. Le grand intérêt en pratique est de disposer d'un algorithme constructif pour le calcul des solutions au sens d'approximations d'ordre croissant par rapport à la période d'échantillonnage. Les solutions nominales retrouvant la solution continue.

La principale difficulté dans le contexte des données échantillonnées est de récupérer une structure Hamiltoniennes à ports appropriée. Ce problème a été résolu à la fois dans le contexte non linéaire et linéaire. La solution proposée indique que, lors de l'échantillonnage, la fonction hamiltonienne peut être maintenue. Par contre, la procédure d'échantillonnage nécessite une transformation des matrices d'interconnexion et d'amortissement. Ces nouvelles matrices sont paramétrées par la période d'échantillonnage et décrites en termes de séries asymptotiques autour des matrices décrivant

le modèle continu. En ce qui concerne la stabilisation à un point d'équilibre souhaité, il est possible dans ce contexte échantillonné d'exploiter la solution continue IDA-PBC pour concevoir une stratégie de commande qui vise à reproduire, aux instants d'échantillonnage, le comportement du bouclage continu idéal. La solution proposée peu en pratique être approchée à tout ordre d'approximation autour de la solution continue et en puissances de la période d'échantillonnage.

Concernant les exemples traités. Trois exemples simulés représentant des cas d'étude classiques pour ce type de modélisation Hamiltonienne sont étudiés dans la thèse (électrique, mécanique et électro-mécanique). Ils valident la modélisation et le contrôle des systèmes Hamiltoniens à ports proposés. On constante un gain important sur l'ampleur admissible avec les performances souhaitées de la période d'échantillonnage.

Concernant les perspectives. L'intérêt de la méthodologie proposée réside dans le fait que les modèles à données échantillonnées proposés trouvent une application dans tous les domaines où les systèmes Hamiltoniens à ports sont utilisés, mais numériquement actionnés. De plus, les propriétés structurelles et énergétiques du modèle temps discret proposé peuvent être exploitées dans le contexte de la commande optimale, de la commande des systèmes complexes interconnectés et en réseaux ainsi que dans des domaines moins traditionnels (réduction du bruit en traitement d'images, modélisation de systèmes économiques, ...).

List of publications

Journal Articles

J.4 A. Moreschini, S. Monaco and D. Normand-Cyrot, "Dirac structures of discrete-time port-Hamiltonian systems", 2021. Submitted to IEEE Transactions on Automatic Control (TAC). (Under review)

J.3 M. Mattioni, A. Moreschini, S. Monaco and D. Normand-Cyrot, "Discrete-time energy-balance passivity-based control ", 2021. Submitted to Automatica. (Under review)

J.2 S. Monaco, D. Normand-Cyrot, M. Mattioni and A. Moreschini, "Nonlinear Hamiltonian systems under sampling", 2021. Submitted to IEEE Transactions on Automatic Control (TAC). (Under review)

J.1 A. Moreschini, M. Mattioni, S. Monaco and D. Normand-Cyrot, "Stabilization of Discrete Port-Hamiltonian Dynamics via Interconnection and Damping Assignment," in IEEE Control Systems Letters, vol. 5, no. 1, pp. 103-108, Jan. 2021, doi: 10.1109/LCSYS.2020.3000705.
Presented also at 2020 IEEE 59th Conference on Decision and Control (CDC).

Publications in Proceedings

C.5 M. Mattioni, A. Moreschini, S. Monaco and D. Normand-Cyrot, "On feedback passivation under sampling", 2021 American Control Conference (ACC).

C.4 M. Mattioni, A. Moreschini, S. Monaco and D. Normand-Cyrot, "Reduction-based stabilization of nonlinear discrete-time systems through delayed

state measurements," IFAC-PapersOnLine,Volume 53, Issue 2, 2020, pp. 5851-5856, ISSN 2405-8963, https://doi.org/10.1016/j.ifacol.2020.12.1632.

C.3 A. Moreschini, M. Mattioni, S. Monaco and D. Normand-Cyrot, "Interconnection through u-average passivity in discrete time," 2019 IEEE 58th Conference on Decision and Control (CDC), Nice, France, 2019, pp. 4234-4239, doi: 10.1109/CDC40024.2019.9029357.

C.2 A. Moreschini, M. Mattioni, S. Monaco and D. Normand-Cyrot, "Discrete port-controlled Hamiltonian dynamics and average passivation," 2019 IEEE 58th Conference on Decision and Control (CDC), Nice, France, 2019, pp. 1430-1435, doi: 10.1109/CDC40024.2019.9029809.

C.1 A. Moreschini, S. Monaco and D. Normand-Cyrot, Gradient and Hamiltonian dynamics under sampling, IFAC-PapersOnLine, Volume 52, Issue 16, 2019, pp. 472-477, ISSN 2405-8963, https://doi.org/10.1016/j.ifacol.2019.12.006.

Communications in Conferences without Proceedings

W.1 A. Moreschini, S. Monaco and D. Normand-Cyrot. *Structure preserving for gradient and Hamiltonian dynamics under sampling.* Automatica.it 2019. September, 2019. Ancona (Italy).

Contents

Introduction **1**

Some historical notes on Hamiltonian systems 1
Context of the manuscript 5
Literature overview 10
Goals and contributions 13
Manuscript organization 17

Part I Fundamentals on passive systems **23**

1 Recalls in the continuous-time framework **25**

1.1 Continuous-time models 26
1.2 Dissipativity and passivity 29
1.2.1 Interconnections of passive systems 32
1.2.2 Stability of passive systems 34
1.2.3 Passivity-based control 35
1.3 Port-Hamiltonian systems 37
1.3.1 Port-Hamiltonian dynamics 38
1.3.2 Recalls on Dirac structures 40
1.4 Interconnection and damping assignment 42
1.5 Concluding remarks 46

2 Passivity concepts in discrete time **47**

2.1 Generalities on discrete-time systems 48
2.1.1 Discrete gradient function 50
2.1.2 Discrete Jacobian 52
2.1.3 Difference and differential representation 53
2.2 Passivity in discrete time 55
2.2.1 The u-average passivity 57

2.2.2 Passivity-based control 61
2.2.3 Constructive approximate solutions 61
2.3 Linear-time invariant case 62
2.4 Interconnection of u-average passive systems 64
2.4.1 The parallel interconnection 66
2.4.2 Feedback interconnection 67
2.4.3 Computational aspects 70
2.4.4 Interconnection of average passive LTI systems 71
2.5 Example: interconnection of passive oscillators 73
2.5.1 Interconnection structure design 73
2.5.2 Analysis and simulation results 75
2.6 Concluding remarks 80

3 Generalities on sampled-data systems 83
3.1 The sampled-data representation 84
3.2 Difference and differential representation 87
3.3 Passivity property 89
3.3.1 The u-average passivity 89
3.3.2 Passivity-based control 92
3.4 Linear-time invariant case 93
3.5 Feedback passivation under sampling 95
3.5.1 Problem statement: feedback passivation under sampling . . . 97
3.5.2 Digital passivation and stabilization 98
3.5.3 Illustrative example: Backstepping as feedback passivation . . 102
3.6 Concluding remarks 105

Part II Port-Hamiltonian systems in discrete time 107

4 Modeling of DT port-Hamiltonian systems 109
4.1 Port-Hamiltonian systems in discrete time 110
4.1.1 A new definition 110
4.1.2 A port-Hamiltonian representation proposed in the literature . 115
4.1.3 The case of quadratic Hamiltonians 116
4.2 Dirac structures of port-Hamiltonian systems in DT 118
4.2.1 Discrete-time Dirac structures 119

4.2.2 Port-Hamiltonian systems as Dirac structures 121
4.2.3 Power-preserving interconnection 123
4.2.4 An illustrative example: the mechanical isolation system . . . 129
4.3 Concluding remarks 131

5 Control of DT port-Hamiltonian systems 133
5.1 Negative output feedback 134
5.1.1 The Dirac structure under negative output feedback 135
5.1.2 Some constructive aspects 138
5.1.3 The input-affine dynamics case with quadratic Hamiltonian . . 139
5.2 Interconnection and damping assignment 141
5.2.1 Constructive aspects: an approximate IDA-PBC design 145
5.2.2 IDA-PBC for input-affine systems 147
5.3 Concluding remarks 149

6 LTI port-Hamiltonian systems in DT 151
6.1 Port-Hamiltonian systems in discrete time 151
6.2 Negative output feedback 153
6.3 IDA-PBC in discrete time 154
6.4 Concluding remarks 158

Part III Port-Hamiltonian systems under sampling 159

7 Modeling of SD port-Hamiltonian systems 161
7.1 Formal instrumental results 162
7.2 Constructive aspects 165
7.3 Gradient dynamics under sampling 167
7.4 Port-Hamiltonian dynamics under sampling 172
7.4.1 Conservative dynamics 177
7.4.2 Dissipative dynamics 179
7.5 Input-state-output port-Hamiltonian systems 180
7.6 Comparison with the literature model 184
7.7 Concluding remarks 185

8 Control of SD port-Hamiltonian systems 187
8.1 Negative output feedback 187

8.2 IDA-PBC: Input-Hamiltonian matching 189
8.3 Concluding remarks 194

9 LTI port-Hamiltonian systems under sampling 195
9.1 Gradient dynamics 195
9.2 Port-Hamiltonian systems 198
9.3 Negative output feedback 203
9.4 IDA-PBC: Direct discrete design 203
9.5 Concluding remarks 205

Part IV Case studies 207

10 The RLC circuit 209
10.1 Continuous-time modeling 210
10.2 Sampled-data modeling 211
10.3 Digital damping feedback 218
10.4 Discrete IDA-PBC design 225

11 The Gravity Pendulum 231
11.1 Continuous-time modeling 232
11.2 Sampled-data modeling 233
11.3 Damping feedback design 242
11.4 Energy-based digital stabilization 250

12 The Magnetic Levitation Ball 259
12.1 Continuous-time modeling 260
12.2 Sampled-data modeling 261
12.3 Energy-based digital stabilization 271

CONCLUSIONS 277

BIBLIOGRAPHY 284

List of notations

$\mathbb{N}$	The set of natural numbers including 0.
$\mathbb{R}$	The set of real numbers.
$\mathbb{R}_{\geq 0}$	The set of non-negative real numbers.
$\mathrm{Mat}_{\mathbb{R}}(n,m)$	The space $n \times m$ of the $\mathbb{R}$-valued matrices.
$\mathrm{Sym}_{\mathbb{R}}(n)$	The space $n \times n$ of the $\mathbb{R}$-valued symmetric matrices.
$\mathrm{Skew}_{\mathbb{R}}(n)$	The space $n \times n$ of the $\mathbb{R}$-valued skew-symmetric matrices.
I	The identity operator.
I_d	The identity function.
$\mathbf{0}_{n\times m}$	The $n \times m$ $\mathbb{R}$-valued matrix whose entries are all zeros.
$\|\| \cdot \|\|$	The Euclidean norm.
$\langle \cdot, \cdot \rangle$	The inner product.
$x^\top$	Transpose operation on a vector x.
$\nabla_{x_i} g(x)$	The partial derivative of a smooth function $g : \mathbb{R}^n \to \mathbb{R}$ with respect to the i^{th} component; i.e. $\nabla_{x_i} g(x) = \frac{\partial g}{\partial x_i}$.
$g^\perp$	Left hand-side annihilator of g, i.e. $g^\perp g = 0$.
$g^\dagger$	Left pseudo-inverse of g, i.e. $(g^\top g)^{-1} g^\top$.
$\nabla \lambda(x)$	The column vector derivative of a scalar-valued function $\lambda : \mathbb{R}^n \to \mathbb{R}$; i.e. $\nabla \lambda(x) = col\left(\nabla_{x_1} \lambda(x), \cdots, \nabla_{x_n} \lambda(x)\right)$.
$\nabla^2 \lambda(x)$	The Hessian matrix of a scalar-valued function $\lambda : \mathbb{R}^n \to \mathbb{R}$.

L_f	The Lie derivative operator; i.e. $f : \mathbb{R}^n \to \mathbb{R}^n$, $\mathrm{L}_f = \sum_{i=1}^n f_i(x)\frac{\partial}{\partial x_i}$.
L_f^l	The l^{th}-order Lie derivative operator; i.e. $\mathrm{L}_f^l = \mathrm{L}_f\mathrm{L}_f^{l-1}$ and $\mathrm{L}_f^0 = I$.
$\mathrm{ad}_f\lambda$	The Lie bracket between vector fields $f : \mathbb{R}^n \to \mathbb{R}^n$ and $\lambda : \mathbb{R}^n \to \mathbb{R}^n$; i.e. $\mathrm{ad}_f\lambda = [f, \lambda] = \frac{\partial \lambda}{\partial x} f - \frac{\partial f}{\partial x}\lambda$.
$\mathrm{ad}_f^l\lambda$	The l^{th}-order Lie bracket between vector fields; i.e. $\mathrm{ad}_f^l\lambda = \mathrm{ad}_f\mathrm{ad}_f^{l-1}\lambda$.
e^{L_f}	The exponential Lie operator along the vector field $f : \mathbb{R}^n \to \mathbb{R}^n$; i.e. $e^{\mathrm{L}_f} := I + \sum_{i\geq 1} \frac{\mathrm{L}_f^i}{i!}$.
$e^{\mathrm{L}_f}x$	The exponential Lie operator evaluated at x; i.e. $e^{\mathrm{L}_f}x = e^{\mathrm{L}_f}I_d\|_x$.
$\otimes$	The tensor product of two vector space.
$\frac{\partial}{\partial x} \otimes \lambda$	The derivative of a matrix-valued function $\lambda : \mathbb{R}^n \to \mathrm{Mat}_{\mathbb{R}}(n, n)$; i.e. $\frac{\partial}{\partial x} \otimes \lambda = \left(\frac{\partial \lambda}{\partial x_1}, \cdots, \frac{\partial \lambda}{\partial x_n}\right) \in \mathrm{Mat}_{\mathbb{R}}(n, n^2)$.
$\mathrm{L}_\lambda^{\otimes l}$	The l^{th}-order tensor product of the Lie operator L_λ; i.e. $\mathrm{L}_\lambda^{\otimes l} = \mathrm{L}_\lambda \otimes \mathrm{L}_\lambda^{\otimes l-1}$.
$\mathcal{C}^p$	The class of the function which can be differentiated p times ($n > 1$), leaving a continuous p^{th} derivative.
$O(\delta^p)$	The Big O notation.

List of acronyms

AS	Asymptotically Stable
CT	Continuous Time
DDR	Difference and Differential Representation
DT	Discrete Time
EB	Energy Balancing
ES	Energy Shaping
GAS	Global Asymptotically Stable
IDA	Interconnection and Damping Assignment
IH_dM	Input-H_d-Matching
ILM	Input-Lyapunov-Matching
KYP	Kalman-Yakubovich-Popov
LTI	Linear Time Invariant
PBC	Passivity-Based Control
PH	Port-Hamiltonian
SD	Sampled Data
ZOH	Zero-Order Hold
ZSD	Zero-State-Detectable
ZSO	Zero-State-Observable

Introduction

The thesis discusses modeling and control of port-Hamiltonian systems in the discrete-time framework and then, more specifically, for dynamics issued from sampling. The cases of linear and nonlinear dynamics defined on finite-dimensional state-space representations are studied essentially for the single-input case. Typical examples and case studies are presented to illustrate the results with simulations. We begin with a brief survey on port-Hamiltonian systems and their origins and impact on the actual technological advances and needs to proceed then with the objectives and contributions of the thesis. At the end of this introduction, an outline of the content of the subsequent chapters is described along with the concerned published works.

Some historical notes on Hamiltonian systems

Hamiltonian dynamics made their appearance in the scientific literature when the irish mathematician Sir William Rowan Hamilton published two milestones on a general method in dynamics, Hamilton (1834, 1835). They are basically a straight adaptation to dynamics of methods that Hamilton developed for the most in his researches on optical systems. Indeed, Hamilton investigated the evolution of a *conservative* system - one that satisfies the conservation of energy - and found that it is determined by a characteristic function, he named the *principal function*, analogous to the one introduced for optical systems, Hankins (1980). This principal function - defined for describing the mechanics of a system - is determined by the evolution of the dynamical system from an initial to a final configuration and of the energy associated with the motion. Nowadays, this function is conveniently known as *Hamiltonian function*. A classical interpretation of the Hamiltonian function comes from applications in mechanics where it represents the total energy of the system, which is

respectively the sum of kinetic and potential energy.

Since the 60s, the control community has directed its efforts towards the analysis and control of nonlinear systems, focusing on dynamics continuously evolving over time. The concept of "energy" has lent useful tools for the expansion of this research line. It is in fact possible to study many systems from their energy sources and losses, such as mechanical, electrical, thermal, and many others. Among these, we can classify dissipative and Hamiltonian systems. Dissipative systems can be generally defined as systems that have the property of dissipating energy rather than producing it; any increase of stored energy happening to it is always due to external sources. Hamiltonian systems are systems that, in absence of dissipating elements, have the property of preserving the amount of stored energy at any time instant of their evolution. Indeed, Hamiltonian systems are conservative systems which stand in contrast to dissipative systems. Hamiltonian systems have no friction or other resistive components to dissipate energy, and thus, their dynamics does not shrink over time. These systems have in common to present highly desirable properties which may simplify system analysis and control design. More insight into this aspect can be found in the milestones van der Schaft (2000); Wiggins (2003); Brogliato et al. (2007); van der Schaft et al. (2014) and references therein.

Hamiltonian-based and port-based network modeling has been an upward trend in systems and control theory since the nineties. Pioneered by the work Breedveld (1984), port-based modeling aims to describe a complex system such as the interconnection of several subsystems of different physical nature (electrical, mechanical, hydraulic, etc...), through variables whose product describes the *power* of each subsystem (voltages and currents, velocities and forces, flows and pressures, etc...). Port-based modeling aims to describe the energy exchange between parts composing a system, (such as between mass-spring, inductor-capacitor, etc). Seeing ports as interfaces among independent subsystems, the formulation defines an input-output structure among these subsystems. Further, in the pioneering work Maschke et al. (1992); Maschke and van der Schaft (1992), combining port-based and Hamiltonian modeling, emphasis has been put on dynamical systems able to interact with the environment via inputs and outputs ports, and susceptible to control interaction. This has given birth to a new class of systems properly called *port-Hamiltonian systems*.

As seen in Maschke and van der Schaft (1992), arising from the bond graph formalism, port-Hamiltonian systems can be defined by a Dirac structure introduced in

Courant (1990) as the generalization of symplectic and Poisson geometric structures. The Dirac structure formalizes the power-conserving interconnection among subsystems and is mainly defined by an energy function (the Hamiltonian function) and suitable additional resistive algebraic relation which provides energy dissipation. Indeed, the main extension of port-Hamiltonian systems theory with respect to classical Hamiltonian theory is the inclusion of energy-dissipating elements into the description of the dynamics. The essence of port-Hamiltonian systems modeling is thus regarded as the linkage and exchange of energy between energy-storing, energy-dissipating, and energy-routing components characterizing the port-Hamiltonian system as highlighted in Figure 1.

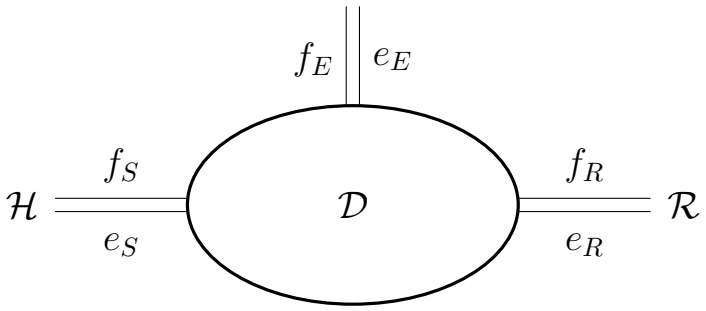

Figure 1: Dirac structure

Essentially, the storing $\mathcal{H}$ and the dissipating $\mathcal{R}$ are interconnected to an energy routing device $\mathcal{D}$, which provides a power balance in the structure. In the Dirac structure, the linkage is made through ports, which are vectors of flows and efforts: energy-storing port (f_S, e_S), energy-dissipating port (f_R, e_R), and external port (f_E, e_E). The inner product between the flows and efforts denotes the power flowing through the links. Notably, in the mechanical context, Dirac structures are of great interest as they can directly incorporate algebraic constraints that arise in Lagrangian systems, Leok and Ohsawa (2011); van der Schaft and Maschke (2020), and might be extended to thermodynamic processes as recently discussed in the work of van der Schaft and Maschke (2018).

In this present thesis, we focus on an important special case of port-Hamiltonian systems so-called *input-state-output* port-Hamiltonian systems, where there are no algebraic constraints on the state-space variables, and the flow and effort variables of control and interaction ports are split into conjugated input–output pairs. Input–state–output port-Hamiltonian systems are generally given as the graph of the

skew-symmetric map

$$\begin{pmatrix} f_S \\ f_R \\ f_E \end{pmatrix} = \begin{pmatrix} -J(x) & -g_R(x) & -g(x) \\ g_R^\top(x) & 0 & 0 \\ g^\top(x) & 0 & 0 \end{pmatrix} \begin{pmatrix} e_S \\ e_R \\ e_E \end{pmatrix}$$

leading to a port-Hamiltonian system,

$$\begin{aligned} \dot{x} &= (J(x) - R(x))\nabla H(x) + g(x)u \\ y &= g^\top(x)\nabla H(x) \end{aligned}$$

with state vector $x \in \mathcal{X} \subset \mathbb{R}^n$, output vector $y \in \mathbb{R}^m$, input vector $u \in \mathbb{R}^m$, Hamiltonian function $H(\cdot) : \mathcal{X} \to \mathbb{R}$ and power conjugates variables $\dot{x} = -f_S$, $\nabla H(x) = e_S$, $e_R = -r(x)f_R$ with matrix $r(x) = r^\top(x) \succeq 0$, $y = f_E$, $u = e_E$. The matrices $J(x) = J^\top(x)$, $R(x) = g_R(x)r(x)g_R^\top(x) = R^\top(x) \succeq 0$ are the interconnection and dissipation matrices, respectively, g_R represents the input matrix corresponding to the resistive port, and the vector field $g(x)u$ models the interaction with the environment.

For a broad and thorough overview of port-Hamiltonian formalism see van der Schaft et al. (2014); van der Schaft (2000); Duindam et al. (2009).

The main advantage of invoking port-Hamiltonian system theory is that due to its particular structure, a port-Hamiltonian system determines whether or not the system is affected by a dissipation term, so providing dissipation or, alternatively, conservation of energy. In this sense, the port-Hamiltonian theory broadens the range of applicability to more class of systems, unlike the classic Hamiltonian, and provides a natural framework for *passivity-based control* (PBC). Fundamental references on passive systems can be found in the works of Ortega et al. (2001, 2002a,b, 2008); Duindam et al. (2009). Input-state-output port-Hamiltonian systems are a very special class of passive systems as their conservative or dissipative, dynamics guarantee that the associated energy evolution equals, or lower than, the power injected from the external source.

The notions of passivity, and dissipativity, are emerged in the analysis of physical systems with the aim to formalize the energy behavior associated with the dissipation of the system provided by the dissipating components. From the very first works on those topics by Willems (1972a), the concept of passivity has been proved to be fundamental for the analysis and control of nonlinear systems at large due to the intrinsic connection of energy dissipation to Lyapunov-stability theory Hill and

Moylan (1976). Nowadays, the PBC paradigm is the underlying leitmotiv of many energy-based control strategies which have been developed to feedback stabilize systems exploiting the energy function. Basically, these energy-based controllers aim to shape the energy function to achieve stabilization to a desired equilibrium by assigning the transient behavior via energy transfer between the interconnected parts of the dynamical system. In this framework, a different and admissible storage function is chosen to properly design the controller ensuring passivity. Since the early '80s PBC design has become an upward trend thanks to the pioneering works Takegaki and Arimoto (1981); Spong et al. (2020); Slotine and Li (1987); Ortega and Spong (1989); Byrnes et al. (1991) that pave the way to a substantial amount of research and application problems such as in Kokotovic (1992); Kokotovic et al. (1992); Krstić et al. (1994); Loria et al. (1998); Battilotti et al. (1997); Lorıa et al. (2001); Astolfi et al. (2001); Di Gennaro (2003); Astolfi and Ortega (2003); Stramigioli (2015); Chopra and Spong (2006); Ortega et al. (2001, 2002b,a).

The control of port-Hamiltonian systems through energy management and structure assignment for the interconnected system has been widely investigated in the past decade and applied to many different fields. The results are highly interesting as they suggest that the concepts of energy and energy exchange between different components of the system, act as a common denominator in the modeling and control of complex networked dynamical systems of different natures so that they can be modeled and controlled with the same tools. The literature is widely developed and in addition to the authors' work already referred we also recommend van der Schaft et al. (2014); Brogliato et al. (2007); Duindam et al. (2009) and the references therein for a broad and thorough overview on the port-Hamiltonian formalism.

Context of the manuscript

Technological advances have led to fast growth and usage of digital computation and computer-aided design. Digital computation, as its name suggests, refers to computation using digital representations dealing with a discrete or finite set of data. Systems and control engineering is one of the many areas that took benefits of digital computation, particularly, technology for simulation and control. Discrete-time and digital control systems analysis and design is a branch of control theory rooted in the early '50s under the pioneering work by John R. Ragazzini, wherein Ragazzini and

Franklin (1958) can be found the bases for the analysis and design of the emerging technologies of computer controllers.

The first steps towards the investigations on discrete-time systems in the nonlinear context have been moved parallel to the study on the nonlinear control in continuous time since the early '80s in some basic works concerning the analysis Sontag (1979); Jakubczyk (1980a,b); Fliess and Normand-Cyrot (1981) and Normand-Cyrot (1983); followed from the first results in the design Sontag and Sussmann (1982); Monaco and Normand-Cyrot (1982, 1983, 1984); Jakubczyk and Normand-Cyrot (1984); Grizzle (1985); Grizzle and Kokotovic (1988). Afterwards, a continuous growth of interest in the discrete-time context enabled the settlement of a body of analysis and design methods with contributions of several scientists in the last 30 years; among them Castillo et al. (1993); Barbot et al. (1996); Castillo et al. (1997); Barbot et al. (1999); Di Gennaro et al. (1999); Goodwin et al. (2001); Grüne and Nesic (2003); Nešić and Grüne (2005); Yuz and Goodwin (2005); Kotta (2006).

Since the early 2000s, a few works have been devoted to the issues that are taken up in this manuscript with the aim of extending the analysis and control methods of Hamiltonian systems to the discrete-time and sampled-data contexts such as Stramigioli et al. (2002, 2005); Laila and Astolfi (2004, 2006a); Laila et al. (2006); Monaco et al. (2008, 2010); Tiefensee et al. (2010); Monaco and Normand-Cyrot (2011).

Two major aspects noted before, which are at the bases of Hamiltonian design approaches, were not well understood and employed in the discrete-time and sampled-data contexts: **passivity** and **the Hamiltonian structure itself**. These aspects, which will be clarified in the sequel, represent the starting point of this dissertation. With this in mind let us first specify what we mean with *discrete-time* and *sampled-data* systems.

Discrete-time systems can be represented in state-space form by a first-order difference equation described by a map as

$$\begin{aligned} x(k+1) &= F(x(k), u(k)) \\ y(k) &= h(x(k)) \end{aligned}$$

with state vector $x \in \mathcal{X} \subset \mathbb{R}^n$, control vector $u \in \mathcal{U} \subset \mathbb{R}^m$, output vector $y \in \mathcal{Y} \subset \mathbb{R}^q$ and iteration variable $k \in \mathbb{Z}$ named *time instant*. Such a model is generally used to

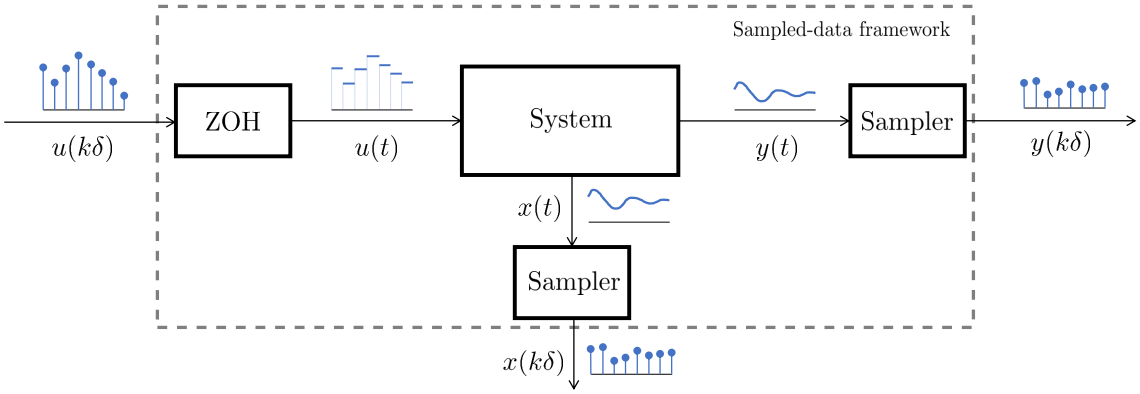

Figure 2: Sampled-data framework

represent discrete phenomena from different contexts, such as evolution at discrete-time instants, algorithms, or to represent at periodic instant of times, sampled state and output evolutions fed by piecewise constant inputs over time intervals of amplitude equal to the sampling period (sampled-data systems).

In this thesis, we refer to sampled-data systems issued from an uniform sampling of continuous-time signals as illustrated in Figure 2. The continuous-time system is interfaced with the digital environment through analog to digital (Sampler) and digital to analog (ZOH) converter devices. The Sampler aims at producing sampled signals $x(k)$ and $y(k)$, respectively, of the continuous-time state $x(t)$ and output $y(t)$ at the sampling instants $t = k\delta$ with $k \in \mathbb{N}$, so that $k\delta = 0, \delta, 2\delta, 3\delta, \ldots$, over sampling periods of fixed step-size δ. Accordingly, the control input $u(k\delta)$ is a discrete sequence of signals that is injected into the sampled-data framework in order to control the continuous-time system. The control input $u(k\delta)$ is converted through a Zero-Order-Holder (ZOH) device to a piecewise constant signal $u(k) = u(t)$ with $t \in [k\delta, (k+1)\delta[$. According to such a sampling procedure, a Sampled-Data (SD) system admits a state-space representation in the map form

$$\text{CT}: \begin{cases} \dot{x}(t) &= f(x(t), u(t)) \\ y(t) &= h(x(t)) \end{cases} \longrightarrow \text{SD}: \begin{cases} x((k+1)\delta) &= x(k\delta) + F^{\delta}(x(k\delta), u(k\delta)) \\ y(k\delta) &= h(x(k\delta)) \end{cases}$$

so recovering, for each fixed step-size δ, a discrete-time model described by a map that is by construction parameterized by the sampling period. This sampled-data SD system reproduces by construction both the state $x(t)$ and output $y(t)$ time evolutions

Example 1

Consider the one-dimensional discrete-time system described by the first-order difference equations

$$x(k+1) = ax(k) + bu(k)$$
$$y(k) = cx(k).$$

Informally, the discrete-time system is said passive if the following inequality is satisfied for all $x(k)$ and $u(k)$

$$S(x(k+1)) - S(x(k)) \leq u^{\top}(k)y(k)$$

for a suitable positive semi-definite function $S(x)$, the *storage function*. Pick $S(x) = \frac{1}{2}x^2(k)$ as a suitable storage function, then when substituting $y(k) = cx(k)$ the inequality above reads

$$\frac{1}{2}(a^2-1)x^2(k) + (ab-c)x(k)u(k) + \frac{1}{2}b^2u^2(k) \leq 0. \tag{1}$$

Clearly, the inequality (1) cannot be satisfied for all $x(k)$ and $u(k)$ due to the effect of the term $b^2u^2(k)$ which is always positive for any $b \neq 0$.

of the Continuous-Time (CT) system at any sampling instants $t = k\delta, k \geq 0$, when properly initialized at the same state condition $x(0)$.

As pointed out in previous works passivity and port-Hamiltonian structure, admit a clear counterpart neither in discrete time nor under sampling. Concerning passivity, as discussed in Monaco and Normand-Cyrot (1997b); Stramigioli et al. (2005); Navarro-López (2005); Monaco et al. (2008); Monaco and Normand-Cyrot (2011), a common pathology arising in the discrete-time setting is that the system cannot be passive (adopting the more standard definition) if the associated output $y(k)$ is solely defined as a function of the measured state $x(k)$ and not affected by the control $u(k)$. Example 1 illustrates this pathology that occurs already in the linear context. The same issue arises when handling sampled-data systems since the SD model usually violates the standard passivity condition with respect to an output $y(t)$ assumed passive for the continuous-time system; this means that passivity under sampling is not preserved.

The other aspect is the port-Hamiltonian structure in the digital context, Stramigioli et al. (2005); Talasila et al. (2006); Laila and Astolfi (2006a, 2007); Monaco et al. (2009); Tiefensee et al. (2010). Unlike the continuous-time port-Hamiltonian

definition, in discrete time there are no universal representations of these forms. The modeling in the literature usually arises from some sampling procedure applied to the smooth continuous-time model, or directly modeling the dynamics at a discrete level, and this may lead to confusion.

On the other hand, in a sampled-data thinking, even when the sampled-data system is perfectly able to describe the continuous-time evolution at all the sampling instants, the sampled-data equivalent model does not naturally show a port-Hamiltonian-like structure, which is an essential structural property of the system to properly design energy-based controller in a digital context. To understand the lack of a Hamiltonian structure under sampling see Example 2.

Example 2

Consider the simplest Hamilton's canonical dynamics over $\mathbb{R}^2$

$$\begin{pmatrix} \dot{x}_1 \\ \dot{x}_2 \end{pmatrix} = \begin{pmatrix} 0 & 1 \\ -1 & 0 \end{pmatrix} \begin{pmatrix} \frac{\partial H}{\partial x_1} \\ \frac{\partial H}{\partial x_2} \end{pmatrix}$$

with quadratic Hamiltonian $H(x) = \frac{1}{2}x_1^2 + \frac{1}{2}x_2^2$. As well known, this dynamics is described by a skew-symmetric matrix and a infinitesimal variation of the Hamiltonian function with respect to x and is conservative, meaning that

$$\dot{H}(x) = \frac{\partial H}{\partial x}\dot{x} = \frac{\partial H}{\partial x_1}\dot{x}_1 + \frac{\partial H}{\partial x_2}\dot{x}_2 = 0.$$

Commonly in the literature it is customary to consider sampled data models which aim to preserve some Hamiltonian structure to be defined in discrete time, see McLachlan et al. (1999); Yalçin et al. (2015); Aoues et al. (2017); Hairer et al. (2006). However, by computing the sampled-data equivalent model, one easily gets

$$\begin{pmatrix} x_1((k+1)\delta) \\ x_2((k+1)\delta) \end{pmatrix} = e^{\delta \begin{pmatrix} 0 & 1 \\ -1 & 0 \end{pmatrix}} \begin{pmatrix} x_1(k\delta) \\ x_2(k\delta) \end{pmatrix} = \begin{pmatrix} \cos\delta & \sin\delta \\ -\sin\delta & \cos\delta \end{pmatrix} \begin{pmatrix} x_1(k\delta) \\ x_2(k\delta) \end{pmatrix}$$

which preserves the conservation of energy (as a consequence of the exact state matching), namely

$$H(x((k+1))) - H(x(k\delta)) = \int_{k\delta}^{(k+1)\delta} \dot{H}(x(\tau))\, \mathrm{d}\tau = 0,$$

but the sampled-data model does not exhibit, at least in first attempt, some Hamiltonian-like structure in discrete time.

This thesis work aims to give steps towards filling the gap in the literature related to the aforementioned aspects. It will be shown that the concept of u-average passiv-

ity introduced in Monaco and Normand-Cyrot (2011) can be profitably employed to overcome the problem of a direct input-output link. It thus can be a powerful tool for relying passivity to port-Hamiltonian structures in both discrete-time and sampled-data contexts. Moreover, making use of the Difference and Differential Representation (DDR) introduced in Monaco and Normand-Cyrot (1995), a novel state-space representation of port-Hamiltonian systems is proposed that appears suitably shaped to stress straight connections between continuous-time, discrete-time and sampled-data modeling.

Literature overview

Due to the lack of a universal definition of port-Hamiltonian system in the digital context, many different representations have been introduced in the literature with their advantages in the attempt to preserving energetic properties as well as the interconnected structures of standard continuous-time port-Hamiltonian models. These studies are often based on suitable approximations.

Discrete spaces. A general approach for defining port-Hamiltonian modeling through a discrete-time setting comes in describing systems on discrete manifold (structure discretization), which are spaces that locally look like discretization grids over the set of floating-point numbers. In Talasila et al. (2006, 2004); Šešlija et al. (2012) the authors showed that the change of energy over a sampling interval is only approximated by a product of a new introduced discrete operator along with the increment between the current and the successive state.

Sampled-data approach. In a sampled-data perspective a first attempt of providing sampled-data port-Hamiltonian system is given in Stramigioli et al. (2002, 2005) in which the authors showed how to sample a continuous-time port-Hamiltonian flow for preserving a properly defined passivity property. In Laila and Astolfi (2006a) an approximate sampled-data port-Hamiltonian model which guarantees Hamiltonian conservation of energy is proposed through midpoint discretization method. In Castaños et al. (2015) a sampled-data version of an implicit port-Hamiltonian system is given adopting a flow-splitting numerical integration method. The generated discrete-time model preserves up to an approximation error the storage function and the output of the continuous-time system. The splitting method, along with the approximation of the partial derivative of the Hamiltonian function, is considered also

in Celledoni and Høiseth (2017) to design discrete port-Hamiltonian flows preserving energy balance and stability. Recently, a different definition has been given in Kotyczka and Lefèvre (2019); Kotyczka et al. (2018); Kotyczka and Maschke (2017) providing an higher-order approximation of the continuous-time energy balance and symplectic integration by collocation methods, such as Gauss-Legendre.

Discrete-gradient method. Major contributions of the literature make use of the discrete gradient function to model discrete-time port-Hamiltonian systems. In fact, the discrete gradient function arose in geometric numerical integration to express the variation of a function between two points, see Gonzalez (1996). In the sampled-data context, the discrete gradient function is used to reproduce the qualitative behaviour of the solution to the sampling of differential equation. Its definition is firstly introduced in Gonzalez (1996) to guarantee first-order conservation of energy of the Hamiltonian dynamics at discrete level. This conservation of energy is based on a geometric integration scheme and extends the concept of symplecticity, so that the conserved density of the flow, which is usually implicitly defined, is preserved at the sampling instants, McLachlan et al. (1999); Hairer et al. (2006); Quispel and McLaren (2008). In McLachlan (1995) composition methods are exploited to increase the integration order. A second-order improvement of the implicit scheme which provides preservation of the coadjoint orbits and energy is proposed in Engø and Faltinsen (2001). In Laila and Astolfi (2007); Gören-Sümer and Yalçın (2008); Yalçin et al. (2015); Aoues et al. (2017) a symplectic first-order model is given by replacing the partial derivative of the Hamiltonian function with the discrete gradient function and enhancing the same interconnection and dissipation matrices associated with the continuous-time flow. Among all the port-Hamiltonian structures discussed, these port-Hamiltonian models based on the discrete gradient function are the most comparable with the proposed form in this manuscript in terms of state-space representation.

Structure-preserving approximations for distributed parameters. Several results have been proposed also for distributed parameter port-Hamiltonian systems to properly sampled the continuous-time partial differential equation preserving the associated port-Hamiltonian structure. One of the earliest result on on structure preservation of port-Hamiltonian system is found in Golo et al. (2004) exploiting the approximation of the differential forms through Whitney forms. This method lay the foundation for further development given in Baaiu et al. (2006); Eberard et al. (2007);

Wu et al. (2015); Bassi et al. (2007). A different structure-preserving discretization is given in Kotyczka (2016); Trenchant et al. (2017, 2018); Serhani et al. (2018) providing a structure based on finite differences and finite volumes. A more recent method is given in Cardoso-Ribeiro et al. (2018); Serhani et al. (2019a,b) introducing a new discretization method named Partitioned Finite Element, and in Moulla et al. (2011); Harkort and Deutscher (2012); Vu et al. (2017) using pseudo-spectral discretization methods exploiting Galerkin projection and Bessel function.

About the control design Alongside the discretized modeling, the usage of a discrete gradient-based design is fruitful in defining associated energy-based stabilization method to apply to the sampled-data port-Hamiltonian system. Thus, the digital stabilization is tackled through a proper direct digital design based on the discretized model. The direct discrete-time IDA-PBC design have been firstly proposed in Laila and Astolfi (2005, 2006b) and further extended in Sümer and Yalçın (2011). Those stabilization design massively improve the emulation control, that is obtained by the holding between the sampling instants of the continuous-time controller. In Aoues et al. (2013, 2015b,a) and Aoues et al. (2017) the direct digital design of the IDA-PBC and negative output feedback design is respectively provided. The result clearly improves the former direct digital implementations but still, for sufficiently high sampling period, the energy balance equation still leads to a numerical drift. This is due to the fact that the sampled-data system over which the design was made is approximated to the first-order and loses some information on the exact solution of the continuous time system.

This, even though a partial overview of the literature, gives various advice and highlights the main difficulties.

In particular:

- the discrete gradient turns out to be an adequate tool for modeling port-Hamiltonian dynamics both in the discrete-time context and in the sampled-data context, allowing to express the system in terms of some rate of change of the Hamiltonian function;
- the discrete gradient introduces an implicitly defined first-order difference equation characterizing the system dynamics. Therefore, in the case of controlled dynamics, it is necessary to decouple the free evolution from the controlled one;

- the dynamics considered in the sampled-data framework are usually approximated even when an exact and analytic solution exists.

Goals and contributions

Several aspects are at the basis of the present study. Two of them are introductory to the thesis work.

Because dissipativity concepts and port-Hamiltonian structures are intricately nested, a first intuition is to exploit in this Hamiltonian context the notion of passivity introduced in Monaco and Normand-Cyrot (2011) to overcome the necessity of a direct input-output link (or the relative degree zero obstacle). This means to set the question of defining port-Hamiltonian structures in a differential algebraic framework making use of the Differential/Difference representation proposed in Monaco and Normand-Cyrot (1995) to model nonlinear discrete-time dynamics as two coupled equations. This structure was discussed in several works, such as Monaco and Normand-Cyrot (1998, 2005); Monaco et al. (2007), and shown to be suitable at first to understand and characterize analysis properties like controllability, observability, invariance, so providing key instrumental tools to go further more classical studies.

A second aspect relies upon the notion of gradient function associate with the Hamiltonian function that is instrumental to pass from energy balance to power balance equations through time derivatives and is fundamental to define the state-space representation of Hamiltonian dynamics in continuous time. As manipulations over time derivatives are substituted with algebraic manipulations over first-order difference equations in the attempt to characterize dynamics over time in discrete time, the second intuition lays in the use of the discrete gradient function in place of the gradient. This is less surprising, as the use of the discrete gradient function given in Gonzalez (1996) is typical in dynamic programming or optimizing problems and is perfectly suited to model the variational balance equations in discrete time. In fact, port-Hamiltonian structures are defined in McLachlan et al. (1999); Yalçin et al. (2015); Aoues et al. (2017) in terms of the discrete gradient of the Hamiltonian so resulting in well-shaped energy balance equalities in discrete time.

The contributions of this thesis are based on the combined use of these notions.

We distinguish the contributions relying upon the discrete-time context from those obtained for sampled-data dynamics.

Discrete-time context

1. A novel representation of discrete-time port-Hamiltonian dynamics is proposed making use of the discrete gradient function and adopting the DDR representation, Definition 4.1.1 and Theorem 4.1.1. This form is totally new as it splits the dynamics into the free evolution and the controlled one recovering the one in McLachlan et al. (1999); Yalçin et al. (2015); Aoues et al. (2017) in the control-free case only.

2. An output that qualifies to be a power conjugate output (its product with the control variable is a unity of power) is defined exploiting the notion of average passivity. The energy balance equation or dissipativity inequality follows, verifying the properties of average passivity and negative output damping feedback proposed in Monaco and Normand-Cyrot (2011) and presently specified to port-Hamiltonian dynamics in Theorem 4.1.1 and Theorem 5.1.1.

3. To further validate the proposed port-Hamiltonian form and set a bridge with discrete Dirac oriented modeling, the Dirac structure associated with the proposed port-Hamiltonian structure is described in Theorem 4.2.1 as well as the Dirac structure associated with the closed-loop system under negative average output feedback Theorem 5.1.2. This is very interesting as the Dirac structure enables us to describe the associated port-Hamiltonian structure that is defined in closed loop in an extended state space splitting the free flow variable from the controlled one again.

4. Finally regarding the analysis, it is shown that the power-conserving interconnection of two port-Hamiltonian systems is again a port-Hamiltonian system with Hamiltonian function the sum of the two respective Hamiltonian, Theorem 4.2.1. This result is very interesting as it makes reference to the power-preserving interconnection introduced in Definition 2.4.1 and as the usual feedback interconnection defined with respect to the respective average output of average passive systems, Theorem 2.4.1. This again is a totally new result that exploits the possibility to rewrite the

proposed port-Hamiltonian form through a Dirac structure and verifying that the composition of Dirac structure recovers the feedback interconnection of average passive systems.

5. The broad question of control through energy management is a very intricate problem in discrete time in spite of the well-shaped proposed structure because of several difficulties. The structure is implicitly due to the discrete gradient function, it is generally nonlinear in the control variable and the output is control-dependent. All these aspects make the computation of control solutions a difficult problem that relies on nonlinear algebraic equation to solve. Among energy-based control goals is the favorite interconnection and damping assignment passivity based control (IDA-PBC) that opens the road of the second generation of passivity based control. Sufficient conditions are however given in Theorem 5.2.1 that can be solved for particular classes of systems or in an approximate meaning.

6. All the five aforementioned aspects apply to the linear time-invariant case so providing original solutions with respect to the literature. Regarding point 5, a complete IDA-PBC solution is described and computed in Theorem 6.3.1, as it is always the case in the linear case, involving manipulations over matrices rather than nonlinear functions.

Sampled-data context

Generally speaking, there are two ways for addressing the sampled-data context, either to sample (according to the approach we described) the state dynamics, fix the sampling time and treat the system as a discrete-time one or to restrict sampling to the control design goal (input-output matching, energy decreasing), disregarding the exact sampling of the state evolutions. In this second approach, the solution may simplify even though exist, so providing appealing results, but the properties of the sampled-data state-space structure are surely lost. Both approaches are pursued making use of the description of the state or output solutions to the sampling problem as series expansions in powers of the sampling period. This is performed along the lines developed in Monaco and Normand-Cyrot (1990) according to a formal calculus approach and combinatorial manipulations over the flows associated with the

solutions of nonlinear differential equations. As documented in several works Monaco and Normand-Cyrot (2001, 2007); Monaco et al. (2010), these descriptions get the benefits to be algorithmically computable and the constructive solutions in an approximate sense also, when referring to homogeneous truncations with respect to the successive powers in the sampling period. Accordingly, all points 1 to 6 are revisited for sampled dynamics and the solutions proposed, described by the first terms of the expansions. However, we focus on the main difficulties or contributions that have been reached.

1. Pursuing the first approach, the main difficulty is to recover a port-Hamiltonian structure under sampling, in particular, due to its implicit structure. It is solved both in the nonlinear and in the linear case. The solution says that while the Hamiltonian function can be the same, the sampling procedure implies a transformation of the interconnection and damping matrices in the sampled structure. These matrices come out to be described around the continuous-time by their series expansions in powers of the sampling period as discussed in Theorem 7.4.1 for the nonlinear case and Theorem 9.2.1 for the linear case. This first aspect is totally original in the literature and allows us to revisit all the 6 points so proposing new solutions.

2. Pursuing the second approach it is possible in this sampled-data framework to go further by exploiting the continuous-time IDA-PBC solution to design, at least in an approximate sense, the first terms of the IDA-PBC controller which assign the second-order approximation of the desired sampled-data port-Hamiltonian system, Theorem 8.2.1.

Case studies

Three classical physical case studies in this context have been pursued to validate all the results in the modeling and control sampled-data port-Hamiltonian systems making reference to different application fields such as electrical, mechanical, and electro-mechanical systems.

1. First, we consider the standard continuous-time RLC system. Based on its linear dynamics we compute its associated exact sampled-data

port-Hamiltonian representation. This sampled-data structure has been exploited further for digital stabilization purpose. First, we stabilize the system at its zero equilibrium point through the injection of the digital negative output feedback computed over the sampled-data port-Hamiltonian model. Then, we consider the problem of stabilizing the system at the desired equilibrium point through the design of digital IDA-PBC feedback.

2. Secondly, we consider the gravity pendulum system, which is a nonlinear port-Hamiltonian system affected by a separable Hamiltonian function. We compute an approximate port-Hamiltonian system of higher-order with respect to the model proposed by McLachlan et al. (1999); Yalçin et al. (2015); Aoues et al. (2017). Again the model has been exploited to stabilize the origin of the system under digital negative output feedback. Finally, an approximate sampled-data IDA-PBC control has been computed to stabilize the continuous-time system at the desired equilibrium point.

3. Finally, the same results have been applied to a magnetic levitation ball system which is a nonlinear system affected by a non-separable Hamiltonian function. In particular, we show and discuss how to compute an approximate sampled-data model and how to stabilize the system by computing an approximate digital IDA-PBC feedback based on the continuous-time solution.

Manuscript organization

The contribution of the thesis is distributed in 4 parts that make up the core of the manuscript. Below we report the detailed list of chapters discussing their content.

Part I

The *Chapter 1* is devoted to recalling the main continuous-time concepts that will be treated within the manuscript. Thus, we begin with the definition of continuous-time system and stability, to then introduce the formal notion of dissipativity and

passivity along with their properties. After the definiton of the port-Hamiltonian system the chapter ends with the definition of passivity-based control (PBC) and interconnection and damping assignment (IDA-PBC).

In *Chapter 2* we enter the world of discrete-time systems providing the basic mathematical background for the forthcoming chapters. After the definitions of discrete-time system, difference and differential representation of a discrete-time system, and stability concepts we recast the notion of passivity and dissipativity and finally we recall the main notion of u-average passivity. Then a first result is presented, related to the interconnection of u-average passive systems. This result is given in Moreschini et al. (2019b):

> *A. Moreschini, M. Mattioni, S. Monaco and D. Normand-Cyrot, "Interconnection through u-average passivity in discrete time," 2019 IEEE 58th Conference on Decision and Control (CDC), Nice, France, 2019, pp. 4234-4239, doi: 10.1109/CDC40024.2019.9029357.*

The *Chapter 3* concerns the sampled-data framework. Firstly, we recall the definitions of sampled-data system, and difference and differential representation and passivity and u-average passivity notions under sampling. Then, we discuss the feedback passivation problem under sampled-data design as presented in Mattioni et al. (2021):

> *M. Mattioni, A. Moreschini, S. Monaco and D. Normand-Cyrot, On feedback passivation under sampling. 2020. Submitted to 2021 American Control Conference (ACC). (Accepted)*

Part II

In *Chapter 4* we introduce a novel formal definition of discrete-time port-Hamiltonian systems. We show that the port-Hamiltonian system arises with a particular passive output defined by a discrete gradient function but coinciding with the u-average output map related to the u-average passivity property. The discrete-time structure is validated presenting the relation between the proposed port-Hamiltonian system with its associated Dirac structure. The contents of this chapter are given in Moreschini et al. (2019a); Moreschini et al. (2021):

A. Moreschini, M. Mattioni, S. Monaco and D. Normand-Cyrot, "Discrete port-controlled Hamiltonian dynamics and average passivation," 2019 IEEE 58th Conference on Decision and Control (CDC), Nice, France, 2019, pp. 1430-1435, doi: 10.1109/CDC40024.2019.9029809.

A. Moreschini, S. Monaco and D. Normand-Cyrot, "Dirac structures of discrete-time port-Hamiltonian systems," Submitted to IEEE Transactions on Automatic Control (TAC). (Under review)

In *Chapter 5* we specify in the discrete-time port-Hamiltonian framework the notion of negative output damping feedback for general nonlinear discrete-time port-Hamiltonian systems. Then we discuss the achieved Dirac structure under negative output feedback. Further, we address the problem of IDA-PBC stabilization in discrete-time. The problem is first set in the general nonlinear case so providing sufficient conditions, then the problem is specialized for a special class of discrete gradient associated with the Hamiltonian function. The results of this chapter are partially published in Moreschini et al. (2021):

A. Moreschini, M. Mattioni, S. Monaco and D. Normand-Cyrot, "Stabilization of Discrete Port-Hamiltonian Dynamics via Interconnection and Damping Assignment," in IEEE Control Systems Letters, vol. 5, no. 1, pp. 103-108, Jan. 2021, doi: 10.1109/LCSYS.2020.3000705.

In *Chapter 6* we revisit all the results presented in the previous chapters concerning discrete-time port-Hamiltonian systems in the linear time invariant case. In particular, we specialize the structure of LTI discrete-time port-Hamiltonian system associated with quadratic Hamiltonian functions. Then, the associated negative output feedback is characterized. Finally, necessary and sufficient conditions for solving the discrete-time IDA-PBC problem for LTI port-Hamiltonian systems are presented, as given in Moreschini et al. (2021).

Part III

The *Chapter 7* concerns the modeling of gradient and port-Hamiltonian systems under sampling. In particular, we provide exact sampled-data equivalent models to

gradient and port-Hamiltonian Hamiltonian structures preserving the continuous-time energetic properties at all sampling instants. Then, the proposed sampled-data representations for uncontrolled dynamics are generalized to input-state-output structures to exactly reveal the energy balance equation in terms of a suitable output map that qualifies as a power-conjugate output. The content of this chapter is partially submitted in Monaco et al. (2021):

> *S. Monaco, D. Normand-Cyrot, M. Mattioni and A. Moreschini, "Nonlinear Hamiltonian systems under sampling", Submitted to IEEE Transactions on Automatic Control (TAC). (Under review)*

In *Chapter 8* we specify the stabilization of sampled-data port-Hamiltonian system in terms of negative output feedback and IDA-PBC under sampling. First, we recall the negative output feedback design for sampled-data system and the result is revisited in the present context. Then, the problem of IDA-PBC under sampling is addressed making reference to the Input-Hamiltonian-Matching design discussed in Part I.

The *Chapter 9* restates all the results achieved under sampling in the linear context. In this respect, we describe the exact linear gradient and port-Hamiltonian structures under sampling. Then, the negative output feedback is properly designed and, finally, the IDA-PBC problem introduced in Part II is properly reshaped providing an exact solution to the matching equation. The modeling of gradient and port-Hamiltonian dynamics in the linear case is published in Moreschini et al. (2019):

> *A. Moreschini, S. Monaco and D. Normand-Cyrot, Gradient and Hamiltonian dynamics under sampling, IFAC-PapersOnLine, Volume 52, Issue 16, 2019, Pages 472-477, ISSN 2405-8963, https://doi.org/10.1016/j.ifacol.2019.12.006.*

Part IV

This part focuses upon three different case studies with the aim to underline the computational aspects and the effectiveness of the methodologies and the results presented in the main part of the manuscript.

In *Chapter 10* we consider a linear-time invariant RLC system and an exact sampled-data port-Hamiltonian system is computed. Further, we discuss and illus-

trate the digital stabilization problem through negative output feedback and direct discrete IDA-PBC by means of illustrative simulations.

In *Chapter 11* the same modeling and stabilization results are performed for the nonlinear gravity pendulum which comes with a separable Hamiltonian function. First, we perform approximate port-Hamiltonian models under sampling and then we address the stabilization problem through negative output feedback and IDA-PBC under sampled-data design.

Finally, to complete the discussion in *Chapter 12* we focus upon a magnetic levitation ball system which is a nonlinear system affected by a non-separable Hamiltonian function. We perform approximate port-Hamiltonian models under sampling and we discuss the achieved approximate structure. Accordingly, to stabilize the system, we exploit the IDA-PBC feedback to achieve stabilization at the desired equilibrium of the closed-loop magnetic levitation ball system under digital feedback.

The manuscript ends with concluding remarks, open perspectives and open works on these discrete-time and sampled-data frameworks.

Part I

FUNDAMENTALS ON PASSIVE SYSTEMS

Chapter 1

Recalls in the continuous-time framework

Contents

1.1 Continuous-time models **26**

1.2 Dissipativity and passivity **29**

1.2.1 Interconnections of passive systems 32

1.2.2 Stability of passive systems 34

1.2.3 Passivity-based control 35

1.3 Port-Hamiltonian systems **37**

1.3.1 Port-Hamiltonian dynamics 38

1.3.2 Recalls on Dirac structures 40

1.4 Interconnection and damping assignment **42**

1.5 Concluding remarks **46**

In this chapter, some recalls and preliminary results are presented for continuous-time systems by emphasizing physical properties such as port-Hamiltonian modeling and passivity that are then exploited throughout the manuscript together with basic notions regarding control design such as general passivity-based control and Interconnection and Damping Assignment (IDA-PBC). The notions used hereinafter are recalled from Khalil (2002); Wiggins (2003); Isidori (2013); Sepulchre et al. (2012); van der Schaft (2000); van der Schaft et al. (2014).

1.1 Continuous-time models

Throughout this thesis, nonlinear continuous-time systems are described in state space form by a set of ordinary differential equations

$$\dot{x} = f(x, u) \tag{1.1a}$$
$$y = h(x). \tag{1.1b}$$

The state $x = (x_1, \ldots, x_n)$ is assumed to belong to a subset $\mathcal{X}$ of $\mathbb{R}^n$, the input $u = (u_1, \ldots, u_m)$ is assumed to belong to a subset $\mathcal{U}$ of $\mathbb{R}^m$, and the output $y = (y_1, \ldots, y_p)$ is assumed to belong to a subset $\mathcal{Y}$ of $\mathbb{R}^p$. The function $f : \mathcal{X} \times \mathcal{U} \to \mathcal{X}$ and $h : \mathcal{X} \times \mathcal{U} \to \mathcal{X}$ are assumed smooth. It is assumed also that (1.1a) is forward complete, meaning that its solution exists for all $t \geq 0$, $x_0 = x(0) \in \mathcal{X}$ and $u \in \mathcal{U}$. A continuous-time system of the form (1.1) is referred as time-invariant as mappings f, h are not explicitly depending on t.

The state $x_\star \in \mathcal{X}$ is said to be an *equilibrium point* of the system (1.1a) if $f(x_\star, 0) = 0$. This class of systems includes the following sub-classes of systems:

- Input-affine system:

$$\dot{x} = f(x) + g(x)u \tag{1.2a}$$
$$y = h(x) \tag{1.2b}$$

- Linear system (LTI):

$$\dot{x} = Ax + Bu \tag{1.3a}$$
$$y = Cx \tag{1.3b}$$

  with matrices (A, B, C) of appropriate dimensions.

Once determined the equilibrium point $x_\star$ of the autonomous system (1.1a), with input $u = 0$, it is natural to verify if its solution is stable.

Definition 1.1.1 (Stability)**.** The state $x = x_\star$ is said *stable* equilibrium of the system (1.1a) if for all $\epsilon > 0$, there exists a $\delta_\epsilon > 0$ such that

$$||x_0 - x_\star|| < \delta_\epsilon \Longrightarrow ||x(t) - x_\star|| < \epsilon, \quad \text{for all} \quad t \geq 0.$$

This stability condition requires that all the trajectories of (1.1a) are contained within an arbitrarily small enough ball centered at the equilibrium point $x_\star$ of radius ϵ, when released from a ball of radius δ_ϵ sufficiently small.

Definition 1.1.2 (Unstability)**.** The state $x = x_\star$ is said *unstable* if is not stable.

Definition 1.1.3 (Asymptotic Stability)**.** The state $x = x_\star$ is said *asymptotically stable* equilibrium of the system (1.1a) if it is stable and if there exists a $B_r(x) = \{x \in \mathbb{R}^n : ||x|| < r\}$ such that

$$\lim_{t\to\infty} ||x(t) - x_\star|| = 0 \quad \forall x_0 \in B_r(x).$$

The state $x_\star$ is said to be a global asymptotic stable equilibrium of the system (1.1a) if $B_r(x)$ is $\mathbb{R}^n$.

Asymptotic stability claims that the equilibrium state $x_\star$ besides being stable in the sense of Definition 1.1.1 guarantees that nearby solutions to $x_\star$ actually converge to $x_\star$ as $t \to \infty$. The aforementioned stability definitions are also known as *stability in the sense of Lyapunov*, and if the asymptotic stability condition is not satisfied, the stability in the sense of Lyapunov refers to a *marginally stable* equilibrium point.

Once introduced the notion of stability of an equilibrium point it is important to find a way to determine it. In this respect, in 1892, Lyapunov introduced a certain function with specific properties to establish stability of an equilibrium point studying the evolution of the trajectories of the vector field $f(x, 0)$ associated with (1.1a), without explicitly computing the solution of (1.1a). In particular, he considered a continuously differentiable function $V : \mathcal{X} \to \mathbb{R}$ to provide that if the evolution of the trajectories of the vector field $f(x, 0)$, verifying $f(0, 0) = 0$, converges to 0 then function V will decrease along the solution of $f(x, 0)$. The function $V(x)$ is referred as Lyapunov function.

Definition 1.1.4. A function $f : \mathbb{R}^n \to \mathbb{R}^n$ is called *radially unbounded*, if $||x|| \to \infty$ implies $f(x) \to \infty$.

The Lyapunov stability theorem is given below and is recalled from Wiggins (2003).

Theorem 1.1.1. *Let $x = x_\star$ be an equilibrium point for the continuous-time dynamics* (1.1a) *and let $\mathcal{X} \subset \mathbb{R}^n$ such that $x_\star \in \mathcal{X}$. Let $V : \mathcal{X} \to \mathbb{R}$ be a continuous function such that $V(x_\star) = 0$ and $V(x) > 0$, $\forall x \in \mathcal{X} - \{0\}$. Hence,*

- *If $\dot{V}(x(t)) \leq 0$, for all $x(t) \in \mathcal{X} - \{0\}$ then $x_\star$ is a stable equilibrium for the system;*
- *If $\dot{V}(x(t)) < 0$, for all $x(t) \in \mathcal{X} - \{0\}$ then $x_\star$ is an asymptotic stable equilibrium for the system;*
- *If D coincides with $\mathbb{R}^n$, V is radially unbounded and $\dot{V}(x(t)) < 0$, for all $x(t) \in \mathbb{R}^n - \{0\}$ then $x_\star$ is a global asymptotically stable equilibrium for the system.*

The asymptotic stability notion is a very important property of a system and much more fundamental for control purpose, and the Lyapunov Theorem is often difficult to apply as it usually happens that the variation in time of V is only negative definite. Therefore, to conclude asymptotic stability let recall the following important notions.

Definition 1.1.5 (Invariant set)**.** A set $\mathcal{X}$ is said to be an *invariant set* with respect to (1.1a) if

$$x(0) \in \mathcal{X} \implies x(t) \in \mathcal{X}, \quad \forall t \in \mathbb{R}.$$

$\mathcal{X}$ is said to be a *positively invariant set* if

$$x(0) \in \mathcal{X} \implies x(t) \in \mathcal{X}, \quad \forall t \geq 0.$$

Theorem 1.1.2 (LaSalle's theorem)**.** *Let $\Omega \subset \mathcal{X}$ be a compact set that is positively invariant with respect to* (1.1a)*. Let $V : \mathcal{X} \to R$ be a continuously differentiable function such that $\dot{V}(x) \leq 0$ in Ω. Let E be the set of all points in Ω where $\dot{V}(x) = 0$. Let M be the largest invariant set in E. Then every solution starting in Ω approaches M as $t \to \infty$.*

Theorem 1.1.3 (Barbashin-Krasovskii theorem)**.** *Let $x = 0$ be an equilibrium point for* (1.1a)*. Let $V : \mathcal{X} \to \mathbb{R}$ be a continuously differentiable positive definite function on a domain $\mathcal{X}$ containing the origin $x = 0$, such that $\dot{V} \leq 0$ in $\mathcal{X}$. Let $S = \{x \in \mathcal{X} \mid \dot{V}(x) = 0\}$ and suppose that no solution can stay identically in S, other than the trivial solution $x(t) \equiv 0$. Then, the origin is asymptotically stable.*

Theorem 1.1.4. *Let $x = 0$ be an equilibrium point for* (1.1a)*. Let $V : \mathcal{X} \to \mathbb{R}$ be a continuously differentiable, radially unbounded, positive definite function such that $\dot{V} \leq 0$ for all $x \in \mathbb{R}^n$. Let $S = \{x \in \mathbb{R}^n \mid \dot{V}(x) = 0\}$ and suppose that no solution can stay identically in S, other than the trivial solution $x(t) \equiv 0$. Then, the origin is globally asymptotically stable.*

Remark 1.1.1. The equilibrium point $x_\star = 0$ of the linear system (1.3) with $u = 0$, is globally asymptotically stable with respect to the Lyapunov function $S(x) = \frac{1}{2}x^\top Px$ and positive definite $P \in \mathrm{Sym}_{\mathbb{R}}(n, n)$, verifying

$$PA + A^\top P < 0. \tag{1.4}$$

Then, all eigenvalues of the matrix A have negative real part.

1.2 Dissipativity and passivity

In the early 1970's, the concept of passive systems have been introduced for electrical circuit theory in Popov (1973) and further energetic properties has been formalized introducing the notions of *storage function* and *supply rate*, see Willems (1972b,c). These notions provide information on the energy behavior of the system with respect to its environment. Particularly, Willems managed the passivity concept as a fundamental input-output property which may be defined in terms of energy dissipation and transformation, and provided an energy balance of the system which generates a family of output related to external input mapping. In the context of this manuscript, since the system (1.1) must be modeled in such a way it exchanges power with its environment, the input space $\mathcal{U} \subset \mathbb{R}^m$ and output space $\mathcal{Y} \subset \mathbb{R}^m$ are assumed having same dimension, i.e. $\dim \mathcal{U} = \dim \mathcal{Y}$ and the dynamical system (1.1) is considered, as in Figure 1.1, in the following input-affine representation

$$\dot{x} = f(x) + g(x)u \tag{1.5a}$$

$$y = h(x) \tag{1.5b}$$

with smooth mappings $f : \mathbb{R}^n \to \mathbb{R}^n$, $g : \mathbb{R}^n \to \mathbb{R}^m$, $h : \mathbb{R}^n \to \mathbb{R}^m$, and without feedthrough term.

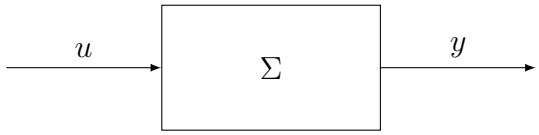

Figure 1.1: System (1.5) in an input-output representation with no feedthrough term.

In the following needed definitions are recalled from Sepulchre et al. (2012). The interested reader might find further insight in Willems (1972b,c); van der Schaft (2000); Vidyasagar (2002); Brogliato et al. (2007); Astolfi et al. (2007); Aliyu (2011).

Definition 1.2.1 (Dissipativity)**.** Assume that associated with the system (1.5) is a function $\omega : \mathcal{U} \times \mathcal{Y} \to \mathbb{R}$, called *supplied rate*, which is locally integrable for every $u \in \mathcal{U}$, that is, it satisfies

$$\int_{t_0}^{t_1} |\omega(u(t), y(t))| \, dt < \infty, \quad \text{for all } t_0 \leq t_1.$$

Let $\mathcal{X}$ be a connected subset of $\mathbb{R}^n$ containing the equilibrium point $x_\star$. The system (1.1) is said *dissipative* in $\mathcal{X}$ with supply rate $\omega(u, y)$ if there exists a $\mathcal{C}^1$ nonnegative function $S : \mathcal{X} \to \mathbb{R}_{\geq 0}$, $S(x_\star) = 0$, such that

$$S(x(T)) - S(x(0)) \leq \int_0^T \omega(u(t), y(t)) \, dt \tag{1.6}$$

for all $u \in \mathcal{U}$ and $T \geq 0$ such that $x(t) \in \mathcal{X}$ for all $t \in [0, T]$. The function $S(x)$ is then called a *storage function*.

Definition 1.2.2 (Passivity)**.** The system (1.5) is said *passive* if it is dissipative with supply rate

$$\omega(u(t), y(t)) = u^\top y.$$

If the storage function $S(x)$ is differentiable with $S(x) \geq 0$, a passive system is equivalently defined as satisfying the differential dissipation inequality

$$\dot{S}(x) \leq u^\top y, \tag{1.7}$$

along all solutions $x(t)$ with respect to the input function $u(t)$. From the passivity condition a physical interpretation of $S(x)$ can be deduced. Indeed, in many physical systems the storage function is nothing else that a generalization of the energy of the

system as the supply rate $\omega(u, y)$ is a generalization of the power supplied by the system. Thus, the physical interpretation of the dissipation inequality (1.7) states that the rate of increase of the internal energy is never greater than the power provided by the input power. Moreover, a passive system is dissipative if the energy variation of a system with zero input decreases over time, i.e. $\dot{S}(x) \leq 0$.

A particular interpretation of this condition is when the stored energy is exactly equal to the supplied one.

Definition 1.2.3. The system (1.1) is said *lossless* with supply rate $\omega(u, y)$ if there exists a differentiable storage function $S(x)$, such that for all $x \in \mathcal{X}$ and $u \in \mathcal{U}$

$$\dot{S}(x) = \omega(u, y). \tag{1.8}$$

Moreover, it is said *conservative* if it is lossless and for zero input $u = 0$ the supply rate verifies $\omega(0, y) = 0$.

The aforementioned definition states that a lossless system with supply rate $\omega(u, y) = u^\top y$, stores the same amount of energy than it is supplied with. Moreover, a passive system is conservative if the energy variation of a system with zero input remains constant over time, i.e. $\dot{S}(x) = 0$.

The necessary and sufficient conditions for providing passivity of a system of the form (1.5) are given by Kalman, Yakubovich and Popov and known in the literature as KYP properties. The next theorem is given by Hill and Moylan (1976).

Theorem 1.2.1. *A system* (1.5) *is passive if and only if there exists a* $\mathcal{C}^1$ *nonnegative function* $S : \mathcal{X} \to \mathbb{R}_{\geq 0}$ *which verifies the KYP properties*

$$\mathrm{L}_f S(x) \leq 0 \tag{1.9a}$$

$$\mathrm{L}_g S(x) = h^\top(x) \tag{1.9b}$$

for all $x \in \mathcal{X}$.

Remark 1.2.1. A linear system of the form (1.3) with $D = 0$, is passive with respect to a quadratic storage function $S(x) = \frac{1}{2}x^\top Px$ and positive definite $P \in \mathrm{Sym}_{\mathbb{R}}(n, n)$, and verifies KYP properties

$$PA + A^\top P < 0 \tag{1.10a}$$
$$B^\top P = C. \tag{1.10b}$$

Alternatively, if the system (1.3) is lossless, then verifies

$$PA + A^\top P = 0 \tag{1.11a}$$
$$B^\top P = C. \tag{1.11b}$$

1.2.1 Interconnections of passive systems

A useful feature of passive systems theory is the parallel interconnection and the negative feedback interconnection of passive systems is still passive. These results have inspired and motivated a huge number of control techniques typically exploited in control engineering Willems (2007); van der Schaft (2000). Indeed, these interconnection properties lead to nowadays well consolidated methodologies making reference to the so-called Passivity-Based Control (PBC) embedding, among many, Interconnection and Damping Assignment (IDA-PBC) and Control by Interconnection (CbI), where the role and the properties of the interconnection are extensively exploited for the design in several control problems Ortega et al. (2001, 2008, 2002b). Moreover, a variety of problems involving complex systems can be recast in the framework of energy-dissipation by modelling the complexity as a suitable power preserving interconnection; as an example, multi-agent and networked systems can be seen as an interconnection between passive subsystems Giordano et al. (2013); Reyes-Báez et al. (2018); Yao et al. (2009); Hatanaka et al. (2015).

The parallel interconnection and the negative feedback interconnection of passive systems are illustrated in Figure 1.2. To begin with, consider the interconnections depicted in where Σ_1 and Σ_2 are time-invariant dynamical system represented as

$$\dot{x}_i = f_i(x_i, u_i) \tag{1.12}$$
$$y_i = h_i(x_i). \tag{1.13}$$

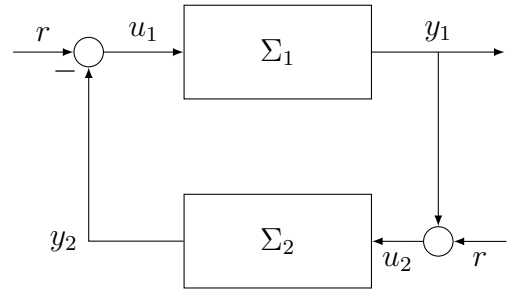

(a) Feedback interconnection

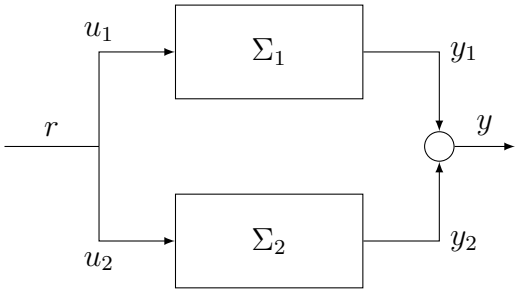

(b) Parallel interconnection

Figure 1.2: Interconnection of passive systems

Whether as a result of negative feedback interconnection (Figure 1.2a) or parallel interconnection (Figure 1.2b), the closed-loop state model takes the form

$$\dot{x} = f(x, r) \tag{1.14}$$

$$y = h(x) \tag{1.15}$$

where r is the new external input source and the state $x = (x_1, x_2)$. In this respect, the feedback interconnection is represented by an interconnecting law given by the following conditions

$$u_1 = r - h_2(x_2) \tag{1.16a}$$

$$u_2 = r + h_2(x_1) \tag{1.16b}$$

which results from the interconnection given in (Figure 1.2a), while the parallel interconnections is simply given by the condition

$$r = u_1 = u_2 \tag{1.17}$$

resulting from the interconnection illustrated in (Figure 1.2b).

Theorem 1.2.2. *Assume Σ_1 and Σ_2 are two passive system. Then the resulting feedback and parallel interconnection yield a passive system.*

The result can be deduced by requiring the storage function S of the whole interconnected system as the sum of the individual storage functions, i.e.

$$S(x_1, x_2) = S_1(x_1) + S_2(x_2).$$

1.2.2 Stability of passive systems

The concept of passivity and dissipativity are closely related to the Lyapunov stability theory in case the storage function $S(x)$ serves as a Lyapunov function. Indeed, if the passivity of the system is assured, then stability and stabilization problems can be handled, Sepulchre et al. (2012). The passivity property implies more than stability. It associates the input and output to the storage function and characterizes useful input-output properties.

The following notions are very useful in the problem of zero-state stabilization of the system. The problem of zero-state stabilization of controlled system was intensively studied in literature, see e.g. Byrnes et al. (1991). However the following are recalled from Sepulchre et al. (2012).

Definition 1.2.4 (Zero-state detectability)**.** Consider the system (1.1) with equilibrium point $x_\star$ and $\mathcal{K}^* \subset \mathbb{R}^n$ be the largest invariant set contained in $\mathcal{K} := \{x \in \mathbb{R}^n \mid h(x, 0) = 0\}$. The system (1.1) is said *zero-state detectable (ZSD)* if $x_\star$ is an asymptotically stable equilibrium conditionally to $\mathcal{K}^*$; that is for each initial condition $x_0 \in \mathcal{K}^*$ and $\epsilon > 0$ there exists $\delta(\epsilon)$ such that

$$||x_0 - x_\star|| < \delta(\epsilon) \implies ||x(t, x_0) - x^*|| < \epsilon \ \forall t > 0$$

and additionally there exists $\bar{\delta} > 0$ such that

$$||x_0 - x_\star|| < \bar{\delta} \implies \lim_{t\to\infty} x(t, x_0) = x_\star.$$

Definition 1.2.5 (Zero-state observability)**.** The system (1.1) with zero input $u = 0$ is zero-state observable (ZSO) if $x = x_\star$ is asymptotically stable conditionally to the largest positively invariant set $\mathcal{Z} = \{0\}$.

Theorem 1.2.3. *Let a system* (1.1) *with an equilibrium in* $x_\star$ *be passive with a storage function* $S(x)$*. Then the following properties hold:*

- *If* $S(x)$ *is positive definite, then the equilibrium* $x = x_\star$ *of* (1.1) *with* $u = 0$ *is Lyapunov stable;*
- *If* (1.1) *is ZSD, then the equilibrium* $x = x_\star$ *of* (1.1) *with* $u = 0$ *is Lyapunov stable;*
- *In addition, if* $S(x)$ *is positive definite and radially unbounded, i.e.* $S(x) \to \infty$ *as* $x \to \infty$*, then the equilibrium* $x = x_\star$ *in the above conditions is globally stable.*

1.2.3 Passivity-based control

We recalled the notion of passivity and seen its role in feedback interconnections. The ideas of passivity-based control that we are going to recall here is a straightforward application of the passivity condition given above.

Theorem 1.2.4 (Damping feedback)**.** *If the system* (1.5) *is zero-state detectable and passive with radially unbounded positive definite storage function* $S : \mathcal{X} \to \mathbb{R}_{\geq 0}$*,* $S(x_\star) = 0$*, then* $x_\star$ *can be globally stabilized by*

$$u = -\phi(y)$$

where ϕ *is any locally Lipschitz function such that* $\phi(0) = 0$ *and* $y^\top \phi(y) > 0$ *for all* $y \neq 0$*.*

In many cases the storage function is nothing else than the energy of the system, and the passive system has a stable equilibrium point. The Passivity-based control given above is needed to stabilize the equilibrium point of the system by means of an

injection of damping so that energy will dissipate whenever $x(t)$ is not identically $x_\star$. In this framework the damping is feedback injected by $\phi(y)$. Moreover, sometimes the injection is obtained by assigning a gain $\kappa > 0$, so that the PBC will inject to the closed loop system the so called *negative output feedback*

$$u = -\kappa y.$$

In our studies, we will usually deduce stability from the positive definiteness of the storage function and then invoke ZSD property to establish asymptotic stability under negative output feedback.

Example 1.2.1. The system

$$\begin{aligned}\dot{x}_1 &= x_2\\ \dot{x}_2 &= -x_1 + u\\ y &= x_2\end{aligned}$$

is ZSD and passive with positive semidefinite storage function $S(x_1, x_2) = \frac{1}{2}x_1^2 + \frac{1}{2}x_2^2$ since

$$\dot{S} = x_1\dot{x}_1 + x_2\dot{x}_2 = yu,$$

marginally stable for $u = 0$. Selecting the negative output feedback $u = -\kappa y$ with $\kappa > 0$, the origin of the closed-loop system is asymptotically stable since it verifies

$$\dot{S} = -\kappa x_2^2 < 0.$$

We have seen that passive systems are stable (for zero input $u = 0$) and easy to control (such as negative output feedback). Thus the perspective of rendering a system passive via feedback is often useful in control design. For example, we may first passivate a system and then stabilize the passivated system with a passivity-based-controller. Beyond negative output feedback, the feedback passivation paradigm is the underlying leit motiv of several nonlinear control strategies such as backstepping or feedforwarding. See Ortega et al. (2001); Astolfi et al. (2007); Sepulchre et al. (2012) for a thorough understanding.

The definition of feedback passivation is formally given in the definition below.

Definition 1.2.6 (Feedback passivation)**.** The system (1.5) is said *feedback passive* if there exist smooth functions $\gamma : \mathbb{R}^n \to \mathbb{R}$, $h_d : \mathbb{R}^n \to \mathbb{R}$ and $S_d : \mathbb{R}^n \to \mathbb{R}_{\geq}0$ such that the feedback law

$$u = \gamma(x) + v \tag{1.18}$$

makes the closed-loop system

$$\dot{x} = f_d(x) + g(x)v \tag{1.19a}$$

$$y = h_d(x) \tag{1.19b}$$

passive with $f_d(x) := f(x) + g(x)\gamma(x)$ and storage function $S_d(\cdot)$; namely, the dissipation inequality below holds for all $t \geq 0$ and $x_0 \in \mathbb{R}^n$

$$S_d(x(t)) - S_d(x_0) \leq \int_0^t y(s)v(s)\mathrm{d}s. \tag{1.20}$$

Theorem 1.2.5 (Stabilization through feedback passivation)**.** *If the system* (1.5) *is feedback passive under feedback law* (1.18) *and the achieved closed-loop system* (1.19) *is ZSD and passive with radially unbounded positive definite storage function* $S_d : \mathbb{R}^n \to \mathbb{R}_{\geq}0$ *and* $S_d(x_\star) = 0$*, then* $x_\star$ *can be globally asymptotically stabilized by the negative output feedback*

$$v = -\kappa h_d(x), \quad \kappa > 0.$$

1.3 Port-Hamiltonian systems

An important class of passive systems governed by the Hamiltonian function is the port-Hamiltonian, van der Schaft (2000). Port-Hamiltonian systems emerge from network modeling of complex physical systems possibly containing components from different physical domains. They are defined by a Dirac structure, expressing the power-conserving property of the interconnection, an energy function, the Hamiltonian, together with a resistive relation (see van der Schaft et al. (2014) and the references therein). Dirac structures, arising from the bond graph formalism and the Poisson formalization of symplectic forms Courant (1990), have been proposed

to represent power-preserving interconnections (see Maschke et al. (1992); van der Schaft and Maschke (2013)). In particular, in Maschke and van der Schaft (1993) it has been shown how port-Hamiltonian systems naturally lead to a generalized Hamiltonian formulation of the dynamics where the Hamiltonian function is given by the total energy of the energy-storing elements in the system, while the internal structure of the system is properly specified by the power-conserving interconnection between energy-storing elements of each subsystem.

1.3.1 Port-Hamiltonian dynamics

In what follows we recall the definition of input-state-output port-Hamiltonian system from van der Schaft (2000). In the rest of the manuscript, input-state-output port-Hamiltonian system will be simply called port-Hamiltonian.

Definition 1.3.1 (Port-Hamiltonian system)**.** A continuous-time port-Hamiltonian system with state $x \in \mathcal{X} \subset \mathbb{R}^n$, input $u \in \mathcal{U} \subset \mathbb{R}^m$ and output $y \in \mathcal{Y} \subset \mathbb{R}^m$, and Hamiltonian function $H(\cdot) : \mathcal{X} \to \mathbb{R}$ which is a continuously differentiable real-valued function, is given as

$$\dot{x} = (J(x) - R(x))\nabla H(x) + g(x)u \tag{1.21a}$$

$$y = g^\top(x)\nabla H(x) \tag{1.21b}$$

where $J(\cdot) \in \mathrm{Skew}_{\mathbb{R}}(n, n)$, and positive semidefinite $R(\cdot) \in \mathrm{Sym}_{\mathbb{R}}(n, n)$.

Port-Hamiltonian systems naturally arise from the energy interpretation of the system and they are defined in terms of a Hamiltonian function $H(x)$, representing the total amount of energy contained in the system (stored energy), together with two geometric structures $J(x)$ and $R(x)$ corresponding to power-conserving interconnection and energy dissipation, respectively. Finally, u and y are conjugated variables whose product has units of power. In the case of port-Hamiltonian systems endowed with a lower bounded Hamiltonian function, the passivity property can be directly inferred from the special geometric structure of the system, exploiting the Hamiltonian function as a storage function, and providing a suitable output for which the passivity property holds true with respect to the Hamiltonian function. In particular, by the geometric structure of $J(x)$ and $R(x)$, it follows that:

- considering $H(x)$ as a storage function ($H : \mathcal{X} \to \mathbb{R}_{\geq 0}$), the port-Hamiltonian system (1.21) is passive and verifies the dissipation inequality

$$\dot{H} = -\nabla^\top H(x) R(x) \nabla H(x) + y^\top u \leq u^\top y, \tag{1.22}$$

and integrating with respect to time for $t > t_0$, one gets the energy balance equality

$$H(x(t)) = H(x(t_0)) - \int_{t_0}^{t} \nabla^\top H(x(\tau)) R(x(\tau)) \nabla H(x(\tau))\, d\tau + \int_{t_0}^{t} u^\top(\tau) y(\tau)\, d\tau,$$

where $\nabla^\top H(x) R(x) \nabla H(x)$ describes the internal dissipation and the inner product $u^\top y$ describes the externally supplied power;

- if $x_\star$ is a (local) strict minimum of the Hamiltonian function $H(x)$, namely

$$x_\star = \arg\min H(x),$$

according to Lyapunov stability and La Salle's invariance principle any equilibrium $x_\star$ of the port-Hamiltonian system which coincides with a local minimum of $H(x)$ are asymptotically stable equilibra of the system if the set $\{x_\star\}$ coincides with the largest invariant set contained in

$$\Omega_\star := \{x \in \mathbb{R}^n \mid \nabla^\top H(x) R(x) \nabla H(x) = 0\};$$

- in the case of zero dissipation $R(x) = 0$, the system is lossless

$$\dot{H} = u^\top y, \tag{1.23}$$

and for zero input $u = 0$ the equality above implies conservation of energy along the dynamics (1.21).

Remark 1.3.1. In the linear case with quadratic Hamiltonian function $H(x) = \frac{1}{2} x^\top P x$ and positive definite $P \in \mathrm{Sym}_{\mathbb{R}}(n, n)$ is represented by the couple of equations

$$\dot{x} = (J - R) P x + B u \tag{1.24a}$$

$$y = B^\top P x \tag{1.24b}$$

with (J, R, B, P) having constant entries. The dissipation inequality along $H(x)$ provides

$$\dot{H}(x) = -x^\top PRPx + x^\top PBu \leq u^\top y. \tag{1.25}$$

1.3.2 Recalls on Dirac structures

Finite-dimensional Dirac structures are defined over finite-dimensional vector space of flows $\mathcal{F}$ and over a field $\mathbb{K}$, where the flow vector f is an element of the vector space of flows $\mathcal{F}$. Accordingly, the effort vector is denoted by e that is an element of the vector space of efforts $\mathcal{E}$. The vector space of efforts is given by the dual space of $\mathcal{F}$, that is $\mathcal{E} = \mathcal{F}^*$. The space of port variables is given by the space of flow and effort variable $\mathcal{F} \times \mathcal{E}$. The duality product between dual spaces $\mathcal{F}$ and $\mathcal{E}$, denoted by

$$\langle \cdot \mid \cdot \rangle : \mathcal{E} \times \mathcal{F} \to \mathbb{K}, \tag{1.26}$$

is non-degenerate, i.e.

$$\begin{aligned} &\langle e \mid f \rangle = 0, \forall e \in \mathcal{E} \implies f = 0 \\ &\langle e \mid f \rangle = 0, \forall f \in \mathcal{F} \implies e = 0, \end{aligned}$$

and linear in each coordinate, i.e.

$$\begin{aligned} &\langle \alpha e_a + \beta e_b \mid f \rangle = \alpha \langle e_a \mid f \rangle + \beta \langle e_b \mid f \rangle \\ &\langle e \mid \alpha f_a + \beta f_b \rangle = \alpha \langle e \mid f_a \rangle + \beta \langle e \mid f_b \rangle, \end{aligned}$$

with $f_a, f_b, f \in \mathcal{F}$, $e_a, e_b, e \in \mathcal{E}$, and $\alpha, \beta \in \mathbb{K}$. The standard definition of a Dirac structure is recalled below, van der Schaft (2000); Duindam et al. (2009).

Definition 1.3.2 (Dirac structure)**.** Consider on the space of the port variables $\mathcal{F} \times \mathcal{E}$ the canonical bilinear form

$$\langle\!\langle \cdot, \cdot \rangle\!\rangle : (\mathcal{F} \times \mathcal{E}) \times (\mathcal{F} \times \mathcal{E}) \to \mathbb{K}, \tag{1.27}$$

defined by $\langle\!\langle (f_a, e_a), (f_b, e_b) \rangle\!\rangle := \langle e_a, f_b \rangle + \langle e_b, f_a \rangle$ with $(f_a, e_a), (f_b, e_b) \in \mathcal{F} \times \mathcal{E}$. Then a *Dirac structure* is a subspace $\mathcal{D} \subset \mathcal{F} \times \mathcal{E}$ such that $\mathcal{D} = \mathcal{D}^{\perp\!\!\!\perp}$, with $\perp\!\!\!\perp$ denoting the orthogonal complement with respect to the bilinear form $\langle\!\langle \cdot, \cdot \rangle\!\rangle$.

Note that the bilinear form $\langle\langle (f,e),(f,e) \rangle\rangle$ is indefinite as it can be positive or negative, and is non-degenerate, in the sense that $\langle\langle (f_a,e_a),(f_b,e_b) \rangle\rangle = 0$ for all (f_a,e_a) implies $(f_a,e_a) = 0$, or viceversa. Furthermore, the duality product (1.26) and the bilinear form (1.27) are related by

$$\langle e \mid f \rangle = \frac{1}{2} \langle\langle (f,e),(f,e) \rangle\rangle \in \mathcal{F} \times \mathcal{E}.$$

For a finite-dimensional real linear space $\mathcal{F}$ the definition of Dirac structure is equivalent to $\dim \mathcal{D} = \dim \mathcal{F}$ and

$$\langle e \mid f \rangle = e^\top f = 0, \quad (f,e) \in \mathcal{D}.$$

The aforementioned property has a physical interpretation as it corresponds to the power-conservation law. Specifically, it expresses the phenomena that the power entering (or leaving) a Dirac structure is always zero.

Remark 1.3.2. It is worth mentioning that if $\Phi : \mathcal{E} \to \mathcal{F}$ is a skew-symmetric linear mapping, that is $\Phi = \Phi^*$ where $\Phi^* : \mathcal{E} \to \mathcal{E}^* = \mathcal{F}$ is the adjoint mapping, then

$$\Phi_{\text{graph}} := \{(f,e) \in \mathcal{F} \times \mathcal{E} \mid f = \Phi e\}$$

is a Dirac structure.

In the case of a linear state space $\mathcal{X}$ and a constant Dirac structure $\mathcal{D}$, is defined as

$$\mathcal{D} \subset \mathcal{F}_S \times \mathcal{E}_S \times \mathcal{F}_R \times \mathcal{E}_E \times \mathcal{F}_P \times \mathcal{E}_P$$

where $(f_S, e_s) \in \mathcal{F}_S \times \mathcal{E}_S$ are the flows and efforts of the energy-storing elements, $(f_R, e_R) \in \mathcal{F}_R \times \mathcal{E}_R$ the flows and efforts of the energy-dissipating elements, and finally $(f_P, e_P) \in \mathcal{F}_P \times \mathcal{E}_P$ are the flows and efforts of the external ports. The vectors of flow variables and effort variables of the energy-storing elements are given as

$$\begin{aligned} f_S &= -\dot{x} \\ e_S &= \frac{\partial H}{\partial x}(x) \end{aligned}$$

while (f_R, e_R) are related by a energy-dissipating (resistive) relation, which can be any subset $\mathcal{R} \subset \mathcal{F}_R \times \mathcal{E}_R$, satisfying the property

$$e_R^\top f_R \leq 0 \quad \forall\ (f_R, e_R) \in \mathcal{R}. \tag{1.28}$$

This leads to the following definition.

Definition 1.3.3. A port-Hamiltonian system is defined by a Dirac structure $\mathcal{D}$, a Hamiltonian function $H : \mathcal{X} \to \mathbb{R}$ and an energy-dissipating relation $\mathcal{R} \subset \mathcal{F}_R \times \mathcal{E}_R$ satisfying (1.28). The dynamics is given by the requirement that for all $t \in \mathbb{R}$

$$\left(-\dot{x}(t), \frac{\partial H}{\partial x}(x(t)), f_R(t).e_R(t), f_P(t), e_P(t)\right) \in \mathcal{D}(x(t))$$
$$(f_R(t), e_R(t)) \in \mathcal{R}$$

Exploiting Remark 1.3.2 the port-Hamiltonian system is given as the graph of the skew-symmetric map

$$\begin{pmatrix} f_S \\ f_R \\ f_P \end{pmatrix} = \begin{pmatrix} -J(x) & -g_R(x) & -g(x) \\ g_R^\top(x) & 0 & 0 \\ g^\top(x) & 0 & 0 \end{pmatrix} \begin{pmatrix} e_S \\ e_R \\ e_P \end{pmatrix},$$

with resistive relation $e_R = -r(x)f_R$, matrix $r(x) = r^\top(x) \succeq 0$, and the input matrix $g_R(x)$ corresponding to the resistive port, which provide energy balance

$$f_S^\top e_S + f_R^\top e_R + f_P^\top e_P = 0.$$

1.4 Interconnection and damping assignment

Port-Hamiltonian systems can be profitably used for solving set-point stabilization based on the feedback passivation problem. The *energy management* is the essence of the second generation of PBC, see Ortega et al. (2001), since the Hamiltonian function, which serves as storage function, is generally defined as the sum of the kinetic and potential energy functions associated with the system. This Hamiltonian function comes with desirable features, one above all is that the energy function has a minimum at the desired operating point to ensure stability. One of the most praised energy-based control is, undoubtedly, the so-called Interconnection and Damping Assignment (IDA-PBC), introduced in Ortega et al. (2002b). Stabilization of a desired equilibrium by IDA-PBC involves assigning for the closed-loop system a new port-Hamiltonian structure with the assigned energy function having a minimum at the desired equilibrium point, for stability reasons.

Problem 1 (IDA-PBC)**.** The objective of the IDA-PBC strategy consists of finding an input feedback $u = u(x)$ such that a desired equilibrium point $x_\star$ of the closed-loop system is (asymptotically) stable and that the closed-loop system is given by

$$\dot{x} = (J_d(x) - R_d(x))\nabla H_d(x) + g(x)u \tag{1.29a}$$

$$y = g^\top(x)\nabla H_d(x) \tag{1.29b}$$

where $J_d(x) \in \mathrm{Skew}_{\mathbb{R}}(n,n)$ and positive semidefinite $R_d(x) \in \mathrm{Sym}_{\mathbb{R}}(n,n)$ are, respectively, the desired interconnection and dissipation matrices and $H_d : \mathbb{R}^n \to \mathbb{R}_{\geq 0}$ is the desired Hamiltonian function. The desired $H_d(x)$ must verify $H_d(x_\star) = 0$, with $x_\star$ a strict (local) minimizer of $H_d(x)$. Moreover, the achieved closed-loop system (1.29) yields the energy balance equality for all $t > t_0$,

$$H_d(x(t)) - H_d(x(t_0)) = -\int_{t_0}^{t} \nabla^\top H_d(x(\tau))R_d(x(\tau))\nabla H_d(x(\tau))\ d\tau + \int_{t_0}^{t} u^\top(\tau)y(\tau)\ d\tau.$$

A static feedback can be computed solving in u the PDE called matching equation of form

$$(J(x) - R(x))\nabla H(x) + g(x)u = (J_d(x) - R_d(x))\nabla H_d(x).$$

The following proposition is recalled.

Proposition 1.4.1 (Ortega et al. (2002b))**.** *Consider the system*

$$\dot{x} = (J(x) - R(x))\nabla H(x) + g(x)u \tag{1.30a}$$

$$y = g^\top(x)\nabla H(x) \tag{1.30b}$$

and a desired equilibrium $x_\star$ to be stabilized. Assume that we can find functions $u(x)$ and $H_a(x)$, and matrices $J_a(x)$ and $R_a(x)$ satisfying the matching equation of form

$$(J(x) - R(x))\nabla H(x) + g(x)u = (J_a(x) + J(x) - R_a(x) - R(x))(\nabla H_a(x) + \nabla H(x))$$

and such that the following conditions occur.

- *Equilibrium assignment: at $x_\star$ the gradient of $H_a(x)$ verifies*

$$\nabla H_a(x_\star) + \nabla H(x_\star) = 0.$$

- *Minimum condition: the Hessian of $H_a(x)$ at $x_\star$ satisfies*

$$\nabla^2 H_a(x_\star) + \nabla^2 H(x_\star) > 0.$$

Then, $x_\star$ will be a (locally) stable equilibrium of the closed-loop system (1.29)*. It will be (locally) asymptotically stable if, in addition, the largest invariant set under the closed-loop dynamics contained in*

$$\{x \in \mathbb{R}^n \mid \nabla^\top H_d(x) R_d(x) \nabla H_d(x) = 0\}$$

equals $\{x_\star\}$*.*

Namely, the matching equation reduces in solving the matching condition

$$g^\perp(x)\left((J(x) - R(x))\nabla H(x) - (J_d(x) - R_d(x))\nabla H_d(x)\right) = 0$$

where $g^\perp(x)$ denotes left annihilator of the mapping g, i.e. $g^\perp(x)g(x) = 0$ for all $x \in \mathbb{R}^n$. Its solution, that is generically necessary for the solvability of the matchign equation, hinges upon suitable construction of $J_d(x)$, $R_d(x)$, and $H_d(x)$, namely defining

$$J_d(x) := J(x) + J_a(x) \quad R_d(x) := R(x) + R_a(x) \quad H_d(x) := H(x) + H_a(x)$$

where $H_a(x)$ is chosen such that $H_d(x)$ has a minimum in $x_\star$, namely $H_a(x)$ must verify at $x_\star$ the relation $H_a(x_\star) = -H(x_\star)$, solving the matching condition

$$g^\perp(x)\left((J(x) - R(x))\nabla H_a(x) + (J_a(x) - R_a(x))(\nabla H(x) + \nabla H_a(x))\right) = 0. \quad (1.31)$$

If the matching condition is satisfied, then the state-feedback u that (asymptotically) stabilizes the equilibrium point $x_\star$ of the closed-loop system (1.29) is given by

$$u = g^\dagger(x)\left((J(x) - R(x))\nabla H_a(x) + (J_a(x) - R_a(x))(\nabla H(x) + \nabla H_a(x))\right) \quad (1.32)$$

with $g^\dagger(x) = (g^\top(x)g(x))^{-1}g^\top(x)$.

Remark 1.4.1. The matching condition which must be solved is parameterized by three ingredients $J_a(x)$, $R_a(x)$, and $g^\perp(x)$ with $J_a(x)$ and $R_a(x)$ defining the degrees of freedom in satisfying the PDE. If the problem is solvable with respect to unchanged $J(x)$ and $R(x)$, i.e. $J_a(x) = 0$ and $R_a(x) = 0$, the matching equation is called the *energy shaping matching equation*, and characterizes the possible $H_a(x)$ which is used to shape $H(x)$ to $H_d(x)$, see van der Schaft (2000); Ortega et al. (2001, 2002a).

However, not all the desired equilibrium points can be assigned to the closed-loop system. The assignable equilibrium point $x_\star$ to the port-Hamiltonian system (1.21), see Castaños et al. (2009), is contained in the set

$$\mathcal{E} := \{x \in \mathbb{R}^n \mid g^\perp(x)(J(x) - R(x))\nabla H(x) = 0\},$$

there is a uniquely defined constant control given by,

$$u_\star = -g^\dagger(x_\star)(J(x_\star) - R(x_\star))\nabla H(x_\star).$$

For the ease of presentation let consider the following example which will be better analyzed in Part IV concerning the case studies.

Example 1.4.1. Assume the LC port-Hamiltonian system of the form

$$\dot{x} = J\nabla H(x) + Bu = \begin{pmatrix} 0 & 1 \\ -1 & 0 \end{pmatrix} \nabla H(x) + \begin{pmatrix} 0 \\ 1 \end{pmatrix} u \tag{1.33}$$

and associated Hamiltonian function given by

$$H(x) = \frac{1}{2C}x_1^2 + \frac{1}{2L}x_2^2. \tag{1.34}$$

with inductor $L > 0$ and capacitor $C > 0$. The control objective is to asymptotically stabilize the closed-loop system at the desired equilibrium point $x_\star = (x_{\star 1}, 0)$, by assigning the desired Hamiltonian function

$$H_d(x) = \frac{1}{2C}(x_1 - x_{\star 1})^2 + \frac{1}{2L}x_2^2.$$

To achieve the control objective the matching condition

$$B^\perp((J - R_d)\nabla H_d(x) - J\nabla H(x)) = 0$$

must be satisfied. However, selecting the dissipation matrix as

$$R_d = \begin{pmatrix} 0 & 0 \\ 0 & r_d \end{pmatrix}$$

the matching condition is satisfied and thus there exists an IDA-PBC feedback of the form

$$\begin{aligned} u &= (B^\top B)^{-1}B^\top((J - R_d)\nabla H_d(x) - J\nabla H(x)) \\ &= \frac{1}{C}x_{\star 1} - \frac{r_d}{L}x_2 \end{aligned} \tag{1.35}$$

which assigns the desired closed-loop system

$$\dot{x} = (J - R_d)\nabla H_d(x) = \begin{pmatrix} 0 & 1 \\ -1 & -r_d \end{pmatrix} \nabla H_d(x).$$

1.5 Concluding remarks

The underlying notions of passivity, port-Hamiltonian modeling, passivity-based control and IDA-PBC have been recalled. A deeper understanding of these concepts can be found in Ortega et al. (2001); van der Schaft (2000); Brogliato et al. (2007); Astolfi et al. (2007); Sepulchre et al. (2012); van der Schaft et al. (2014). We conclude this chapter by mentioning the crucial properties that need particular attention and understanding in discrete time first and then under sampled-data design:

1. definition of passivity for discrete time systems;
2. interconnection of passive systems;
3. definition of port-Hamiltonian dynamics with an associated passive output;
4. the use of passivity in energy-based control in discrete time and under sampling.

Chapter 2

Passivity concepts in discrete time

Contents

2.1 Generalities on discrete-time systems **48**

2.1.1 Discrete gradient function 50

2.1.2 Discrete Jacobian 52

2.1.3 Difference and differential representation 53

2.2 Passivity in discrete time **55**

2.2.1 The u-average passivity 57

2.2.2 Passivity-based control 61

2.2.3 Constructive approximate solutions 61

2.3 Linear-time invariant case **62**

2.4 Interconnection of u-average passive systems **64**

2.4.1 The parallel interconnection 66

2.4.2 Feedback interconnection 67

2.4.3 Computational aspects 70

2.4.4 Interconnection of average passive LTI systems 71

2.5 Example: interconnection of passive oscillators **73**

2.5.1 Interconnection structure design 73

2.5.2 Analysis and simulation results 75

2.6 Concluding remarks **80**

This chapter moves towards passivity properties in a discrete time setting. First, we discuss generalities on discrete-time systems and in particular we recall the definition of Difference/Differential representation (DDR), introduced in Monaco and Normand-Cyrot (1995), and the definition of discrete gradient function, introduced in Gonzalez (1996). Then, we restate the definition of passivity in discrete time and, in this respect, notions and properties of u-average passivity are recalled from Monaco and Normand-Cyrot (2011). Further, we establish a connection between the u-average output, arising from the u-average passivity definition, with a discrete gradient of the associated storage function. Finally, since in the framework of discrete-time u-average passive systems, a complete understanding of the properties under elementary interconnections is still unclear, the properties of the interconnection preserving u-average passivity under interconnection are proposed and new results in this direction will be presented and further discussed by means of an academic example.

2.1 Generalities on discrete-time systems

General nonlinear discrete-time systems are described in the state-space representation by a set of difference equation equations

$$x(k+1) = F(x(k), u(k)) \tag{2.1a}$$

$$y(k) = h(x(k), u(k)). \tag{2.1b}$$

The state $x = (x_1, \ldots, x_n)$ is assumed to belong to a subset $\mathcal{X}$ of $\mathbb{R}^n$, the input $u = (u_1, \ldots, u_m)$ is assumed to belong to a subset $\mathcal{U}$ of $\mathbb{R}^m$, and the output $y = (y_1, \ldots, y_p)$ is assumed to belong to a subset $\mathcal{Y}$ of $\mathbb{R}^p$. $F : \mathcal{X} \times \mathcal{U} \to \mathbb{R}^n$, $h : \mathcal{X} \times \mathcal{U} \to \mathbb{R}^n$ are smooth mappings. The state x, input u, and output y are functions of time k with $k \in \mathbb{N}$ and determined by their initial condition $x(0)$ and $u(0)$. For a deeper understanding on discrete-time systems see Normand-Cyrot (1983); Greenspan (1973); Monaco and Normand-Cyrot (1986); Kotta (2006); Sontag (2013). The point $x_\star \in \mathcal{X}$ is the equilibrium point of the autonomous system (2.1a), that is $F(x(k), 0)$. This general class of systems include the following sub-classes of discrete-time systems:

- Input-affine system:

$$x(k+1) = F(x(k)) + g(x(k))u(k) \tag{2.2a}$$
$$y(k) = h(x(k)) + j(x(k))u(k) \tag{2.2b}$$

- Linear system (LTI):

$$x(k+1) = Ax(k) + Bu(k) \tag{2.3a}$$
$$y(k) = Cx(k) + Du(k) \tag{2.3b}$$

with matrices (A, B, C, D) of appropriate dimensions.

As a counterpart of the Lyapunov stability in continuous-time, below we recall the result for discrete-time systems.

Theorem 2.1.1 (Discrete Lyapunov Stability)**.** *Let $x_k = x_\star$ be an equilibrium point for the discrete-time system* (2.1) *and let $\mathcal{D} \subset \mathbb{R}^n$ such that $x_\star \in \mathcal{D}$. Let $V : \mathcal{D} \to \mathbb{R}$ be continuous function such that $V(x_\star) = 0$ and $V(x(k)) > 0$, $\forall x \in D - \{0\}$. Hence,*

- *If $V(x(k+1)) \leq V(x(k))$, $\forall x \in \mathcal{D} - \{0\}$ then $x_\star$ is a stable equilibrium for the system;*
- *If $V(x(k+1)) < V(x(k))$, $\forall x \in \mathcal{D} - \{0\}$ then $x_\star$ is an asymptotic stable equilibrium for the system;*
- *If $\mathcal{D}$ coincides with $\mathbb{R}^n$, V is radially unbounded and $V(x(k+1)) < V(x(k))$, $\forall x \in \mathbb{R}^n - \{0\}$ then $x_\star$ is a global asymptotically stable equilibrium for the system.*

The LaSalle's theorem, or LaSalle Invariance Principle see Mei and Bullo (2017), is formally extended in discrete-time saying that, differently from the continuous-time, in discrete-time the function $V : \mathcal{D} \to \mathbb{R}$ is such that $V(x(k+1)) \leq V(x(k))$ in Ω, and as $k \to \infty$ every solution starting in Ω approaches the largest invariant set M in

$$E := \{x \in \mathcal{D} \mid V(x(k+1)) = V(x(k))\}.$$

Theorem 2.1.2. *Let $x = 0$ be an equilibrium point for* (2.1a)*. Let $V : \mathcal{D} \to \mathbb{R}$ be a continuous positive definite function on a domain $\mathcal{D}$ containing the origin $x = 0$, such that $V(x(k+1)) \leq V(x(k))$ in $\mathcal{D}$. Let $E = \{x \in \mathcal{D} \mid V(x(k+1)) = V(x(k))\}$ and suppose that no solution can stay identically in E, other than the trivial solution $x(k) \equiv 0$. In addition, if $V(x)$ is also radially unbounded, then the origin is globally asymptotically stable.*

2.1.1 Discrete gradient function

The notion of *discrete gradient function* has been introduced by Gonzalez (1996) with the aim of defining numerical methods suitable for the energy conservation of Hamiltonian systems. The discrete gradient function, or simply discrete gradient, is a function which satisfies two fundamental conditions: the first condition regards the variation of the energy function one-step ahead; the second condition concerns the continuity argument with respect to the continuous-time gradient. Whereas those conditions guarantee a resulting function which yields some geometric property inheriting conservation (or dissipation) of the energy, their solution is not generally unique.

Hereafter, the definition of discrete gradient function adopted in this manuscript is given below considering a discrete gradient computed component-wise through its integral form.

Definition 2.1.1 (Discrete gradient)**.** Given a differentiable real-valued function $S : \mathbb{R}^n \to \mathbb{R}$, its *discrete gradient* function is $\bar{\nabla} S : \mathbb{R}^n \times \mathbb{R}^n \to \mathbb{R}^n$,

$$\bar{\nabla} S(v, w) = \mathrm{col}(\bar{\nabla} S(v_1, w_1), \cdots, \bar{\nabla} S(v_n, w_n)),$$

with

$$\bar{\nabla} S(v_i, w_i) = \frac{1}{w_i - v_i} \int_{v_i}^{w_i} \frac{\partial S(v_1, ..., v_{i-1}, \xi, w_{i+1}, ..., w_n)}{\partial \xi} \, \mathrm{d}\xi,$$

which satisfies for all $v, w \in \mathbb{R}^n$,

$$(w - v)^\top \bar{\nabla} S(v, w) = S(w) - S(v)$$
$$\bar{\nabla} S(v, v) = \nabla S(v).$$

Roughly speaking, a discrete gradient function on a vector space $\mathbb{R}^n$ with inner product $v^\top w$ is a function satisfying the variation between an initial value $S(v)$ and a final value $S(w)$. For the sake of compactness the discrete gradient function of $S(\cdot)$ between v and w will be denoted $\bar{\nabla} S(v,w) := \bar{\nabla} S|_v^w$.

A systematic study of discrete-gradient methods is discussed in McLachlan et al. (1999); Hairer et al. (2006). The following Lemma gives constructive forms of the discrete gradient.

Lemma 2.1.1. *For a given smooth function $S(\cdot) : \mathbb{R}^n \to \mathbb{R}$, by the mean value theorem, one can express the difference $S(w) - S(v)$ as such*

$$S(w) - S(v) = (w-v)^\top \int_0^1 \nabla S|_{v+s(w-v)} ds,$$

which yields the constructive form of the discrete gradient

$$\bar{\nabla} S|_v^w = \int_0^1 \nabla S|_{v+s(w-v)} ds$$

with $v + s(w-v) = col(v_1 + s(w_1 - v_1), \cdots, v_n + s(w_n - v_n))$, for $s \in [0,1]$.

Remark 2.1.1. If the function $S(v)$ is a separable function, meaning that for $v \in \mathbb{R}^n$ and $v = col(v_1, \ldots, v_n)$,

$$S(v) = \sum_{i=1}^n S_i(v_i),$$

then its discrete gradient function in the integral form from v to w reduces to

$$\bar{\nabla} S|_v^w = \sum_{i=1}^n \bar{\nabla}_i S|_{v_i}^{w_i}$$

with for any $i = (1, \cdots, n)$

$$\bar{\nabla} S_i|_{v_i}^{w_i} = \frac{1}{w_i - v_i} \int_{v_i}^{w_i} \frac{\mathrm{d}S_i(\xi)}{\mathrm{d}\xi} \mathrm{d}\xi = \int_0^1 \nabla S_i|_{v_i + s(w_i - v_i)} \mathrm{d}s.$$

Remark 2.1.2. Given $S(v) = \frac{1}{2} v^\top P v$, where P is a matrix with constant entries, then its associated discrete gradient from v to w is given by

$$\bar{\nabla} S|_v^w = \frac{1}{2} \nabla S(w+v) = \frac{1}{2} P(w+v), \tag{2.4}$$

that is directly deduced from the difference $S(w) - S(v) = \frac{1}{2} w^\top P w - \frac{1}{2} v^\top P v = \frac{1}{2}(w-v)^\top P(v+w)$.

2.1.2 Discrete Jacobian

Along with the discrete gradient function an instrumental object involved into the sampled-data representation of port-Hamiltonian dynamics that we will present in Part III is the discrete Jacobian function. Its definition is given below.

Definition 2.1.2 (Discrete Jacobian)**.** Given a vector-valued function $f : \mathbb{R}^n \to \mathbb{R}^n$ its *discrete Jacobian* is a matrix-valued function $\bar{\mathrm{J}}[f]|_{\cdot} : \mathbb{R}^n \times \mathbb{R}^n \to \mathrm{Mat}_{\mathbb{R}}(n, n)$, which satisfies for all $v, w \in \mathbb{R}^n$

$$\bar{\mathrm{J}}[f]|_v^w (w - v) = f(w) - f(v). \tag{2.5}$$

The discrete Jacobian $\bar{\mathrm{J}}[f]|_v^w$ of a function $f = col(f_1, \ldots, f_n) : \mathbb{R}^n \to \mathbb{R}^n$ with $f_i : \mathbb{R}^n \to \mathbb{R}$ is the $n \times n$ matrix-valued function which yields

$$f(w) - f(v) = \begin{pmatrix} (w - v)^\top \bar{\nabla} f_1|_v^w \\ \vdots \\ (w - v)^\top \bar{\nabla} f_n|_v^w \end{pmatrix} = \bar{\mathrm{J}}[f]|_v^w (w - v)$$

with gradient $\bar{\nabla} f_i|_v^w = col(\bar{\nabla}_1 f_i|_v^w \cdots \bar{\nabla}_n f_i|_v^w)$.

The following Lemma gives constructive forms of the discrete Jacobian.

Lemma 2.1.2. *For a given differentiable function $f : \mathbb{R}^n \to \mathbb{R}^n$, the difference $f(w) - f(v)$ can be expressed as such*

$$f(w) - f(v) = \int_0^1 \nabla f|_{v+s(w-v)} ds (w - v)$$

so getting for the discrete Jacobian of f, the integral expression

$$\bar{\mathrm{J}}[f]|_v^w = \int_0^1 \nabla f|_{v+s(w-v)} ds.$$

Generally, as for the discrete gradient function, the discrete Jacobian function computed according to the Lemma above requires for all $v \in \mathbb{R}^n$,

$$\bar{\mathrm{J}}[f]|_v^v = \nabla f(v).$$

2.1.3 Difference and differential representation

The general nonlinear discrete-time dynamics

$$x(k+1) = F(x(k), u(k))$$

is nonlinear in the control variable $u(k)$ and this usually requires a formal algebraic characterization of the map $F(\cdot, u(k))$ with respect to the control variable. However, to cope this aspect an alternative representation has been proposed in Monaco and Normand-Cyrot (1995, 1998); Monaco et al. (2007). The following definition is recalled from Monaco and Normand-Cyrot (1998).

Definition 2.1.3 (Difference and Differential representation)**.** Given smooth functions $F_0 : \mathcal{X} \to \mathcal{X}$ and $G : \mathcal{X} \times \mathcal{U} \to \mathcal{X}$, and assume F_0 invertible. A discrete-time dynamics (2.1a) in its *Difference and Differential representation* (DDR) is defined by the couple of equations of the form

$$x^+ = F_0(x) \tag{2.6a}$$

$$\frac{\mathrm{d}x^+(u)}{\mathrm{d}u} = G(x^+(u), u) \quad \text{with} \quad x^+(0) = x^+ \tag{2.6b}$$

with $x := x(k) \in \mathcal{X}$, $x^+(0) = x^+ \in \mathcal{X}$ and $u := u(k) \in \mathcal{U} \subseteq \mathbb{R}$ for all $k \in \mathbb{N}$.

$F_0(\cdot)$ is a smooth map characterizing the free evolution of the dynamics (2.1a) and $G(\cdot, u)$ is a smooth map defining the forced component as $x^+(u)$ represents a curve in $\mathcal{X}$ parameterized by u. Hence, $x^+(u(k)) := x(k+1)$ represents the one-step ahead controlled evolution as $x^+(0) = x^+ := F(x(k), 0)$ defines the one-step ahead free evolution with jumps under the drift $F_0(\cdot)$ at any instant $k \in \mathbb{N}$.

As a matter of fact, a nonlinear difference equation of the map form (2.1a) can be recovered by integrating (2.6b) between 0 and $u(k)$ for the initial condition $x^+(0)$ computed from (2.37a) setting $x^+ = x^+(0) := F_0(x(k))$. One obtains (2.1a) in its integral form

$$\begin{aligned} x(k+1) :&= F(x(k), u(k)) \\ &= x^+(u(k)) = x^+(0) + \int_0^{u(k)} G(x^+(v), v)\, \mathrm{d}v \end{aligned}$$

with $F(x(k), u(k))$ given in (2.1a) and such that $F(\cdot, 0) = F_0(\cdot)$. For the sake of notation, for systems in their difference and differential representation, the time arguments will be dropped out and the integral form is referred as

$$x^+(u) = x^+(0) + \int_0^u G(x^+(v), v)\ \mathrm{d}v. \tag{2.7}$$

Remark 2.1.3. Under invertibility assumption on $F(x, 0)$, the discrete-time evolution affected by the control has a unique analytic controlled map $G(\cdot, u)$ which satisfies the differential condition, for u sufficiently small,

$$G(x, u) := \frac{\partial F}{\partial u}(x, u)\bigg|_{x=F^{-1}(x,u)}, \tag{2.8}$$

that can be assumed in its expansions in powers of u around $u = 0$, namely

$$G(\cdot, u) = G_1(\cdot) + \sum_{i\geq 1} \frac{u^i}{i!} G_{i+1}(\cdot), \tag{2.9}$$

with $G_i(\cdot)$ vector fields defined from $\mathcal{X}$ to $\mathcal{X}$ characterizing the series for all $i > 0$. The existence of $\bar{u} \in \mathcal{U}$ such that $F(x, \bar{u})$ is invertible suffices to prove that any dynamics in the form of a map admits a DDR, so providing a perfect equivalence between the standard representation and the DDR form, see Monaco and Normand-Cyrot (1995) for details.

Remark 2.1.4. The invertibility assumption upon the drift term $F(x, 0)$ can be weakened by requiring submersivity of $F(x, u)$, see Monaco and Normand-Cyrot (1998); Monaco et al. (2007) for further detail.

A nice property arising from the DDR form is that it allows to split the evolutions of any smooth mapping evolving in $\mathbb{R}$ along the discrete time dynamics $x^+(u)$ as the contribution of the free and forced components. Accordingly, the following proposition is given and recalled from Monaco and Normand-Cyrot (1998).

Proposition 2.1.1. *Given any smooth mapping $\lambda : \mathcal{X} \to \mathbb{R}$ associated with the discrete-time dynamics in DDR* (2.6)*, then along the integral form*

$$x^+(u) = x^+(0) + \int_0^u G(x^+(v), v)\ \mathrm{d}v \tag{2.10}$$

the mapping $\lambda(\cdot)$ *verifies*

$$\lambda(x^+(u)) = \lambda(x^+(0)) + \int_0^u \mathrm{L}_{G(.,v)}\lambda(x^+(v))\mathrm{d}v. \tag{2.11}$$

2.2 Passivity in discrete time

In the following notions of passivity and dissipativity are recalled in discrete time. For further detail see, Byrnes and Lin (1994); Lin and Byrnes (1995); Monaco and Normand-Cyrot (1999); Navarro-López et al. (2002); Laila and NešIć (2003); Monaco and Normand-Cyrot (2011).

Definition 2.2.1 (Dissipativity)**.** Assume that associated with the system (2.1) is a function $\omega : \mathcal{U} \times \mathcal{Y} \to \mathbb{R}$, called *supplied rate*, which is locally absolutely summable for every $u \in \mathcal{U}$, that is, it satisfies

$$\sum_{k=k_0}^{k_1} |\omega(u(k), y(k))| < \infty, \quad \text{for all } k_0 \leq k_1.$$

Let $\mathcal{X}$ be a connected subset of $\mathbb{R}^n$ containing the equilibrium point $x_\star$. The system (1.1) is said *dissipative* in $\mathcal{X}$ with supply rate $\omega(u, y)$ if there exists a smooth nonnegative function $S : \mathcal{X} \to \mathbb{R}_{\geq 0}$, $S(x_\star) = 0$ (the storage function), such that

$$S(x(T)) - S(x(0)) \leq \sum_{k=0}^{T} \omega(u(k), y(k)) \tag{2.12}$$

for all $u \in \mathcal{U}$ and $T \geq 0$ such that $x(k) \in \mathcal{X}$ for all $0 \leq k \leq T$ with $k \in \mathbb{N}$.

Definition 2.2.2 (Passivity)**.** The system (2.1) is said *passive* if it is dissipative with supply rate

$$\omega(u(k), y(k)) = u^\top(k)y(k).$$

Again, one computes from the summation version (2.12) its infinitesimal dissipation inequality, between two time steps,

$$S(x(k+1)) - S(x(k)) \leq u^\top(k)y(k), \tag{2.13}$$

along all solutions $x(k)$ with respect to the input function $u(k)$.

Definition 2.2.3 (Lossless)**.** The system (2.1) is said *lossless* with supply rate $\omega(u(k), y(k))$ if there exists a storage function $S(x)$, such that for all $x \in \mathcal{X}$ and $u \in \mathcal{U}$

$$S(x(k+1)) - S(x(k)) = u^\top(k)y(k). \tag{2.14}$$

Moreover, it is said *conservative* if it is lossless and for zero input $u = 0$ the supply rate verifies $\omega(0, y(k)) = 0$.

Remark 2.2.1. Due to (2.13) (respectively (2.14)) a passive system (respectively lossless) with a positive definite storage function $S(x)$ is Lyapunov stable in the sense of Theorem 2.1.1, meaning that the storage function $S(x)$ is nonincreasing also along trajectories for which the output is $y(k) \equiv 0$.

The passivity condition discussed above seems to be a direct discrete-time counterpart of the continuous-time case, but it is interesting to note that unlike the continuous-time condition in the discrete-time case the condition requires that the output not only is a function of the state but that it is also dependent on the control variable u. This is treated in the general linear case below.

Example 2.2.1. Consider the linear discrete-time system

$$\begin{aligned} x(k+1) &= Ax(k) + Bu(k) \\ y(k) &= Cx(k) \end{aligned}$$

with A having eigenvalues into the unit circle, and assume a storage function $S(x) = \frac{1}{2}x^\top Px$ with $P \succeq 0$. Then, from the passivity condition (2.13) the following inequality must be satisfied

$$\begin{aligned} &S(x(k+1)) - S(x(k)) = \frac{1}{2}\left(x(k+1)\right)^\top P\left(x(k+1)\right) - \frac{1}{2}x^\top(k)Px(k) \leq u^\top(k)y(k). \\ &= \frac{1}{2}x^\top(k)\left(A^\top PA - P\right)x(k) + u^\top(k)B^\top PAx(k) + \frac{1}{2}u^\top(k)B^\top PBu(k) \leq u^\top(k)Cx(k) \end{aligned}$$

It is easy to note that the inequality above, due to the eigenvalues of A reduces to

$$u^\top(k)\left(B^\top PA - C\right)x(k) + \frac{1}{2}u^\top(k)B^\top PBu(k) \leq 0$$

saying that the passivity condition is not satisfied for all $x(k)$ and $u(k)$ due to the positive quadratic term

$$\frac{1}{2}u^\top(k)B^\top PBu(k) \geq 0.$$

We will see in the forthcoming section that a different definition of passivity in discrete-time may prevent this issue arising form the output $y(k) = Cx(k)$.

2.2.1 The u-average passivity

The concept of average passivity has been introduced in Monaco and Normand-Cyrot (2011) to weaken the necessity of a throughput, that is unavoidable to well pose the concept in discrete time.

To begin with it is necessary to define the so-called u-average output associated with a discrete time system.

Definition 2.2.4 (u-average output)**.** Given the system

$$x^+ = F_0(x) \tag{2.16a}$$

$$\frac{\partial x^+(u)}{\partial u} = G(x^+(u), u) \quad \text{with} \quad x^+(0) = x^+ \tag{2.16b}$$

$$y = h(x) \tag{2.16c}$$

with output map $h(x) : \mathcal{X} \to \mathcal{Y}$ then for any $(x, u) \in \mathcal{X} \times \mathcal{U}$ the mapping $h_{\text{av}}(x, u)$ denotes the *u-average output* defined as

$$h_{\text{av}}(x, u) := \frac{1}{u}\int_0^u h(x^+(v))\mathrm{d}v \tag{2.17}$$

with $h_{\text{av}}(x, 0) := h(x^+(0), 0)$ and $x^+(0) = F_0(x) := F(x, 0)$.

At this point, it is possible to introduce the concept of u-average passivity.

Definition 2.2.5 (u-average passivity)**.** The system (2.16) is *u-average passive* if there exists a smooth nonnegative function $S : \mathcal{X} \to \mathbb{R}_{\geq 0}$ such that for all $(x, u) \in \mathcal{X} \times \mathcal{U}$

$$S(x^+(u)) - S(x) \leq \int_0^u h(x^+(v), v)\mathrm{d}v = uh_{\text{av}}(x, u). \tag{2.18}$$

Definition 2.2.6 (u-average lossless)**.** The system (2.16) is *u-average lossless* if there exists a smooth nonnegative function $S : \mathcal{X} \to \mathbb{R}_{\geq 0}$ such that for all $(x, u) \in \mathcal{X} \times \mathcal{U}$

$$S(x^+(u)) - S(x) = \int_0^u h(x^+(v))\mathrm{d}v = uh_{\mathrm{av}}(x, u). \tag{2.19}$$

Remark 2.2.2. In this respect, it is worth mentioning that u-average passivity (respectively, u-average lossless) of the discrete-time system (2.16) with respect to the given output function $h(x)$ coincides with the passivity given in (2.13) (respectively, lossless) with respect to the u-average output mapping $h_{\mathrm{av}}(x, u)$ (that properly depends on u by construction).

Remark 2.2.3. A necessary condition to achieve u-average passivity with respect to the output function $h(x)$ is that $\mathrm{L}_{G(.,0)}h(x^+(0)) \neq 0$, (identically, relative degree 0 of the output map $h_{\mathrm{av}}(x, u)$).

We have seen in continuous time that a system to be passive has to meet KYP properties, as given in Theorem 1.2.1, which are necessary and sufficient conditions. In this discrete-time context, KYP properties have not been established for general discrete-time system of the form (2.1), and only partial results have been proposed in the literature. In particular, some conditions are performed requiring quadraticity in the control variable u, see Byrnes and Lin (1993); Lin and Byrnes (1995); Monaco and Normand-Cyrot (1999, 1997a, 2011); Navarro-López and Fossas-Colet (2004).

The following proposition defines an alternative output map for which u-average passivity (respectively, passivity) is achieved. The result is recalled from Monaco and Normand-Cyrot (2011) and its proof is given as it is instrumental to developments presented throughout the manuscript.

Proposition 2.2.1. *If the system* (2.16) *is u-average passive with respect to the output map* (2.16c) *and a smooth nonnegative function $S : \mathcal{X} \to \mathbb{R}_{\geq 0}$, then it is also u-average passive with respect to the output map*

$$Y(x, u) = \mathrm{L}_{G(.,u)}S(x) \tag{2.20}$$

and respectively passive with respect to the u-average output map

$$Y_{av}(x, u) = \frac{1}{u}\int_0^u \mathrm{L}_{G(.,v)}S(x^+(v))\mathrm{d}v. \tag{2.21}$$

Proof. By the assumption of u-average passivity of the system (2.16), it verifies the inequality

$$S(x^+(u)) - S(x) \leq \int_0^u h(x^+(v))\mathrm{d}v.$$

for all $(x, u) \in \mathcal{X} \times \mathcal{U}$, meaning that also for $u = 0$ the equality above is satisfied, which yields $S(x^+(0)) - S(x) \leq 0$. Thus, exploiting the integral expression (2.11), one gets that

$$\begin{aligned} S(x^+(u)) - S(x) &= S(x^+(0)) - S(x) + S(x^+(u)) - S(x^+(0)) \\ &\leq \int_0^u \mathrm{L}_{G(.,v)} S(x^+(v))\mathrm{d}v \leq \int_0^u h(x^+(v))\mathrm{d}v. \end{aligned}$$

Finally, from the inequality above one achieves

$$\begin{aligned} S(x^+(u)) - S(x) &\leq \int_0^u \mathrm{L}_{G(.,v)} S(x^+(v))\mathrm{d}v \\ &= \int_0^u Y(x^+(v), u)\mathrm{d}v = uY_{\mathrm{av}}(x, u) \end{aligned}$$

so concluding the proof. □

The following lemma provides an equivalent representation of the u-average output in terms of the discrete gradient function, which will be essential for properly defining port-Hamiltonian systems in discrete time given in Part II.

Lemma 2.2.1. *The u-average output map*

$$Y_{av}(x, u) = \frac{1}{u} \int_0^u \mathrm{L}_{G(.,v)} S(x^+(v))\mathrm{d}v \tag{2.22}$$

associated with the system (2.16) *rewrites in terms of discrete gradient as follows*

$$Y_{av}(x, u) = g^\top(x, u)\bar{\nabla} S\big|_{x^+}^{x^+(u)} \tag{2.23}$$

with

$$g(x, u) := \frac{1}{u} \int_0^u G(x^+(v), v)\mathrm{d}v.$$

Proof. The proof is simply performed exploiting the definition of the discrete gradient function in Definition 2.1.1. Since the u-average output (2.22) arises from the variation

$$S(x^+(u)) - S(x^+) = \int_0^u \mathrm{L}_{G(.,v)} S(x^+(v))\mathrm{d}v = uY_{\mathrm{av}}(x,u),$$

then by definition of discrete gradient and by the integral form (2.7) of the system (2.16) one gets that

$$\begin{aligned} S(x^+(u)) - S(x^+) &= (x^+(u) - x^+)^\top \bar{\nabla} S\big|_{x^+}^{x^+(u)} \\ &= \left(\int_0^u G(x^+(v), v)\mathrm{d}v\right)^\top \bar{\nabla} S\big|_{x^+}^{x^+(u)} \\ &= u\left(\frac{1}{u}\int_0^u G(x^+(v), v)\mathrm{d}v\right)^\top \bar{\nabla} S\big|_{x^+}^{x^+(u)} \\ &= ug^\top(x,u)\bar{\nabla} S\big|_{x^+}^{x^+(u)} = uY_{\mathrm{av}}(x,u) \end{aligned}$$

thus the result. □

To complete the notions related to the u-average passivity concept, the definition of u-average passivity from some nominal control value $\bar{u}$ is recalled. It has been introduced in Mattioni et al. (2019) to deal with incremental-like passivity properties in discrete time. From the u-average passivity inequality one can pick a nominal value $\bar{u}$ for which the inequality rewrites as

$$\begin{aligned} S(x^+(u)) - S(x) &= S(x^+(u)) - S(x^+(\bar{u})) + S(x^+(\bar{u})) - S(x) \\ &= S(x^+(\bar{u})) - S(x) + \int_{\bar{u}}^u \mathrm{L}_{G(.,v)} S(x^+(v))\mathrm{d}v \leq \int_{\bar{u}}^u h(x^+(v), v)\mathrm{d}v. \end{aligned}$$

The inequality above leads to the u-average passivity from $\bar{u}$ property which is formally given below.

Definition 2.2.7 (u-average passivity from $\bar{u}$)**.** The system (2.16) is *u-average passive from $\bar{u}$*, with $\bar{u} \in \mathcal{U} \subseteq \mathbb{R}$ if there exists a storage function $S(\cdot) : \mathcal{X} \to \mathbb{R}_{\geq 0}$ such that, for all $(x,u) \in \mathcal{X} \times \mathcal{U}$,

$$S(x^+(u)) - S(x) \leq (u - \bar{u}) h_{\mathrm{av}}(\bar{u})(x,u) \tag{2.24}$$

with u-average output from $\bar{u}$ of the form

$$h_{\mathrm{av}}(\bar{u})(x,u) = \frac{1}{u - \bar{u}} \int_{\bar{u}}^u h(x^+(v), v)\mathrm{d}v.$$

2.2.2 Passivity-based control

The u-average passivity notion is profitably used to achieve asymptotic stabilization of the origin of a u-average passive system by injecting its u-average output. The following result recall the negative u-average output feedback proposed in Monaco and Normand-Cyrot (2011).

Theorem 2.2.1. *Let the discrete-time system*

$$x^+ = F_0(x) \tag{2.25a}$$

$$\frac{\partial x^+(u)}{\partial u} = G(x^+(u), u) \quad \textit{with} \quad x^+(0) = x^+ \tag{2.25b}$$

$$y = h(x) \tag{2.25c}$$

be u-average passive with storage function $S(\cdot) : \mathcal{X} \to \mathbb{R}_{\geq 0}$ with $S(0) = 0$ and ZSD, then any feedback $u = \gamma(x)$ solving the algebraic equation

$$u + \kappa h_{av}(x, u) = 0 \tag{2.26}$$

with positive gain $\kappa > 0$ achieves asymptotic stabilization of the origin.

2.2.3 Constructive approximate solutions

A solution to the algebraic equation (2.26) is generally difficult to characterize as it is nonlinear in the control variable u. However, an approximate solution can be computed by truncating the u-average output

$$h_{\text{av}}(x, u) = h(\cdot)|_{F_0(x)} + \frac{u}{2}\mathrm{L}_{G(\cdot,0)}h(\cdot)|_{F_0(x)} + O(u^2) \tag{2.27}$$

which can be substituted in (2.26) to get the algebraic equation $\Gamma(x, u) = 0$ with

$$\Gamma(x, u) = u + \kappa(h(\cdot)|_{F_0(x)} + \frac{u}{2}\mathrm{L}_{G(\cdot,0)}h(\cdot)|_{F_0(x)}) + O(u^2).$$

Accordingly one gets the corollary below.

Corollary 2.2.1. *Let the system (2.25) be u-average passive with storage function $S(\cdot) : \mathcal{X} \to \mathbb{R}_{\geq 0}$ with $S(0) = 0$ and ZSD. Then the feedback*

$$u = -z(x)h(F_0(x)) \tag{2.28}$$

with suitably chosen

$$z(x) = \left.\frac{\kappa}{1 + \frac{\kappa}{2}\mathrm{L}_{G(\cdot,0)}h(\cdot)}\right|_{F_0(x)}, \qquad \kappa > 0, \tag{2.29}$$

and $\frac{\kappa}{2}\mathrm{L}_{G(\cdot,0)}h(\cdot)|_{F_0(x)} \neq -1$*, achieves local asymptotic stabilization of the origin.*

2.3 Linear-time invariant case

In this section the discussion performed for the general nonlinear discrete-time systems is specialized in the linear time invariant case.

Given a linear-time invariant system defined on $\mathcal{X}$

$$x(k+1) = Ax(k) + Bu(k) \tag{2.30a}$$
$$y(k) = Cx(k) \tag{2.30b}$$

with matrices (A, B, C) of appropriate dimensions and $u := u(k) \in \mathcal{U} \subseteq \mathbb{R}$, it follows that in DDR form the dynamics (2.30a) is expressed by the couple of difference and differential equations

$$x^+ = Ax \tag{2.31a}$$
$$\frac{\partial x^+(u)}{\partial u} = B \tag{2.31b}$$
$$y = h(x) = Cx. \tag{2.31c}$$

Integrating the differential equation (2.31b) from 0 to $u(k)$ with initial conditions $x^+ = x^+(0)$ given in (2.31a) one recovers the dynamics (2.30a), namely

$$x(k+1) := x^+(u(k)) = Ax(k) + \int_0^{u(k)} B \, \mathrm{d}v = Ax(k) + Bu(k).$$

The u-average passivity property in the LTI case arises with a special structure of the u-average output associated with the system. Notably, the LTI system (2.31) is *u-average passive* with respect to the output map (2.31c) and storage function $S(\cdot) : \mathcal{X} \to \mathbb{R}_{\geq 0}$ with $S(0) = 0$ if for all $(x, u) \in \mathcal{X} \times \mathcal{U}$ the inequality is satisfied

$$S(x^+(u)) - S(x) \leq uh_{\mathrm{av}}(x, u)$$

with u-average output mapping $h_{\rm av}(x,u)$ of the form

$$h_{\rm av}(x,u)=\frac{1}{u}\int_0^u Cx^+(v)\,\mathrm{d}v=CAx+\frac{1}{2}CBu.$$

In this linear case, Proposition 2.2.1 is specified below with respect to the quadratic storage function $S(x)=\frac{1}{2}x^\top Px$ with symmetric matrix $P=P^\top\succ 0$.

Proposition 2.3.1. *If the LTI system* (2.31) *is u-average passive with respect to the output map* (2.31c) *and a quadratic storage function $S(x)=\frac{1}{2}x^\top Px$ with symmetric matrix $P=P^\top\succ 0$, then it will be also u-average passive with respect to the output map*

$$Y(x)=B^\top Px \tag{2.32}$$

and respectively passive with respect to the u-average output map

$$Y_{av}(x,u)=B^\top PAx+\frac{1}{2}B^\top PBu. \tag{2.33}$$

Remark 2.3.1. Due to Lemma 2.2.1, the u-average output (2.33) is rewritten in terms of the discrete gradient function. Namely, in this linear case it takes the form

$$\begin{aligned}Y_{\rm av}(x,u)&=B^\top\bar{\nabla}S\big|_{x^+}^{x^+(u)}\\&=\frac{1}{2}B^\top P(x^+(u)+x^+)\\&=B^\top PAx+\frac{1}{2}B^\top PBu.\end{aligned}$$

As seen for general nonlinear discrete-time systems, the u-average passivity notion can be profitably used for providing asymptotic stabilization. In this respect one may notice that, due to the special structure of the u-average output related to the LTI system, the implicit equality (2.26) specializes as

$$u+\kappa(CAx+\frac{1}{2}CBu)=0, \tag{2.34}$$

so reducing a first-order algebraic equation. Thus, the following theorem specializes the result in Theorem 2.2.1 to the LTI case showing that the stabilization properties hold globally.

Theorem 2.3.1. *Let the discrete-time system*

$$x^+ = Ax \tag{2.35a}$$

$$\frac{\partial x^+(u)}{\partial u} = B \quad with \quad x^+(0) = x^+ \tag{2.35b}$$

$$y = h(x) = Cx \tag{2.35c}$$

be ZSD and u-average passive with storage function $S(x) = \frac{1}{2}x^\top Px$ *with* $P = P^\top \succ 0$, *then the feedback*

$$u = -\frac{\kappa CA}{1 + \frac{\kappa}{2}CB}x \tag{2.36}$$

with positive gain $\kappa > 0$ *and* $\frac{\kappa}{2}CB \neq -1$ *achieves global asymptotic stabilization of the origin.*

2.4 Interconnection of u-average passive systems

In this section we discuss the interconnection of u-average passive systems in discrete time. We have seen that in continuous-time the passivity property is preserved under parallel and feedback interconnection. In this respect, it is desirable to preserve basic passivity property under power-preserving interconnection. How to define power preserving interconnection in discrete time? Is the u-average passivity property preserved under interconnection? In this section we give answers to these questions.

According to the discrete-time model given in the difference and differential representation (2.6), let two discrete-time systems $\Sigma_i(h_i)$, for $i = 1, 2$, of the form

$$x_i^+ = F_0(x) \tag{2.37a}$$

$$\frac{\partial x_i^+(u_i)}{\partial u_i} = G_i(x_i^+(u_i), u_i) \quad \text{with} \quad x_i^+(0) = x_i^+ \tag{2.37b}$$

$$y_i = h_i(x_i) \tag{2.37c}$$

with associated output maps $h_i(\cdot) : \mathbb{R}^n \to \mathbb{R}$ be passive with respect to the u-average outputs

$$h_{i\text{av}}(x_i, u_i) = \frac{1}{u_i}\int_0^{u_i} h_i(x_i^+(w))\mathrm{d}w$$

and storage functions $S_i : \mathbb{R}^n \to \mathbb{R}_{\geq 0}$, and respectively u-average passive with respect to the output maps $h_i(x_i)$ in (2.37c). For the sake of compactness, we denote $x = \mathrm{col}(x_1, x_2)$.

In what follows, given two discrete-time dynamics of the form (2.37), we investigate the average passivity properties arising when an output-to-input connection is established through an interconnecting pattern between the inputs and the associated outputs. Precisely, we investigate connections in terms of a power-preserving interconnection ensuring no loss of energy throughout the interconnection process (lossless interconnection). The following definition is proposed.

Definition 2.4.1: u-average power-preserving interconnection

The interconnection between $\Sigma_1(h_1)$ and $\Sigma_2(h_2)$ given in (2.37) for $i = 1, 2$ is said *power preserving* if the pair (u_1, u_2) satisfies

$$\int_0^{u_1} h_1(x_1^+(w))\, dw + \int_0^{u_2} h_2(x_2^+(w))\, dw = 0. \tag{2.38}$$

The integral form (2.38) can be rewritten in terms of u-average outputs, namely

$$u_1 h_{1\mathrm{av}}(x_1, u_1) + u_2 h_{2\mathrm{av}}(x_2, u_2) = 0, \tag{2.39}$$

so emphasizing that the power-preserving interconnection involves precisely the u-average outputs of the two systems. Then, among these power preserving interconnections, the simplest solution to (2.39) is obtained by setting

$$\begin{pmatrix} u_1 \\ u_2 \end{pmatrix} = \begin{pmatrix} 0 & -1 \\ 1 & 0 \end{pmatrix} \begin{pmatrix} h_{1\mathrm{av}}(x_1, u_1) \\ h_{2\mathrm{av}}(x_2, u_2) \end{pmatrix}. \tag{2.40}$$

An immediate comment is that such connection is implicitly defined so setting the problem of its solution. Again, the existence of a solution is guaranteed by the Implicit Function Theorem. This is specified later in Section 2.4.3.

2.4.1 The parallel interconnection

Let us study the average passivity properties of the simple parallel interconnection of (2.37) for $i = 1, 2$ when setting

$$u = u_1 = u_2 \tag{2.41a}$$

$$h(x) = h_1(x_1) + h_2(x_2). \tag{2.41b}$$

Proposition 2.4.1 (u-average parallel interconnection)**.** *Consider the parallel interconnection of two u-average passive systems of the form (2.37), then the resulting system*

$$x_1^+(u) = F_1(x_1, u) \tag{2.42a}$$

$$x_2^+(u) = F_2(x_2, u) \tag{2.42b}$$

with output $h(x) := h_1(x_1) + h_2(x_2)$ is u-average passive with storage function $S(x) = S_1(x_1) + S_2(x_2)$.

Proof. Because each subsystem $\Sigma_i(h_i)$ in (2.37) ($i = 1, 2$) u-average passive, one gets the forward difference inequality

$$S(x^+(u)) - S(x) \leq \int_0^{u_1} h_1(x_1^+(w))\mathrm{d}w + \int_0^{u_2} h_2(x_2^+(w))\mathrm{d}w.$$

Due to the interconnection $u = u_1 = u_2$ one gets

$$\begin{aligned} S(x^+(u)) - S(x) &\leq \int_0^u \left(h_1(x_1^+(w)) + h_2(x_2^+(w))\right) \mathrm{d}w \\ &= \int_0^u h(x^+(v))\mathrm{d}v = u h_{\mathrm{av}}(x, u) \end{aligned}$$

and thus the result. □

The above result shows that, when considering the parallel interconnection of u-average passive systems (2.37), passivity in the u-average sense is preserved with respect to the natural output induced by the sum of the single ones. It is worth to note that the resulting u-average output, in this case, is also equal to the sum of the averaged outputs associated with (2.37) when setting $u = u_i$ for $i = 1, 2$.

2.4.2 Feedback interconnection

Let us now consider a suitable feedback interconnection of (2.37) enhancing u-average passivity of the resulting system. To this end, let us consider the input

$$u = \bar{u} + v. \tag{2.43}$$

with $u = \mathrm{col}(u_1, u_2)$ composed by two terms: $v = \mathrm{col}(v_1, v_2)$ is the external inputs; $\bar{u} = \mathrm{col}(u_1, u_2)$ is the power-preserving feedback computed as the solution to the power-preserving interconnection (2.38) (equivalently, (2.39)) in Definition 2.4.1. Namely $\bar{u} = \mathrm{col}(u_1, u_2)$ verifies

$$\bar{u}_1 h_{1\mathrm{av}}(x_1, \bar{u}_1) + \bar{u}_2 h_{2\mathrm{av}}(x_2, \bar{u}_2) = 0,$$

The following theorem can be thus proved.

Theorem 2.4.1: u-average feedback interconnection

Let, for $i = 1, 2$, the systems $\Sigma_i(h_i)$ be u-average passive with storage functions $S_i : \mathbb{R}^n \to \mathbb{R}_{\geq 0}$. Consider the input (2.43) with $\bar{u} = u(x)$ being the power-preserving interconnection (2.38). Then, the interconnected system

$$x_1^+(\bar{u}_1(x) + v_1) = F_1(x_1, \bar{u}_1(x) + v_1) \tag{2.44a}$$
$$x_2^+(\bar{u}_2(x) + v_2) = F_2(x_2, \bar{u}_2(x) + v_2) \tag{2.44b}$$

with output $y = (h_1(x_1), h_2(x_2))^\top$ is v-average passive from $\bar{u}$ with storage function $S_c(x) := S_1(x_1) + S_2(x_2)$. Namely, the dissipation inequality

$$S_c(x^+(u)) - S_c(x) \leq v^\top h(\bar{u})(x, \bar{u} + v) \tag{2.45}$$

holds with v-average output

$$h_{\mathrm{av}}(\bar{u})(x, \bar{u} + v) = \begin{pmatrix} \frac{1}{v_1} \int_0^{v_1} h_1(x_1^+(\bar{u}_1 + \ell))\mathrm{d}\ell \\ \frac{1}{v_2} \int_0^{v_2} h_2(x_2^+(\bar{u}_2 + \ell))\mathrm{d}\ell \end{pmatrix}. \tag{2.46}$$

Proof. Under $\bar{u}$, that is the internal state power-preserving interconnection solution to (2.39), one has

$$\int_0^{\bar{u}_1} h_1(x_1^+(w))\mathrm{d}w + \int_0^{\bar{u}_2} h_2(x_2^+(w))\mathrm{d}w = 0.$$

Accordingly, by computing the forward difference $S_c(x^+(u)) - S_c(x)$ and exploiting u-average passivity of (2.37) and because of the power-preserving condition (2.38), one gets

$$\begin{aligned} S_c(x^+(u)) - S_c(x) &= S_c(x^+(u)) - S_c(x^+(\bar{u})) + S_c(x^+(\bar{u})) - S_c(x) \\ &\leq \int_0^{u_1} h_1(x_1^+(w))\mathrm{d}w + \int_0^{u_2} h_2(x_2^+(w))\mathrm{d}w \\ &= \int_0^{\bar{u}_1} h_1(x_1^+(w))\mathrm{d}w + \int_0^{\bar{u}_2} h_2(x_2^+(w))\mathrm{d}w + \int_{\bar{u}_1}^{u_1} h_1(x_1^+(w))\mathrm{d}w \\ &+ \int_{\bar{u}_2}^{u_2} h_2(x_2^+(w))\mathrm{d}w = \int_{\bar{u}_1}^{u_1} h_1(x_1^+(w))\mathrm{d}w + \int_{\bar{u}_2}^{u_2} h_2(x_2^+(w))\mathrm{d}w \end{aligned}$$

verifying the dissipativity inequality

$$S_c(x^+(u)) - S(x) \leq (u - \bar{u})^\top h_{c,\bar{u}}^{av}(x, u) \tag{2.47}$$

with

$$h_{\mathrm{av}}(\bar{u})(x, u) = \begin{pmatrix} \frac{1}{u_1 - \bar{u}_1} \int_{\bar{u}_1}^{u_1} h_1(x_1^+(w))\mathrm{d}w \\ \frac{1}{u_2 - \bar{u}_2} \int_{\bar{u}_2}^{u_2} h_2(x_2^+(w))\mathrm{d}w \end{pmatrix}. \tag{2.48}$$

Thus, u-average passivity of (2.44) from (2.38) holds. Thus, by plugging the input (2.43) into the dissipation inequality (2.47) one gets

$$\begin{aligned} S_c(x^+(u)) - S_c(x) &\leq \int_{\bar{u}_1}^{u_1} h_1(x_1^+(w))\mathrm{d}w + \int_{\bar{u}_2}^{u_2} h_2(x_2^+(w))\mathrm{d}w \\ &= \int_0^{v_1} h_1(x_1^+(\bar{u}_1 + \ell))\mathrm{d}\ell + \int_0^{v_2} h_2(x_2^+(\bar{u}_2 + \ell))\mathrm{d}\ell \\ &= v^\top h_{\mathrm{av}}(\bar{u})(x, \bar{u} + v) \end{aligned}$$

so getting the result (2.53) with v-average output (2.46). □

Theorem 2.4.1 provides that the feedback interconnection between two u-average passive systems yields a passive system with respect to the v-average output from $\bar{u}$ in (2.46), i.e. $h_{\mathrm{av}}(\bar{u})(x, \bar{u} + v)$, and respectively it provides u-average passivity

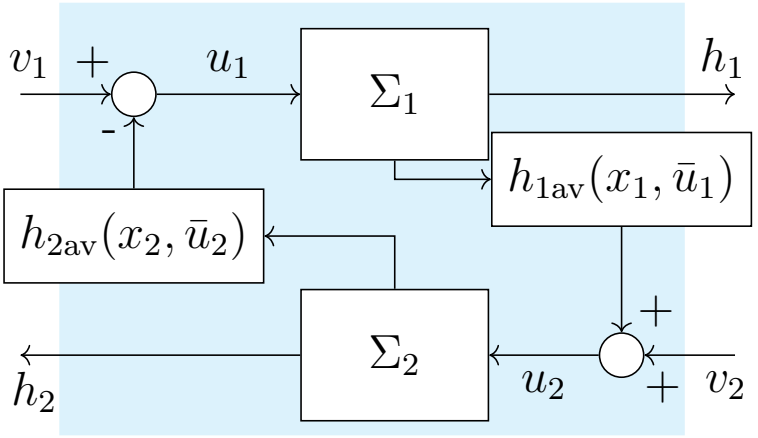

Figure 2.1: Power-preserving feedback interconnection between $\Sigma_1(h_1)$ and $\Sigma_2(h_2)$ via average outputs with external v.

from $\bar{u}$ with respect to the natural output $h(x) := \mathrm{col}(h_1(x_1), h_2(x_2))$. In particular, as it is clear from (2.53), under an external source v and for a fixed $\bar{u}$ in (2.38), the average outputs are defined starting from the same outputs of the single systems (2.37) but averaged over the new interconnected dynamics (2.44) deduced from (2.43). Thus, starting from average passivity of the single systems (2.37) with outputs $h_i(x_i)$, the interconnected system is u-average passive under the power preserving stated feedback $\bar{u} = \bar{u}(x)$ solving (2.38).

Remark 2.4.1. The input (2.43) is composed as the sum of two terms: the exogenous signal v and an interconnecting feedback $\bar{u} = \bar{u}(x)$ defining the pattern as the solution to (2.38). This latter term is a power preserving state feedback computed over the averaged outputs $h_{i\mathrm{av}}(x_i, u_i)$ when setting the exogenous signal in (2.43) $v_i = 0$ (that is $u = \bar{u}$). Such an interconnection $u = \bar{u} + v$ is not realized through the direct input/averaged-output ports hat should be obtained when computing the feedback $u = u(x, v)$ solution to

$$\begin{pmatrix} u_1 \\ u_2 \end{pmatrix} = \begin{pmatrix} 0 & -1 \\ 1 & 0 \end{pmatrix} \begin{pmatrix} h_{i\mathrm{av}}(x_1, u_1) \\ h_{2\mathrm{av}}(x_2, u_2) \end{pmatrix} + v. \tag{2.49}$$

2.4.3 Computational aspects

The power preserving interconnecting feedback (2.38) is defined as the implicit solution of a nonlinear equality induced by the averaged outputs. Although exact computations are tough to be carried out in general, an approximate solution to (2.38) does exist (at least locally) as specified in the following proposition. To this end, assume, without loss of generality that for $i = 1, 2$, (2.37) possesses an equilibrium at the origin. For the sake of facility, let us assume the interconnecting pattern be defined by (2.40). Thus, the following result holds true.

Proposition 2.4.2. *Consider, for $i = 1, 2$, the discrete-time systems $\Sigma_i(h_i)$ in (2.37) with equilibrium at $x = 0$ and being u-average passive. Consider the interconnection (2.40). Then, for all x in a neighborhood of the origin, the power-preserving feedback*

$$\begin{pmatrix} \bar{u}_1 \\ \bar{u}_2 \end{pmatrix} = \begin{pmatrix} 0 & -1 \\ 1 & 0 \end{pmatrix} \begin{pmatrix} h_{1av}(x_1, \bar{u}_1) \\ h_{2av}(x_2, \bar{u}_2) \end{pmatrix} \tag{2.50}$$

locally admits a solution $\bar{u}_a = \bar{u}_a(x)$ verifying $\bar{u}(0) = 0$. Thus, the interconnected system (2.44) is locally passive when setting $u = \bar{u}_a(x) + v$ with

$$\bar{u}_a(x) = \Psi^{-1}(x) \begin{pmatrix} -h_2(F_2(x_2, 0)) \\ h_1(F_1(x_1, 0)) \end{pmatrix}.$$

and

$$\Psi(x) := \begin{pmatrix} 1 & \mathrm{L}_{G_2(\cdot,0)} h_2(F_2(x_2, 0)) \\ -\mathrm{L}_{G_1(\cdot,0)} h_1(F_1(x_1, 0)) & 1 \end{pmatrix}$$

Proof. First, consider the expansion of the average outputs associated with $h_i(x_i)$ as given, for $i = 1, 2$, as

$$h_{i\mathrm{av}}(x_i, u_i) = h_i(F_i(x_i, 0)) + u_i \mathrm{L}_{G_i} h_i(F_i(x_i, 0)) + O(u_i^2),$$

where $O(u_i^2)$ contains all the remaining terms of a higher order of the control variable u_i. By substituting such an expansion in the implicit equality (2.50) one gets

$$\begin{aligned} \bar{u}_1 &= -h_2(F_2(x_2, 0)) + \bar{u}_2 \mathrm{L}_{G_2} h_2(F_2(x_2, 0)) + O(u_2^2) \\ \bar{u}_2 &= h_1(F_1(x_1, 0)) + \bar{u}_1 \mathrm{L}_{G_1} h_1(F_1(x_1, 0)) + O(u_1^2) \end{aligned}$$

Form the equations above one sets the operator

$$\Gamma(x,u) = \begin{pmatrix} \bar{u}_1 + h_2(F_2(x_2,0)) + \bar{u}_2 \mathrm{L}_{G_2} h_2(F_2(x_2,0)) + O(u_2^2) \\ \bar{u}_2 - h_1(F_1(x_1,0)) + \bar{u}_1 \mathrm{L}_{G_1} h_1(F_1(x_1,0)) + O(u_1^2) \end{pmatrix}$$

By invoking the implicit function theorem, for all x in the neighborhood of the origin,

$$\Big| \frac{\partial \Gamma(x,u)}{\partial u} \Big|_{u=0} = \Big| \Psi(x) \Big| \neq 0$$

with

$$\Psi(x) := \begin{pmatrix} 1 & \mathrm{L}_{G_2(\cdot,0)} h_2(F_2(x_2,0)) \\ -\mathrm{L}_{G_1(\cdot,0)} h_1(F_1(x_1,0)) & 1 \end{pmatrix}$$

proves that for any (x,u) in a neighborhood of $(0,0)$ there exists a solution. Accordingly, when the implicit equality is solved truncating it in u^2, one gets local passivity from Theorem 2.4.1 when $u = \bar{u}_a(x) + v$ with the approximate solution

$$\bar{u}_a(x) = \Psi^{-1}(x) \begin{pmatrix} -h_2(F_2(x_2,0)) \\ h_1(F_1(x_1,0)) \end{pmatrix}.$$

□

2.4.4 Interconnection of average passive LTI systems

The feedback interconnection provided in the previous section can be specified in the linear case. In this case, all the solutions can be explicitly computed. The following theorem holds.

Theorem 2.4.1. *Let, for $i = 1, 2$, the LTI systems*

$$x_i^+(u_i) = A_i x_i + B_i u_i \tag{2.51a}$$

$$y_i = C_i x_i \tag{2.51b}$$

be u-average passive with quadratic storage function $S_i(x) = \frac{1}{2} x_i^\top P_i x_i$ and $P_i > 0$. Consider the input (2.43) with $\bar{u} = Kx$ and

$$K = \begin{pmatrix} K_1 & K_2 \\ K_3 & K_4 \end{pmatrix} = \begin{pmatrix} 1 & \frac{1}{2} C_2 B_2 \\ -\frac{1}{2} C_1 B_1 & 1 \end{pmatrix}^{-1} \begin{pmatrix} \mathbf{0} & -C_2 A_2 \\ C_1 A_1 & \mathbf{0} \end{pmatrix}$$

the unique solution to the power-preserving interconnection (2.38). Then, the interconnected system

$$x_1^+(\bar{u}_1 + v_1) = (A_1 + B_1K_1)x_1 + B_1K_2x_2 + B_1v_1 \tag{2.52a}$$

$$x_2^+(\bar{u}_2 + v_2) = B_2K_3x_1 + (A_2 + B_2K_4)x_2 + B_2v_2 \tag{2.52b}$$

$$y_1 = C_1x_1, \quad y_2 = C_2x_2 \tag{2.52c}$$

is v-average passive from $\bar{u}$ with storage function $S_c(x) := S_1(x_1) + S_2(x_2)$. Namely, the dissipation inequality

$$S_c(x^+(u)) - S_c(x) \leq v^\top h_{av}(\bar{u})(x, \bar{u} + v) \tag{2.53}$$

holds with v-average output (2.46) *which takes the form*

$$h_{av}(\bar{u})(x, \bar{u} + v) = \begin{pmatrix} C_1(A_1 + B_1K_1)x_1 + C_1B_1K_2x_2 + \frac{1}{2}C_1B_1v_1 \\ C_2B_2K_3x_1 + C_2(A_2 + B_2K_4)x_2 + \frac{1}{2}C_2B_2v_2 \end{pmatrix}.$$

Proof. In the linear case the power-preserving interconnection (2.40) is specified as

$$\begin{pmatrix} u_1 \\ u_2 \end{pmatrix} = \begin{pmatrix} \mathbf{0} & -C_2A_2 \\ C_1A_1 & \mathbf{0} \end{pmatrix} \begin{pmatrix} x_1 \\ x_2 \end{pmatrix} + \begin{pmatrix} 0 & -\frac{1}{2}C_2B_2 \\ \frac{1}{2}C_1B_1 & 0 \end{pmatrix} \begin{pmatrix} u_1 \\ u_2 \end{pmatrix}$$

which is satisfied by $\bar{u} = Kx$ with

$$K = \begin{pmatrix} K_1 & K_2 \\ K_3 & K_4 \end{pmatrix} = \begin{pmatrix} 1 & \frac{1}{2}C_2B_2 \\ -\frac{1}{2}C_1B_1 & 1 \end{pmatrix}^{-1} \begin{pmatrix} \mathbf{0} & -C_2A_2 \\ C_1A_1 & \mathbf{0} \end{pmatrix},$$

where the invertibility of the matrix is guaranteed by the u-average passivity of the LTI systems. Then, injecting $u = \bar{u} + v$ into both the system $\Sigma(h_1)$ and $\Sigma(h_2)$ one achieves the interconnected system (2.52), where v-average passivity is deduced by Theorem 2.4.1. Finally, setting $S_c(x) = \frac{1}{2}x_1^\top P_1x_1 + \frac{1}{2}x_1^\top P_1x_1$, the v-average output $h_{\mathrm{av}}(\bar{u})(x, \bar{u} + v)$ along the dynamics $x^+(\bar{u} + v)$ in (2.52) specializes as

$$\begin{aligned} h_{\mathrm{av}}(\bar{u})(x, \bar{u} + v) &= \begin{pmatrix} \frac{1}{v_1}\int_0^{v_1} C_1x_1^+(\bar{u}_1 + \ell)\mathrm{d}\ell \\ \frac{1}{v_2}\int_0^{v_2} C_2x_2^+(\bar{u}_2 + \ell)\mathrm{d}\ell \end{pmatrix} \\ &= \begin{pmatrix} \frac{1}{v_1}\int_0^{v_1} C_1((A_1 + B_1K_1)x_1 + B_1K_2x_2 + B_1\ell)\mathrm{d}\ell \\ \frac{1}{v_2}\int_0^{v_2} C_2(B_2K_3x_1 + (A_2 + B_2K_4)x_2 + B_2\ell)\mathrm{d}\ell \end{pmatrix} \\ &= \begin{pmatrix} C_1(A_1 + B_1K_1)x_1 + C_1B_1K_2x_2 + \frac{1}{2}C_1B_1v_1 \\ C_2B_2K_3x_1 + C_2(A_2 + B_2K_4)x_2 + \frac{1}{2}C_2B_2v_2 \end{pmatrix}. \end{aligned}$$

□

2.5 Example: interconnection of passive oscillators

This section illustrates computational aspects by means of an academic example concerning the interconnection of a couple of input-affine nonlinear passive oscillators. Due to the input-affinine structure a global solution exists and is exactly computable.

Consider a couple of nonlinear discrete-time passive oscillators $\Sigma_1(h_1)$ and $\Sigma_2(h_2)$ described by the equations of the form, for $i = 1, 2$,

$$x_{1i}(k+1) = \frac{a x_{2i}(k)}{1 + x_{1i}^2(k)} \tag{2.54a}$$

$$x_{2i}(k+1) = \frac{a x_{1i}(k)}{1 + x_{2i}^2(k)} + u_i(k) \tag{2.54b}$$

$$y_i(k) = x_{2i}(k), \tag{2.54c}$$

with coefficient $a^2 \leq 1$ and state $x_i = col(x_{1i}, x_{2i})$. Systems modeled by equations of the form (2.54) are average passive with respect to the associated output mapping (2.54c), and associated storage function

$$S_i(x_i) = \frac{1}{2} x_i^\top x_i \tag{2.55}$$

with average output respectively depending on the control input u_i that is given by the expression

$$h_{i\mathrm{av}}(x_i, u_i) = \frac{a x_{1i}(k)}{1 + x_{2i}^2(k)} + \frac{1}{2} u_i(k). \tag{2.56}$$

2.5.1 Interconnection structure design

Consider the feedback interconnecting between $\Sigma_1(h_1)$ and $\Sigma_2(h_2)$ under the proposed u-average interconnection (2.43), that is

$$u = \bar{u} + v,$$

with $u = col(u_1, u_2)$, $\bar{u} = col(\bar{u}_1, \bar{u}_2)$, and $v = col(v_1, v_2)$. As previously discussed, $\bar{u} = \bar{u}_i(x)$ denotes the preliminary power-preserving state-feedback given in Definition

2.4.1 as v defines the virtual input, that is the new input channel of the overall interconnected system.

According to Theorem 2.4.1, the power-preserving interconnection of average passive systems is achieved by computing the preliminary feedback $\bar{u}(x)$ solution to (2.38), which yields

$$\bar{u}(x) = \begin{pmatrix} \bar{u}_1 \\ \bar{u}_2 \end{pmatrix} = \begin{pmatrix} -\frac{1}{2}\frac{ax_{11}(k)}{1+x_{21}^2(k)} - \frac{1}{2}\frac{ax_{12}(k)}{1+x_{22}^2(k)} \\ \frac{1}{2}\frac{ax_{11}(k)}{1+x_{21}^2(k)} - \frac{1}{2}\frac{ax_{12}(k)}{1+x_{22}^2(k)} \end{pmatrix}. \tag{2.57}$$

The interconnected system through the proposed u-average interconnecting law

$$u = \begin{pmatrix} \bar{u}_1 + v_1 \\ \bar{u}_2 + v_2 \end{pmatrix} = \begin{pmatrix} -\frac{1}{2}\frac{ax_{11}(k)}{1+x_{21}^2(k)} - \frac{1}{2}\frac{ax_{12}(k)}{1+x_{22}^2(k)} + v_1 \\ \frac{1}{2}\frac{ax_{11}(k)}{1+x_{21}^2(k)} - \frac{1}{2}\frac{ax_{12}(k)}{1+x_{22}^2(k)} + v_2 \end{pmatrix}, \tag{2.58}$$

is thus given by the equations

$$x_{11}(k+1) = \frac{ax_{21}(k)}{1+x_{11}^2(k)} \tag{2.59a}$$

$$x_{21}(k+1) = \frac{1}{2}\frac{ax_{11}(k)}{1+x_{21}^2(k)} - \frac{1}{2}\frac{ax_{12}(k)}{1+x_{22}^2(k)} + v_1(k) \tag{2.59b}$$

$$x_{12}(k+1) = \frac{ax_{22}(k)}{1+x_{12}^2(k)} \tag{2.59c}$$

$$x_{22}(k+1) = \frac{1}{2}\frac{ax_{11}(k)}{1+x_{21}^2(k)} + \frac{1}{2}\frac{ax_{12}(k)}{1+x_{22}^2(k)} + v_2(k) \tag{2.59d}$$

$$y_1 = x_{21}(k) \tag{2.59e}$$

$$y_2 = x_{22}(k) \tag{2.59f}$$

that is, according to the proposed feedback interconnection (2.43), average passive with respect to the output $y = col(y_1, y_2)$ and total storage function given by $S(x) = S_1(x_1) + S_2(x_2)$, that is

$$S(x_1, x_2) = \frac{1}{2}x_1^\top x_1 + \frac{1}{2}x_2^\top x_2, \tag{2.60}$$

and passive with respect to the average output mapping of the form

$$h_{\text{av}}(\bar{u})(x, \bar{u}+v) = \begin{pmatrix} \frac{ax_{11}(k)}{1+x_{21}^2(k)} + \bar{u}_1(k) + \frac{1}{2}v_1(k) \\ \frac{ax_{12}(k)}{1+x_{22}^2(k)} + \bar{u}_2(k) + \frac{1}{2}v_2(k) \end{pmatrix},$$

which reads

$$h_{\text{av}}(\bar{u})(x, \bar{u}+v) = \frac{1}{2}\begin{pmatrix} \frac{ax_{11}(k)}{1+x_{21}^2(k)} - \frac{ax_{12}(k)}{1+x_{22}^2(k)} + v_1(k) \\ \frac{ax_{11}(k)}{1+x_{21}^2(k)} + \frac{ax_{12}(k)}{1+x_{22}^2(k)} + v_2(k) \end{pmatrix}. \tag{2.61}$$

Accordingly, under zero-state detectability property on $h_{\text{av}}(\bar{u})(x, \bar{u}+v)$, one can asymptotically stabilize the system at the origin by injecting the damping feedback $v = -\kappa h_{\text{av}}(\bar{u})(x, \bar{u}+v)$ for damping improvement $\kappa > 0$. The damping feedback is the solution to the implicit equation

$$\begin{pmatrix} v_1 \\ v_2 \end{pmatrix} = -\frac{\kappa}{2}\begin{pmatrix} \frac{ax_{11}(k)}{1+x_{21}^2(k)} - \frac{ax_{12}(k)}{1+x_{22}^2(k)} + v_1 \\ \frac{ax_{11}(k)}{1+x_{21}^2(k)} + \frac{ax_{12}(k)}{1+x_{22}^2(k)} + v_2 \end{pmatrix},$$

which in its explicit form yields

$$v = \begin{pmatrix} v_1 \\ v_2 \end{pmatrix} = -\frac{\kappa}{2+\kappa}\begin{pmatrix} \frac{ax_{11}(k)}{1+x_{21}^2(k)} - \frac{ax_{12}(k)}{1+x_{22}^2(k)} \\ \frac{ax_{11}(k)}{1+x_{21}^2(k)} + \frac{ax_{12}(k)}{1+x_{22}^2(k)} \end{pmatrix}. \tag{2.62}$$

2.5.2 Analysis and simulation results

Consider $\Sigma_1(h_1)$ and $\Sigma_2(h_2)$ given by the equations (2.54) with associated average output given by the mapping (2.56). Set the parameter of the systems as $a = 1$ and initial conditions of $\Sigma_1(h_1)$ and $\Sigma_2(h_2)$ respectively set as $x_1(0) = col(0.5, 3)$, $x_2(0) = col(-0.5, -3)$.

The simulations are considered in three different scenarios:

- The first scenario illustrates the case of $\Sigma_1(h_1)$ and $\Sigma_2(h_2)$ without their feedback interconnection, namely in the case of $u_1 = 0$ and $u_2 = 0$.

  In this respect, Figure 2.2a depicts the evolution of the states associated with $\Sigma_1(h_1)$ and $\Sigma_2(h_2)$. Their evolutions are not converging to the equilibrium point, that is $x_\star = 0$, as their evolution oscillates along the iterations $k > 0$. Therefore the equilibrium of the system is stable, but

not asymptotically stable. For the same reason, as illustrated in Figure 2.2b, both the outputs of $\Sigma_1(h_1)$ and $\Sigma_2(h_2)$, represented by the equation (2.54c), oscillate along k-iterations and both the storage functions $S_1(x_1)$ and $S_2(x_2)$ have the same dynamics (they overlap like shown in Figure 2.2b due to the initial conditions), showing passivity of both the involved dynamics $\Sigma_1(h_1)$ and $\Sigma_2(h_2)$ since both the storage functions $S_1(x_1)$ and $S_2(x_2)$ decrease at the first k-step and remain constant along the other k-iterations.

■ The second scenario illustrates the interconnection of $\Sigma_1(h_1)$ and $\Sigma_2(h_2)$ under the power-preserving interconnection (2.57), namely in the case of $v_1 = 0$ and $v_2 = 0$.

To this end, Figure 2.3a depicts the evolution of the states associated with $\Sigma_1(h_1)$ and $\Sigma_2(h_2)$ under power-preserving interconnection which involves the associated average passive output of both $\Sigma_1(h_1)$ and $\Sigma_2(h_2)$, namely the state trajectories of the augmented system (2.59). The augmented system under preliminary feedback $\bar{u}(x)$ provides a different oscillatory behavior as $\Sigma_1(h_1)$ affects the dynamics of $\Sigma_2(h_2)$ and vice versa. As in the previous case, through power preserving interconnection their evolution is not converging to the equilibrium point as their behavior oscillates along the iterations $k > 0$.

The power-preserving effect is reported by the bottom-right Figure 2.2b, where the total storage function of the interconnected system is depicted. One may notice that the storage function preserves the energy as it is composed by the sum of $S_1(x_1)$ and $S_2(x_2)$ and accordingly there is no energy loss after the first k-step.

The bottom-left Figure 2.3b shows the evolution of the preliminary feedback yielding the power-preserving interconnection. Finally, the top left and right Figure 2.3b depict the oscillatory behavior of output functions (2.59e)-(2.59f) and average output functions (2.56), respectively.

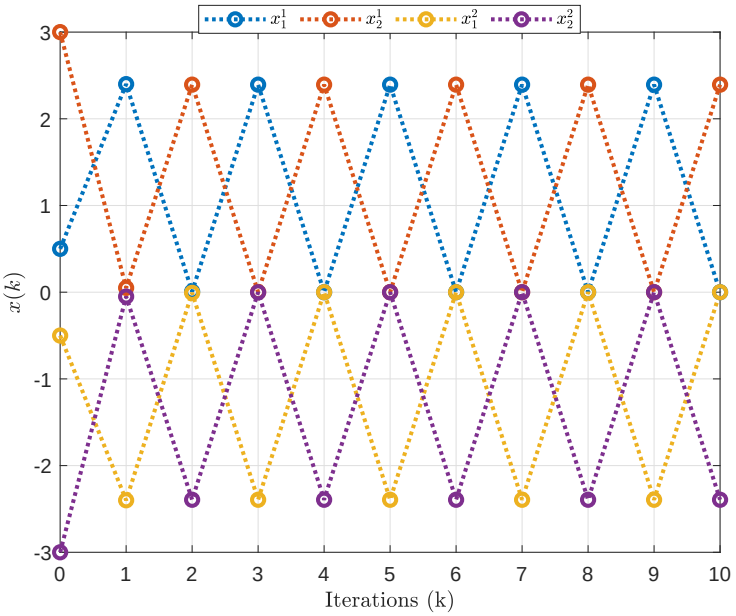

(a) State trajectories

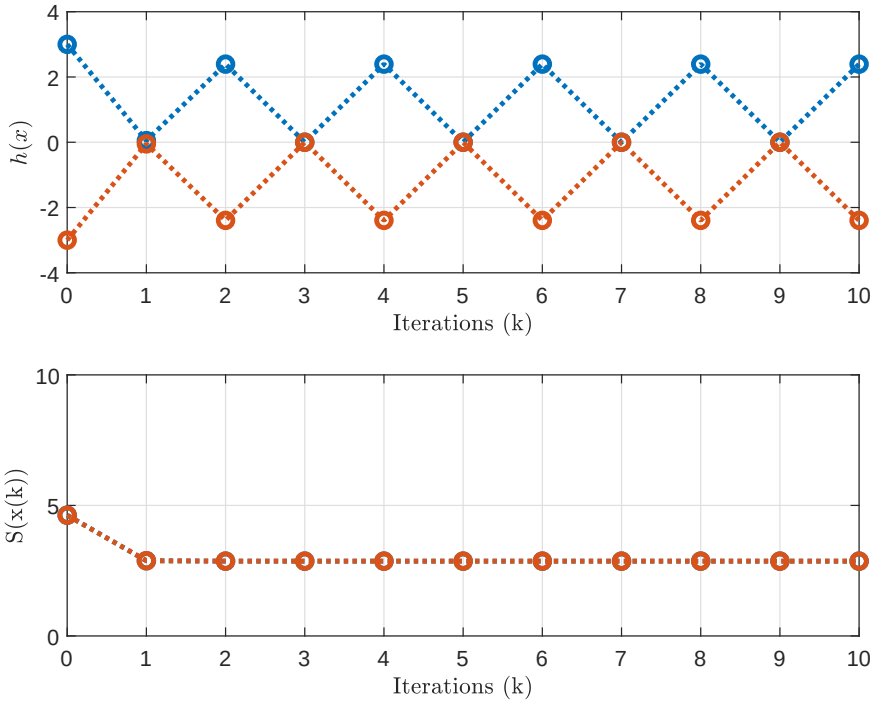

(b) Outputs h_1 (blue), h_2 (red) and Storage functions S_1 (blue), S_2 (red).

Figure 2.2: u-average interconnection of $\Sigma_1(h_1)$ and $\Sigma_2(h_2)$.

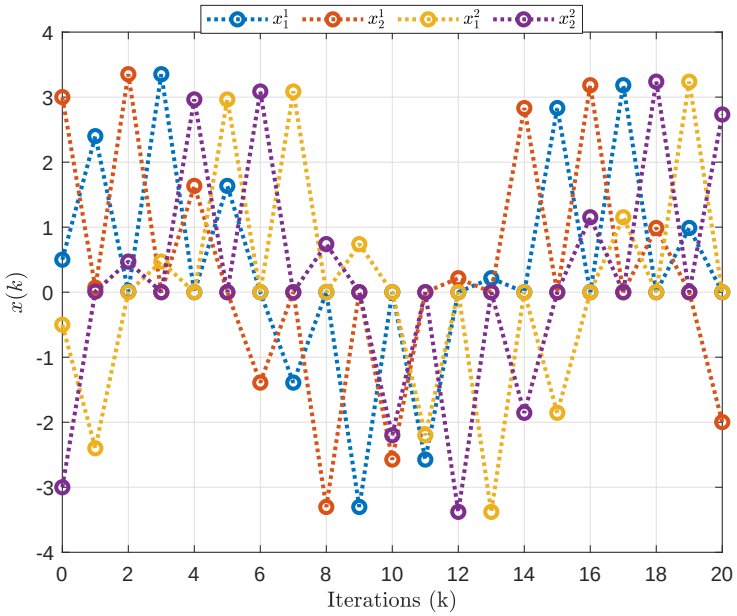

(a) State trajectories

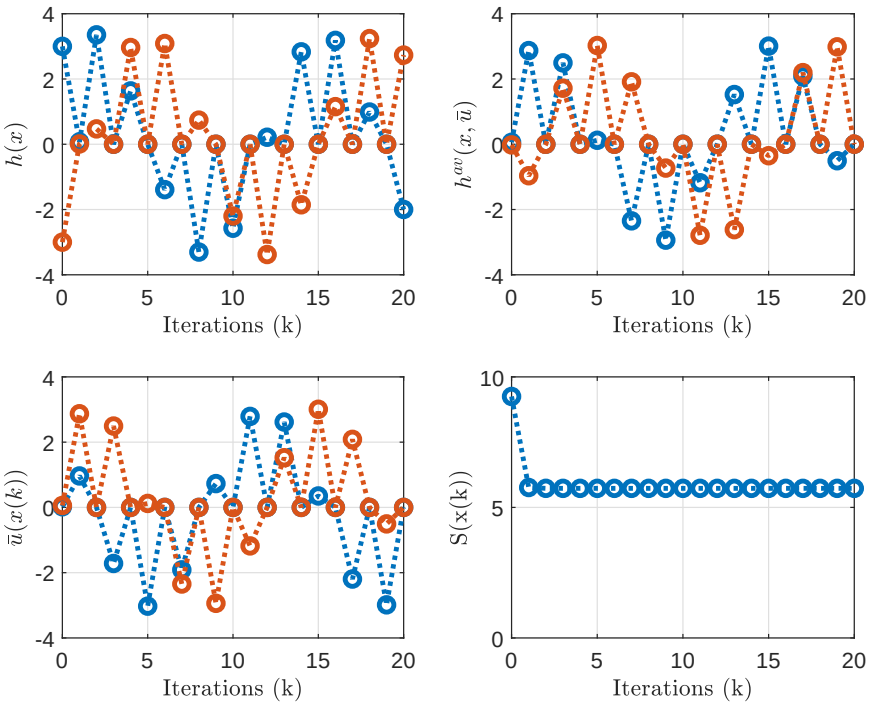

(b) Output functions h_1 (blue), h_2 (red), average output functions h_1^{av} (blue), h_2^{av} (red), preliminary feedback $\bar{u}_1$ (blue), $\bar{u}_2$ (red), and total storage function S (blue).

Figure 2.3: u-average interconnection of the system $\Sigma_1(h_1)$ and $\Sigma_2(h_2)$ with preliminary feedback $u = \bar{u}(x)$ given in (2.57).

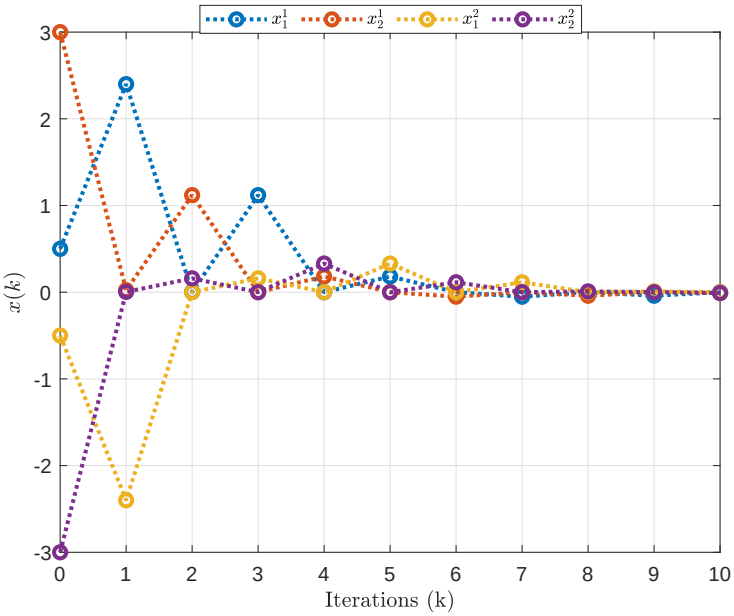

(a) State trajectories

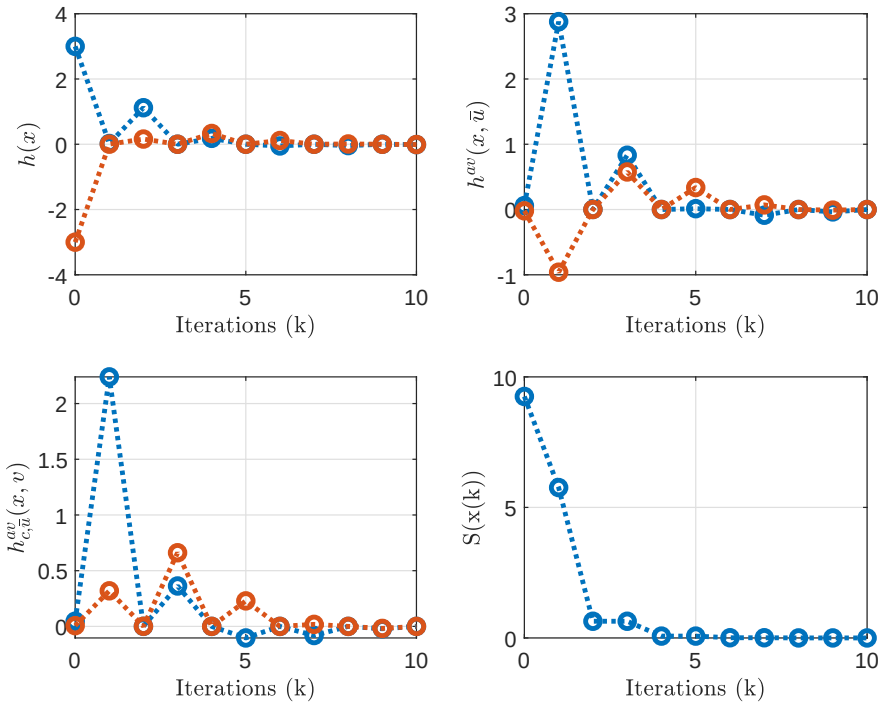

(b) Output functions h_1 (blue), h_2 (red), average output functions h_1^{av} (blue), h_2^{av} (red), new average output of the interconnected system $h_{1c,\bar{u}}^{\text{av}}$ (blue), $h_{2c,\bar{u}}^{\text{av}}$ (red), and total storage function S (blue).

Figure 2.4: u-average interconnection of the system $\Sigma_1(h_1)$ and $\Sigma_2(h_2)$ with addition damping injection of v given in (2.62).

■ The third scenario illustrates the effect of the additional injection of the damping feedback v, computed in (2.62) with a damping improvement $\kappa = 1$, after the u-average interconnection (2.58) of $\Sigma_1(h_1)$ and $\Sigma_2(h_2)$ under the preliminary feedback (2.57).

Differently from the other scenarios, Figure 2.4a shows the effect of the damping injection (2.62) into the u-average interconnected system (2.59). The state trajectories approach the zero sate equilibrium of the interconnected system providing asymptotic stability.

The bottom-left Figure 2.4b depicts the evolution of the new average output function (2.61), as the top left and right Figure 2.4b depict, respectively, the behavior of output functions (2.59e)-(2.59f) and average output functions (2.56). Their evolution converges to the zero value after k-iterations.

The passivity effect of the interconnected system (2.59) is reflected into the bottom-right Figure 2.4b where the total storage function (2.60) is reported. The total storage function shows to be a decreasing function and approached the zero value, that is its lower bound.

2.6 Concluding remarks

At the beginning of this chapter, the notions of DDR, discrete gradient function, and u-average passivity and passivity-based control in discrete time have been recalled. The interested reader can find additional details in Monaco and Normand-Cyrot (1997a, 1998, 2011). Afterwards, in Lemma 2.2.1, we established a connection between the u-average output arising from the definition of u-average passivity and the discrete gradient function of the storage function associated with the discrete-time system. We have discussed the interconnection between u-average passive systems and, in doing so, a proper definition of power-preserving interconnection has been set in Definition 2.4.1 which clearly involves u-average outputs of the systems. The results presented for the feedback interconnection of u-average passive systems in Theorem 2.4.1 yield v-average passivity property from $\bar{u}$ with respect to the natural output of the systems and, respectively, passivity with respect to the v-average output from $\bar{u}$. Computational aspects have been addressed to provide the existence of a

solution by invoking the implicit function theorem. Finally, we have characterized the solution to LTI u-average passive systems and an illustrative example showing the effectiveness of the result. The content of the Section 2.4 related to the interconnection of u-average passive systems is in:

A. Moreschini, M. Mattioni, S. Monaco and D. Normand-Cyrot, "Interconnection through u-average passivity in discrete time," 2019 IEEE 58th Conference on Decision and Control (CDC), Nice, France, 2019, pp. 4234-4239, doi: 10.1109/CDC40024.2019. 9029357.

Chapter 3

Generalities on sampled-data systems

Contents

3.1 The sampled-data representation **84**

3.2 Difference and differential representation **87**

3.3 Passivity property **89**

3.3.1 The u-average passivity 89

3.3.2 Passivity-based control 92

3.4 Linear-time invariant case **93**

3.5 Feedback passivation under sampling **95**

3.5.1 Problem statement: feedback passivation under sampling . 97

3.5.2 Digital passivation and stabilization 98

3.5.3 Illustrative example: Backstepping as feedback passivation 102

3.6 Concluding remarks **105**

The sampled-data framework we deal within this manuscript is formally introduced in this chapter and the underlying properties of the original continuous time system can be reformulated over the sampled-data equivalent model. The preliminaries we are giving are based on previous works of Monaco and Normand-Cyrot (1998, 2005); Monaco et al. (2008). Firstly, we recall the definition of sampled-data equivalent representation and we recall the DDR structure associated

with the sampled-data equivalent model. Then, the passivity and u-average passivity properties are recalled. Lastly, we discuss the problem of feedback passivation under sampled-data design providing an original solution and computational aspects are performed by means of an academic example.

3.1 The sampled-data representation

In what follows, we discuss sampled-data equivalent models of sampled-data systems based on the relation among uniform sampling periods of the states and outputs.

Consider a continuous-time dynamics assumed input affine of the form

$$\dot{x}(t) = f(x(t)) + g(x(t))u(t) \tag{3.1a}$$
$$y(t) = h(t). \tag{3.1b}$$

Assume that the control signal is piecewise constant over time-intervals of fixed length $\delta > 0$, namely for $k \geq 0$

$$u(t) = u(k\delta) \quad \forall\, t \in [k\delta, (k+1)\delta[$$

and that the measures of the states and output are available only at the sampling instants $k\delta$, namely for $k \geq 0$

$$x(t) = x(k\delta) \quad \forall\, t \in [k\delta, (k+1)\delta[$$
$$y(t) = y(k\delta) \quad \forall\, t \in [k\delta, (k+1)\delta[$$

Under these assumptions, the evolution of a continuous-time system (3.1a) affected by the piecewise control $u(k\delta)$ is described by the equations

$$\dot{x}(t) = f(x(t)) + g(x(t))u(k\delta) \tag{3.2a}$$
$$y(t) = h(k\delta) \tag{3.2b}$$

where $u(t) = u(k\delta)$ and $y(t) = y(k\delta)$ for all $t \in [k\delta, (k+1)\delta[$. The sampled-data system is computed by integrating the continuous dynamics (3.2a) at the sampling instants $t = k\delta$, over $t \in [k\delta, (k+1)\delta[$, so obtaining the sampled-data system

$$\begin{aligned} x((k+1)\delta) :&= x(k\delta) + F^{\delta}(x(k\delta), u(k\delta)) \\ &= x(k\delta) + \int_{k\delta}^{(k+1)\delta} f(x(\tau)) + g(x(\tau))u(k\delta)\mathrm{d}\tau \qquad (3.3a) \\ y(t) &= h(k\delta), \qquad (3.3b) \end{aligned}$$

with map $F^{\delta}(\cdot,\cdot) : \mathbb{R}^n \times \mathbb{R} \to \mathbb{R}^n$ parametrized by δ which admits the formal Taylor series expansion in power of δ,

$$\begin{aligned} F^{\delta}(x(k\delta), u(k\delta)) &= \delta\dot{x}(t)|_{k\delta} + \frac{\delta^2}{2}\ddot{x}(t)|_{k\delta} + \cdots \\ &= \sum_{i\geq 1} \frac{\delta^i}{i!}(\mathrm{L}_f + u(k\delta)\mathrm{L}_g)I_d|_{x(k\delta)} \\ &= e^{\delta\mathrm{L}_f + u(k\delta)\mathrm{L}_g} I_d|_{x(k\delta)} - x(k\delta). \qquad (3.4) \end{aligned}$$

The sampled-data model (3.3), with sampling period of fixed length $\delta \in]0, T^*[$ and $T^* > 0$ denoting the upper bound of the convergence interval of the exponential expansion (3.4), defines the so-called sampled-data equivalent model of (3.2a) which is formally defined below.

Definition 3.1.1 (SD equivalent model)**.** Given a continuous-time system of the form (3.2), for any $t = k\delta$ with $\delta \in]0, T^*[$, $T^* > 0$, and $k \in \mathbb{N}$, then its Sampled-Data (SD) equivalent model is given by the equations

$$\begin{aligned} x^+(u) &= x + F^{\delta}(x, u) \qquad (3.5a) \\ y &= h(x), \qquad (3.5b) \end{aligned}$$

with $x^+(u) = x_{k+1} := x((k+1)\delta)$, $x = x_k := x(k\delta)$, $u = u_k := u(k\delta)$, and

$$F^{\delta}(x, u) = e^{\delta(\mathrm{L}_f + u\mathrm{L}_g)} I_d|_x - x.$$

For any piecewise constant input u in Definition 3.1.1 and sampling period δ small enough the discrete model (3.5) gives an exact sampled-data representation, meaning that when both the sampled-data and the continuous-time models are initialized at the same value the sampled-data model provides input-state matching. The expression of the system (3.5) is exactly computable if the formal series in δ of the mapping

$F^\delta(\cdot,\cdot)$ admits a closed form or alternatively is finitely discretizable in the sense of the definition below.

Definition 3.1.2 (Finite discretizability)**.** The system (3.2) is said *finitely discretizable* if it admits a sampled-data equivalent model (3.5) in a finite series expansion in powers of δ, namely for $q \geq 1$

$$F^\delta(x,u) = \sum_{i\geq 1}^{q} \frac{\delta^i}{i!}(\mathrm{L}_f + u\mathrm{L}_g)^i I_d|_x.$$

In spite of the exact form given by $F^\delta(\cdot,\cdot)$, obtaining a closed-form might be tough as its existence directly depends on the integrability of (3.2a). Therefore, it is usual in the sampled-data context to consider an approximate map $F^{\delta[p]}(\cdot,\cdot)$, corresponding to the truncation of the series expansion at a fixed order $p \in \mathbb{N}$ of the sampling period δ. The approximate map $F^{\delta[p]}(\cdot,\cdot)$ is defined as a finite series in power of δ and verifies

$$F^\delta(x,u) = F^{\delta[p]}(x,u) + \mathcal{O}(\delta^{p+1}).$$

Accordingly, the formal definition of approximate model follows.

Definition 3.1.3 (Approximate SD model)**.** Given a continuous-time system of the form (3.2), for any $t = k\delta$ with $\delta \in]0, T^*[$, $T^* > 0$, and $k \in \mathbb{N}$, then for $p \in \mathbb{N}$ its p^{th}-approximate SD model is given by the equations

$$x^+(u) = x + F^{\delta[p]}(x,u) \tag{3.6a}$$
$$y = h(x), \tag{3.6b}$$

with p^{th}-approximate map

$$F^{\delta[p]}(x,u) = \sum_{i\geq 1}^{p} \frac{\delta^i}{i!}(\mathrm{L}_f + u\mathrm{L}_g)^i I_d|_x.$$

From the approximate SD model one gets that as long as the sampling period δ is sufficiently small for $k \geq 0$ one gets that the approximate map verifies

$$||F^\delta(x,u) - F^{\delta[p]}(x,u)|| \leq O(\delta^{p+1}),$$

meaning that the trajectories of the approximate model (3.6) evolves in a neighborhood of the trajectories of the SD equivalent (3.5). In addition, for zero input $u = 0$ the properties of the equilibrium of the autonomous system yield practically upon the approximate dynamics, see Nešić et al. (1999).

Remark 3.1.1. Unsurprisingly, the 1^{th}-approximate SD model to (3.2) coincides with the Forward Euler discrete model and yields

$$x^+(u) = x + F^{\delta[1]}(x, u) = x + \delta(f(x) + g(x)u).$$

The Forward Euler discrete model usually requires a very small sampling period δ to keep its trajectories in a neighborhood of the SD equivalent model. Notably in the nonlinear case, the Forward Euler discrete suffers the nonlinearity induced by the continuous-time model.

Remark 3.1.2. The p^{th}-approximate SD model to the system (3.2) for truncation order $p \geq 2$ does not hold an affine structure with respect to the control variable. Indeed the second order approximate model, say $p = 2$, yields a quadratic term in u, namely

$$F^{\delta[2]}(x, u) = \delta(f(x) + g(x)u) + \frac{\delta^2}{2}\left(\mathrm{L}_f f(x) + u\mathrm{L}_f g(x) + u\mathrm{L}_g f(x) + u^2\mathrm{L}_g g(x)\right).$$

3.2 Difference and differential representation

Even if difference equations of the form are considered far away from differential equations, the involvement of a DDR form (in Definition 2.1.3) in this sampled-data context defines a sampled-data model represented as coupled differential/difference equations, see Monaco and Normand-Cyrot (1998, 2005). To this end, the sampled-data dynamics (3.5) admits an equivalent state-space representation defined by

$$x^+ = x + F_0^\delta(x), \quad x^+ = x^+(0) \tag{3.7a}$$

$$\frac{\partial x^+(u)}{\partial u} = G^\delta(x^+(u), u) \tag{3.7b}$$

a differential equation (3.7a) which describes the variation with respect to the control variable u, while the difference equation (3.7a) describes the free evolution with the maps

$$F_0^\delta(x) = F^\delta(x,0) = e^{\delta \mathrm{L}_f} I_d|_x - x \tag{3.8a}$$

$$G^\delta(x^+(u),u) = \int_0^\delta e^{-s\ \mathrm{ad}_{f+ug}} g(x)\mathrm{d}s \tag{3.8b}$$

where $G^\delta(x^+(u),u)$ is complete and verifies

$$\frac{\partial F^\delta(x,u)}{\partial u} = G^\delta(x^+(u),u).$$

As seen in the discrete time, both (3.5) and (3.7) are perfectly equivalent. By integrating (3.7b) over $[0,u[$ with initial condition (3.7a) one gets the integral form

$$x^+(u) = x + F^\delta(x,u) = x + F_0^\delta(x) + \int_0^u G^\delta(x^+(v),v)\mathrm{d}v. \tag{3.9}$$

Also in this context, a powerful benefit of exploiting the DDR form, as seen in Proposition 2.1.1, is that it allows to split the evolutions of a given smooth mapping $\lambda : \mathbb{R}^n \to \mathbb{R}$ along the sampled trajectories of (3.5) as the contribution of the free and controlled components, namely

$$\lambda(x^+(u)) = \lambda(x^+(0)) + \int_0^u \mathrm{L}_{G^\delta(.,v)}\lambda(x^+(v))\mathrm{d}v. \tag{3.10}$$

Remark 3.2.1. The representation (3.7) in the sampled-data context always exists and is uniquely defined due to the invertibility of the drift term (3.8a). In particular, for a sampling period δ sufficiently small ensuring series convergence, (3.5) is drift invertible meaning that for $x + F_0^\delta(x) = e^{\delta \mathrm{L}_f} I_d|_x$, one gets $(I_d + F_0^\delta)^{-1}|_x = e^{-\delta \mathrm{L}_f} I_d|_x$. Thus, the map $x + F^\delta(x,u)$ is invertible for u in the neighborhood of 0. See Monaco and Normand-Cyrot (1998); Monaco et al. (2007) for further details.

Remark 3.2.2. It is worth mentioning that a sampled-data DDR form does not require additional condition on the existence of the map $G^\delta(.,v)$ since it is computed in (3.8b) as an exponential series of the Lie bracket between vector fields characterizing the continuous-time dynamics.

3.3 Passivity property

Passivity concepts discussed in Section 2.2 for discrete time dynamics can be reinterpreted in this present sampled-data context. Assuming the continuous-time system (3.2) passive, meaning that

$$\dot{S}(x) \leq uy$$

for the storage function $S : \mathcal{X} \to \mathbb{R}_{\geq 0}$ and output map $y = \mathrm{L}_g S(x)$ required by the KYP properties in Theorem 1.2.1, we obtain for the piecewise constant control variable $u(t) = u_k$ and by integrating the above dissipation inequality over $[k\delta, (k+1)\delta[$ the following passivity condition between two time instants

$$S(x^+(u)) - S(x) \leq u \int_0^\delta \mathrm{L}_g S(x(s))\mathrm{d}s. \tag{3.11}$$

with $x(s) = e^{\delta(\mathrm{L}_f + u\mathrm{L}_g)} I_d|_{x(k)}$. It is clear from the passivity condition above that passivity of the original system, in the sense of Definition 1.2.2, with respect to the output map y is not preserved under sampling with respect to the same output. Though, the above inequality suggests that its sampled-data dynamics (3.5) is passive with respect to a new output map suitably computed.

Remark 3.3.1. The approach of Costa-Castelló and Fossas (2006); Stramigioli et al. (2005) to avoid this problem is to consider the δ-average output

$$y^\delta = \frac{1}{\delta} \int_{k\delta}^{(k+1)\delta} y(s)\mathrm{d}s = \frac{1}{\delta} \int_0^\delta \mathrm{L}_g S(x(s))\mathrm{d}s,$$

in place of the original output $y(k\delta)$. The δ-average output is directly deduced from (3.11) by averaging with respect to δ the continuous-time dynamics (3.1a) over the sampling period and along the trajectories of (3.2a). Although this output map seems natural for sampled-data systems, its representation does not meet a counterpart in the pure discrete-time context. Therefore, this notion of δ-average output is not taken into account within this work.

3.3.1 The u-average passivity

The notion of u-average passivity previously discussed has proven to serve as an original and alternative definition of passivity which introduces an appropriate u-average output for which passivity is guaranteed also under sampled-data design.

Assuming passivity of the continuous-time system (3.2) and exploiting the sampled-data DDR form (3.7) associated to the sampled-data equivalent model (3.5), one notices that from the integral expression one has the following inequality

$$S(x^+(0)) - S(x) = \int_0^\delta \mathrm{L}_f S(x(s))\mathrm{d}s \leq 0$$

which holds true by the KYP condition $\mathrm{L}_f S(x) \leq 0$. Therefore, one can rewrite the passivity condition (3.11) as a dissipation inequality of the form

$$\begin{aligned} S(x^+(u)) - S(x) &= S(x^+(0)) - S(x) + S(x^+(u)) - S(x^+(0)) \\ &\leq \int_0^u \mathrm{L}_{G^\delta(.,v)} S(x^+(v))\mathrm{d}v. \end{aligned}$$

This leads to the theorem below where the result is recalled from Monaco et al. (2010).

Theorem 3.3.1. *Let the continuous-time system*

$$\dot{x} = f(x) + g(x)u \tag{3.12}$$
$$y = h(x) \tag{3.13}$$

be passive with storage function $S : \mathbb{R}^n \to \mathbb{R}_{\geq 0}$. Then, the sampled-data equivalent system

$$x^+ = x + F_0^\delta(x), \quad x^+ = x^+(0) \tag{3.14a}$$
$$\frac{\partial x^+(u)}{\partial u} = G^\delta(x^+(u), u) \tag{3.14b}$$
$$Y^\delta(x, u) = \mathrm{L}_{G^\delta(.,u)} S(x), \tag{3.14c}$$

is u-average passive; namely, the sampled-data equivalent DDR system (3.14) *is passive with respect to the u-average output*

$$Y_{av}^\delta(x, u) = \frac{1}{\delta u} \int_0^u \mathrm{L}_{G^\delta(.,v)} S(x^+(v))\mathrm{d}v \tag{3.15}$$

and verifies the dissipation inequality

$$S(x^+(u)) - S(x) \leq u Y_{av}^\delta(x, u).$$

The theorem above provides preservation of the passivity under sampling through the u-average output function $Y^{\delta}_{\rm av}(x,u)$, and respectively u-average passivity with respect to the output map $Y^{\delta}(x,u)$. However, for sake of completeness we recall that the u-average passivity property is a tool holding for discrete-time and sampled-data designs, and does not meet a counterpart in continuous time.

Remark 3.3.2. The u-average output map $Y^{\delta}_{\rm av}(x,u)$ which ensures passivity under sampled-data design, can be expressed as a series expansion in powers of δ around the continuous-time passive output map $h(x)=\mathrm{L}_gS(x)$ as such

$$Y^{\delta}_{\rm av}(x,u)=\sum_{i\geq 0}\frac{\delta^i}{(i+1)!}Y^{\delta}_{{\rm av}_i}(x,u) \tag{3.16}$$

with the first terms

$$\begin{aligned}
Y^{\delta}_{{\rm av}_i0}(x)&=h(x)=\mathrm{L}_gS(x)\\
Y^{\delta}_{{\rm av}_i1}(x,u)&=(\mathrm{L}_f+u\mathrm{L}_g)\,\mathrm{L}_gS(x)+\mathrm{L}_g\mathrm{L}_fS(x)\\
Y^{\delta}_{{\rm av}_i2}(x,u)&=(\mathrm{L}_f+u\mathrm{L}_g)^2\,\mathrm{L}_gS(x)+\mathrm{L}_f\mathrm{L}_g\mathrm{L}_fS(x)+u\mathrm{L}_g^2\mathrm{L}_fS(x).
\end{aligned}$$

The following lemma gives an equivalent representation of the sampled-data u-average output in terms of the discrete gradient function.

Lemma 3.3.1. *The u-average output map associated with the sampled-data system* (3.14) *rewrites in terms of discrete gradient as follows*

$$Y^{\delta}_{av}(x,u)=g^{\delta\top}(x,u)\bar{\nabla}S|_{x^+}^{x^+(u)} \tag{3.17}$$

with map

$$g^{\delta}(\cdot,u)=\frac{1}{\delta u}\left(e^{\delta(L_f+uL_g)}I_d-e^{\delta L_f}I_d\right) \tag{3.18}$$

verifying also

$$g^{\delta}(x,u)=\frac{1}{\delta u}\left(e^{\delta(L_f+uL_g)}I_d|_x-e^{\delta L_f}I_d|_x\right)=\frac{1}{\delta u}\int_0^u G^{\delta}(x^+(v),v)dv. \tag{3.19}$$

Proof. Due to the definition of discrete gradient between x^+ and $x^+(u)$ and by definition of u-average output one gets by construction the equivalence

$$\begin{aligned} Y^\delta_{\mathrm{av}}(x,u) &= \frac{1}{\delta u}\int_0^u Y^\delta(x^+(v),v)\mathrm{d}v \\ &= \frac{1}{\delta u}\left(S(x^+(u)) - S(x^+)\right) \\ &= \frac{1}{\delta u}\left(x^+(u) - x^+)\right)^\top \bar{\nabla} S|_{x^+}^{x^+(u)} \\ &= \frac{1}{\delta u}\left(e^{\delta(\mathrm{L}_f + u\mathrm{L}_g)} I_d|_x - e^{\delta \mathrm{L}_f} I_d|_x\right)^\top \bar{\nabla} S|_{x^+}^{x^+(u)} = g^{\delta\top}(x,u)\bar{\nabla} S|_{x^+}^{x^+(u)}. \end{aligned}$$

Finally, the mapping $g^\delta(\cdot,u)$ yields the equivalence condition (3.19) which is obtained from (3.9) with map $G^\delta(x,u)$ in (3.8b). □

3.3.2 Passivity-based control

We have seen that the u-average passivity notion is profitably used to achieve asymptotic stabilization of the origin for the discrete-time model provided ZSD property. In the present framework, due to the structure of the sampled-data equivalent model (3.14) its ZSD property arises from the assumption on the ZSD of the continuous-time system (3.12); namely if the origin of the continuous-time system is asymptotically stable conditionally to the largest invariant set contained in $\{x \in \mathbb{R}^n \mid \mathrm{L}_g S(x) = 0\}$, then the sampled-data equivalent model (3.14) is asymptotically stable conditionally to the largest invariant set contained in $\{x \in \mathbb{R}^n \mid Y^\delta(x,0) = 0\}$.

Accordingly, one can state the following theorem which specializes the Theorem 2.2.1 in the sampled-data framework, as given in Monaco et al. (2010).

Theorem 3.3.2. *Let the continuous-time system* (3.12) *be passive with positive definite storage function with storage function $S : \mathbb{R}^n \to \mathbb{R}_{\geq 0}$ and ZSD. Then, the digital feedback $u = \gamma^\delta(x)$ solution to*

$$\gamma^\delta(x) + \kappa Y^\delta_{av}(x, \gamma^\delta(x)) = 0 \tag{3.20}$$

with damping $\kappa > 0$, makes the origin of the sampled-data system (3.14) *asymptotically stable.*

3.4 Linear-time invariant case

Despite the fact that a solution to the ODE (3.12) is difficult to calculate for general nonlinear systems, in the LTI case the SD equivalent model to (3.12) can be expressed in its closed form. Indeed, assuming a linear-time invariant in continuous time, of the form

$$\dot{x} = Ax + Bu \tag{3.21a}$$

$$y = Cx \tag{3.21b}$$

with $A \in \mathrm{Mat}_{\mathbb{R}}(n,n)$, $B \in \mathrm{Mat}_{\mathbb{R}}(n,1)$, and $C \in \mathrm{Mat}_{\mathbb{R}}(1,n)$, its equivalent sampled-data model is expressed by the difference equation

$$x^+(u) = A^\delta x + \delta B^\delta u \tag{3.22a}$$

$$y = Cx \tag{3.22b}$$

with

$$A^\delta = e^{\delta A} = I + \sum_{i\geq 1} \frac{\delta^i}{i!} A^i$$

$$B^\delta = \frac{1}{\delta}\int_0^\delta e^{\tau A} B \mathrm{d}\tau = \frac{1}{\delta} B + \sum_{i\geq 1} \frac{\delta^{i-1}}{i!} A^{i-1} B,$$

where A^i is the repeated matrix product of A with itself.

Remark 3.4.1. Unlike the exponential of a vector field, which in general is not exactly computable producing an infinite exponential series, the exponential of a matrix as for the matrix A^δ can be calculated in closed form since it is always a convergent series and therefore is well defined. See Bhatia (2013); Hall (2015) for a thorough overview on matrix exponentials.

The sampled-data equivalent model (3.22) yields an equivalent state-space DDR form under sampling which is defined by the pair of difference and differential equations

$$x^+ = A^\delta, \quad x^+ = x^+(0) \tag{3.23a}$$

$$\frac{\partial x^+(u)}{\partial u} = \delta B^\delta \tag{3.23b}$$

$$y = Cx \tag{3.23c}$$

which restores the LTI system in the form of a map, by integrating (3.23b) over $[0, u[$ with initial condition (3.23a) so that one gets the integral form

$$x^+(u) = x^+(0) + \delta \int_0^u B^\delta \mathrm{d}v = A^\delta x + \delta B^\delta u \tag{3.24a}$$

$$y = Cx. \tag{3.24b}$$

The passivity properties related to LTI sampled-data system can be reformulated. Without loss of generalities, due to the necessary and sufficient conditions provided by the KYP properties in Chapter 1, we assume that the LTI continuous-time system (3.21) which is passive comes with an output of the form

$$y(t) = B^\top P x(t)$$

with positive definite $P \in \mathrm{Sym}_{\mathbb{R}}(n, n)$ defining the quadratic storage function $S(x) = \frac{1}{2} x^\top P x$. Thus, we specialize the Theorem 3.4.1 in this linear case.

Theorem 3.4.1. *Let the continuous-time system*

$$\dot{x} = Ax + Bu \tag{3.25a}$$

$$y = B^\top P x \tag{3.25b}$$

be passive with quadratic storage function $S(x) = \frac{1}{2} x^\top P x$ and positive definite $P \in \mathrm{Sym}_{\mathbb{R}}(n, n)$. Then, the LTI sampled-data equivalent system

$$x^+(u) = A^\delta x + \delta B^\delta u \tag{3.26a}$$

$$Y^\delta(x, u) = B^{\delta\top} P x, \tag{3.26b}$$

is u-average passive; namely, the sampled-data equivalent dynamics (3.26a) *is passive with respect to the u-average output*

$$Y^\delta_{av}(x, u) = B^{\delta\top} P A^\delta x + \frac{\delta}{2} B^{\delta\top} P B^\delta u. \tag{3.27}$$

Remark 3.4.2. The u-average output map (3.27) associated to the sampled-data system (3.26) rewrites in terms of discrete gradient as follows

$$\begin{aligned} Y^\delta_{\mathrm{av}}(x, u) &= B^{\delta\top}(x, u) \bar{\nabla} S \big|_{x^+}^{x^+(u)} \\ &= \frac{1}{2} B^{\delta\top} P (x^+(u) + x^+) \\ &= B^{\delta\top} P A^\delta x + \frac{\delta}{2} B^{\delta\top} P B^\delta u. \end{aligned}$$

We have already discussed for the nonlinear case that the u-average output can be exploited to provide asymptotic stabilization under ZSD property. In this linear context, clearly, if the origin of the continuous-time system is globally asymptotically stable conditionally to the largest invariant set contained in $\{x \in \mathbb{R}^n \mid B^\top Px = 0\}$, then the LTI sampled-data equivalent model (3.26) is globally asymptotically stable conditionally to the largest invariant set contained in $\{x \in \mathbb{R}^n \mid B^{\delta\top} Px = 0\}$. In addition, the passivity-based-control $u = \gamma^\delta(x)$ which asymptotically stabilizes the origin of the closed-loop system, yields as the solution to

$$\gamma^\delta(x) + \kappa B^{\delta\top} PA^\delta x + \kappa \frac{\delta}{2} B^{\delta\top} PB^\delta \gamma^\delta(x) = 0, \tag{3.28}$$

which admits a proper and unique solution. Thus, below we specialize the Theorem 2.3.1 for LTI sampled-data systems.

Theorem 3.4.2. *Let the LTI continuous-time system* (3.25) *be passive with quadratic storage function* $S(x) = \frac{1}{2}x^\top Px$ *and positive definite* $P \in \mathrm{Sym}_{\mathbb{R}}(n, n)$ *and ZSD. Then, the feedback* $u = \gamma^\delta(x)$ *given by*

$$\gamma^\delta(x) = -\frac{\kappa B^{\delta\top} PA^\delta x}{1 + \kappa \frac{\delta}{2} B^{\delta\top} PB^\delta} \tag{3.29}$$

with damping $\kappa > 0$*, makes the origin of the sampled-data system* (3.26a) *globally asymptotically stable.*

3.5 Feedback passivation under sampling

We have discussed in Chapter 1 the benefit of defining feedback passivation design in continuous time, that is to find a control law which aims to passivate the continuous-time system and then stabilize it through passivity-based-controller. Feedback passivation is instrumental in celebrated nonlinear control strategies such as backstepping or feedforwarding regarding cascade dynamics Sepulchre et al. (2012) or Interconnection and Damping Assignment (IDA-PBC) for Hamiltonian dynamics, Ortega et al. (2002b).

In this section we investigate what happens under sampled-data design. We show that feedback passivation under sampling can be preserved under digital control by

means of a new output map, for which the sampled-data system is passive, which depends on the sampling period. In particular, we show that whenever the continuous-time dynamics is feedback passive, then passivation under sampling can be always pursued.

Consider the input-affine continuous-time dynamics of the form

$$\dot{x} = f(x) + g(x)u \tag{3.30}$$

with $x \in \mathbb{R}^n$, $u \in \mathbb{R}$ and a desired equilibrium

$$x_\star \in \{x \in \mathbb{R}^n \text{ s.t. } g^\perp(x)f(x) = 0\}$$

which might be assigned to the closed-loop system under the following assumption.

Assumption 1. The dynamics (3.30) is *feedback passive*; i.e., there exist smooth functions $\gamma : \mathbb{R}^n \to \mathbb{R}$, $h_d : \mathbb{R}^n \to \mathbb{R}$ and $H_d : \mathbb{R}^n \to \mathbb{R}_{\geq 0}$ such that the feedback law

$$u = \gamma(x) + v \tag{3.31}$$

makes the closed-loop system

$$\dot{x} = f_d(x) + g(x)v \tag{3.32a}$$
$$y = h_d(x) \tag{3.32b}$$

passive with

$$f_d(x) := f(x) + g(x)\gamma(x)$$
$$h_d(x) := \mathrm{L}_g H_d(x)$$

and storage function $H_d(\cdot)$, namely the dissipation inequality below holds for all $t \geq 0$ and $x_0 \in \mathbb{R}^n$

$$H_d(x(t)) - H_d(x_0) \leq \int_0^t y(s)v(s)\mathrm{d}s. \tag{3.33}$$

Remark 3.5.1. Let us recall that feedback passivation is basically used to stabilize under feedback the closed-loop system to a desired equilibrium $x_\star$ verifying for a fixed function $H_d : \mathbb{R}^n \to \mathbb{R}$ $H_d(x_\star) = 0$. In addition when ZSD is guaranteed with respect

to the new output map $h_d(x)$, the desired equilibrium can be stabilized through damping injection setting $v = -\kappa h_d(x)$ with $\kappa > 0$. As a matter of fact, one verifies

$$\dot{H}_d(x) = \underbrace{\mathrm{L}_{f_d} H_d(x)}_{\leq 0} + v \underbrace{\mathrm{L}_g H_d(x)}_{= h_d(x)} \leq -\kappa \|h_d(x)\|^2 \tag{3.34}$$

and thus asymptotic stability of $x_\star$ for (3.32).

3.5.1 Problem statement: feedback passivation under sampling

Given a continuous-time dynamics (3.30) assumed feedback passive (Assumption 1), than the control objective is to compute a digital feedback $\bar{u} = \gamma^\delta(x)$ with

$$u = \bar{u} + v \tag{3.35}$$

making the closed-loop sampled-data equivalent model

$$x^+(\bar{u} + v) = x + F^\delta(x, \gamma^\delta(x) + v) \tag{3.36}$$

passive for all $k \geq 0$; i.e. under $u = \bar{u} + v$ the closed-loop system verifies the dissipation inequality

$$H_d(x^+(\bar{u} + v)) - H_d(x) \leq v h_d^\delta(x, v),$$

with a suitably defined passifying output map

$$y = h_d^\delta(x, v).$$

In this respect, in what follows we do show that Assumption 1 guarantees feedback passivity of the dynamics (3.30) under digital feedback with the same storage function $H_d(\cdot)$ as in continuous time. In particular, the solution we propose is constructive and based on the notion of Input-H_d-Matching ($\mathrm{IH}_d\mathrm{M}$).

The idea of matching at the sampling instants a target continuous-time the dynamics by means of a piecewise constant feedback is given by Monaco and Normand-Cyrot (2006). In particular, setting the closed-loop continuous-time system as a target dynamics the control design stands in reproducing the target behaviour of

the closed-loop under sampled-data feedback. A solution to this problem is however unfeasible in general under a singe-rate control, and an involvement of a multi-rate control is needed. Afterwords, it has been proposed in ?Tanasa et al. (2015) the idea of matching exclusively a target input-output behavior at the sampling instants; i.e, in Lyapunov-based stabilization it is proposed to match through a piecewise constant feedback the Lyapunov function behaviour under ideal continuous-time feedback at all the sampling instants $k\delta$ for $k \geq 0$. This technique is referred to as Input-Lyapunov Matching (ILM) under digital control. On the basis of this idea, the notion of Input-H_d-Matching ($\mathrm{IH}_d\mathrm{M}$) extends ILM to suitable storage function $H_d(x) : \mathbb{R}^n \to \mathbb{R}_{\geq 0}$ verifying $H_d(x_\star) = 0$.

.

3.5.2 Digital passivation and stabilization

Before stating the main result, the following Proposition is recalled from Tanasa et al. (2015) aimed at reproducing, at all sampling instant $t = k\delta$ for $k \geq 0$, the evolution of the storage function $H_d(\cdot)$ along the closed-loop dynamics (3.32) for $v = 0$.

Proposition 3.5.1. *Let the continuous-time system (3.30) verifies Assumption 1 with storage function $H_d : \mathbb{R}^n \to \mathbb{R}_{\geq 0}$ and $\mathrm{L}_g H_d(x) \neq 0$ for all $x \neq x_\star$. Then, there exists $T^\star > 0$ such that for all $\delta \in [0, T^\star[$ and $t = k\delta$, $k \geq 0$, the IH_dM equality*

$$H_d(x^+(u)) - H_d(x) = \int_{k\delta}^{(k+1)\delta} \mathrm{L}_{f_d} H_d(x(s))\mathrm{d}s \tag{3.37}$$

with $x(s) = e^{s\mathrm{L}_{f_d}} I_d|_{x_k}$ admits unique solution $u = \gamma^\delta(x)$ as a series expansion in powers of δ around $\gamma(\cdot)$; namely,

$$\gamma^\delta(x) = \sum_{i>0} \frac{\delta^i}{(i+1)!} \gamma^i(x). \tag{3.38}$$

Remark 3.5.2. The left and right hand sides of (3.37) define, respectively, the increment between two successive sampling instants of $H_d(x)$ over the sampled-data dynamics (3.36) and the continuous-time one (3.32) when both initialized, at each step $k \geq 0$, as $x(k\delta) = x_k$. Roughly speaking, the feedback $\gamma^\delta(\cdot)$ ensures at all sampling instants matching of the energy dissipation along the closed-loop system (3.32).

The IH$_d$M feedback is implicitly defined by the nonlinear IH$_d$M equality (3.37) so that seeking for exact solutions might be tough. However, as it is always the case in the sampled-data context a unique solution admitting the series expansion of series (8.15) can be computed through an iterative procedure solving, at each step, a linear equation in the unknown $\gamma^i(x)$. For the first terms, one gets

$$\begin{aligned}\gamma^1(x) &= \mathrm{L}_{f_d}\gamma(x)\\ \gamma^2(x) &= \mathrm{L}^2_{f_d}\gamma(x) + \frac{\mathrm{L}_{ad_f g}H_d(x)}{2\mathrm{L}_g H_d(x)}\mathrm{L}_{f_d}\gamma(x)\end{aligned} \tag{3.39}$$

so that as $\delta \to 0$, $\gamma^\delta(x) \to \gamma(x)$ and recovers the continuous-time solution.

We are ready to state the theorem concerning the feedback passivation under sampling.

Theorem 3.5.1: Feedback passivation under sampling

Let the continuous-time dynamics

$$\dot{x} = f(x) + g(x)u \tag{3.40}$$

verify Assumption 1 with storage function $H_d : \mathbb{R}^n \to \mathbb{R}_{\geq 0}$ such that $\mathrm{L}_g H_d(x) \neq 0$ for all $x \neq x_\star$. Then, the dynamics (3.40) is feedback passive under digital feedback; namely, the control (3.35), that is

$$u = \bar{u} + v$$

with $\bar{u} = \gamma^\delta(x)$ solution to the IH$_d$M equality (3.37) makes the closed-loop sampled-data equivalent model

$$x^+(\bar{u} + v) = x + F^\delta(x, \gamma^\delta(x) + v) \tag{3.41}$$

passive with storage function $H_d(\cdot)$ and output map $Y^\delta_{d_{\mathrm{av}}}(\bar{u})(x, v)$ being the v-average output from $\bar{u}$ of the form

$$Y^\delta_{d_{\mathrm{av}}}(\bar{u})(x, v) = g_d^{\delta\top}(x, v)\bar{\nabla}H_d\big|^{x^+(\bar{u}+v)}_{x^+(\bar{u})} \tag{3.42}$$

with map

$$g^\delta_d(x, v) = \frac{1}{\delta v}\left(F^\delta(x, \gamma^\delta(x) + v) - F^\delta(x, \gamma^\delta(x))\right),$$

verifying

$$vY^{\delta}_{d_{\text{av}}}(\bar{u})(x,v) = \int_0^v Y(x^+(\bar{u}+w),(\bar{u}+w))\mathrm{d}w.$$

In addition, if $H_d(x_\star) = 0$ and the continuous-time system with output $y = h_d(x)$ is ZSD, then the damping feedback $v = v^{\delta}_{\text{di}}(x)$ defined as the unique solution to the implicit damping equality

$$v + \kappa Y^{\delta}_{d_{\text{av}}}(\bar{u})(x,v) = 0, \quad \kappa > 0 \tag{3.43}$$

makes $x_\star$ asymptotically stable in closed loop.

Proof. First, let us prove that (3.36) with output (3.42) is made passive by the IH$_d$M control (3.35). By Assumption 1 $\mathrm{L}_{f_d} H_d(x) \leq 0$ and the feedback $\gamma^\delta(\cdot)$ solution to (3.37) ensures $H_d(x + F^\delta(x,\gamma^\delta(x))) - H_d(x) \leq 0$. As a consequence, exploiting the discrete gradient and the definition of u-average passivity from $\bar{u}$, one gets the dissipation inequality

$$\begin{aligned}
H_d(x^+(u)) - H_d(x) &= H_d(x^+(\bar{u}+v)) - H_d(x^+(\bar{u})) + H_d(x^+(\bar{u})) - H_d(x) \\
&\leq H_d(x^+(\bar{u}+v)) - H_d(x^+(\bar{u})) \\
&\leq H_d(x + F^\delta(x,\gamma^\delta(x)+v)) - H_d(x + F^\delta(x,\gamma^\delta(x))) \\
&= v g_d^{\delta\top}(x,v)\bar{\nabla} H_d\big|_{x^+(\bar{u})}^{x^+(\bar{u}+v)} \\
&= v Y^{\delta}_{d_{\text{av}}}(\bar{u})(x,v)
\end{aligned}$$

and equivalently that

$$\begin{aligned}
H_d(x^+(u)) - H_d(x) &= H_d(x^+(\bar{u})) - H_d(x) + H_d(x^+(u)) - H_d(x^+(\bar{u})) \\
&\leq \frac{1}{u-\bar{u}} \int_{\bar{u}}^{u} Y(x^+(w),w)\mathrm{d}w \\
&= \frac{1}{v} \int_0^v Y(x^+(\bar{u}+w),(\bar{u}+w))\mathrm{d}w = v Y_{d_{\text{av}}}(\bar{u})(x,v),
\end{aligned}$$

thus the result. The existence of a solution to the damping equality (3.43) is guaranteed by the implicit function theorem (because $\mathrm{L}_g H_d(x) \neq 0$ for all $x \neq x_\star$). Accordingly, substituting $v = v^\delta(x)$ into the dissipation inequality above and exploiting (3.43) one gets

$$H_d(x^+(u)) - H_d(x) \leq -\|Y^{\delta}_{d_{\text{av}}}(\bar{u})(x,v)\|^2$$

so that asymptotic stability of $x_\star$ follows from ZSD in continuous time along the lines of Monaco and Normand-Cyrot (2011). □

Remark 3.5.3. The sampled-data output (3.42) providing passivity for the closed-loop sampled-data system admits a power expansion in powers of δ; rewriting

$$g_d^\delta(x,v) = \sum_{i\geq 0} \frac{\delta^i}{(i+1)!} g_d^i(x,v)$$

with $g_d^0(x) = g(x)$ and $g_d^1(x,v) = (\mathrm{L}_{f_d} + v\mathrm{L}_\mathrm{g})\mathrm{L}_g x + \mathrm{L}_g\mathrm{L}_f x + \gamma(x)\mathrm{L}_g^2 x$, one gets for the first terms

$$Y_{d_\mathrm{av}}^\delta(\bar{u})(x,v) = h_d(x) + \frac{\delta}{2}\Big((\mathrm{L}_{f_d} + v\mathrm{L}_g)h_d(x) + \nabla^\top H_d(x)(\mathrm{L}_g\mathrm{L}_f + \gamma(x)\mathrm{L}_g^2)\Big)x + O(\delta^2).$$

The stabilizing controller, setting $v = v^\delta(x)$ solution to (3.43), gets the form series expansion in powers of δ

$$v^\delta(x) = v^0(x) + \sum_{i>0} \frac{\delta^i}{(i+1)!} v^i(x) \tag{3.44}$$

with, for the first terms

$$\begin{aligned} v^0(x) =& -\kappa h_d(x) \\ v^1(x) =& -\kappa(\mathrm{L}_{f_d} + v^0(x)\mathrm{L}_g)v^0(x) \\ & -\kappa\nabla^\top H_d(x)(\mathrm{L}_g\mathrm{L}_f + \gamma(x)\mathrm{L}_g^2)x. \end{aligned}$$

As a consequence, the stabilizing controller $u^\delta(x) = \gamma^\delta(x) + v^\delta(x)$ consists of two components: the passifying feedback, based on $\mathrm{IH}_d\mathrm{M}$, plus output damping for asymptotic stabilization. It can be shown that such a control ensures *one-step consistency* of the closed-loop system Nešić et al. (1999). However, as commented so far, exact forms for the stabilizing controller might not be computed so that only approximate solutions are implemented in practice. Accordingly, we define the p^{th} order approximate solution of the final feedback as truncations of the corresponding series expansions at any finite order p in δ; i.e., setting the so-called *correcting terms* $u^i(x) = \gamma^i(x) + v^i(x)$

$$u_{[p]}^\delta(x) = \gamma(x) - \kappa h_d(x) + \sum_{i=1}^{p} \frac{\delta^i}{(i+1)!} u^i(x). \tag{3.45}$$

Remark 3.5.4. Consistency under the exact solution allows to deduce that those controllers ensure practical asymptotic stability of the closed-loop system, as shown in Tanasa et al. (2015); namely, convergence to a ball containing the origin of radius in $O(\delta^{p+1})$. In particular, setting $p = 0$ in (3.45), one recovers the standard emulation-based solution as the continuous-time feedback directly implemented through ZOH devices. Along the lines of Tanasa et al. (2015), it can be shown that increasing the approximation order of the controller (i.e., $p > 0$) significantly improves the stabilizing performances in closed loop for the dissipation matching by reducing the residual error in (3.37) in $O(\delta^{p+2})$.

3.5.3 Illustrative example: Backstepping as feedback passivation

In this section we illustrate how feedback passivation under sampling is instrumental in the continuous-time backstepping design, see Kokotovic (1992), by means of a two dimensional cascade system.

Consider the continuous-time two dimensional system of the form

$$\dot{x}_1 = x_1^2 - x_1^3 + x_2 \tag{3.46a}$$

$$\dot{x}_2 = u, \tag{3.46b}$$

As discussed in Khalil (2014), to backstep the dynamics (3.46) set the change of coordinates $z_2 = x_2 + x_1 + x_1^2$ for which (3.46) is transformed into

$$\dot{x}_1 = -x_1 - x_1^3 + z_2 \tag{3.47a}$$

$$\dot{z}_2 = u - (1 + 2x_1)(x_1 + x_1^3 - z_2). \tag{3.47b}$$

Continuous-time design

As presented in Khalil (2014), the control

$$u = \gamma(x_1, z_2) + v$$

applied to the transformed dynamics (3.47), with backstepping feedback

$$\gamma(x_1, z_2) = -x_1 + (1 + 2x_1)(x_1 + x_1^3 - z_2) - z_2, \tag{3.48}$$

yields a closed-loop system of the form

$$\dot{x}_1 = -x_1 - x_1^3 + z_2 \tag{3.49a}$$

$$\dot{z}_2 = -x_1 - z_2 + v, \tag{3.49b}$$

that is feedback passive with respect to the storage function $H(x_1, z_2) = \frac{1}{2}x_1 + \frac{1}{2}z_2$ and passive output

$$y = h(x_1, z_2) = z_2, \tag{3.50}$$

namely the storage function along (3.49) satisfies

$$\dot{H}(x_1, z_2) = -d(x_1, z_2) + vy \tag{3.51}$$

with $d(x_1, z_2) = x_1^2 + x_1^4 + z_2^2$.

Sampled-data design

According to Theorem 3.5.1, one can compute the digital feedback for which the feedback passivation under sampling is ensured; i.e., one computes a digital feedback

$$u_k = \gamma^\delta(x_{1k}, z_{2k}) + v_k \tag{3.52}$$

with the digital feedback $\gamma^\delta(x_k)$ given in (8.15) specified for the first two terms as follows

$$\gamma^\delta(x_{1k}, z_{2k}) = \gamma(x_{1k}, z_{2k}) + \frac{\delta}{2}\gamma_1(x_{1k}, z_{2k}) + O(\delta^2) \tag{3.53}$$

with

$$\gamma_1(x_{1k}, z_{2k}) = (z_{2k} - x_{1k}^3 - x_{1k})(8x_{1k}^3 + 3x_{1k}^2 + 4x_{1k} - 2z_{2k}) + 2(x_{1k} + 1)(x_{1k} + z_{2k}).$$

The control (3.52) yields a closed-loop sampled-data dynamics of the form

$$\begin{aligned} x_{1k+1} &= x_{1k} - \delta(x_{1k}^3 + x_{1k} - z_{2k}) + \frac{\delta^2}{2}v_k \\ &\quad - \frac{\delta^2}{2}(-3x_{1k}^5 - 4x_{1k}^3 + 3z_{2k}x_{1k}^2 + 2z_{2k}) + O(\delta^3) \end{aligned} \tag{3.54a}$$

$$\begin{aligned} z_{2k+1} &= z_{2k} - \delta(x_{1k} + z_{2k}) + \frac{\delta^2}{2}x_{1k}(x_{1k}^2 + 2) \\ &\quad + \delta v_k + \frac{\delta^2}{2}v_k(2x_{1k} + 1) + O(\delta^3). \end{aligned} \tag{3.54b}$$

According to Theorem 3.5.1, the closed-loop sampled-data system (3.54) is feedback passive with respect to the same storage function of the continuous-time design, i.e. $H(x_{1k}, z_{2k}) = \frac{1}{2}x_{1k} + \frac{1}{2}z_{2k}$, but with modified output map of the form (3.42) and specified as follows

$$Y^{\delta}_{d_{\text{av}}}(\bar{u})(x_{1k},z_{2k}, v_k) = z_{2k} + \frac{\delta}{2}(v_k - x_{1k} - z_{2k} + 2x_{1k}z_{2k}) + O(\delta^2).$$

Clearly, the above modified output, which is affected by the feedthrough term v_k, differs from the one in (3.50) at the sampling instants. However, the above modified output map $Y^{\delta}_{d}(\bar{u})(x_{1k}, z_{2k}, v_k)$ is obtained from the truncation in $O(\delta^2)$ of the inner product between the input map

$$g^{\delta}_{d}(x_{1k}, z_{2k}) = \begin{pmatrix} 0 \\ 1 \end{pmatrix} + \frac{\delta}{2}\begin{pmatrix} 1 \\ 2x_{1k} + 1 \end{pmatrix} + O(\delta^2)$$

and the discrete gradient given by

$$\bar{\nabla} H|^{x^+(\bar{u}+v)}_{x^+(\bar{u})} = \frac{1}{2}(e^{\delta(f+(\gamma^{\delta}+v_k)g)}I_d|_{x_k} + e^{\delta(f+\gamma^{\delta}g)}I_d|_{x_k}),$$

which yields for the first terms the following expression,

$$\begin{aligned}\bar{\nabla} H|^{x^+(\bar{u}+v)}_{x^+(\bar{u})} = \begin{pmatrix} x_{1k} \\ z_{2k} \end{pmatrix} &+\delta \begin{pmatrix} z_{2k} - x_{1k} - x^3_{1k} \\ \frac{v_k}{2} - x_{1k} - z_{2k} \end{pmatrix} \\ &+ \frac{\delta^2}{2}\begin{pmatrix} \frac{v_k}{2} - 2z_{2k} + 4x^3_{1k} + 3x^5_{1k} - 3x^2_{1k}z_{2k} \\ \frac{v_k}{2} + 2x_{1k} + x^3_{1k} + vx_{1k} \end{pmatrix} + O(\delta^3).\end{aligned}$$

Finally, the digital control (3.52), that provides feedback passivation under sampling, yields the following discrete EB equation of the form

$$H_d(x_{1k+1}, z_{2k+1}) - H_d(x_{1k}, z_{2k}) = -\delta d(x_{1k}, z_{1k}) + \delta v Y^{\delta}_{d_{\text{av}}}(\bar{u})(x_{1k},z_{2k}, v_k)$$

with supply rate given by

$$vY^{\delta}_{d_{\text{av}}}(\bar{u})(x_{1k}, z_{2k}, v_k) = z_{2k}v_k + \frac{\delta}{2}(v^2_k - x_{1k}v_k - z_{2k}v_k) + \delta x_{1k}z_{2k}v_k + O(\delta^2)$$

and dissipation term described by

$$d(x_{1k}, z_{1k}) = x^4_{1k} + x^2_{1k} + z^2_{2k} + \delta(2x^6_{1k} + 3x^4_{1k} - 2x^3_{1k}z_{2k} + x^2_{1k} + z^2_{2k}) + O(\delta^2).$$

3.6 Concluding remarks

At first, we have recalled the notion of sampled-data equivalent model and DDR forms under sampling. Then the notion of passivity, u-average passivity, and passivity based control have been restated in the sampled-data framework. Further, it has been shown that feedback passivation can be preserved under sampled-data control with respect to the same target storage function as in continuous time and suitably modified output mapping, which takes the form of a v-average output from $\bar{u}$. The result is appealing for systems that may not be passive in open-loop. The proposed method has been illustrated on the celebrated backstepping stabilization design Kokotovic (1992), by means of an academic example, providing computational aspects of the proposed sampled-data feedback in terms of feedback passivation under sampling. The result given in Section 3.5 is partially contained in:

> *M. Mattioni, A. Moreschini, S. Monaco and D. Normand-Cyrot, "On feedback passivation under sampling", 2021 American Control Conference (ACC).*

Part II

PORT-HAMILTONIAN SYSTEMS IN DISCRETE TIME

Chapter 4

Modeling of discrete-time port-Hamiltonian systems

Contents

4.1 Port-Hamiltonian systems in discrete time **110**

4.1.1 A new definition 110

4.1.2 A port-Hamiltonian representation proposed in the literature 115

4.1.3 The case of quadratic Hamiltonians 116

4.2 Dirac structures of port-Hamiltonian systems in DT **118**

4.2.1 Discrete-time Dirac structures 119

4.2.2 Port-Hamiltonian systems as Dirac structures 121

4.2.3 Power-preserving interconnection 123

4.2.4 An illustrative example: the mechanical isolation system . 129

4.3 Concluding remarks **131**

In this chapter, a novel definition of port-Hamiltonian systems is introduced in a pure discrete-time setting. Firstly, we give a proper definition of discrete-time port-Hamiltonian system exploiting the notions of DDR and discrete gradient function. Then, we compare the proposed model with a comparable discrete-time port-Hamiltonian system proposed in the literature. Accordingly, we associate a proper Dirac structure to the proposed discrete-time port-Hamiltonian system. Finally, the notion of power-preserving interconnection between u-average pas-

sive system is used to show that the power-preserving interconnection of two port-Hamiltonian systems is again a port-Hamiltonian system. The chapter ends with an example concerning the computation of flow and efforts associated with a mechanical isolation system.

4.1 Port-Hamiltonian systems in discrete time

In this section, inspired from the fact that several applications require models that describe physical phenomena in a pure discrete-time domain instead of discrete-time models obtained by the sampling of a smooth system, a novel class of discrete port-Hamiltonian systems is proposed referring to the DDR form (2.6) along with the discrete gradient function.

4.1.1 A new definition

To begin with, consider the case of autonomous dynamics.

Definition 4.1.1. Given a differentiable real valued Hamiltonian function $H(\cdot) : \mathbb{R}^n \to \mathbb{R}_{\geq 0}$, a discrete-time autonomous port-Hamiltonian dynamics over $\mathbb{R}^n$ can be described by the implicit state space representation

$$x^+ = x + (J(x) - R(x))\bar{\nabla} H|_x^{x^+} \tag{4.1}$$

with $x \in \mathbb{R}^n$, n-dimensional matrices $J(x) = -J^\top(x)$ and $R(x) = R^\top(x) \succeq 0$ catching, respectively, the (power-preserving) interconnection and dissipative structure of the dynamics.

The autonomous port-Hamiltonian representation recovers the models of the literature introduced in McLachlan et al. (1999). This model has been further exploited in a sampled-data context in Yalçin et al. (2015); Aoues et al. (2017) extending also the structure to controlled dynamics.

Discrete-time port-Hamiltonian dynamics of the form (4.1) verify by construction energy properties as described in the proposition below.

Proposition 4.1.1. *Consider the Hamiltonian dynamics* (4.1)*, then, the following properties hold*

P1. *the dynamics* (4.1) *is dissipative with respect to* $H(x)$*, that is*

$$H(x^+) - H(x) = -\bar{\nabla}H^\top|_x^{x^+} R(x)\bar{\nabla}H|_x^{x^+} \leq 0, \quad \forall x \in \mathbb{R}^n; \tag{4.2}$$

P2. *the dynamics* (4.1) *is conservative with respect to* $H(x)$ *for zero dissipation term* $R(\cdot) = 0$*, that is*

$$H(x^+) - H(x) = 0, \quad \forall x \in \mathbb{R}^n; \tag{4.3}$$

P3. *any critical point* $x_\star$ *of* $H(x)$ *is an equilibrium of* (4.1)*;*

P4. *if* $H(x_\star) \leq H(x)$ *for all* x *in the neighborhood of* $x_\star$*, then the equilibrium point* $x_\star$ *is stable and* $H(x)$ *serves (at least locally) as a Lyapunov function for the stable equilibrium of* (4.1)*. If* $\{x_\star\}$ *is the largest invariant set for which*

$$\bar{\nabla}H^\top|_x^{x^+} R(x)\bar{\nabla}H|_x^{x^+} = 0,$$

then $x_\star$ *is asymptotically stable.*

Proof. By computing the forward difference of $H(\cdot)$ along (4.1) one gets

$$\begin{aligned} H(x^+) - H(x) &= (x^+ - x)^\top \bar{\nabla}H|_x^{x^+} \\ &= ((J(x) - R(x))\bar{\nabla}H|_x^{x^+})^\top \bar{\nabla}H|_x^{x^+} \\ &= -\bar{\nabla}H^\top|_x^{x^+} R(x)\bar{\nabla}H|_x^{x^+} \leq 0, \end{aligned}$$

so that **P1** and **P2** immediately follow. Any critical point $x_\star$ of $H(x)$ verifies that $\bar{\nabla}H|_{x_\star}^{x_\star} = \nabla H(x_\star) = 0$, so that along (4.1) yields $x_{k+1} = x_k = x_\star$, thus **P3** is verified.

To prove **P4** on might infer by stability theory, if the critical point $x_\star$ is a minimum of the Hamiltonian $H(x)$ then the dynamics is stable in the sense of Lyapunov and the condition $H(x_\star) \leq H(x)$ holds true for all x. Additionally, by Barbashin-Krasovskii theorem, $x_\star$ is an asymptotically stable equilibrium as the dissipation is strictly negative outside the set $\{x_\star\}$, that is

$$H(x^+) - H(x) = -\bar{\nabla}H^\top|_x^{x^+} R(x)\bar{\nabla}H|_x^{x^+} < 0, \quad \forall x \in \mathbb{R}^n \setminus \{x_\star\}.$$

□

Let us now extend the Definition 4.1.1 to controlled dynamics so defining an input-state-output port-Hamiltonian system in discrete time (or simply port-Hamiltonian system).

Definition 4.1.1: Discrete-time port-Hamiltonian system

Given a differentiable real-valued function $H(\cdot) : \mathbb{R}^n \to \mathbb{R}_{\geq 0}$, a discrete-time port-Hamiltonian system over $\mathbb{R}^n$, with $u \in \mathbb{R}$, is described in DDR form as

$$x^+ = x + (J(x) - R(x))\bar{\nabla} H|_x^{x^+} \tag{4.4a}$$

$$\frac{\partial x^+(u)}{\partial u} = G(x^+(u), u) \quad \text{with} \quad x^+(0) = x^+ \tag{4.4b}$$

$$Y(\cdot, u) = \mathrm{L}_{G(\cdot,u)} H(\cdot) \tag{4.4c}$$

or equivalently in the map form as

$$x^+(u) = x + (J(x) - R(x))\bar{\nabla} H|_x^{x^+} + g(x, u)u \tag{4.5a}$$

$$Y_{\mathrm{av}}(x, u) = g^\top(x, u)\bar{\nabla} H|_{x^+}^{x^+(u)} \tag{4.5b}$$

with matrices $J(x) = -J^\top(x)$ and $R(x) = R^\top(x) \succeq 0$ and map

$$g(x, u)u := \int_0^u G(x^+(v), v)\mathrm{d}v.$$

Some general comments on the proposed structure:

- The controlled port-Hamiltonian dynamics

  $$x^+(u) = x + (J(x) - R(x))\bar{\nabla} H|_x^{x^+} + g(x, u)u,$$

  is computed by blending the autonomous implicit port-Hamiltonian dynamics, that is the difference equation (4.4a) which yields a leap at the instant (k), along with the differential equation (4.20b) which models the effect of the control variable u.

- The control map $G(\cdot, u)$ is assumed to exist and thus, as usual for DDR forms, a discrete-time port-Hamiltonian dynamics in the form of a map (5.1a) can be deduced through integration of (4.20b) between 0 and u with initial condition $x^+(0) = x^+$.

■ Discrete port-Hamiltonian dynamics of the form (4.4) arises with energy properties in terms of u-average passivity in straight relation with the definition of discrete gradient function. Exploiting the integral form for the Hamiltonian function (2.11), that is

$$H(x^+(u)) = H(x^+(0)) + \int_0^u \mathrm{L}_{G(.,v)} H(x^+(v))\mathrm{d}v,$$

for computing the forward difference of the Hamiltonian function $H(x)$ along the dynamics (4.4), one directly gets the *u-average energy balance* equality between two time steps as

$$\underbrace{H(x^+(u)) - H(x)}_{\text{stored energy}} = -\underbrace{\bar{\nabla}H^\top|_x^{x^+} R(x)\bar{\nabla}H|_x^{x^+}}_{\text{dissipated energy}} + \underbrace{\int_0^u Y(x^+(v),v)\mathrm{d}v}_{\text{supplied energy}}, \quad (4.6)$$

and equivalently *energy balance* between two time steps as

$$\underbrace{H(x^+(u)) - H(x)}_{\text{stored energy}} = -\underbrace{\bar{\nabla}H^\top|_x^{x^+} R(x)\bar{\nabla}H|_x^{x^+}}_{\text{dissipated energy}} + \underbrace{ug^\top(x,u)\bar{\nabla}H\big|_{x^+}^{x^+(u)}}_{\text{supplied energy}}, \quad (4.7)$$

holding for all $(x,u) \in \mathbb{R}^n \times \mathbb{R}$, which is in the entire time horizon $[0,k]$

$$\underbrace{H(x_k) - H(x_0)}_{\text{total stored energy}} = \underbrace{-\sum_{i=0}^{k-1} \bar{\nabla}^\top H|_{x_i}^{x_i^+} R(x_i)\bar{\nabla}H|_{x_i}^{x_i^+}}_{\text{total dissipated energy}} + \underbrace{\sum_{i=0}^{k-1} u_i g^\top(x_i,u_i)\bar{\nabla}H\big|_{x_i^+}^{x_i^+(u_i)}}_{\text{total supplied energy}},$$

where the dissipated energy, that is defined by a dissipation matrix and a discrete gradient characterizing the autonomous dynamics, is not depending on the variable u, and the supplied energy contains all the effect of the control variable u with a discrete gradient computed between the autonomous dynamics x^+ and the controlled system $x^+(u)$.

On this basis the following theorem can be proved.

Theorem 4.1.1

Given a discrete-time port-Hamiltonian system (4.4) with Hamiltonian $H(\cdot) : \mathbb{R}^n \to \mathbb{R}_{\geq 0}$, then the following holds:

(i) the dynamics (4.4) with output (4.4c) is u-average passive with dissipation rate

$$d(x) := \bar{\nabla} H^\top|_x^{x^+} R(x) \bar{\nabla} H|_x^{x^+} \geq 0,$$

and *u-average energy balance* equality between two time steps as

$$H(x^+(u)) - H(x) = -d(x) + \int_0^u Y(x^+(v), v)\mathrm{d}v, \tag{4.8}$$

(ii) the dynamics (4.4) is u-average lossless for zero dissipation $R(\cdot) = 0$;

(iii) the average output to (4.4c) for which dynamics (4.4) is passive is given by (4.5b) and achieve the *energy balance* equality between two time steps as

$$H(x^+(u)) - H(x) = -d(x) + u g^\top(x, u) \bar{\nabla} H\big|_{x^+}^{x^+(u)}; \tag{4.9}$$

(iv) the u-average output (4.5b) associated with (4.4c) recovers the discrete gradient of the Hamiltonian $H(\cdot)$ between x^+ and $x^+(u)$; i.e.

$$Y_{\mathrm{av}}(x, u) = \frac{H(x^+(u)) - H(x^+(0))}{u} = g^\top(x, u) \bar{\nabla} H|_{x^+}^{x^+(u)}.$$

Proof. (i) and (ii) follow from the energy dissipation inequality,

$$\begin{aligned} H(x^+(u)) - H(x) &= H(x^+) - H(x) + H(x^+(u)) - H(x^+) \\ &= -\bar{\nabla} H^\top|_x^{x^+} R(x) \bar{\nabla} H|_x^{x^+} + H(x^+(u)) - H(x^+) \\ &\leq H(x^+(u)) - H(x^+) \\ &= \int_0^u Y(x^+(v), v)\mathrm{d}v = u Y_{\mathrm{av}}(x, u) \end{aligned}$$

holding with a strict equality for zero dissipation $R(\cdot) = 0$ (due to Proposition (4.1.1)). From Proposition 4.1.1, one has that $H(x^+) - H(x) = -\bar{\nabla} H^\top|_x^{x^+} R(x) \bar{\nabla} H|_x^{x^+} = -d(x)$ whereas, by definition of discrete gradient function (Definition 2.1.1) one gets that

$$H(x^+(u)) - H(x^+) = (x^+(u) - x^+)^\top \bar{\nabla} H|_{x^+}^{x^+(u)}$$

with $x^+(u) - x^+ = g(x,u)u$, then (iii) and (iv) are proved simply computing

$$H(x^+(u)) - H(x^+) = ug^\top(x,u)\bar{\nabla}H|_{x^+}^{x^+(u)} = uY_{\mathrm{av}}(x,u),$$

with by definition of u-average passivity providing the average output as in Lemma 2.2.1 which yields

$$Y_{\mathrm{av}}(x,u) = \frac{1}{u}\int_0^u Y(x^+(v),v)\mathrm{d}v = g^\top(x,u)\bar{\nabla}H|_{x^+}^{x^+(u)}.$$

□

Theorem 4.1.1 expresses that the energy is non-increasing (conservative) or decreasing (dissipative) up to an isolated minimum of $H(x)$ and the change of internal energy is governed by both the energy-storage and energy-dissipation. Moreover, it is shown that, as usual in continuous time, port-Hamiltonian systems arise with straightforward energy interpretation and direct passivity property. However, those features naturally involve, in discrete time, u-average passivity arguments. Moreover, in this scenario, the u-average output (4.5b) comes in terms of the discrete gradient evaluated along the controlled evolution in a way that is strictly reminiscent of the continuous-time counterpart.

4.1.2 A port-Hamiltonian representation proposed in the literature

The introduced discrete port-Hamiltonian system (4.5), based on the DDR form of a discrete-time system, comes with a very particular structure which differs from the representation given in Aoues et al. (2017) arising with a structure of the form

$$x^+(u) = x + (J(x) - R(x))\bar{\nabla}H|_x^{x^+(u)} + g(x,u)u \tag{4.10a}$$

$$y_\ell(x,u) = g^\top(x,u)\bar{\nabla}H|_x^{x^+(u)}. \tag{4.10b}$$

This port-Hamiltonian structure essentially differs from the proposed structure in (4.5) in many aspects:

- the port-Hamiltonian dynamics (4.10a) arises with a discrete gradient $\bar{\nabla}H|_x^{x^+(u)}$ which is affected by the control variable u, while the proposed model (4.5) arises with a discrete gradient of the form $\bar{\nabla}H|_x^{x^+}$ which is used to characterize the autonomous dynamics;

- the passive output (4.10b) associated with the port-Hamiltonian dynamics (4.10a), again arises with a discrete gradient $\bar{\nabla} H|_x^{x^+(u)}$, while the proposed passive output arises with a discrete gradient of the form $\bar{\nabla} H|_{x^+}^{x^+(u)}$ which encodes the rate of change produced by the control variable u;

- unlike the proposed model which clearly splits the effect of the input source into the energy balance equation with respect to the autonomous behavior (say the energy balance (4.8)), the system (4.10) yields an associated energy balance

$$\underbrace{H(x^+(u)) - H(x)}_{\text{stored energy}} = \underbrace{-\bar{\nabla} H^\top|_x^{x^+(u)} R(x) \bar{\nabla} H|_x^{x^+(u)}}_{\text{dissipation + partial supplied}} + \underbrace{u y_\ell(x,u)}_{\text{partial supplied energy}} \tag{4.11}$$

  where by construction the dissipated energy includes internal dissipation (due to control-free dynamics) and an input-dependent component (due to discrete gradient $\bar{\nabla} H|_x^{x^+(u)}$).

It results that the energy balance equality (4.11) which comes from (4.10) does not decouple in the total energy the contribution given by the external source from the internal dissipated energy. Then, this may be a problem in characterizing the contribution of the input source into the energy balance equality and thus in designing energy-based control strategies in discrete-time which are computed over the energy-balance equality.

4.1.3 The case of quadratic Hamiltonians

It is worth to emphasize that the discrete port-Hamiltonian system (4.1) yields an implicit dynamics with respect to the coordinate x^+. An explicit representation is in general tough to determine as such form directly depends on the nonlinearity of the Hamiltonian function except for some polynomial cases. An important class is associated with a quadratic Hamiltonian function, that is

$$H(x) = \frac{1}{2} x^\top P x \tag{4.12}$$

with symmetric and positive definite matrix P, that is $P = P^\top \succ 0$.

The following proposition holds and his proof is based on the definition of discrete gradient.

Proposition 4.1.2. *Given a quadratic Hamiltonian function $H(\cdot) : \mathbb{R}^n \to \mathbb{R}_{\geq 0}$ of the form* (4.12)*, then the associated discrete-time port-Hamiltonian system is described in DDR form as*

$$x^+ = x + \frac{1}{2}(J(x) - R(x))P(x + x^+) \tag{4.13a}$$

$$\frac{\partial x^+(u)}{\partial u} = G(x^+(u), u) \quad \textit{with} \quad x^+(0) = x^+ \tag{4.13b}$$

$$Y(x, u) = G^\top(x, u)Px \tag{4.13c}$$

or equivalently in the map form as

$$x^+(u) = x + \frac{1}{2}(J(x) - R(x))P(x^+ + x) + g(x, u)u \tag{4.14a}$$

$$Y_{av}(x, u) = g^\top(x, u)Px^+ + \frac{u}{2}g^\top(x, u)Pg(x, u) \tag{4.14b}$$

with matrices $J(x) = -J^\top(x)$ and $R(x) = R^\top(x) \succeq 0$ and vector field

$$g(x, u)u := \int_0^u G(x^+(v), v)\mathrm{d}v.$$

Accordingly, if $(I - \frac{1}{2}(J(\cdot) - R(\cdot))P)$ is invertible for each entry, then there exists an explicit form for the free dynamics (4.13a) *that is*

$$x^+ = F_0(x) = (I - \frac{1}{2}(J(x) - R(x))P)^{-1}(I + \frac{1}{2}(J(x) - R(x))P)x, \tag{4.15}$$

so that the controlled dynamics (4.14a) *yields*

$$x^+(u) = (I - \frac{1}{2}(J(x) - R(x))P)^{-1}(I + \frac{1}{2}(J(x) - R(x))P)x + ug(x, u). \tag{4.16}$$

Proof. The port-Hamiltonian dynamics (4.13a) (and thus (4.14a)) are obtained by substituting the discrete gradient between x and x^+ of the quadratic Hamiltonian $H(x) = \frac{1}{2}x^\top Px$, that is

$$\bar{\nabla}H|_x^{x^+} = \frac{1}{2}P(x + x^+).$$

Accordingly, the conjugate output (4.14b) is simply achieved by manipulating the discrete gradient between x^+ and $x^+(u)$, so that

$$\begin{aligned} Y_{\text{av}}(x,u) &= g^\top(x,u)\bar{\nabla}H|_{x^+}^{x^+(u)} \\ &= \frac{1}{2}g^\top(x,u)P(x^+ + x^+(u)) \\ &= \frac{1}{2}g^\top(x,u)P(2x^+ + ug(x,u)) \\ &= g^\top(x,u)Px^+ + \frac{u}{2}g^\top(x,u)Pg(x,u). \end{aligned}$$

Finally, the explicit dynamics is simply obtained by expressing x^+ due to the particular form of the discrete gradient associated with the quadratic Hamiltonian function. □

Remark 4.1.1. Computing the difference of the Hamiltonian function one step ahead one gets the relation

$$H(x^+(u)) - H(x) = -d(x) + ug^\top(x,u)PF_0(x) + \frac{u^2}{2}g^\top(x,u)Pg(x,u),$$

with quadratic dissipation term

$$d(x) = \frac{1}{4}(F_0(x) + x)^\top P^\top R(x)P(F_0(x) + x) \geq 0$$

for all $x \in \mathbb{R}^n$, and vector field $F_0(x)$ given in (4.15).

4.2 Dirac structures of port-Hamiltonian systems in discrete time

The concept of Dirac structure is essential for validating the implicit discrete-time port-Hamiltonian representation here introduced and set the bridge with discrete Dirac structure oriented modeling. We show hereinafter how to properly define Dirac structures associated with the definition of port-Hamiltonian systems we proposed.

4.2.1 Discrete-time Dirac structures

Given a differentiable real-valued function $H(\cdot) : \mathcal{X} \to \mathbb{R}$, the port variables of the Dirac structure associated with the energy storing elements are denoted by (f_S, e_S), two vectors of equal dimension with their product $e_S^\top f_S$ denoting the total power flowing into the Dirac from the energy-storing element. More in detail:

- the vector of flow variables is given by the first order difference

  $$x(k+1) - x(k)$$

  that is the rate of change of x;

- the vector of effort variables of the energy-storing element is given by the discrete gradient $\bar{\nabla} H|_{x(k)}^{\cdot}$ which is an element of its dual space of $\mathcal{X}$;

- the interconnection of energy-storing elements to storage ports of the Dirac structure is accomplished by

  $$\begin{aligned} f_S(k) &= -(x(k+1) - x(k)), \\ e_S(k) &= \bar{\nabla} H|_{x(k)}^{x(k+1)}. \end{aligned}$$

Hence, the energy balance for the energy-storing multi-port can be written as

$$\begin{aligned} H(x(k+1)) - H(x(k)) &= \bar{\nabla}^\top H|_{x(k)}^{x(k+1)}(x(k+1) - x(k)) \\ &= -e_S(k)^\top f_S(k), \end{aligned}$$

where $\bar{\nabla}^\top H|_{x(k)}^{x(k+1)}(x(k+1) - x(k))$ is the power flowing into the energy storing while $e_S(k)^\top f_S(k)$ is the power flowing into the Dirac structure.

The second multiport corresponds to internal energy dissipation with port variables denoted as (f_R, e_R) determined by a static relation $\mathcal{R} \in \mathcal{F}_R \times \mathcal{E}_R = 0$ such that $e_R^\top f_R \leq 0$, that is the power flowing into the Dirac structure. Thus, the condition

$$e_S(k)^\top f_S(k) + e_R(k)^\top f_R(k) = 0 \tag{4.17}$$

leads by substitution to

$$\begin{aligned} H(x(k+1)) - H(x(k)) &= -e_S(k)^\top f_S(k) \\ &= e_R(k)^\top f_R(k) \leq 0. \end{aligned} \tag{4.18}$$

Flows	Efforts
$f_S(k) = -(x^+ - x(k))$	$e_S(k) = \bar{\nabla} H\|_{x(k)}^{x^+}$
$f_R(k) = g_R^\top(x(k)) \bar{\nabla} H\|_{x(k)}^{x^+}$	$e_R(k) = -r(x(k)) f_R(k)$
$f_C(k) = -(x^+(u(k)) - x^+)$	$e_C(k) = \bar{\nabla} H\|_{x^+}^{x^+(u(k))}$
$f_I(k) = Y_{\mathrm{av}}(x(k), u(k))$	$e_I(k) = u(k)$

Table 4.1

The external ports (f_P, e_P) model the interaction of the system with its environment. Thus (4.17) extends to

$$e_S(k)^\top f_S(k) + e_R(k)^\top f_R(k) + e_P(k)^\top f_P(k) = 0$$

and the variation (4.18) to

$$\begin{aligned} H(x(k+1)) - H(x(k)) &= -e_S(k)^\top f_S(k) \\ &= e_R(k)^\top f_R(k) + e_P(k)^\top f_P(k) \leq e_P(k)^\top f_P(k) \end{aligned} \tag{4.19}$$

expressing that the increase of the internally stored energy is less or equal to the externally supplied power. The external port (f_P, e_P) can be split into control port (f_C, e_C) and external interaction (f_I, e_I) so getting the energy balance

$$H(x(k+1)) - H(x(k)) = e_R(k)^\top f_R(k) + e_C(k)^\top f_C(k) + e_I(k)^\top f_I(k).$$

In conclusion one sets the following definition.

Definition 4.2.1. Let a state space $\mathcal{X}$ and an Hamiltonian function $H(\cdot) : \mathcal{X} \to \mathbb{R}$ defining energy storage. A port-Hamiltonian system on $\mathcal{X}$ is defined by a Dirac structure

$$\mathcal{D} \subset \mathcal{X} \times \mathcal{X}^\star \times \mathcal{F}_R \times \mathcal{E}_R \times \mathcal{F}_P \times \mathcal{E}_P$$

with energy storing port $(f_S, e_S) \in \mathcal{X} \times \mathcal{X}^\star$ and a resistive structure $(f_R, e_R) \in \mathcal{F}_R \times \mathcal{E}_R$. Its dynamics is specified by

$$\Big(-(x(k+1) - x(k)), \bar{\nabla}^\top H\|_{x(k)}^{x(k+1)}, f_R(k), e_R(k), f_P(k), e_P(k) \Big) \in \mathcal{D}(k)$$
$$(f_R(k), e_R(k)) \in \mathcal{R}(k).$$

4.2.2 Port-Hamiltonian systems as Dirac structures

The following theorem specifies the Dirac structure associated with the discrete-time port-Hamiltonian structure described in Definition 4.1.1.

Theorem 4.2.1: Port-Hamiltonian systems as Dirac structures

The port-Hamiltonian system defined in Definition 4.1.1, that is in DDR form as

$$x^+ = x + (J(x) - R(x))\bar{\nabla}H|_x^{x^+} \tag{4.20a}$$

$$\frac{\partial x^+(u)}{\partial u} = G(x^+(u), u) \quad \text{with} \quad x^+(0) = x^+ \tag{4.20b}$$

$$Y(\cdot, u) = \mathrm{L}_{G(\cdot,u)}H(\cdot) \tag{4.20c}$$

or equivalently in the map form as

$$x^+(u) = x + (J(x) - R(x))\bar{\nabla}H|_x^{x^+} + g(x,u)u \tag{4.21a}$$

$$Y_{\mathrm{av}}(x,u) = g^\top(x,u)\bar{\nabla}H|_{x^+}^{x^+(u)} \tag{4.21b}$$

is a port-Hamiltonian system with power conjugate input-output pair $(u, Y_{\mathrm{av}}(x,u))$ and Dirac structure

$$\mathcal{D} \subset \mathcal{X} \times \mathcal{X}^\star \times \mathcal{F}_R \times \mathcal{E}_R \times \mathcal{F}_C \times \mathcal{E}_C \times \mathcal{F}_I \times \mathcal{E}_I$$

with flow and effort variables in Table 4.1 satisfying the energy balance

$$e_S(k)^\top f_S(k) + e_R(k)^\top f_R(k) + e_P(k)^\top f_P(k) = 0$$

with $e_P(k)^\top f_P(k) = e_C(k)^\top f_C(k) + e_I(k)^\top f_I(k)$. The Dirac structure is given by the skew-symmetric graph map specified below, omitting the k-dependency:

$$\begin{bmatrix} f_S \\ f_R \\ f_C \\ f_I \end{bmatrix} = \begin{bmatrix} -J(x) & -g_R(x) & 0 & 0 \\ g_R^\top(x) & 0 & 0 & 0 \\ 0 & 0 & 0 & -g(x,e_I) \\ 0 & 0 & g^\top(x,e_I) & 0 \end{bmatrix} \begin{bmatrix} e_S \\ e_R \\ e_C \\ e_I \end{bmatrix},$$

with dissipation given by $R(x) = g_R(x)r(x)g_R^\top(x)$ with matrix $r(x) = r^\top(x) \succeq 0$, and the input matrix $g_R(x)$ corresponding to the resistive port.

Proof. The proof works out by comparing the energy balance written in the Dirac setting:

$$e_S(k)^\top f_S(k) + e_R(k)^\top f_R(k) + e_P(k)^\top f_P(k) = 0$$

with $H(x^+(u(k)) - H(x(k))$ decomposed according to the properties of the discrete gradient as

$$\begin{aligned} H(x^+(u(k)) - H(x(k)) &= H(x^+(u(k))) - H(x^+) + H(x^+) - H(x(k)) \\ &= -e_C(k)^\top f_C(k) - e_S(k)^\top f_S(k) \end{aligned}$$

with

$$\begin{aligned} -e_S(k)^\top f_S(k) &= \bar{\nabla}^\top H|_{x(k)}^{x^+}(x^+ - x(k)) \\ -e_C(k)^\top f_C(k) &= \bar{\nabla}^\top H|_{x^+}^{x^+(u(k))}(x^+(u(k)) - x^+). \end{aligned}$$

By definition of the output $y(x,u)$, one gets

$$\begin{aligned} e_I(k)^\top f_I(k) &= \bar{\nabla}^\top H|_{x^+}^{x^+(u(k))}(x^+(u(k)) - x^+) \\ &:= \int_0^{u(k)} \mathrm{L}_{G(\cdot,v)} H(x^+(v))dv := u(k)Y_{\mathrm{av}}(x(k),u(k)) \end{aligned}$$

with $f_I = g(x,u)^\top \bar{\nabla} H|_{x^+}^{x^+(u)}$, $e_I = u$, which concludes $e_C^\top f_C + e_I^\top f_I = 0$. Regarding the resistive part one verifies

$$\begin{aligned} -e_S^\top f_S &= \bar{\nabla}^\top H|_x^{x^+}(x^+ - x) = \bar{\nabla}^\top H|_x^{x^+}(J(x) - R(x))\bar{\nabla} H|_x^{x^+} \\ &= -\bar{\nabla}^\top H|_x^{x^+} R(x)\bar{\nabla} H|_x^{x^+} = -\bar{\nabla}^\top H|_x^{x^+} g_R(x) r(x) g_R^\top(x)\bar{\nabla} H|_x^{x^+} = e_R^\top f_R \end{aligned}$$

which finally concludes $e_S^\top f_S + e_R^\top f_R = 0$ and

$$e_S(k)^\top f_S(k) + e_R(k)^\top f_R(k) + e_P(k)^\top f_P(k) = 0.$$

□

Remark 4.2.1. Theorem 4.2.1 proves that the average output defines properly a power conjugate variable because the product with $u(k)$ is a unity of power,

$$u(k)Y_{\mathrm{av}}(x(k),u(k)) = \int_0^{u(k)} \mathrm{L}_{G(\cdot,v)} H(x^+(v))dv = e_I(k)^\top f_I(k).$$

The following lemma holds true and provides u-average passivity of the structure.

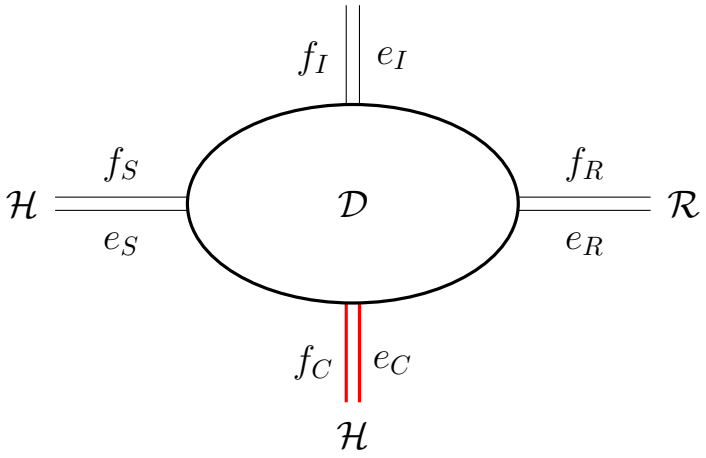

Figure 4.1: Dirac structure having energy-storing port $(f_S, e_S) \in \mathcal{F}_S \times \mathcal{E}_S$, energy-incoming port $(f_C, e_C) \in \mathcal{F}_C \times \mathcal{E}_C$, energy-outgoing port $(f_I, e_I) \in \mathcal{F}_I \times \mathcal{E}_I$, and inner energy-dissipated port $(f_R, e_R) \in \mathcal{F}_R \times \mathcal{E}_R$.

Lemma 4.2.1. *Given a port-Hamiltonian system* (4.5) *with Hamiltonian function* $H : \mathbb{R}^n \to \mathbb{R}_{\geq 0}$*, then the following holds true*

$$H(x^+(u)) - H(x) = e_R^\top f_R - e_C^\top f_C \leq e_I^\top f_I. \tag{4.22}$$

4.2.3 Power-preserving interconnection

This section discusses the preservation of the discrete port-Hamiltonian structure after the interconnection process between discrete port-Hamiltonian systems. Particular attention is given to the ways in which new composed systems can be formed from given families of systems by means of interconnections. Exploiting the fact that the composition of Dirac structures, say the power-conserving interconnection of Dirac structures, again defines a Dirac structure, we conclude that the so defined feedback interconnection of port-Hamiltonian systems again exhibits a port-Hamiltonian structure in discrete time.

Let first recall the composition of Dirac structure.

Definition 4.2.2 (van der Schaft (2000))**.** Given two Dirac structures ($\mathcal{D}_1$,$\mathcal{D}_2$) defined respectively on $\mathcal{F}_1 \times \mathcal{F}_C$ and $\mathcal{F}_C \times \mathcal{F}_2$ where $\mathcal{F}_C$ is the space of shared flow and

Flows	Efforts
$f_{C_{v_i}} = -(x^+(\bar{u}_i + v_i) - x^+(\bar{u}_i))$	$e_{C_{v_i}} = \bar{\nabla} H_i \vert_{x^+(\bar{u}_i)}^{x^+(\bar{u}_i+v_i)}$
$f_{I_i} = Y_{i\mathrm{av}}(\bar{u}_i)(x_i, v_i)$	$e_{I_i} = v_i$

Table 4.2

effort. Their composition is defined on $\mathcal{F}_1 \times \mathcal{F}_2$ under the interconnection constraint

$$f_{C_1} = -f_{C_2}$$
$$e_{C_1} = e_{C_2}$$

or equivalently

$$e_{C_1}^\top f_{C_1} + e_{C_2}^\top f_{C_2} = 0 \tag{4.23}$$

on the shared flows and efforts (f_{C_1}, e_{C_1}) and (f_{C_2}, e_{C_2}).

The definition above describes the composition of Dirac structure. An important result concerns the fact that the composition of two Dirac structures recovers the power-preserving interconnection presented in Definition 2.4.1.

Lemma 4.2.2. *The composition of Dirac structures satisfying the equality* (4.23) *equals the power-preserving interconnection described in Definition 2.4.1, namely*

$$e_{C_1}^\top f_{C_1} + e_{C_2}^\top f_{C_2} \equiv \int_0^{\bar{u}_1} Y_1(x_1^+(s), s)\mathrm{d}s + \int_0^{\bar{u}_2} Y_2(x_2^+(s), s)\mathrm{d}s \equiv 0.$$

The Lemma above expresses the concept of energy conservation of two dynamics Σ_1 and Σ_2 under interconnection; that is, the power supplied by Σ_2 to Σ_1 is compensated by the one supplied by Σ_1 to Σ_2. This rewrites by definition of conjugate output the external power balance equation

$$\bar{u}_1 Y_{1\mathrm{av}}(x_1, \bar{u}_1) + \bar{u}_2 Y_{2\mathrm{av}}(x_2, \bar{u}_2) = 0,$$

where the i-th conjugate output is the u-average output with respect to the map $Y_i(x_i^+(u_i), u_i)$.

The following result holds.

Theorem 4.2.1. *Given two port-Hamiltonian systems* $(\Sigma_{d1}, \Sigma_{d2})$ *of the form* (4.21)*, their feedback interconnection*

$$(\bar{u}_1, \bar{u}_2) = (-Y_{2av}(x_2, \bar{u}_2), Y_{1av}(x_1, \bar{u}_1)),$$

is a port-Hamiltonian system defined on $\mathcal{X}_1 \times \mathcal{X}_2$ *with Hamiltonian* $H(\cdot) = H_1(\cdot) + H_2(\cdot)$*; i.e.*

$$\begin{aligned} x_1^+(\bar{u}_1) &= x_1 + (J_1(x_1) - R_1(x_1))\bar{\nabla} H_1|_{x_1}^{x_1^+} - g_1(x_1, \bar{u}_1) g_2^\top(x_2, \bar{u}_2) \bar{\nabla} H_2|_{x_2^+}^{x_2^+(\bar{u}_2)} \\ x_2^+(\bar{u}_2) &= x_2 + (J_2(x_2) - R_2(x_2))\bar{\nabla} H_2|_{x_2}^{x_2^+} + g_2(x_2, \bar{u}_2) g_1^\top(x_1, \bar{u}_1) \bar{\nabla} H_1|_{x_1^+}^{x_1^+(\bar{u}_1)}. \end{aligned}$$

The associated Dirac structure is defined by the skew-symmetric extended graph

$$\begin{bmatrix} f_S \\ f_R \\ f_{C_{\bar{u}}} \end{bmatrix} = \begin{bmatrix} -\mathbf{J} & -\mathbf{g_R} & 0 \\ \mathbf{g_R}^\top & 0 & 0 \\ 0 & 0 & \mathbf{Q} \end{bmatrix} \begin{bmatrix} e_S \\ e_R \\ e_{C_{\bar{u}}} \end{bmatrix}$$

with flows $f_S = (f_{S_1}, f_{S_2})$*,* $f_R = (f_{R_1}, f_{R_2})$*,* $f_{C_{\bar{u}}} = (f_{C_{\bar{u}_1}}, f_{C_{\bar{u}_2}})$*, efforts* $e_S = (e_{S_1}, e_{S_2})$*,* $e_R = (e_{R_1}, e_{R_2})$*,* $e_{C_{\bar{u}}} = (e_{C_{\bar{u}_1}}, e_{C_{\bar{u}_2}})$ *and*

$$\begin{aligned} \mathbf{J}(x) &:= \begin{bmatrix} J_1(x_1) & 0 \\ 0 & J_2(x_2) \end{bmatrix}, \qquad \mathbf{g_R}(x) := \begin{bmatrix} g_{R1}(x_1) & 0 \\ 0 & g_{R2}(x_2) \end{bmatrix}, \\ \mathbf{Q}(x, \bar{u}) &:= \begin{bmatrix} 0 & g_1(x_1, \bar{u}_1) g_2^\top(x_2, \bar{u}_2) \\ -g_2(x_2, \bar{u}_2) g_1^\top(x_1, \bar{u}_1) & 0 \end{bmatrix}, \end{aligned}$$

with dissipation given by $R_i(x_i) = g_{Ri}(x_i) r_i(x_i) g_{Ri}^\top(x_i)$ *matrix* $r_i(x_i) = r_i^\top(x_i) \succeq 0$*, and the input matrix* $g_{Ri}(x)$ *corresponding to the resistive port.*

Proof. First, we note that according to the Definition 2.4.1 and Definition 4.2.2, the feedback interconnection of two port-Hamiltonian system according to

$$\begin{aligned} \bar{u}_1 &= -Y_{2\text{av}}(x_2, \bar{u}_2) \\ \bar{u}_2 &= Y_{1\text{av}}(x_1, \bar{u}_1) \end{aligned}$$

is power preserving and recovers the composition of the associated Dirac. On one hand, the algebraic constraint $\bar{u}_1 Y_{1\text{av}}(x_1, \bar{u}_1) + \bar{u}_2 Y_{2\text{av}}(x_2, \bar{u}_2)$ rewrites in the Dirac structures as $e_{I_1}^\top f_{I_1} + e_{I_2}^\top f_{I_2} = 0$. On the other hand, the port in the external supplied

part which refers to the power-conserving feedback interconnection is properly the pair (e_{I_1}, f_{I_1}) in the Dirac structure $\mathcal{D}_1$ and $(e_{C_{2\bar{u}_2}}, f_{C_{2\bar{u}_2}})$ in the Dirac structure $\mathcal{D}_2$. Because a Dirac composition (power preserving) is characterized by the constraints

$$e_{I_1}^\top f_{I_1} = e_{C_{2\bar{u}_2}}^\top f_{C_{2\bar{u}_2}}$$
$$e_{I_2}^\top f_{I_2} = -e_{C_{1\bar{u}_1}}^\top f_{C_{1\bar{u}_1}}$$

and by definition

$$e_{I_1}^\top f_{I_1} + e_{C_{1\bar{u}_1}}^\top f_{C_{1\bar{u}_1}} = 0$$
$$e_{I_2}^\top f_{I_2} + e_{C_{2\bar{u}_2}}^\top f_{C_{2\bar{u}_2}} = 0,$$

one gets the equality

$$e_{C_{1\bar{u}_1}}^\top f_{C_{1\bar{u}_1}} + e_{C_{2\bar{u}_2}}^\top f_{C_{2\bar{u}_2}} = 0 \tag{4.24}$$

which is nothing else than a power-preserving feedback interconnection between the two associated port-Hamiltonian systems. Accordingly, a solution is given by $f_{C_{1\bar{u}_1}} = -e_{C_{2\bar{u}_2}}$ and $e_{C_{1\bar{u}_1}} = f_{C_{2\bar{u}_2}}$. Moreover any system Σ_{d1} and Σ_{d2} contains under feedback additional terms of the form $g_1 g_2^\top \bar{\nabla} H_2 \big|_{x_2^+}^{x_2^+(\bar{u}_2)}$ and $g_2 g_1^\top \bar{\nabla} H_1 \big|_{x_1^+}^{x_1^+(\bar{u}_1)}$ respectively which compose a skew-symmetric matrix due to the flows $f_{C_{\bar{u}_1}}, f_{C_{\bar{u}_2}}$ satisfying the skew-symmetric graph

$$f_{C_{\bar{u}}} = \mathbf{Q}(x, \bar{u}) e_{C_{\bar{u}}}.$$

It results that even if the internal interconnection matrix is modified, the power-balance equality remains unchanged. □

Accordingly, the following extended result holds.

Theorem 4.2.2: Power-preserving interconnection

The interconnection between two port-Hamiltonian systems $(\Sigma_{d1}, \Sigma_{d2})$ under

$$u_1 = \bar{u}_1 + v_1$$
$$u_2 = \bar{u}_2 + v_2$$

with power-preserving feedback

$$\bar{u}_1 = -Y_{2\text{av}}(x_2, \bar{u}_2)$$
$$\bar{u}_2 = Y_{1\text{av}}(x_1, \bar{u}_1),$$

is again a port-Hamiltonian system with Hamiltonian $H(x_1, x_2) = H_1(x_1) + H_2(x_2)$; i.e.

$$x_1^+(u_1) = x_1 + (J_1(x_1) - R_1(x_1))\bar{\nabla}H_1|_{x_1}^{x_1^+} - g_1(x_1)g_2^\top(x_2)\bar{\nabla}H_2|_{x_2^+}^{x_2^+(\bar{u}_2)} + v_1\tilde{g}_1(x_1, \bar{u}_1, v_1)$$
$$x_2^+(u_1) = x_2 + (J_2(x_2) - R_2(x_2))\bar{\nabla}H_2|_{x_2}^{x_2^+} + g_2(x_2)g_1^\top(x_1)\bar{\nabla}H_1|_{x_1^+}^{x_1^+(\bar{u}_1)} + v_2\tilde{g}_2(x_1, \bar{u}_2, v_2)$$
$$Y_{1\text{av}}(\bar{u}_1)(x_1, v_1) = \tilde{g}_1^\top(x_1, \bar{u}_1, v_1)\bar{\nabla}H_1|_{x_1^+(\bar{u}_1)}^{x_1^+(\bar{u}_1+v_1)}$$
$$Y_{2\text{av}}(\bar{u}_2)(x_2, v_2) = \tilde{g}_2(x_1, \bar{u}_2, v_2)\bar{\nabla}H_2|_{x_2^+(\bar{u}_2)}^{x_2^+(\bar{u}_2+v_2)}$$

with $(\bar{u}_i + v_i)g_i(x_i, \bar{u}_i + v_i) = \bar{u}_i g_i(x_i, \bar{u}_i) + v_i\tilde{g}_i(x_i, \bar{u}_i, v_i)$. The associated Dirac structure is defined by the skew-symmetric graph composed by

$$\begin{bmatrix} f_S \\ f_R \\ f_{C_{\bar{u}}} \\ f_{C_{\bar{v}}} \\ f_I \end{bmatrix} = \begin{bmatrix} -\mathbf{J} & -\mathbf{g_R} & 0 & 0 & 0 \\ \mathbf{g_R}^\top & 0 & 0 & 0 & 0 \\ 0 & 0 & \mathbf{Q} & 0 & 0 \\ 0 & 0 & 0 & 0 & -\mathbf{g} \\ 0 & 0 & 0 & \mathbf{g}^\top & 0 \end{bmatrix} \begin{bmatrix} e_S \\ e_R \\ e_{C_{\bar{u}}} \\ e_{C_{\bar{v}}} \\ e_I \end{bmatrix}$$

with flows $f_S = (f_{S_1}, f_{S_2})$, $f_R = (f_{R_1}, f_{R_2})$, $f_{C_{\bar{u}}} = (f_{C_{\bar{u}_1}}, f_{C_{\bar{u}_2}})$, $f_{C_{\bar{v}}} = (f_{C_{\bar{v}_1}}, f_{C_{\bar{v}_2}})$, $f_I = (f_{I_1}, f_{I_2})$, efforts $e_S = (e_{S_1}, e_{S_2})$, $e_R = (e_{R_1}, e_{R_2})$, $e_{C_{\bar{u}}} = (e_{C_{\bar{u}_1}}, e_{C_{\bar{u}_2}})$, $e_{C_{\bar{v}}} = (e_{C_{\bar{v}_1}}, e_{C_{\bar{v}_2}})$, $e_I = (e_{I_1}, e_{I_2})$ with the additional part

$$\mathbf{g}(x, \bar{u}, v) := \begin{bmatrix} g_1(x_1, \bar{u}_1 + v_1) & 0 \\ 0 & g_2(x_2, \bar{u}_2 + v_2) \end{bmatrix}$$

The power conjugate output vector is again composed by each v_i-average from $\bar{u}_i$ output associated with $\mathrm{L}_{\bar{G}_i(\cdot, u_i)}H_i$; i.e.

$$Y_{\text{av}}(\bar{u}_i)(x_i, v_i) = \frac{1}{v_i}\int_0^{v_i} \mathrm{L}_{\bar{G}_{i(\cdot, \bar{u}_i + w)}}H_i(x^+(\bar{u}_i + w))dw.$$

Proof. Setting $u_i = \bar{u}_i + v_i$, the proof is based on the fact that the composition of two Dirac structures satisfies the constraint (4.23), each one described according

to the energy balance

$$e_{\bar{S}_i}^\top f_{\bar{S}_i} + e_{R_i}^\top f_{R_i} + e_{P_i}^\top f_{P_i} = 0$$

with decomposition of the stored and resistive port according to the preliminary feedback $\bar{u}_i$ as

$$e_{\bar{S}_i}^\top f_{\bar{S}_i} = e_{S_i}^\top f_{S_i} + e_{C_{i\bar{u}_i}}^\top f_{C_{i\bar{u}_i}}$$

and external interconnection

$$e_{P_i}^\top f_{P_i} = e_{\bar{C}_{v_i}}^\top f_{C_{v_i}} + e_{I_i}^\top f_{I_i}.$$

The energy balance of each Dirac structure associated with the interconnected structure is thus given by the sum

$$e_{S_i}^\top f_{S_i} + e_{R_i}^\top f_{R_i} + e_{C_{i\bar{u}_i}}^\top f_{C_{i\bar{u}_i}} + e_{\bar{C}_{v_i}}^\top f_{C_{v_i}} + e_{I_i}^\top f_{I_i} = 0$$

with by skew-symmetric graph $e_{C_{1\bar{u}_1}}^\top f_{C_{1\bar{u}_1}} + e_{C_{2\bar{u}_2}}^\top f_{C_{2\bar{u}_2}} = 0$, so concluding for the sum

$$\begin{aligned} e_{S_1}^\top f_{S_1} + e_{S_2}^\top f_{S_2} &= -e_{R_1}^\top f_{R_1} - e_{R_2}^\top f_{R_2} \\ &= \bar{\nabla}^\top H_1|_{x_1}^{x_1^+} R_1(x_1) \bar{\nabla} H_1|_{x_1}^{x_1^+} + \bar{\nabla}^\top H_2|_{x_2}^{x_2^+} R_2(x_2) \bar{\nabla} H_2|_{x_2}^{x_2^+}, \end{aligned}$$

and

$$e_{I_{1v_1}}^\top f_{I_{1v_1}} + e_{I_{2v_2}}^\top f_{I_{2v_2}} = -e_{\bar{C}_{v_1}}^\top f_{C_{v_1}} - e_{\bar{C}_{v_2}}^\top f_{C_{v_2}} = v_1 Y_{1\mathrm{av}}(\bar{u}_1)(x_1, v_1) + v_2 Y_{2\mathrm{av}}(\bar{u}_2)(x_2, v_2)$$

with power

$$v_i Y_{I\mathrm{av}}(\bar{u}_i)(x_i, v_i) = v_i \tilde{g}_i(x, \bar{u}_i, v_i) \bar{\nabla} H_i|_{x_i^+(\bar{u}_1)}^{x_1^+(\bar{u}_1+v_1)} = \int_0^{v_i} \mathrm{L}_{G_{i(\cdot,\bar{u}_i+w)}}(x_i^+(\bar{u}_i + w)) dw.$$

□

The result establishes that any feedback interconnection of discrete port-Hamiltonian systems turns again in a discrete port-Hamiltonian system in the sense of (4.5). This provides a novel direction in controlling complex physical systems in a pure discrete domain taking into account different discrete gradients evaluated along intermediate values provided by the effort variables.

4.2.4 An illustrative example: the mechanical isolation system

The objective of this example is to illustrate the involved computations for constructing discrete port-Hamiltonian systems in a pure discrete-time setting. Although the resulting system is not a discretization of the continuous-time, the proposed method recasts the continuous-time energetic behavior by defining flows and efforts at a discrete level.

Consider a mechanical isolation system presented in Tang and Brennan (2013), which consists of a mass $m > 0$ and spring with stiffness $k > 0$, affected by a nonlinear damping force $F_d = \ell(q)\dot{q}$ moving as a harmonic oscillator. The damper causes energy dissipation through the nonlinear function

$$\ell(q) = \frac{bq^2}{a^2 + q^2},$$

where $a \geq 0$ denotes the length of the damper, $b \geq 0$ the damper coefficient, and q the position of the center of mass of m. Accordingly, the model involves a quadratic potential energy so that total energy function is given by

$$H(q,p) = \frac{k}{2}q^2 + \frac{1}{2m}p^2,$$

with $p = m\dot{q}$, where $\dot{q}$ is the velocity of the mass, one computes the associated discrete gradient function

$$\bar{\nabla}H|_{x}^{x^+} = \begin{pmatrix} \bar{\nabla}H|_{q}^{q^+} \\ \bar{\nabla}H|_{p}^{p^+} \end{pmatrix} = \begin{pmatrix} \frac{k}{2}(q^+ + q) \\ \frac{1}{2m}(p^+ + p) \end{pmatrix}.$$

A passive isolation system, in general contains mass, spring, and damping elements and moves as a harmonic oscillator. The mass and spring stiffness dictate a natural frequency of the system. Damping causes energy dissipation and has a secondary effect on natural frequency.

According to the Dirac structure we derive the discrete relation between the physical components in terms of flows and efforts, that is

$$\begin{cases} f_k &= q - q^+ \\ e_k &= \frac{k}{2}(q^+ + q) \end{cases},$$

$$\begin{cases} f_m &= p - p^+ \\ e_m &= \frac{1}{2m}(p^+ + p) \end{cases}.$$

Thus coupling them through a power-preserving interconnection, namely $e_k^\top f_k + e_m^\top f_m = 0$, one gets $e_m = -f_k$, $e_k = f_m$ which characterizes the exchange of energy among the components, one deduces the following implicit representation of a discrete mass-spring dynamics,

$$q^+ = q + \frac{1}{2m}(p^+ + p)$$
$$p^+ = p - \frac{k}{2}(q^+ + q).$$

Furthermore, to include the nonlinear resistive term $b(q)$ acting upon the Dirac structure so as the velocity of the mass is damped, define the resistive ports satisfying the power resistive relation

$$f_r^\top e_r = -\bar{\nabla}^\top H|_p^{p^+} \ell(q) \bar{\nabla} H|_p^{p^+}$$

so that the flow f_m of the mass becomes $f_m + f_r = e_k$ so yielding

$$q^+ = q + \frac{1}{2m}(p^+ + p) \tag{4.25}$$
$$p^+ = p - \frac{k}{2}(q^+ + q) - \frac{\ell(q)}{2m}(p^+ + p). \tag{4.26}$$

Again, to further control the velocity of the mass, one consider the addition external port $e_U = u$ and its conjugate external flow

$$f_I(k) = \bar{\nabla} H|_{p^+}^{p^+(u)} = \frac{1}{2m}(p^+(u) + p^+)$$

which provides the input-state-output port-Hamiltonian representation,

$$q^+(u) = q + \frac{1}{2m}(p^+ + p) \tag{4.27}$$
$$p^+(u) = p - \frac{k}{2}(q^+ + q) - \frac{\ell(q)}{2m}(p^+ + p) + u \tag{4.28}$$
$$Y_{\text{av}} = \frac{1}{2m}(p^+(u) + p^+). \tag{4.29}$$

The different behavior of the model computed over the discrete-time Dirac structure can be seen in Figure 4.2, respectively providing dissipation of energy for $b \neq 0$ and conservation of energy with $b = 0$. Note also that, the nonlinear damping in case of $a = 0$ yields the classical linear damping affecting the system.

Furthermore, when considering the interconnection of two mechanical systems of the form (4.27), the resulting power-preserving interconnection through $\bar{u}$ reads an

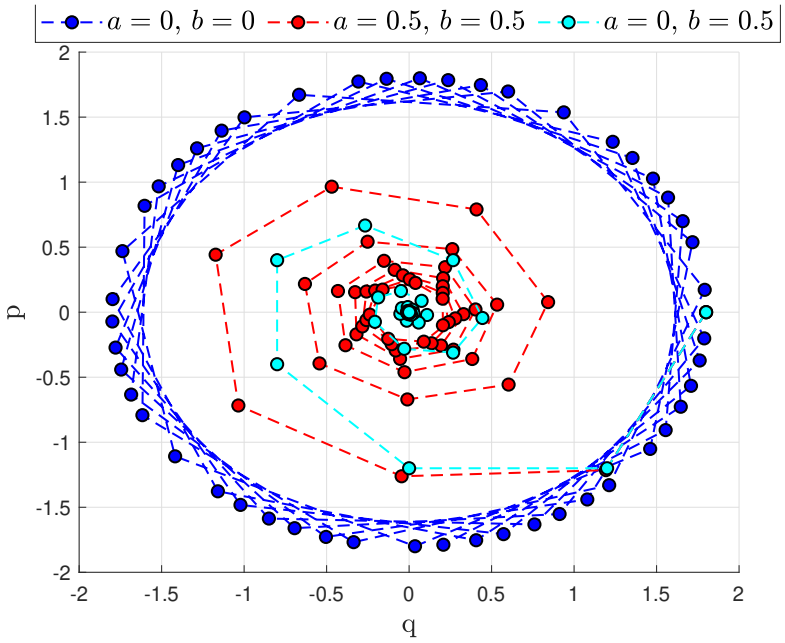

Figure 4.2: Phase portrait of (4.25) by varying the parameters a and b, with $m = k = 1$ and $x(0) = (1.8, 0)$.

interconnected system

$$
\begin{aligned}
q_1^+(\bar{u}_1) &= q_1 + \frac{1}{2m_1}(p_1^+ + p_1) \\
q_2^+(\bar{u}_2) &= q_2 + \frac{1}{2m_2}(p_2^+ + p_2) \\
p_1^+(\bar{u}_1) &= p_1 - \frac{k_1}{2}(q_1^+ + q_1) - \frac{\ell_1(q_1)}{2m_1}(p_1^+ + p_1) - \frac{1}{2m_2}(p_2^+(\bar{u}_2) + p_2^+) \\
p_2^+(\bar{u}_2) &= p_2 - \frac{k_2}{2}(q_2^+ + q_2) - \frac{\ell_2(q_2)}{2m_2}(p_2^+ + p_2) + \frac{1}{2m_1}(p_1^+(\bar{u}_1) + p_1^+),
\end{aligned}
$$

which is a discrete port-Hamiltonian system with total energy

$$H_c(q, p) = H_1(q_1, p_1) + H_2(q_2, p_2)$$

verifying $H_c(q^+(\bar{u}), p^+(\bar{u})) - H_c(q, p) \leq 0$ and clearly conservative $H_c(q^+(\bar{u}), p^+(\bar{u})) - H_c(q, p) = 0$ when resistive elements are set as $b_1 = b_2 = 0$.

4.3 Concluding remarks

In this section, inspired by the fact that several applications require models that describe physical phenomena in a pure discrete-time domain instead of discrete-time

models obtained by the sampling of a smooth system, a novel class of discrete port-Hamiltonian systems have been proposed referring to DDR form along with the discrete gradient function. We have seen that the proposed model, with respect to the literature model, comes with a straightforward energy interpretation and direct passivity property. However, those features naturally involve u-average passivity arguments. Accordingly, we have defined the Dirac structure associated with the introduced port-Hamiltonian system and we have identified its associated graph. Finally, by invoking the notion of power-preserving interconnection of u-average passive systems we have seen that the power-preserving interconnection of two port-Hamiltonian systems is again a port-Hamiltonian system, and the solution is achieved fact that the power-preserving interconnection of two systems recovers the composition of the respective Dirac structures. An illustrative example concerning a mechanical isolation system showed how to compute respectively flows and efforts associated with the system in a discrete-time setting. The results presented within this chapter are partially given in:

> *A. Moreschini, M. Mattioni, S. Monaco and D. Normand-Cyrot, "Discrete port-controlled Hamiltonian dynamics and average passivation," 2019 IEEE 58th Conference on Decision and Control (CDC), Nice, France, 2019, pp. 1430-1435, doi: 10.1109/CDC40024.2019.9029809.*
>
> *A. Moreschini, S. Monaco and D. Normand-Cyrot, "Dirac structures of discrete-time port-Hamiltonian systems," Submitted to IEEE Transactions on Automatic Control (TAC). (Under review)*

Chapter 5

Control of discrete-time port-Hamiltonian systems

Contents

5.1 Negative output feedback **134**

5.1.1 The Dirac structure under negative output feedback . . . 135

5.1.2 Some constructive aspects 138

5.1.3 The input-affine dynamics case with quadratic Hamiltonian 139

5.2 Interconnection and damping assignment **141**

5.2.1 Constructive aspects: an approximate IDA-PBC design . . 145

5.2.2 IDA-PBC for input-affine systems 147

5.3 Concluding remarks **149**

This chapter deals with the stabilization problem of port-Hamiltonian systems in discrete time introduced in the previous chapter. For, we discuss the negative output feedback design associated with this particular structure of the dynamics. Accordingly, we give a particular characterization of the stabilizing feedback in the case of input-affine port-Hamiltonian systems arising with a quadratic Hamiltonian function. Finally, we set the IDA-PBC problem in this discrete-time setting giving sufficient condition to solve the problem. Again, the result is specialized in the case of input-affine dynamics assuming a particular structure of the Hamiltonian function.

5.1 Negative output feedback

This section is devoted to present how u-average passivity and stability properties can be used to design passivity based controllers stabilizing the discrete port-Hamiltonian systems introduced in the previous section. Due to the nice passivity and u-average passivity properties of the discrete-time port-Hamiltonian system, it is considerably desirable to provide stabilization by its gain output-feedback. However, in this framework, the system comes with a passive output containing the feedthrough term, therefore the conjugate output of the system can not be directly injected into the closed-loop system but an implicit equality must be solved. Then the following theorem specializes the result given in Monaco and Normand-Cyrot (2011) in this discrete-time port-Hamiltonian framework.

This is set in the sequel.

Theorem 5.1.1: Negative output feedback in discrete time

Let the discrete port-Hamiltonian system

$$x^+(u) = x + (J(x) - R(x))\bar{\nabla}H\big|_x^{x^+} + g(x,u)u \tag{5.1a}$$

$$Y_{\text{av}}(x,u) = g^\top(x,u)\bar{\nabla}H\big|_{x^+}^{x^+(u)} \tag{5.1b}$$

be ZSD with $H(\cdot) : \mathbb{R}^n \to \mathbb{R}_{\geq 0}$, having a minimum in $x_\star$. Then, the feedback $u = \gamma(x)$ solution to the implicit damping equality

$$\gamma(x) + \kappa g^\top(x,\gamma(x))\bar{\nabla}H\big|_{x^+}^{x^+(\gamma(x))} = 0 \tag{5.2}$$

achieves asymptotic stabilization of the closed-loop equilibrium $x_\star$ with gain $\kappa > 0$.

Proof. It is directly deduced by the u-average dissipation inequality

$$H(x^+(u)) - H(x) \leq uY_{\text{av}}(x,u)$$

so that the solution $u = \gamma(x)$ to the implicit damping equality (5.2) ensures in closed-loop the negativity of difference $H(x^+(\gamma(x))) - H(x)$, namely one gets

$$H(x^+(\gamma(x))) - H(x) \leq -\kappa \left(g^\top(x,\gamma(x))\bar{\nabla}H\big|_{x^+}^{x^+(\gamma(x))}\right)^2 \leq 0,$$

for positive values of κ. As for Theorem 2.2.1, the points for which the above equality is zero coincides with those points belong to the set $\mathcal{K} := \{x \in \mathbb{R}^n \mid Y(x^+(0), 0) = 0\}$, so that, from ZSD condition, one concludes that $x_\star$ is asymptotically stable. □

Remark 5.1.1. The feedback solution to (5.2) can be equivalently seen as a negative u-average output feedback

$$Y_{\text{av}}(x, u) = g^\top(x, u)\bar{\nabla}H\big|_{x^+}^{x^+(u)} = \frac{1}{u}\int_0^u Y(x^+(v), v)\mathrm{d}v$$

with respect to the output map

$$Y(\cdot, u) = G^\top(\cdot, u)\nabla H(\cdot) = \mathrm{L}_{G(\cdot,u)}H(\cdot).$$

5.1.1 The Dirac structure under negative output feedback

Interestingly enough is the preservation of port-Hamiltonian structure under negative output feedback (5.2). We study the effect over the Dirac structure of the negative average output feedback $\bar{u}(x)$, defined as the solution with $\kappa > 0$ to the algebraic equality

$$\bar{u} + \kappa Y_{\text{av}}(x, \bar{u}) = 0 \tag{5.3}$$

that yields

$$\bar{u}^2 + \kappa \int_0^{\bar{u}} \mathrm{L}_{G(\cdot,v)}H(x^+(v))dv = 0.$$

We show that a Dirac structure and thus a port-Hamiltonian system is preserved in closed loop. The following result holds.

Theorem 5.1.2: Dirac structure under negative output feedback

Under the feedback $u = \bar{u} + v$ with negative average output feedback $\bar{u}(x)$ satisfying (5.3) and external input v, the system in (5.1a) that is

$$x^+(u) = x + (J(x) - R(x))\bar{\nabla}H|_x^{x^+} + g(x, u)u$$

is transformed into a PH system with Dirac structure described by the skew-

symmetric graph

$$\begin{bmatrix} f_S \\ f_R \\ f_{C_{\bar{u}}} \\ f_{R_{\bar{u}}} \\ f_{C_v} \\ f_I \end{bmatrix} = \begin{bmatrix} -J(x) & -g_R(x) & 0 & 0 & 0 & 0 \\ g_R^\top(x) & 0 & 0 & 0 & 0 & 0 \\ 0 & 0 & 0 & S(x,\bar{u}) & 0 & 0 \\ 0 & 0 & -S^\top(x,\bar{u}) & 0 & 0 & 0 \\ 0 & 0 & 0 & 0 & 0 & -\tilde{g}(x,\bar{u},v) \\ 0 & 0 & 0 & 0 & \tilde{g}^\top(x,\bar{u},v) & 0 \end{bmatrix} \begin{bmatrix} e_S \\ e_R \\ e_{C_{\bar{u}}} \\ e_{R_{\bar{u}}} \\ e_{C_v} \\ e_I \end{bmatrix} \tag{5.4}$$

with dissipation given by $R(x) = g_R(x)r(x)g_R^\top(x)$, $r(x) = r^\top(x) \geq 0$, input matrix $g_R(x)$ corresponding to the resistive port., $S(x,\bar{u}) = \kappa g(x,\bar{u})g^\top(x,\bar{u})$, $\tilde{g} = \tilde{g}(\cdot,\bar{u},v)$, satisfying $(\bar{u}+v)g(\cdot,\bar{u}+v) = \bar{u}g(\cdot,\bar{u}) + v\tilde{g}(\cdot,\bar{u},v)$ with $v = e_I$. Passivity holds with respect to the output map

$$Y_{\text{av}}(\bar{u})(x,v) = \frac{1}{v}\int_0^v \mathrm{L}_{G(\cdot,v)}H(x^+(\bar{u}+v))dv \tag{5.5}$$

that again can be rewritten in terms of the discrete gradient of the function $H(\cdot)$ between $x^+(\bar{u})$ and $x^+(\bar{u}+v)$; i.e.

$$vY_{\text{av}}(\bar{u})(x,v) = \tilde{g}^\top(x,\bar{u},v)\bar{\nabla}H|_{x^+(\bar{u})}^{x^+(\bar{u}+v)}$$

satisfying $vY_{\text{av}}(\bar{u})(x,v) = e_I^\top f_I$.

Proof. The proof works out showing first that a Dirac structure oh the port-Hamiltonian system is preserved under the feedback $\bar{u}$ with flow and effort variables in Table 5.1 when setting $v = 0$ so getting the skew symmetric graph

$$\begin{bmatrix} f_S \\ f_R \\ f_{C_{\bar{u}}} \\ f_{R_{\bar{u}}} \end{bmatrix} = \begin{bmatrix} -J(x) & -g_R(x) & 0 & 0 \\ g_R^\top(x) & 0 & 0 & 0 \\ 0 & 0 & 0 & S(x,\bar{u}) \\ 0 & 0 & -S^\top(x,\bar{u}) & 0 \end{bmatrix} \begin{bmatrix} e_S \\ e_R \\ e_{C_{\bar{u}}} \\ e_{R_{\bar{u}}} \end{bmatrix}$$

with $S(x,\bar{u}) = \kappa g(x,\bar{u})g^\top(x,\bar{u})$. Indeed, the feedback $\bar{u}$ generates the constructive resistive component given by

$$\begin{aligned} f_{R_{\bar{u}}} &= -\kappa(g(x,\bar{u})g^\top(x,\bar{u}))^\top\bar{\nabla}H|_{x^+}^{x^+(\bar{u})} \\ e_{R_{\bar{u}}} &= \bar{\nabla}H|_{x^+}^{x^+(\bar{u})}. \end{aligned}$$

Flows	Efforts
$f_S(k) = -(x^+ - x(k))$	$e_S(k) = \bar{\nabla} H\|_{x(k)}^{x^+}$
$f_R(k) = g_R^\top(x(k))\bar{\nabla} H\|_{x(k)}^{x^+}$	$e_R(k) = -r(x(k))f_R(k)$
$f_{C_{\bar{u}}}(k) = -(x^+(\bar{u}(k)) - x^+)$	$e_{C_{\bar{u}}}(k) = \bar{\nabla} H\|_{x^+}^{x^+(\bar{u})}$
$f_{R_{\bar{u}}}(k) = -\kappa g(x,\bar{u})g^\top(x,\bar{u})\bar{\nabla} H\|_{x^+}^{x^+(\bar{u})}$	$e_{R_{\bar{u}}}(k) = \bar{\nabla} H\|_{x^+}^{x^+(\bar{u})}$
$f_{C_v}(k) = -(x^+(\bar{u}+v) - x^+(\bar{u}))$	$e_{C_v}(k) = \bar{\nabla} H\|_{x^+(\bar{u})}^{x^+(\bar{u}+v)}$
$f_I(k) = Y_{\mathrm{av}}(\bar{u})(x(k), v(k))$	$e_I(k) = v(k)$

Table 5.1

Applying now the feedback $u = \bar{u} + v$, one gets again a Dirac structure with skew symmetric graph (5.4) satisfying

$$e_S^\top f_S + e_R^\top f_R + e_{C\bar{u}}^\top f_{C\bar{u}} + e_{R\bar{u}}^\top f_{R\bar{u}} + e_{Cv}^\top f_{Cv} + e_I^\top f_I = 0.$$

More in detail, the stored energy is split into two parts, $e_S^\top f_S + e_{C\bar{u}}^\top f_{C\bar{u}}$, the resistive part into $e_R^\top f_R + e_{R\bar{u}}^\top f_{R\bar{u}}$ so getting under the feedback $\bar{u}$ the energy balance equality

$$e_S^\top f_S + e_{C\bar{u}}^\top f_{C\bar{u}} = -e_R^\top f_R - e_{R\bar{u}}^\top f_{R\bar{u}}.$$

Finally, the external port is split into the external control and external interaction satisfying $e_{Cv}^\top f_{Cv} + e_I^\top f_I = 0$. □

Remark 5.1.2. We note that the closed-loop port-Hamiltonian system can be defined on the augmented space $\mathcal{X}_e = \mathcal{X} \times \mathcal{X}$ by splitting the dynamics into its free and controlled evolution again setting $x_e = (x_f, x_c)$. According to a variational approach, one gets in closed loop with $u = \bar{u}$, $(x^+(\bar{u}) - x) = (x_f^+ - x_f) + (x_c^+ - x_c)$ when setting as initial condition for each time instant k, $x_f = x, x_c^+ = x^+(\bar{u}), x_c = x_f^+ = x^+(0)$. Accordingly, the dynamics over $\mathcal{X}_e$ adopts the state-space representation of the form (4.1), that is

$$x_e^+ - x_e = (J_e(x_e) - R_e(x_e))\nabla H|_{x_e}^{x_e^+}$$

with augmented skew symmetric and resistive matrices

$$J_e(x_e) = \begin{pmatrix} J(x_f) & 0 \\ 0 & 0 \end{pmatrix}, \quad R_e(x_e) = \begin{pmatrix} R(x_f) & 0 \\ 0 & \kappa g(x_f,\bar{u})g^\top(x_f,\bar{u}) \end{pmatrix}$$

and augmented discrete gradient function

$$\nabla H|_{x_e}^{x_e^+} = (\bar{\nabla} H|_{x_f}^{x_f^+}, \bar{\nabla} H|_{x_c}^{x_c^+})^\top \in \mathcal{X}_e$$

satisfying by construction the energy variation

$$(x^+(\bar{u}) - x)^\top \bar{\nabla} H|_x^{x^+(\bar{u})} = (x_f^+ - x_f)^\top \bar{\nabla} H|_{x_f}^{x_f^+} + (x_c^+ - x_c)^\top \bar{\nabla} H|_{x_c}^{x_c^+}.$$

5.1.2 Some constructive aspects

We have seen that the stabilizing negative output feedback $u = \gamma(x)$ is computed as the implicit solution to the equality (5.2), that is

$$\gamma(x) + \kappa g^\top(x, \gamma(x)) \bar{\nabla} H\big|_{x^+}^{x^+(\gamma(x))} = 0$$

with damping improvement $\kappa > 0$, and an exact solution might be tough to be computed in general. The following corollary given in Monaco and Normand-Cyrot (2011) specializes in this case providing the existence of a local solution for the discrete-time port-Hamiltonian system (5.1).

Corollary 5.1.1. *Let the discrete port-Hamiltonian system* (5.1) *be ZSD with Hamiltonian function $H(\cdot) : \mathbb{R}^n \to \mathbb{R}_{\geq 0}$, having a minimum in $x_\star$. Then, the feedback*

$$u = -z(x) \left(\mathrm{L}_{G_1} H(\cdot) \right) \big|_{F(x,0)} \tag{5.6}$$

with

$$z(x) = \left. \frac{\kappa}{1 + \frac{\kappa}{2} \mathrm{L}_{G_1}^2 H(\cdot) + \frac{\kappa}{2} \mathrm{L}_{G_2} H(\cdot)} \right|_{F(x,0)}, \qquad \kappa > 0 \tag{5.7}$$

achieves local asymptotic stabilization of the closed-loop equilibrium $x_\star$.

Proof. First, consider the series expansion around u of the mapping $Y(\cdot, u)$ up to an error in $O(u^2)$ that is

$$Y(\cdot, u) = G^\top(\cdot, u) \nabla H(\cdot) = G_1^\top(\cdot) \nabla H(\cdot) + u G_2^\top(\cdot) \nabla H(\cdot) + O(u^2)$$

with $G_1(\cdot), G_2(\cdot)$ vector fields characterizing the series expansion of $G(\cdot)$ and $O(u^2)$ which contains all the remaining terms of a higher order of the control variable u. The average output associated with it is given by the expression

$$Y_{\mathrm{av}}(x, u) = \mathrm{L}_{G_1} H(\cdot)|_{F(x,0)} + \frac{u}{2} \mathrm{L}_{G_2} H(\cdot)|_{F(x,0)} + \frac{u}{2} \mathrm{L}_{G_1}^2 H(\cdot)|_{F(x,0)} + O(u^2).$$

Finally, by substituting such an expansion into the equality (5.2) one gets

$$u\left(1+\frac{\kappa}{2}\mathrm{L}_{G_2}H(\cdot)|_{F(x,0)}+\frac{\kappa}{2}\mathrm{L}^2_{G_1}H(\cdot)|_{F(x,0)}\right)+\kappa\mathrm{L}_{G_1}H(\cdot)|_{F(x,0)}=0,$$

which yields in turn (5.6). Its existence is guaranteed by nonsingularity condition $1+(\frac{\kappa}{2}\mathrm{L}^2_{G_1}H+\frac{\kappa}{2}\mathrm{L}_{G_2}H)|_{F(x,0)}\neq 0$ at $x_\star$ which is verified with $\kappa>0$ in the neighborhood of $x_\star$ since $\nabla H(x_\star)=0$. □

5.1.3 The input-affine dynamics case with quadratic Hamiltonian

A remarkable case of port-Hamiltonian systems for which the feedback solution to the implicit equality (5.2) can be computed is the one associated with a quadratic Hamiltonian function $H(x)=\frac{1}{2}x^\top Px$ with $P=P^\top\succ 0$ together with an input map $g(x):=g(x,0)$ affine in the control variable, namely

$$g(x,u):=\frac{1}{u}\int_0^u G(x^+(v),v)\mathrm{d}v=g(x,0).$$

Hence, exploiting the property (2.4) the dynamics (5.1a) takes the form

$$x^+(u)=F(x,u)=x+\frac{1}{2}(J(x)-R(x))P(x^++x)+g(x)u \tag{5.8}$$

and, from the fact that $x^+(u)+x^+=2F(x,0)+g(x)u$, the associated conjugate output (5.1b) rewrites as

$$Y_{\mathrm{av}}(x,u)=g^\top(x)PF(x,0)+\frac{1}{2}g^\top(x)Pg(x)u. \tag{5.9}$$

Corollary 5.1.2. *Given an input-affine discrete port-Hamiltonian dynamics with $H(x)=\frac{1}{2}x^\top Px$ with $P=P^\top\succ 0$ of the form*

$$x^+(u)=F(x,u)=x+\frac{1}{2}(J(x)-R(x))P(x^++x)+g(x)u \tag{5.10a}$$

$$Y_{av}(x,u)=g^\top(x)PF(x,0)+\frac{1}{2}g^\top(x)Pg(x)u. \tag{5.10b}$$

assumed ZSD, then $u=\gamma(x)$ with

$$\gamma(x)=-\frac{\kappa g^\top(x)P}{1+\frac{\kappa}{2}g^\top(x)Pg(x)}F(x,0), \tag{5.11}$$

globally asymptotically stabilize through $\kappa>0$ the closed-loop equilibrium $x_\star=0$.

Proof. It is a matter of computation to provide that the passivity-based control given by $u = -\kappa Y_{\text{av}}(x, u)$ for (5.10b) recovers (5.11). Its existence is guaranteed as the non-singularity condition $\frac{\kappa}{2} g^\top(x) P g(x) \neq -1$ is always verified by construction. Then, due to ZSD, $u = \gamma(x)$ achieves asymptotic stability of $x = 0$ and it achieves globally as the assumed $H(x)$ is postitive semidefinite, radially unbounded, and $H(0) = 0$ satisfying $\gamma(x) Y_{\text{av}}(x, \gamma(x)) < 0$ for all $x \neq 0$. □

On the optimality of the negative output feedback

From the special structure of the negative output feedback (5.11) one might define inverse optimality in which the a priori designed feedback (5.11) is shown to be optimal for a posteriori determined cost functional of the form

$$\mathcal{J} = \sum_{n \geq k} l(x_n) + ||u_n||^2. \tag{5.12}$$

A more general result in this discrete-time framework can be found in Monaco and Normand-Cyrot (2015). The following result provide inverse optimal control for the associated port-Hamiltonian dynamics and the output damping feedback (5.11).

Theorem 5.1.1. *Given a discrete port-Hamiltonian dynamics* (5.10a) *assumed ZSD with output* (5.10b) *and a passivity-based control* $u_\star = \frac{1}{2}\gamma(x)$ *where*

$$\gamma(x) = -\frac{g^\top(x) P}{1 + \frac{1}{2} g^\top(x) P g(x)} F(x, 0). \tag{5.13}$$

Then $u_\star$ *which achieves global asymptotic stability of* $x = 0$ *is inverse optimal as it minimizes*

$$\mathcal{J} = \sum_{n \geq k} l(x_n) + ||u_n||^2 \tag{5.14}$$

with, for all $x \neq 0$,

$$l(x) = H(x) - H(x^+) + \frac{(g^\top(x) P F(x, 0))^2}{4 + 2 g^\top(x) P g(x)} > 0. \tag{5.15}$$

Proof. The necessary condition for the optimality of $u_\star$ is given by the equation

$$\frac{\partial}{\partial u}\big(l(x) + ||u||^2 + H(x^+(u)) - H(x)\big)\Big|_{u_\star} = 0,$$

which is satisfied by the choice of $u_\star = \frac{1}{2}\gamma(x)$. Moreover, the global asymptotic stability is inherited by the feedback $\gamma(x)$ itself. From the necessity condition one deduces $l(x) = H(x) - H(x^+(u_\star)) - ||u_\star||^2$ which reads

$$\begin{aligned} l(x) &= H(x) - H(x^+(u_\star)) - ||u_\star||^2 \\ &= H(x) - H(x^+) + H(x^+) - H(x^+(u_\star)) - ||u_\star||^2 \\ &= H(x) - H(x^+) - u_\star Y_{\text{av}}(x, u_\star) - ||u_\star||^2 \\ &= H(x) - H(x^+) + \frac{1}{4}\left(\frac{(g^\top(x)Px^+)^2}{1 + \frac{1}{2}g^\top(x)Pg(x)}\right) \end{aligned}$$

so that the function (5.15) is deduced. Finally, the positivity (5.15) is guaranteed since $g^\top(x)Pg(x) \geq 0$ implies $1 + \frac{1}{2}g^\top(x)Pg(x) > 0$ and

$$H(x) - H(F(x,0)) = \frac{1}{4}(F(x,0) + x)^\top PR(x)P(F(x,0) + x) \geq 0$$

for all x as $R(x) \succeq 0$ by assumption. □

5.2 Interconnection and damping assignment

In this section the problem of asymptotic stabilization towards a target equilibrium is tackled in terms of feedback passivation with respect to a new Hamiltonian function which must be assigned to the closed-loop system. The control objective stands in the assignment of a given equilibrium to the controlled system while preserving the port-Hamiltonian structure. More precisely, the problem consists of stabilizing the discrete port-Hamiltonian system at a desired equilibrium point, say $x_\star$, by possibly assigning through feedback a new Hamiltonian function $H_d(x)$ with a minimum in $x_\star$, namely

$$x_\star = \arg\min\{H_d(x)\}.$$

It is however clear that not all $x_\star \in \mathbb{R}^n$ can be assigned to the closed-loop system. Then, to begin with let the class of admissible equilibria be characterized.

Definition 5.2.1. The point $x_\star \in \mathbb{R}^n$ is said *admissible equilibrium* for the system (4.5) if it is contained in the set

$$\mathcal{E} := \{x \in \mathbb{R}^n \mid g^\perp(x,u)(J(x) - R(x))\nabla H(x) = 0, \quad \text{for some } u \in \mathbb{R}\},$$

with $g^\perp(x,u)$ denoting the left-hand side annihilator of $g(x,u)$, namely $g^\perp(x,u)g(x,u) = 0$, for all $(x,u) \in \mathbb{R}^n \times \mathbb{R}$.

The following discrete-time IDA-PBC problem can be formulated.

Problem 2 (DT IDA-PBC)**.** Given discrete port-Hamiltonian systems of the form

$$x^+(u) = x + (J(x) - R(x))\bar{\nabla} H|_x^{x^+} + g(x,u)u \tag{5.16a}$$
$$Y_{\text{av}}(x,u) = g^\top(x,u)\bar{\nabla} H|_{x^+}^{x^+(u)} \tag{5.16b}$$

and $x_\star \in \mathcal{E}$, find $\bar{u}(x) : \mathbb{R}^n \to \mathbb{R}$ such that for $u = \bar{u}(x) + v$ the system takes the port-Hamiltonian form

$$x^+(\bar{u}(x) + v) = x + (J_d(x) - R_d(x))\bar{\nabla} H_d|_x^{x^+(\bar{u}(x))} + g_d(x,v)v \tag{5.17}$$

with new Hamiltonian function $H_d : \mathbb{R}^n \to \mathbb{R}_{\geq 0}$ such that

$$x_\star = \arg\min\{H_d(x)\},$$

$J_d(x) = -J_d^\top(x)$, $R_d(x) = R_d^\top(x) \succeq 0$ and $g_d(x,v)$ satisfying by construction

$$vg_d(x,v) = \bar{u}(x)(g(x,\bar{u}(x)+v) - g(x,\bar{u}(x))) + vg(x,\bar{u}(x)+v). \tag{5.18}$$

Accordingly, the closed-loop (5.17) verifies the new energy balance equality

$$H_d(x_k) - H_d(x_0) = \sum_{i=0}^{k-1} v_i Y_{d_{\text{av}}i}(\bar{u}) - \sum_{i=0}^{k-1} w_{d_i}, \qquad \forall k \in \mathbb{N},$$

with dissipation $w_d \geq 0$ and new passive output

$$Y_{d_{\text{av}}}(\bar{u})(x,v) = g_d^\top(x,v)\bar{\nabla} H_d|_{x^+(\bar{u}(x))}^{x^+(\bar{u}(x)+v)}. \tag{5.19}$$

Remark 5.2.1. For sake of completeness, one may note that the new passive output (8.10) is properly the v-average output from $\bar{u}$ when setting $u = \bar{u} + v$ from Definition 2.2.7.

A first characterization of the solution to the DT IDA-PBC problem is given below when the interconnection and damping matrices are assumed preserved, namely when

$$J_d(x) = J(x), \quad R_d(x) = R(x).$$

For the ease of notation, in the following $\bar{u}(x)$ is denoted by $\bar{u}$.

Proposition 5.2.1 (Energy shaping)**.** *Given the discrete port-Hamiltonian system* (5.16) *and* $x_\star \in \mathcal{E}$*, the DT IDA-PBC problem is solvable for* $J_d(x) = J(x)$ *and* $R_d(x) = R(x)$*, if there exists a desired Hamiltonian function* $H_d(\cdot) : \mathbb{R}^n \to \mathbb{R}_{\geq 0}$ *verifying*

(i) $\quad \nabla H(x_\star) = -\nabla H_a(x_\star)$

(ii) $\quad H(x_\star) - H(x) < H_a(x) - H_a(x_\star) \quad \forall x \in \mathcal{B}/\{x_\star\},$

with $H_a(x) = H_d(x) - H(x)$ *and* $\mathcal{B}$ *an open neighborhood of* $x_\star$ *and a feedback* $\bar{u}(x)$ *solution to the matching equation*

$$(J(x) - R(x))(\bar{\nabla} H_a|_x^{x^+(\bar{u})} + \bar{\nabla} H|_x^{x^+(\bar{u})} - \bar{\nabla} H|_x^{x^+}) = g(x, \bar{u})\bar{u}. \tag{5.20}$$

Moreover, the equilibrium $x_\star \in \mathcal{E}$ *is stable for the closed-loop port-Hamiltonian dynamics*

$$x^+(\bar{u}) = x + (J(x) - R(x))\bar{\nabla} H_d|_x^{x^+(\bar{u})} \tag{5.21}$$

with Lyapunov function $H_d(x)$*.* $x_\star$ *is asymptotically stable if the largest invariant set contained in* $\{x \in \mathbb{R}^n \mid ||\bar{\nabla} H_d|_x^{x^+(\bar{u})}||_R^2 = 0\}$ *is* $\{x_\star\}$*.*

Proof. According to $\nabla H(x_\star) = -\nabla H_a(x_\star)$, $H_d(x)$ has a critical point at $x_\star$, say $\nabla H_d(x_\star) = 0$, while the condition *(ii)* provides that $x_\star$ is a minimum. The feedback $\bar{u}(x)$ solution to (5.20) achieves the target dynamics (5.21) by construction. Moreover, by specifying (5.20) at $x = x_\star$ one gets from the condition *(i)*,

$$-(J(x_\star) - R(x_\star))\nabla H(x_\star) = g(x_\star, \bar{u}(x_\star))\bar{u}(x_\star)$$

which is solvable only for $x_\star \in \mathcal{E}$. Finally, by qualifying $H_d(x)$ as a Lyapunov function for (5.21), (asymptotic) stability of $x_\star$ follow from the property **P4** in Proposition 4.1.1. □

Any solution $\bar{u}$ to the matching equation (5.20) is only related to the choice of a function $\bar{\nabla} H_a|_x^{x^+(\bar{u})}$, and this fact leads to limiting the solutions exclusively to possible choices of $H_a(\cdot)$ and admissible closed-loop flow $x^+(\bar{u})$. However, it is important to stress that a solution $\bar{u}$ to the matching equation (5.20) is tough to be computed for the general nonlinear case due to the nonlinearity in $\bar{u}$ provided by $g(x,\bar{u})$, $\bar{\nabla} H|_x^{x^+(\bar{u})}$, and $\bar{\nabla} H_a|_x^{x^+(\bar{u})}$.

In this formulation the solution $\bar{u}$ is an energy shaping control which modifies the Hamiltonian of the system (4.5) so achieving a closed-loop system which possesses a desired equilibrium $x_\star$ coinciding with the minimum of the desired energy function $H_d(x)$. The closed-loop system possesses the same dissipation term $R(x)$, ensuring stability (asymptotic stability if the system is ZSD) of the desired equilibrium $x_\star$.

The modification of the interconnection and damping matrices, to respectively $J_d(\cdot)$ and $R(\cdot)$, provide a broad set of suitable solutions assignable to the closed-loop system.

Theorem 5.2.1: IDA-PBC in discrete time

Consider the discrete port-Hamiltonian system (5.16), that is

$$x^+(u) = x + (J(x) - R(x))\bar{\nabla} H|_x^{x^+} + g(x,u)u \tag{5.22a}$$

$$Y_{\text{av}}(x,u) = g^\top(x,u)\bar{\nabla} H|_{x^+}^{x^+(u)} \tag{5.22b}$$

and $x_\star \in \mathcal{E}$, the DT IDA-PBC problem is solvable if there exists a desired Hamiltonian function $H_d(x) : \mathbb{R}^n \to \mathbb{R}$ satisfying *(i)*, *(ii)* of Proposition 5.2.1 with $H_a(x) = H_d(x) - H(x)$, matrices $J_a(x), R_a(x)$ and a feedback, $\bar{u} = \bar{u}(x) : \mathbb{R}^n \to \mathbb{R}$ verifying the matching equation

$$\begin{aligned}(J(x) - R(x) + J_a(x) - R_a(x))(\bar{\nabla} H|_x^{x^+(\bar{u})} - \bar{\nabla} H|_x^{x^+} + \bar{\nabla} H_a|_x^{x^+(\bar{u})}) \\ = g(x,\bar{u})\bar{u} - (J_a(x) - R_a(x))\bar{\nabla} H|_x^{x^+}\end{aligned} \tag{5.23}$$

with matrices

$$\begin{aligned}J_d(x) &:= J(x) + J_a(x) = -J_d^\top(x) \\ R_d(x) &:= R(x) + R_a(x) = R_d^\top(x) \succeq 0.\end{aligned}$$

Moreover, $x_\star$ is a stable equilibrium of the closed-loop system (5.17) with new Lyapunov function $H_d(x)$; it is asymptotically stable if $\{x_\star\}$ is the largest invariant set contained in

$$\{x \in \mathbb{R}^n \mid ||\bar{\nabla} H_d|_x^{x^+(\bar{u})}||_{R_d}^2 = 0\}.$$

Proof. The matching equation (5.23) is deduced by equating the desired closed-loop dynamics (5.17) with the right-hand side of (5.22) under feedback $u = \bar{u}(x)$ provided that $x_\star \in \mathcal{E}$. Straightforwardly, the control $u = \bar{u} + v$ makes (5.22) a port-Hamiltonian dynamics of the form (5.17). Due to properties *(i)* and *(ii)* in Proposition 5.2.1 along with the property **P4** in Proposition 4.1.1, the stability of $x_\star \in \mathcal{E}$ is ensured. □

Remark 5.2.2. A necessary condition for the solvability of the matching equation (5.23) is that there exists $\bar{u}(x)$ satisfying, for all $x \in \mathbb{R}^n$, the matching condition

$$g^\perp(x,\bar{u})\big[(J_d(x) - R_d(x))(\bar{\nabla} H|_x^{x^+(\bar{u})} - \bar{\nabla} H|_x^{x^+} + \bar{\nabla} H_a|_x^{x^+(\bar{u})}) + (J_a(x) - R_a(x))\bar{\nabla} H|_x^{x^+}\big] = 0. \tag{5.24}$$

5.2.1 Constructive aspects: an approximate IDA-PBC design

Albeit Theorem 5.2.1 characterizes all the possible solutions to the DT IDA-PBC problem, a general solution $\bar{u}(x)$ to the matching equation (5.23) is difficult to be characterized due to the implicit structure involved into the equation. However, due to the mean value theorem, one rewrites the discrete gradient in $\mathcal{O}(\|x^+(u) - x^+\|^2)$, namely

$$\bar{\nabla} H|_x^{x^+(u)} = \bar{\nabla} H|_x^{x^+} + \frac{1}{2}\nabla^2 H(x)(x^+(u) - x^+) + \mathcal{O}(\|x^+(u) - x^+\|^2)$$

where $\mathcal{O}(\|x^+(u) - x^+\|^2)$ contains all the remaining terms of a higher order of $x^+(u) - x^+$, with $x^+(u) - x^+ = g(x,u)u$ and $g(x,u) = g(x,0) + \mathcal{O}(|u|)$. Accordingly, an approximate solution can be inferred as states the proposition below.

Proposition 5.2.2. *Given the discrete port-Hamiltonian system* (5.16) *and* $x_\star \in \mathcal{E}$, *if there exist* $H_d(x) : \mathbb{R}^n \to \mathbb{R}$ *satisfying* (i), (ii) *of Proposition 5.2.1 with* $H_a(x) = H_d(x) - H(x)$, *matrices* $J_a(x), R_a(x)$ *which solve in* $\mathcal{O}(|\bar{u}|^2)$ *the matching equation*

$$\begin{aligned}(J(x) - R(x) + J_a(x) - R_a(x))\bar{\nabla} H_a|_x^{x^+} + (J_a(x) - R_a(x))\bar{\nabla} H|_x^{x^+} \\ = N_d(x)\bar{u} + \mathcal{O}(|\bar{u}|^2)\end{aligned} \tag{5.25}$$

with $N_d(x) = \left(I - \frac{1}{2}(J_d(x) - R_d(x))\nabla^2 H_d(x)\right) g(x,0)$, *then the solution* $\bar{u}$ *takes the form*

$$\bar{u} = N_d^\dagger(x)\big((J_a(x) - R_a(x))\bar{\nabla} H|_x^{x^+} + (J_d(x) - R_d(x))\bar{\nabla} H_a|_x^{x^+}\big) \tag{5.26}$$

which locally stabilizes the desired equilibrium $x_\star$ *with matrices*

$$\begin{aligned}J_d(x) &:= J(x) + J_a(x) = -J_d^\top(x) \\ R_d(x) &:= R(x) + R_a(x) = R_d^\top(x) \succeq 0.\end{aligned}$$

Proof. The result is obtained by rewriting the matching equation (5.23) in terms of the approximate discrete gradient of $H_a(x)$ and $H(x)$, namely

$$\begin{aligned}(J_d(x) - R_d(x))(\bar{\nabla} H_d|_x^{x^+} - \bar{\nabla} H|_x^{x^+} + \frac{1}{2}\nabla^2 H_d(x)(x^+(\bar{u}) - x^+)) \\ = g(x,\bar{u})\bar{u} - (J_a(x) - R_a(x))\bar{\nabla} H|_x^{x^+} + \mathcal{O}(\|x^+(\bar{u}) - x^+\|^2),\end{aligned}$$

which gives the approximate matching equation (5.25) and consequently the approximate control (5.26). □

Remark 5.2.3. The approximate matching equation (5.25) suggests that when the higher order terms in $\bar{u}$ are zeroed, namely $\mathcal{O}(|\bar{u}|^2) = 0$, a solution to the matching equation is not approximate but it turns into an exact solution. This particular case is studied below.

5.2.2 IDA-PBC for input-affine systems

Due to the approximate solution given in Proposition 5.2.2 one can investigate a particular case in which the solution is not only locally defined and, consequently stability, is not only locally valid. Indeed, a special exact solution can be inferred if the problem satisfies the following assumption:

A1. The controlled port-Hamiltonian dynamics has an input-affine structure, that is

$$x^+(u) = x + (J(x) - R(x))\bar{\nabla}H|_x^{x^+} + g(x)u, \tag{5.27}$$

where the input mapping $g(x)$ is independent from the control variable u;

A2. The desired Hamiltonian function $H_d(x)$ comes with a discrete gradient from x to $x^+(u)$ affine in u, namely

$$\bar{\nabla}H_d|_x^{x^+(u)} := \bar{\nabla}H_d|_x^{x^+} + s(x)u \tag{5.28}$$

for some function $s : \mathbb{R}^n \to \mathbb{R}^n$.

Under these assumptions, the matching equation simplifies as

$$\begin{aligned}(J_d(x) - R_d(x))\bar{\nabla}H_a|_x^{x^+} + (J_a(x) - R_a(x))\bar{\nabla}H|_x^{x^+} \\ = (g(x) - (J_d(x) - R_d(x))s(x))\,\bar{u}\end{aligned} \tag{5.29}$$

which is liner with respect to the control variable $\bar{u}$.

In this respect, the following proposition is presented.

Proposition 5.2.3. *Consider an input-affine system of the form* (5.27) *and* $x_\star \in \mathcal{E}$ *the desired equilibrium to be assigned. If there exists a desired Hamiltonian function* $H_d(x) : \mathbb{R}^n \to \mathbb{R}$ *satisfying* (5.28) *and conditions* (i), (ii) *of Proposition 5.2.1 with* $H_d(x) = H(x) + H_a(x)$, *matrices* $J_a(x), R_a(x)$ *which solves for all* $x \in \mathbb{R}^n$ *the matching condition*

$$N_d^\perp(x)\left((J(x) - R(x) + J_a(x) - R_a(x))\bar{\nabla}H_a|_x^{x^+} + (J_a(x) - R_a(x))\bar{\nabla}H|_x^{x^+}\right) = 0 \tag{5.30}$$

with $N_d(x) = (g(x) - (J_d(x) - R_d(x))s(x))$, then $\bar{u}$ is a discrete IDA-PBC of the form

$$\bar{u} = N_d^{\dagger}(x)\big((J_d(x) - R_d(x))\bar{\nabla}H_d|_x^{x^+} - (J(x) - R(x))\bar{\nabla}H|_x^{x^+}\big). \tag{5.31}$$

Proof. The proof follows the lines of Proposition 5.2.2. Thus, from the condition (5.25) and property (5.28) one rewrites the matching equation (5.29) for which $N_d(x) = (g(x) - (J_d(x) - R_d(x))s(x))$ can be set and due to the necessary condition (5.24) one deduces the matching condition (5.30). Selecting J_a, R_a and satisfying the matching condition than the control $\bar{u}$ of the form (5.31) follows. □

Remark 5.2.4. Due to Proposition 5.2.1, the control given in (5.31) assigns the desired equilibrium $x_\star$ through the Hamiltonian $H_d(x)$ to the closed-loop system verifying (5.28). Moreover, the assigned $x_\star$ is stable, or in addition, asymptotically stable if the largest invariant set contained in $\{x \in \mathbb{R}^n \mid ||\bar{\nabla}H_d|_x^{x^+(\bar{u})}||_{R_d}^2 = 0\}$ is $\{x_\star\}$.

Remark 5.2.5. A particular desired Hamiltonian function which satisfies the condition (5.30) is for instance the quadratic Hamiltonian function given by

$$H_d(x) = \frac{1}{2}(x - x_\star)^\top P_d(x - x_\star)$$

computed from x to $x^+(u)$. The associated discrete gradient yields the following expression

$$\bar{\nabla}H_d|_x^{x^+(u)} = \frac{1}{2}P_d(x^+(u) + x - 2x_\star),$$

which is by construction

$$\bar{\nabla}H_d|_x^{x^+(u)} = \bar{\nabla}H_d|_x^{x^+} + s(x)u = \frac{1}{2}P_d(x^+ + x - 2x_\star) + s(x)u,$$

with $s(x) = \frac{1}{2}P_d g(x)$ because of the affinity in the control variable of (5.27).

5.3 Concluding remarks

We have seen how port-Hamiltonian systems in discrete time can be properly stabilized by means of proper passivity-based control. First, we specialize in this port-Hamiltonian framework the passivity-based control computed upon the u-average output of the system. As usual in discrete time, the control is given by the solution to an implicit damping equality. Then, we showed how the Dirac structure of the port-Hamiltonian system is modified under the passivity-based feedback, to conclude that the closed-loop system is again in a port-Hamiltonian structure. In the input-affine case, we give a proper structure to the solution of the implicit damping equality, and in this case, we showed that the stabilizing control achieves inverse optimal properties with respect to a particular suitably defined cost functional. Finally, the IDA-PBC problem is set in the nonlinear case and sufficient conditions have been presented in Theorem 5.2.1. Despite the fact that a general solution is tough to determine in the nonlinear case, the problem is specialized to input-affine port-Hamiltonian systems, assumption **A1**, together with a desired Hamiltonian function satisfying the assumption **A2**. The particular solution is given in Proposition 5.2.3 providing a solution to the IDA-PBC problem in discrete time. The results concerning this chapter are included in the following published works:

A. Moreschini, M. Mattioni, S. Monaco and D. Normand-Cyrot, "Discrete port-controlled Hamiltonian dynamics and average passivation," 2019 IEEE 58th Conference on Decision and Control (CDC), Nice, France, 2019, pp. 1430-1435, doi: 10.1109/CDC40024.2019.9029809.

A. Moreschini, M. Mattioni, S. Monaco and D. Normand-Cyrot, "Stabilization of Discrete Port-Hamiltonian Dynamics via Interconnection and Damping Assignment," in IEEE Control Systems Letters, vol. 5, no. 1, pp. 103-108, Jan. 2021, doi: 10.1109/LCSYS.2020.3000705.

A. Moreschini, S. Monaco and D. Normand-Cyrot, "Dirac structures of discrete-time port-Hamiltonian systems," Submitted to IEEE Transactions on Automatic Control (TAC). (Under review)

Chapter 6

LTI port-Hamiltonian systems in discrete time

Contents

6.1 Port-Hamiltonian systems in discrete time **151**

6.2 Negative output feedback **153**

6.3 IDA-PBC in discrete time **154**

6.4 Concluding remarks **158**

In this chapter we focus on the linear time-invariant (LTI) port-Hamiltonian systems and we show how both modeling and stabilization properties specialize. In particular, it is interesting to emphasize that all the local properties arising in the nonlinear port-Hamiltonian systems have global validity in the linear case. More importantly, the solutions can be exactly computed and regarding the IDA PBC problem a closed-form solution is performed for LTI port-Hamiltonian dynamics and necessary and sufficient conditions for solving the problem are given.

6.1 Port-Hamiltonian systems in discrete time

Differently from the nonlinear representation all the matrices characterizing the system have constant entries and the Hamiltonian function has a quadratic form, that is

$$H(x) = \frac{1}{2} x^\top P x \tag{6.1}$$

with symmetric and positive definite matrix P, that is $P = P^\top \succ 0$. The following definition is achieved exploiting the discrete gradient function of the quadratic Hamiltonian function.

Definition 6.1.1: LTI port-Hamiltonian system in discrete time

A LTI port-Hamiltonian system in discrete time is described in DDR form, over $\mathbb{R}^n$ with $u \in \mathbb{R}$, as follows

$$x^+ = x + \frac{1}{2}(J - R)P(x^+ + x) \tag{6.2a}$$

$$\frac{\partial x^+(u)}{\partial u} = B \quad \text{with} \quad x^+(0) = x^+ \tag{6.2b}$$

$$Y(x) = B^\top P x \tag{6.2c}$$

or equivalently in the map form as

$$x^+(u) = x + \frac{1}{2}(J - R)P(x^+ + x) + Bu \tag{6.3a}$$

$$Y_{\text{av}}(x, u) = B^\top P x^+ + \frac{u}{2} B^\top P B. \tag{6.3b}$$

with matrices $J = -J^\top \in \mathbb{R}^{n\times n}$, $R = R^\top \succeq 0 \in \mathbb{R}^{n\times n}$, and $B \in \mathbb{R}^{n\times 1}$.

Remark 6.1.1. The LTI port-Hamiltonian system comes with an energy balance equation between two time steps as

$$\underbrace{H(x^+(u)) - H(x)}_{\text{stored energy}} = -\underbrace{\bar{\nabla} H^\top|_x^{x^+} R \bar{\nabla} H|_x^{x^+}}_{\text{dissipated energy}} + \underbrace{u B^\top \bar{\nabla} H\big|_{x^+}^{x^+(u)}}_{\text{supplied energy}}, \tag{6.4}$$

which satisfies the following relation

$$H(x^+(u)) - H(x) = -d(x) + u B^\top P x^+ + \frac{u^2}{2} B^\top P B,$$

with dissipation term

$$d(x) = \frac{1}{4}(x^+ + x)^\top P^\top R P (x^+ + x) > 0$$

for all $x \neq 0$.

The LTI port-Hamiltonian system given above can be rewritten in the explicit and the stability of the dynamics is deduced.

Proposition 6.1.1. *Consider the LTI port-Hamiltonian system* (6.2)*. Then, if* $(I - \frac{1}{2}(J-R)P)$ *is invertible, then there exists an explicit LTI port-Hamiltonian system with*

$$x^+ = Ax = \left(I - \frac{1}{2}(J-R)P\right)^{-1}\left(I + \frac{1}{2}(J-R)P\right)x, \tag{6.5}$$

so that the controlled dynamics (6.3a) *yields*

$$x^+(u) = Ax + Bu \tag{6.6a}$$

$$Y_{av}(x,u) = B^\top PAx + \frac{u}{2}B^\top PB. \tag{6.6b}$$

Moreover, the origin $x = 0$ *is a globally asymptotically stable equilibrium for* (6.5)*.*

Proof. The explicit representation follows by Proposition 6.1.1. Moreover, By Barbashin-Krasovskii theorem, $x = 0$ is the minimum of $H(x)$ and is an asymptotically stable equilibrium as

$$H(x^+) - H(x) = -\frac{1}{4}x^\top(A+I)^\top P^\top RP(A+I)x < 0,$$

for any $x \neq 0$ and A given in (6.5). Moreover, since $H(x)$ is radially unbounded, then the asymptotic stability of $x = 0$ is globally guaranteed. □

6.2 Negative output feedback

In this LTI framework the negative output feedback given in Theorem 5.1.1 can be specialized. In particular, the problem achieves a unique solution to the implicit damping equality and provides global asymptotic stability of the origin.

Theorem 6.2.1: LTI negative output feedback in discrete time

Given a LTI port-Hamiltonian system of the form (6.6) assumed ZSD. Then the implicit damping equality

$$\gamma(x) + \kappa Y_{\text{av}}(x,u) = 0 \tag{6.7}$$

admits a unique solution $u = \gamma(x)$ with

$$\gamma(x) = -\frac{\kappa B^\top P A}{1 + \frac{\kappa}{2} B^\top P B} x \tag{6.8}$$

with $\kappa > 0$, which globally asymptotically stabilize the equilibrium $x = 0$.

The optimality result can be specialized to the port-Hamiltonian system (6.6), that are the linear version of the discrete port-Hamiltonian dynamics associated with the conjugate output (6.3b) with feedthrough term.

Corollary 6.2.1. *The feedback*

$$u_\star = \frac{1}{2}\gamma(x),$$

with feedback $\gamma(x)$ *in* (6.8) *and* $\kappa = 1$ *is inverse optimal as it minimizes*

$$\mathcal{J} = \sum_{n \geq k} l(x_n) + ||u_n||^2 \tag{6.9}$$

with, for all $x \neq 0$,

$$l(x) = H(x) - H(x^+) + \frac{(B^\top P A x)^2}{4 + 2B^\top P B} > 0. \tag{6.10}$$

6.3 IDA-PBC in discrete time

We have seen that for general nonlinear port-Hamiltonian system an IDA-PBC feedback is difficult to be characterized. However, a closed-form solution is provided for LTI port-Hamiltonian dynamics where necessary and sufficient conditions for solving the DT IDA-PBC problem are presented. In particular, one computes a stabilizing feedback $\bar{u}$ of the form

$$\bar{u} = Kx + K_\star x_\star,$$

with suitable matrices K and $K_\star$ which assign the desired equilibrium $x_\star$ and the quadratic desired Hamiltonian function $H_d(x)$ to the closed-loop system expressed in its closed-form.

For this purpose, assume a LTI discrete port-Hamiltonian dynamics of the form (6.2a) with quadratic Hamiltonian $H(x) = \frac{1}{2} x^\top P x$ and $P = P^\top \succ 0$. As in (6.3a)

the explicit state-space representation is computed by solving (6.2a) in $x^+(0) = x^+$ with $u = 0$ so getting the controlled dynamics

$$x^+(u) = Ax + Bu \tag{6.11}$$

where $x^+(0) = x^+ = Ax$ with state matrix

$$A = \big(I - \frac{1}{2}(J - R)P\big)^{-1}\big(I + \frac{1}{2}(J - R)P\big).$$

The set $\mathcal{E}$, defining all the admissible equilibria for the closed-loop LTI discrete port-Hamiltonian dynamics (6.2a), is specified as such

$$\mathcal{E} := \ker\big\{B^\perp(J - R)P\big\},$$

with $B^\perp$ denoting the left-hand side annihilator of B, namely $B^\perp B = 0$.

In this framework the DT-IDA-PBC problem reduces in finding the feedback

$$u = \bar{u} + v$$

which makes the equilibrium $x_\star \in \mathcal{E}$ stable for the closed-loop port-Hamiltonian system associated with the desired Hamiltonian

$$H_d(x) = \frac{1}{2}(x - x_\star)^\top P_d(x - x_\star).$$

More in detail, the state feedback $u = \bar{u} + v$ achieves the target LTI port-Hamiltonian structure

$$\begin{aligned} x^+(\bar{u} + v) &= x + (J_d - R_d)\bar{\nabla} H_d|_x^{x^+(\bar{u})} + Bv \\ &= x + \frac{1}{2}(J_d - R_d)P_d(x^+(\bar{u}) + x - 2x_\star) + Bv \end{aligned}$$

with matrices $J_d \in \mathrm{Skew}_{\mathbb{R}}(n, n)$, $R_d \in \mathrm{Sym}_{\mathbb{R}}(n, n)$, and $P_d \in \mathrm{Sym}_{\mathbb{R}}(n, n)$ with $R_d \succeq 0$, and $P_d \succ 0$. Equivalently, the implicit port-Hamiltonian dynamics can be explicitly expressed in closed-form as such

$$x^+(\bar{u} + v) = A_d x + A_{d,\star} x_\star + Bv \tag{6.12}$$

with $x^+(\bar{u}) = A_d x + A_{d,\star} x_\star$ defining the new controlled free dynamics and matrices

$$\begin{aligned} A_d &= \big(I - \frac{1}{2}(J_d - R_d)P_d\big)^{-1}\big(I + \frac{1}{2}(J_d - R_d)P_d\big) \\ A_{d,\star} &= -\big(I - \frac{1}{2}(J_d - R_d)P_d\big)^{-1}(J_d - R_d)P_d. \end{aligned}$$

The following Theorem is deduced from Proposition 5.2.1 and provides a necessary and sufficient condition for solving the DT IDA-PBC problem in the linear case with matching equation given by

$$(J-R)\frac{P}{2}(x^+ + x) + B\bar{u} = (J_d - R_d)\frac{P_d}{2}(x^+(\bar{u}) + x - 2x_\star) \tag{6.13}$$

or, equivalently in closed form, by

$$Ax + B\bar{u} = A_d x + A_{d,\star} x_\star.$$

Theorem 6.3.1: LTI IDA-PBC in discrete time

Given the LTI port-Hamiltonian dynamics

$$x^+(u) = x + (J-R)\bar{\nabla}H|_x^{x^+} + Bu \tag{6.14}$$

and a desired equilibrium $x_\star \in \mathcal{E}$ to be assigned. Then, the DT IDA-PBC problem is solvable if and only if there exist J_a, R_a and P_a solutions to the matching condition

$$B^\perp(J_a - R_a)P + B^\perp(J_a + J - R_a - R)P_a = 0 \tag{6.15}$$

such that $J_d = (J+J_a) = -J_d^\top$, $R_d = (R+R_a) = R_d^\top \succeq 0$, and $P_d = (P+P_a) \succ 0$. In addition, the feedback assigning the port-Hamiltonian dynamics

$$x^+(\bar{u} + v) = x + (J_d - R_d)\bar{\nabla}H_d|_x^{x^+(\bar{u})} + Bv \tag{6.16}$$

(or, equivalently, (6.12)) is given by

$$\bar{u} = \frac{1}{2}B^\dagger\left[(J_d - R_d)P_d(x^+(\bar{u}) + x - 2x_\star) - (J-R)P(x^+ + x)\right]. \tag{6.17}$$

Moreover if one provides that $(I - \frac{1}{2}(J-R)P)$ and $(I - \frac{1}{2}(J_d - R_d)P_d)$ are invertible then one gets the a closed form, by

$$\bar{u} = B^\dagger(A_d - A)x + B^\dagger A_{d,\star} x_\star. \tag{6.18}$$

with

$$A_d = \big(I - \frac{1}{2}(J_d - R_d)P_d\big)^{-1}\big(I + \frac{1}{2}(J_d - R_d)P_d\big) \tag{6.19a}$$

$$A_{d,\star} = -\big(I - \frac{1}{2}(J_d - R_d)P_d\big)^{-1}(J_d - R_d)P_d. \tag{6.19b}$$

Proof. One must prove that the algebraic condition (6.15) is necessary and sufficient for solving the matching equation (6.13). For necessity, by virtue of Remark 5.2.2, if the problem is solvable (meaning that (6.13) holds true), then the matching condition (5.24), specified in the linear case as

$$B^\perp\left[(J_d - R_d)\frac{P_d}{2}(x^+(\bar{u}) + x - 2x_\star) - (J - R)\frac{P}{2}(x^+ + x)\right] = 0, \tag{6.20}$$

holds. By manipulating the equality above on gets

$$B^\perp\big[(J_d - R_d)\frac{P_d}{2} - (J - R)\frac{P}{2}\big](x^+ + x) = -B^\perp(J_d - R_d)\frac{P_d}{2}(x^+(\bar{u}) - x^+ - 2x_\star)$$

whereby the right-hand-side vanishes, because

$$\begin{aligned} &B^\perp(J_d - R_d)\frac{P_d}{2}(x^+(\bar{u}) - x^+ - 2x_\star) \\ &\quad = B^\perp\big[(x^+(\bar{u}) - x) - (x^+ - x)\big] \\ &\quad = B^\perp[x^+(\bar{u}) - x^+] = B^\perp B\bar{u} = 0, \end{aligned}$$

so leading to the necessary condition

$$B^\perp\left[(J_d - R_d)P_d - (J - R)P\right](x^+ + x) = 0$$

which must hold for all $x \in \mathbb{R}^n$, that coincides with (6.15) by definition of $J_d = J + J_a$, $R_d = R + R_a$ and $P_d = P + P_a$. Then, necessity is proved.

The sufficiency works out by showing that, if (6.15) holds, the feedback (6.17) (or, equivalently, (6.18)) solves the problem. To this end, plugging the feedback (6.17) into (6.13) one gets the equivalence

$$\begin{aligned} BB^\dagger\big[(J_d - R_d)\frac{P_d}{2}(x^+(\bar{u}) + x - 2x_\star) - (J - R)\frac{P}{2}(x^+ + x)\big] \\ = (J_d - R_d)\frac{P_d}{2}(x^+(\bar{u}) + x - 2x_\star) - (J - R)\frac{P}{2}(x^+ + x). \end{aligned}$$

Since $BB^\dagger = I - (B^\perp)^\top[(B^\perp(B^\perp)^\top]^{-1}B^\perp$, the equality above reduces to

$$-(B^\perp)^\top[(B^\perp(B^\perp)^\top]^{-1}B^\perp\big[(J_d - R_d)\frac{P_d}{2}(x^+(\bar{u}) + x - 2x_\star) - (J-R)\frac{P}{2}(x^+ + x)\big] = 0$$

which holds true as (J_a, R_a, P_a) satisfy (6.15) and (6.20). As a consequence, the feedback solution to (6.17) assigns the target dynamics (6.16) to (6.2a). As far as the closed form is concerned, plugging $u = \bar{u} + v$ into (6.11), with $\bar{u}$ as in (6.18), one recovers (6.12). □

Remark 6.3.1. Differently from the general nonlinear case, the matching condition (6.13) takes the form of a linear matrix equality (6.15).

6.4 Concluding remarks

In this section, we have seen how modeling and control design specializes in the case of LTI port-Hamiltonian systems. Firstly, we introduced the definition of LTI discrete-time port-Hamiltonian system showing also its explicit representation. Then, we showed the structure of the negative output feedback computed upon the u-average output of the port-Hamiltonian system which achieves global asymptotic stability. Finally, the IDA-PBC problem is restated in the LTI setting, and a necessary and sufficient condition for solving the problem is given along with the explicit structure of the IDA-PBC feedback. Those results are partially included in:

> *A. Moreschini, M. Mattioni, S. Monaco and D. Normand-Cyrot, "Discrete port-controlled Hamiltonian dynamics and average passivation," 2019 IEEE 58th Conference on Decision and Control (CDC), Nice, France, 2019, pp. 1430-1435, doi: 10.1109/CDC40024.2019.9029809.*

> *A. Moreschini, M. Mattioni, S. Monaco and D. Normand-Cyrot, "Stabilization of Discrete Port-Hamiltonian Dynamics via Interconnection and Damping Assignment," in IEEE Control Systems Letters, vol. 5, no. 1, pp. 103-108, Jan. 2021, doi: 10.1109/LCSYS.2020.3000705.*

Part III

PORT-HAMILTONIAN SYSTEMS UNDER SAMPLING

Chapter 7

Modeling of sampled-data port-Hamiltonian systems

Contents

7.1 Formal instrumental results **162**

7.2 Constructive aspects **165**

7.3 Gradient dynamics under sampling **167**

7.4 Port-Hamiltonian dynamics under sampling **172**

7.4.1 Conservative dynamics 177

7.4.2 Dissipative dynamics 179

7.5 Input-state-output port-Hamiltonian systems **180**

7.6 Comparison with the literature model **184**

7.7 Concluding remarks **185**

This chapter concerns the modeling of gradient and port-Hamiltonian dynamics under sampling. It is well known that gradient and Hamiltonian dynamics have straight relations with fundamental properties of physical systems such as conservation and/or variational principles. Those dynamics are widely investigated in continuous time and are at the basis of *ad hoc* design approaches. In a sampled-data point of view, the following question naturally arises,

> *Does an exact sampled-data equivalent to a gradient and Hamiltonian dynamics exhibit a discrete gradient or Hamiltonian representation?*

To answer the question, a precise characterization of gradient and Hamiltonian dynamics under sampling is in this chapter. In particular, the contribution of this chapter is to provide exact sampled-data equivalent models to gradient and Hamiltonian structures preserving the continuous-time trajectories and energetic properties at all sampling instants. We show that the problem is solvable making reference to the same Hamiltonian as in continuous time but with suitably modified interconnection and damping matrices, parameterized by the sampling period. To achieve the structure under sampling we give first some instrumental results to characterize the sampled-data equivalent dynamics in term of the discrete gradient function. Finally, the proposed sampled-data representations for uncontrolled dynamics are generalized to input-state-output representations and further compared with an alternative sampled-data structure given in the related literature.

7.1 Formal instrumental results

In the present section we present basic formal results that are fundamental to describe the sampled-data structure of port-Hamiltonian dynamics.

In this respect, the first lemma describes the sampled-data autonomous dynamics described by the map $F^\delta(x)$ in terms of the vector field $f(x)$ of the continuous-time system, exploiting the exponential form

$$F^\delta(x) = e^{\delta \mathrm{L}_f} x - x.$$

The characterization of the sampled-data map in terms of the continuous-time vector field is essential for highlighting the continuous-time gradient into port-Hamiltonian dynamics.

Lemma 7.1.1. *Let $f : \mathbb{R}^n \to \mathbb{R}^n$ be a smooth vector-valued function, then for all $\delta \in]0, T^*[$, the associated sampled-data equivalent dynamics*

$$F^\delta(x) = e^{\delta \mathrm{L}_f} x - x,$$

satisfies the equality

$$x^+ - x = F^\delta(x) = \delta \mathcal{M}(\delta, f, x) f(x) \tag{7.1}$$

with $\mathcal{M}(\delta, f, x) \in \mathrm{Mat}_{\mathbb{R}}(n, n)$*, locally non singular, given by*

$$\mathcal{M}(\delta, f, x) = \frac{1}{\delta} \int_0^\delta \mathrm{J}[e^{s\mathrm{L}_f} x] ds \tag{7.2}$$

where "$\mathrm{J}[\cdot]$*" indicates the Jacobian with respect to* x *of the function into the brackets.*

Proof. The proof follows from the definition of $e^{\delta \mathrm{L}_f} x$, which might be written as

$$\begin{aligned}
e^{\delta \mathrm{L}_f} x - x &= \delta f(x) + \frac{\delta^2}{2!} \mathrm{L}_f(f)(x) + \frac{\delta^3}{3!} \mathrm{L}_f^2(f)(x) + \dots \\
&= \left(\delta \mathrm{J}[x] + \frac{\delta^2}{2!} \mathrm{J}[f] + \frac{\delta^3}{3!} \mathrm{J}[\mathrm{L}_f(f)] + \dots \right) f(x) \\
&= \mathrm{J} \left[\delta x + \frac{\delta^2}{2!} f(x) + \frac{\delta^3}{3!} \mathrm{L}_f(f)(x) + \dots \right] f(x) \\
&= \mathrm{J} \left[\int_0^\delta e^{sf} x ds \right] f(x) \\
&= \int_0^\delta \mathrm{J}[e^{s\mathrm{L}_f} x ds] f(x) \\
&= \delta \mathcal{M}(\delta, f, x) f(x)
\end{aligned}$$

with $\mathcal{M}(\delta, f, x)$ as in (7.2). The non singularity of $\mathcal{M}(\delta, f, x)$ follows by construction for δ small enough. □

The second instrumental Lemma generalizes Lemma 7.1.1 to the behaviour of any function $H(\cdot)$ along the sampled-data dynamics.

Lemma 7.1.2. *Let* $f : \mathbb{R}^n \to \mathbb{R}^n$ *be a smooth vector-valued function and* $H(\cdot) : \mathbb{R}^n \to \mathbb{R}$ *a smooth real-valued function, then for all* $\delta \in]0, T^*[$ *the associated sampled-data equivalent dynamics satisfies the variational equality below*

$$H(x^+) - H(x) = \delta \nabla^\top \mathcal{H}(\delta, f, x) f(x) = \delta \mathrm{L}_f \mathcal{H}(\delta, f, x), \tag{7.3}$$

which recovers the usual Lie derivative along f *of a new function* $\mathcal{H}(\delta, f, x)$ *given by*

$$\mathcal{H}(\delta, f, x) = \frac{1}{\delta} \int_0^\delta H(x(s)) ds = \Big(\frac{e^{\delta \mathrm{L}_f} - I}{\delta \mathrm{L}_f} H \Big)(x) = H(x) + \sum_{i \geq 1} \frac{\delta^i}{(i+1)!} \mathrm{L}_f^i H(x)$$

which depends on the f*-dynamics and is parameterized by the sampling period* δ*.*

Proof. The proof follows from the property of the exponential function $H(x^+) = H(e^{\delta \mathrm{L}_f}(x)) = e^{\delta \mathrm{L}_f} H(x)$ so that the variational equality

$$\begin{aligned} e^{\delta \mathrm{L}_f} H(x) - H(x) &= \delta \mathrm{L}_f H(x) + \frac{\delta^2}{2!} \mathrm{L}_f^2 H(x) + \frac{\delta^3}{3!} \mathrm{L}_f^3 H(x) + \dots \\ &= (\delta \nabla^\top H(x) + \frac{\delta^2}{2!} \nabla^\top (\mathrm{L}_f H)(x) + \frac{\delta^3}{3!} \nabla^\top (\mathrm{L}_f^2 H)(x) + \dots) f(x) \\ &= \nabla^\top \Big(\int_0^\delta e^{s \mathrm{L}_f} H(x) ds \Big) f(x) \\ &= \delta \nabla^\top \mathcal{H}(\delta, f, x) f(x) \end{aligned}$$

which yields

$$\mathcal{H}(\delta, f, x) = \frac{1}{\delta} \Big(\int_0^\delta e^{s \mathrm{L}_f} H(x) ds \Big) = \frac{1}{\delta} \Big(\int_0^\delta H(x(s)) ds \Big).$$

□

The third Lemma is a direct consequence of the aforestated Lemma 7.1.1 and Lemma 7.1.2.

Lemma 7.1.3. *Given a smooth vector field $f : \mathbb{R}^n \to \mathbb{R}^n$ and for any fixed $\delta \in]0, T^*[$ the associated sampled-data equivalent dynamics with*

$$e^{\delta \mathrm{L}_f} x - x = F^\delta(x),$$

then the discrete gradient of $H(\cdot)$ along the flow $F^\delta(x)$ satisfies

$$\bar{\nabla}^\top H|_x^{x^+} = \frac{1}{\delta} \nabla^\top \left(\int_0^\delta H(x(s)) ds \right) \mathcal{M}^{-1}(\delta, f, x). \tag{7.4}$$

To conclude this series of lemmas which are instrumental to properly characterize port-Hamiltonian systems under sampling, the next lemma rewrites the discrete gradient function in terms of the gradient itself.

Lemma 7.1.4. *Given a smooth vector field $f : \mathbb{R}^n \to \mathbb{R}^n$ and for any fixed $\delta \in]0, T^*[$ the associated sampled-data equivalent dynamics with*

$$e^{\delta \mathrm{L}_f} x - x = F^\delta(x),$$

then the discrete gradient of $H(\cdot)$ along the flow $F^\delta(x)$ satisfies

$$\bar{\nabla} H|_x^{x^+} = \nabla H(x) + \delta \mathcal{Q}(\delta, H, f, x) f(x) \tag{7.5}$$

with $\mathcal{Q}(\delta, H, f, x) \in \mathrm{Mat}_{\mathbb{R}}(n, n)$ given by

$$\mathcal{Q}(\delta, H, f, x) = \Big(\int_0^1 s \bar{\mathrm{J}}[\nabla H]|_x^{x+sF^\delta(x)} ds \Big) \mathcal{M}(\delta, f, x). \tag{7.6}$$

Proof. The proof follows from the definition of discrete gradient which can be expressed in the integral form

$$\bar{\nabla} H|_x^{x^+} = \bar{\nabla} H|_x^{x+F^\delta(x)} = \int_0^1 \nabla H(x + sF^\delta(x)) \mathrm{d}s.$$

By manipulating the above integral expression and invoking the property of Lemma 7.1.1, namely $F^\delta(x) = \delta \mathcal{M}(\delta, f, x) f(x)$ one gets

$$\begin{aligned}
\bar{\nabla} H|_x^{x^+} &= \nabla H(x) + \int_0^1 s \bar{\mathrm{J}}[\nabla H]|_x^{x+sF^\delta(x)} (e^{\delta \mathrm{L}_f} x - x) \mathrm{d}s \\
&= \nabla H(x) + \int_0^1 s \bar{\mathrm{J}}[\nabla H]|_x^{x+sF^\delta(x)} F^\delta(x) \mathrm{d}s \\
&= \nabla H(x) + \int_0^1 s \bar{\mathrm{J}}[\nabla H]|_x^{x+sF^\delta(x)} \mathrm{d}s \; \mathcal{M}(\delta, f, x) f(x)
\end{aligned}$$

which concludes the expression (7.5). □

7.2 Constructive aspects

In this section we provide constructive expressions of the objects intruduced in the previous section.

Remark 7.2.1. Easy computations provide the following expression of the discrete jacobian of the gradient function ∇H, that is

$$\begin{aligned}
\bar{\mathrm{J}}[\nabla H]|_x^{x+sF^\delta(x)} &= \int_0^1 \nabla^2 H(x + \tau s F^\delta(x)) \mathrm{d}\tau \\
&= \nabla^2 H(x) + \frac{s}{2} \left(\frac{\partial}{\partial x} \otimes \nabla^2 H(x) \right) \big(F^\delta(x) \otimes I \big) \\
&+ \frac{s^2}{3!} \big(F^{\delta\top}(x) \otimes I \big) \left(\frac{\partial^2}{\partial x^2} \otimes \nabla^2 H(x) \right) \big(F^\delta(x) \otimes I \big) + O(s^3),
\end{aligned}$$

so that one deduces the first terms of its integral form

$$\int_0^1 s\bar{\mathrm{J}}[\nabla H]|_x^{x+sF^\delta(x)}\mathrm{d}s = \frac{1}{2}\nabla^2 H(x) + \frac{\delta}{3!}\left(\frac{\partial}{\partial x}\otimes\nabla^2 H(x)\right)\left(\left(f(x)+\frac{\delta}{2}\mathrm{L}_f f(x)\right)\otimes I\right) + \frac{\delta^2}{4!}\left(f^\top(x)\otimes I\right)\left(\frac{\partial^2}{\partial x^2}\otimes\nabla^2 H(x)\right)(f(x)\otimes I) + O(\delta^3).$$

Remark 7.2.2. One can express the discrete gradient in x along the displacement $x + F^\delta(x)$ for the first terms, so obtaining an easy computable expression in terms of the usual gradient, Hessian matrix, and Kroneker product. More precisely the discrete gradient yields for the first terms

$$\bar{\nabla}H|_x^{x+F^\delta(x)} = \nabla H(x) + \frac{\delta}{2}\nabla^2 H(x)f(x) + \frac{\delta^2}{4}\nabla^2 H(x)\mathrm{J}[f]f(x) + \frac{\delta^2}{3!}\mathrm{L}_f\otimes\mathrm{L}_f\nabla H(x) + O(\delta^3)$$

where $\nabla^2 H(x)$ is the Hessian of $H(x)$ and

$$\mathrm{L}_f\otimes\mathrm{L}_f\nabla H(x) = \begin{pmatrix}\mathrm{L}_f\otimes\mathrm{L}_f\nabla_1 H(x)\\ \vdots \\ \mathrm{L}_f\otimes\mathrm{L}_f\nabla_n H(x)\end{pmatrix}$$

with, for all $p = 1,\dots,n$,

$$\mathrm{L}_f\otimes\mathrm{L}_f\nabla_p H(x) = \sum_{j=1}^n\sum_{i=1}^n \frac{\partial^3 H}{\partial x_i\partial x_j\partial x_p}f_i(x)f_j(x).$$

Remark 7.2.3. The function $\mathcal{M}(\delta, f, x)$ might be represented in terms of a formal operator defined by setting

$$\frac{e^{\delta\mathrm{L}_f}-I}{\delta\mathrm{L}_f} = I + \sum_{i\geq 1}\frac{\delta^i}{(i+1)!}\mathrm{L}_f^i,$$

which yields the following expression

$$\mathcal{M}(\delta, f, x) = \mathrm{J}\left[\frac{e^{\delta\mathrm{L}_f}-I}{\delta\mathrm{L}_f}(x)\right]. \tag{7.7}$$

Accordingly, one might provide a computable expression of $\mathcal{M}(\delta, f, x)$ defined as a series expansion in power of δ

$$\mathcal{M}(\delta, f, x) = I + \sum_{i \geq 1} \frac{\delta^i}{(i+1)!} \mathcal{M}_i(x),$$

with

$$\mathcal{M}_i(x) = \mathrm{J}[\mathrm{L}_f^{i-1} f(x)].$$

For the first terms on gets

$$\begin{aligned} \mathcal{M}_1(x) &= \mathrm{J}[f(x)] \\ \mathcal{M}_2(x) &= \mathrm{J}[\mathrm{J}[f(x)]f(x)]. \end{aligned}$$

Remark 7.2.4. Exploiting the computable expression of $\mathcal{M}(\delta, f, x)$ one defines the matrix $\mathcal{Q}(\delta, H, f, x)$ as a series expansion in power of δ

$$\mathcal{Q}(\delta, H, f, x) = \sum_{i \geq 0} \frac{\delta^i}{(i+1)!} \mathcal{Q}_i(x),$$

so that for the first terms one gets

$$\begin{aligned} \mathcal{Q}_0(x) &= \frac{1}{2} \nabla^2 H(x) \\ \mathcal{Q}_1(x) &= \frac{1}{3} \left(\frac{\partial}{\partial x} \otimes \nabla^2 H(x) \right) (f(x) \otimes I) + \nabla^2 H(x) \mathrm{J}[f(x)] \\ \mathcal{Q}_2(x) &= \frac{1}{4} \left(f^\top(x) \otimes I \right) \left(\frac{\partial^2}{\partial x^2} \otimes \nabla^2 H(x) \right) (f(x) \otimes I) + \frac{1}{2} \left(\frac{\partial}{\partial x} \otimes \nabla^2 H(x) \right) (\mathrm{L}_f f(x) \otimes I) \\ &\quad + \left(\frac{\partial}{\partial x} \otimes \nabla^2 H(x) \right) (f(x) \otimes I) \, \mathrm{J}[f(x)] + 3 \nabla^2 H(x) \mathrm{J}[\mathrm{J}[f(x)]f(x)]. \end{aligned}$$

7.3 Gradient dynamics under sampling

Let first consider the problem of representing the class of dynamics called gradient dynamics under sampling. In continuous time the dynamics is characterized by the gradient vector field

$$f(x) = -\nabla H(x)$$

with respect to the storage function $H(x)$ associated with its dynamics. In this respect, let first formally define the gradient dynamics.

Definition 7.3.1. Gradient dynamics are differential equations of the form

$$\dot{x}(t) = f(x(t)) = -\nabla H(x(t)) \tag{7.8}$$

with storage function $H(\cdot) : \mathbb{R}^n \to \mathbb{R}_{\geq 0}$.

The reason that gradient dynamics are grouped with the study of Lyapunov functions is that for gradient dynamics there is a natural Lyapunov candidate, that is $H(\cdot)$. Moreover, such dynamics satisfies by construction the forward difference inequality over the map $H(\cdot)$, for $\delta \in]0, T^*[$ small enough, since

$$H(x^+) - H(x) = \int_{k\delta}^{(k+1)\delta} \dot{H}(x(\tau))\mathrm{d}\tau = -\int_{k\delta}^{(k+1)\delta} \|\nabla H(x(\tau))\|^2 \mathrm{d}\tau \leq 0. \tag{7.9}$$

Except at equilibria the function $H(x)$ is strictly decreasing on orbits. Moreover, the direction $\nabla H(x)$ is the direction of most rapid increase of $H(x)$, while the direction $-\nabla H(x)$ defines the direction of most rapid decrease of $H(x)$.

The challenging problem now relies on the possibility to turn the sampled-data equivalent dynamics to the gradient dynamics (7.8) into discrete-time dynamics suitably equipped with the discrete gradient of $H(x)$, say $\bar{\nabla} H|_x^{x^+}$.

The following theorem achieves the result.

Theorem 7.3.1: Gradient dynamics under sampling

Given the continuous-time gradient dynamics (7.8), then for any fixed $\delta \in]0, T^*[$, its sampled-data equivalent dynamics admits the discrete-time representation

$$x^+ = x - \delta \mathcal{I}(\delta, -\nabla H, x) \bar{\nabla} H|_x^{x^+} \tag{7.10}$$

with non singular matrix

$$\mathcal{I}(\delta, -\nabla H, x) = \mathcal{M}(\delta, -\nabla H, x)(I - \delta \mathcal{Q}(\delta, H, -\nabla H, x))^{-1} \in \mathrm{Mat}_{\mathbb{R}}(n, n). \tag{7.11}$$

Additionally, the Hamiltonian function satisfies the variational equality

$$\begin{aligned} H(x^+) - H(x) &= -\int_0^\delta \nabla^\top H(x(s))\nabla H(x(s))ds \\ &= -\delta\bar{\nabla}^\top H|_x^{x^+}\mathcal{I}(\delta, -\nabla H, x)\bar{\nabla}H|_x^{x^+} \leq 0. \end{aligned} \tag{7.12}$$

Proof. According to the Lemma 7.1.1, one can rewrite the dynamics $F^\delta(x)$, fixing $f = -\nabla H(x)$, as follows

$$F^\delta(x) = -\delta\mathcal{M}(\delta, -\nabla H, x)\nabla H(x).$$

Since $(I - \delta\mathcal{Q}(\delta, f, x))$ is non singular by construction, one can manipulated the above equation so getting

$$F^\delta(x) = -\mathcal{M}(\delta, -\nabla H, x)(I - \delta\mathcal{Q}(\delta, -\nabla H, x))^{-1}(I - \delta\mathcal{Q}(\delta, -\nabla H, x))\nabla H(x).$$

Finally, according to Lemma 7.1.4 one defines the discrete gradient as

$$\bar{\nabla}H|_x^{x^+} = \nabla H(x) + \delta\mathcal{Q}(\delta, H, -\nabla H, x)\nabla H(x),$$

thus one deduces

$$F^\delta(x) = -\delta\mathcal{I}(\delta, -\nabla H, x)\bar{\nabla}H|_x^{x^+}$$

with $\mathcal{I}(\delta, H, -\nabla H, x)$ given in (7.11). The non singularity of $\mathcal{I}(\delta, H, f, x)$ follows from the non singularity of $\mathcal{M}(\delta, f, x)$ and $(I - \delta\mathcal{Q}(\delta, f, x))$. Moreover, the equality (7.12) is direct consequence of the variational equality $H(x^+) - H(x)$ expressed in terms of the discrete gradient and the provided discrete gradient dynamics (7.10) which yields

$$\begin{aligned} H(x^+) - H(x) &= \bar{\nabla}^\top H|_x^{x^+}(x^+ - x) \\ &= \bar{\nabla}^\top H|_x^{x^+}F^\delta(x) \\ &= -\delta\bar{\nabla}^\top H|_x^{x^+}\mathcal{I}(\delta, -\nabla H, x)\bar{\nabla}H|_x^{x^+} \leq 0. \end{aligned}$$

The variational equality $H(x^+) - H(x)$ can be equivalently expressed through the integration of the Hamiltonian function along the continuous-time dynamics

$$H(x^+) - H(x) = \int_0^\delta \dot{H}(x(s))ds$$

that yields

$$H(x^+) - H(x) = -\int_0^\delta \nabla^\top H(x(s))\nabla H(x(s))ds = -\delta\bar{\nabla}^\top H|_x^{x^+}\mathcal{I}(\delta, -\nabla H, x)\bar{\nabla}H|_x^{x^+},$$

both the expressions are equal since the sampled-data dynamics matches at the sampling times the continuous-time one by definition. □

The results of Theorem 7.3.1 ensure the existence of a discrete gradient-like dynamics based on the sampled-data equivalent model of the continuous-time dynamics with respect to the same real-valued function $H(\cdot)$. Differently, the discrete representation introduces a new matrix $\mathcal{I}(\delta, H, -\nabla H, x)$ which depends on the function $H(\cdot)$ itself and on the sampling period δ.

Remark 7.3.1. From the energy variation (7.12) one deduces that the symmetric part of $\mathcal{I}(\delta, -\nabla H, x)$ is positive semidefinite, namely

$$\frac{1}{2}\mathcal{I}(\delta, -\nabla H, x) + \frac{1}{2}\mathcal{I}(\delta, -\nabla H, x) \succeq 0.$$

Remark 7.3.2. Easy computation can be performed exploiting the computable expression of $\mathcal{M}(\delta, f, x)$ and $\mathcal{Q}(\delta, H, f, x)$, and the fact that the inverse matrix $(I - \delta\mathcal{Q}(\delta, H, f, x))^{-1}$ can be formally defined as

$$(I - \delta\mathcal{Q}(\delta, H, f, x))^{-1} = I + \sum_{p\geq 1} \delta^p \left(\mathcal{Q}(\delta, H, f, x)\right)^p.$$

Then the matrix $\mathcal{I}(\delta, H, -\nabla H, x)$ can be described by its series expansion in powers of δ by

$$\mathcal{I}(\delta, -\nabla H, x) = \sum_{i\geq 0} \frac{\delta^i}{(i+1)!}\mathcal{I}_i,$$

which gives the expressions for first terms

$$
\begin{aligned}
\mathcal{I}_0 &= \mathcal{M}_0 = I \\
\mathcal{I}_1 &= \mathcal{M}_1 + 2\mathcal{M}_0\mathcal{Q}_0 = \mathbf{0}_{n\times n} \\
\mathcal{I}_2 &= \mathcal{M}_2 + 3\mathcal{M}_0\mathcal{Q}_1 + 6\mathcal{M}_0\mathcal{Q}_0\mathcal{Q}_0 + 3\mathcal{M}_1\mathcal{Q}_0 = -\frac{1}{2}\nabla^2 H(x)\nabla^2 H(x) \\
&= -\frac{1}{2}\sum_{i=1}^{n}\begin{pmatrix}
\left(\frac{\partial^2 H(x)}{\partial x_1 \partial x_i}\right)^2 & \frac{\partial^2 H(x)}{\partial x_1 \partial x_i}\frac{\partial^2 H(x)}{\partial x_2 \partial x_i} & \cdots & \frac{\partial^2 H(x)}{\partial x_1 \partial x_i}\frac{\partial^2 H(x)}{\partial x_n \partial x_i} \\
\frac{\partial^2 H(x)}{\partial x_1 \partial x_i}\frac{\partial^2 H(x)}{\partial x_2 \partial x_i} & \left(\frac{\partial^2 H(x)}{\partial x_2 \partial x_i}\right)^2 & \cdots & \frac{\partial^2 H(x)}{\partial x_2 \partial x_i}\frac{\partial^2 H(x)}{\partial x_n \partial x_i} \\
\vdots & \vdots & \ddots & \vdots \\
\frac{\partial^2 H(x)}{\partial x_1 \partial x_i}\frac{\partial^2 H(x)}{\partial x_n \partial x_i} & \frac{\partial^2 H(x)}{\partial x_2 \partial x_i}\frac{\partial^2 H(x)}{\partial x_n \partial x_i} & \cdots & \left(\frac{\partial^2 H(x)}{\partial x_n \partial x_i}\right)^2
\end{pmatrix}.
\end{aligned}
$$

Thus, for the first terms the sampled-data gradient dynamics yields the form,

$$
\begin{aligned}
x^+ &= x - \delta(\mathcal{I}_0 + \frac{\delta^2}{6}\mathcal{I}_2)\bar{\nabla}H|_x^{x^+} + O(\delta^4) \\
&= x - \delta\bar{\nabla}H|_x^{x^+} + \frac{\delta^3}{12}\nabla^2 H(x)\nabla^2 H(x)\bar{\nabla}H|_x^{x^+} + O(\delta^4)
\end{aligned}
$$

so recovering in first approximation in δ the discrete gradient dynamics.

Remark 7.3.3. In case of separable Hamiltonian function

$$H(x) = \sum_{i=0}^{n} l_i(x_i)$$

for any continuously differential function $l_i(\cdot) : \mathbb{R} \to \mathbb{R}$ the matrix $\mathcal{I}_2$ is diagonal and is specified as

$$
\mathcal{I}_2 = -\frac{1}{2}\begin{pmatrix}
\left(\frac{\partial^2 l_1(x_1)}{\partial x_1^2}\right)^2 & 0 & \cdots & 0 \\
0 & \left(\frac{\partial^2 l_2(x_2)}{\partial x_2^2}\right)^2 & \cdots & 0 \\
0 & \vdots & \ddots & 0 \\
0 & \cdots & 0 & \left(\frac{\partial^2 l_n(x_n)}{\partial x_n^2}\right)^2
\end{pmatrix}.
$$

Remark 7.3.4. The expression of the discrete gradient given in Lemma 7.1.4 can be specified in the case of gradient dynamics of the form (7.8), which gives for the first terms

$$\begin{aligned}\bar{\nabla} H|_x^{x+F^\delta(x)} &= \Big(I - \delta \mathcal{Q}(\delta, H, -\nabla H, x)\Big)\nabla H(x) \\ &= \nabla H(x) - \delta \mathcal{Q}_0 \nabla H(x) - \frac{\delta^2}{2}\mathcal{Q}_1 \nabla H(x) + O(\delta^3) \\ &= \nabla H(x) - \frac{\delta}{2}\nabla^2 H(x)\nabla H(x) + \frac{\delta^2}{2}\nabla^2 H(x)\nabla^2 H(x)\nabla H(x) \\ &+ \frac{\delta^2}{6}\left(\frac{\partial}{\partial x} \otimes \nabla^2 H(x)\right)(\nabla H(x) \otimes I)\,\nabla H(x) + O(\delta^3).\end{aligned}$$

7.4 Port-Hamiltonian dynamics under sampling

In the previous section we discussed the case of gradient dynamics under sampling. How do these methods extend to port-Hamiltonian dynamics? To answer the question let a continuous-time port-Hamiltonian dynamics given by

$$\dot{x} = f(x) = (J(x) - R(x))\nabla H \tag{7.13}$$

with matrices $J(x) = -J^\top(x)$ and $R(x) = R^\top(x) \succeq 0$ catching, respectively, the (power-preserving) interconnection and dissipative structure of the dynamics, and the Hamiltonian function $H(\cdot) : \mathbb{R}^n \to \mathbb{R}_{\geq 0}$. See Chapter 1 for details.

Also for dynamics of the form (7.13) the instrumental lemmas presented in Section 7.1 can be exploited to define sampled-data representations which preserves their characteristic structure.

The theorem below characterizes the port-Hamiltonian dynamics under sampling.

Theorem 7.4.1: Port-Hamiltonian dynamics under sampling

Given a port-Hamiltonian dynamics (7.13), then for any $\delta \in]0, T^*[$, its sampled equivalent dynamics admits the discrete port-Hamiltonian structure

$$x^+ = x + \delta \mathcal{S}^\delta_{J-R}(\delta, f, x)\bar{\nabla} H|_x^{x^+} \tag{7.14}$$

where

$$\mathcal{S}^\delta_{J-R}(\delta, f, x) = \mathcal{M}(\delta, f, x)(J(x) - R(x))\left(I + \delta \mathcal{Q}(\delta, H, f, x)(J(x) - R(x))\right)^{-1},$$

that satisfies the energy balance equality

$$\begin{aligned} H(x^+) - H(x) &= \delta \bar{\nabla} H|_x^{x^+ \top} \mathcal{S}_{J-R}^{\delta}(\delta, f, x) \bar{\nabla} H|_x^{x^+} \\ &= -\int_0^{\delta} \nabla^\top H(x(s)) R(x) \nabla H(x(s)) ds \leq 0. \end{aligned} \tag{7.15}$$

Proof. According to Lemma 7.1.1, the flow $F^\delta(x)$ modifies as

$$F^\delta(x) = \delta \mathcal{M}(\delta, f, x)(J(x) - R(x)) \nabla H(x)$$

and, from Lemma 7.1.4, the discrete gradient function rewrites

$$\begin{aligned} \bar{\nabla} H|_x^{x+F^\delta(x)} &= \nabla H(x) + \delta \mathcal{Q}(\delta, H, f, x) f(x) \\ &= (I + \delta \mathcal{Q}(\delta, H, f, x)(J(x) - R(x))) \nabla H(x). \end{aligned}$$

Finally by equating $F^\delta(x) = (\mathcal{J} - \mathcal{R})(\delta, f, x) \bar{\nabla} H|_x^{x+F^\delta(x)}$, one gets the following relation

$$\mathcal{M}(\delta, f, x)(J(x) - R(x)) = \mathcal{S}_{J-R}^{\delta}(\delta, f, x) \left(I + \delta \mathcal{Q}(\delta, H, f, x)(J(x) - R(x))\right)$$

which is satisfied for $\mathcal{S}_{J-R}^{\delta}(\delta, f, x)$ stated above in the Theorem. Moreover by definition of discrete gradient the energy balance equality (7.15) holds true, since

$$H(x^+) - H(x) = (x^+ - x)^\top \bar{\nabla} H|_x^{x^+} = \delta \bar{\nabla} H|_x^{x^+ \top} \mathcal{S}_{J-R}^{\delta}(\delta, f, x) \bar{\nabla} H|_x^{x^+}$$

and by the property of the exponential function $H(x^+) = H(e^{\delta \mathrm{L}_f}(x)) = e^{\delta \mathrm{L}_f} H(x)$ one also gets

$$\begin{aligned} H(x^+) - H(x) &= e^{\delta \mathrm{L}_f} H(x) - H(x) \\ &= \int_0^{\delta} \nabla^\top H(x(s))(J(x(s)) - R(x(s))) \nabla H(x(s)) ds \\ &= -\int_0^{\delta} \nabla^\top H(x(s)) R(x(s)) \nabla H(x(s)) ds \leq 0. \end{aligned}$$

then (7.15) follows. □

Theorem 7.4.1 shows that the continuous-time dynamics (7.13) preserves its port-Hamiltonian structure at a discrete-time level with respect to the same energy function $H(\cdot)$ and modified interconnection and dissipative structure, say $\mathcal{S}_{J-R}^{\delta}(\delta, f, x)$,

which depends on the sampling period δ. Moreover, its behavior along the function $H(\cdot)$ is, by construction, the same as the continuous-time one, at the sampling instants.
The construction of the matrix $\mathcal{S}^{\delta}_{J-R}(\delta, f, x)$ aims to guarantee that the sampled-data dynamics exhibits a discrete-port Hamiltonian structure given in Definition 4.1.1 (in case of zero input) through suitably computed δ-dependent matrices.

Remark 7.4.1. The port-Hamiltonian structure introduced in Theorem 7.4.1 are slight generalization of the result presented for the gradient dynamics and given in Theorem 7.3.1. Indeed, this implies that, when setting the matrices $J(x)-R(x) = -I$ one gets under sampling $\mathcal{S}^{\delta}_{J-R}(\delta, f, x) = -\mathcal{I}(\delta, f, x)$.

Remark 7.4.2. Approximations of the sampled-data matrix $\mathcal{S}^{\delta}_{J-R}(\delta, f, x)$ can be iteratively computed exploiting the computable expression of the inverse matrix

$$(I + \delta\mathcal{Q}(\delta, H, f, x)(J(x) - R(x)))^{-1}$$

which can be formally defined as

$$(I + \delta\mathcal{Q}(\delta, H, f, x)(J(x) - R(x)))^{-1} = I + \sum_{p\geq 1}(-1)^p\delta^p \left(\mathcal{Q}(\delta, H, f, x)(J(x) - R(x))\right)^p .$$

Expressing the sampled-data mapping in its series expansion in powers of δ as follows

$$\mathcal{S}^{\delta}_{J-R}(\delta, f, x) = \sum_{i\geq 0} \frac{\delta^i}{(i+1)!}(\mathcal{S}^{\delta}_{\mathcal{J}-\mathcal{R}})_i, \tag{7.16}$$

with matrix

$$(\mathcal{S}^{\delta}_{\mathcal{J}-\mathcal{R}})_i = \sum_{j=0}^{i-1}(\mathcal{M}_i - \frac{(i+1)!}{(j+1)!(i-j)!}(\mathcal{S}^{\delta}_{\mathcal{J}-\mathcal{R}})_j\mathcal{Q}_{i-1-j})(\mathcal{S}^{\delta}_{\mathcal{J}-\mathcal{R}})_0 \tag{7.17}$$

which yields for the first terms

$$(\mathcal{S}^{\delta}_{\mathcal{J}-\mathcal{R}})_0 = (J(x) - R(x)) \tag{7.18a}$$
$$(\mathcal{S}^{\delta}_{\mathcal{J}-\mathcal{R}})_1 = (\mathcal{M}_1 - 2(J(x) - R(x))\mathcal{Q}_0)\,(J(x) - R(x)) \tag{7.18b}$$
$$(\mathcal{S}^{\delta}_{\mathcal{J}-\mathcal{R}})_2 = \big(\mathcal{M}_2 - 3\mathcal{M}_1(J(x) - R(x))\mathcal{Q}_0 - 3(J(x) - R(x))\mathcal{Q}_1 \tag{7.18c}$$
$$+ 6(J(x) - R(x))\mathcal{Q}_0(J(x) - R(x))\mathcal{Q}_0\big)(J(x) - R(x)), \tag{7.18d}$$

with $\mathcal{M}_i$ and $\mathcal{Q}_i$ respectively reported in Remark 7.2.3 and Remark 7.2.4.

Remark 7.4.3. To recover a port-Hamiltonian representation in terms of skew-symmetric and symmetric matrix one can split the matrix $\mathcal{S}^{\delta}_{J-R}(\delta, f, x)$ in a skew-symmetric and symmetric part, so that

$$\mathcal{S}^{\delta}_{J-R}(\delta, f, x) = \mathcal{J}(\delta, f, x) - \mathcal{R}(\delta, f, x) \tag{7.19}$$

with matrices

$$\begin{aligned}\mathcal{J}(\delta, f, x) &= \frac{1}{2}[\mathcal{S}^{\delta}_{J-R}(\delta, f, x) - \mathcal{S}^{\delta\top}_{J-R}(\delta, f, x)] \in \mathrm{Skew}_{\mathbb{R}}(n, n)\\ \mathcal{R}(\delta, f, x) &= -\frac{1}{2}[\mathcal{S}^{\delta}_{J-R}(\delta, f, x) + \mathcal{S}^{\delta\top}_{J-R}(\delta, f, x)] \in \mathrm{Sym}_{\mathbb{R}}(n, n)\end{aligned}$$

and computing their series expansion in δ

$$\mathcal{J}(\delta, f, x) = \sum_{i\geq 0} \frac{\delta^i}{(i+1)!}\mathcal{J}_i \tag{7.20}$$

$$\mathcal{R}(\delta, f, x) = \sum_{i\geq 0} \frac{\delta^i}{(i+1)!}\mathcal{R}_i \tag{7.21}$$

one computes the first terms for the skew-symmetric matrix as

$$\begin{aligned}\mathcal{J}_0 &= J(x)\\ \mathcal{J}_1 &= \frac{1}{2}\left(\mathcal{M}_1(J(x) - R(x)) + (J(x) + R(x))\mathcal{M}_1^{\top}\right) + 2\left(J(x)\mathcal{Q}_0R(x) + R(x)\mathcal{Q}_0J(x)\right)\\ \mathcal{J}_2 &= \frac{1}{2}\Big(\mathcal{M}_2J(x) + J(x)\mathcal{M}_2^{\top} + 3(J(x)\mathcal{Q}_0J(x)\mathcal{M}_1^{\top} - \mathcal{M}_1J(x)\mathcal{Q}_0J(x))\\ &\quad + 3(\mathcal{M}_1R(x)\mathcal{Q}_0J(x) + J(x)\mathcal{Q}_0R(x)\mathcal{M}_1^{\top}) + 3J(x)(\mathcal{Q}_1^{\top} - \mathcal{Q}_1)J(x)\\ &\quad + 12J(x)\mathcal{Q}_0J(x)\mathcal{Q}_0J(x) + 6(J(x)\mathcal{Q}_0J(x)\mathcal{Q}_0R(x) - R(x)\mathcal{Q}_0J(x)\mathcal{Q}_0J(x))\\ &\quad + 6(R(x)\mathcal{Q}_0R(x)\mathcal{Q}_0J(x) + J(x)\mathcal{Q}_0R(x)\mathcal{Q}_0R(x)) + R(x)\mathcal{M}_2^{\top} - \mathcal{M}_2R(x)\\ &\quad + 3(\mathcal{M}_1J(x)\mathcal{Q}_0R(x) + R(x)\mathcal{Q}_0J(x)\mathcal{M}_1^{\top}) + 3(R(x)\mathcal{Q}_0R(x)\mathcal{M}_1^{\top} - \mathcal{M}_1R(x)\mathcal{Q}_0R(x))\\ &\quad + 3(J(x)\mathcal{Q}_1R(x) + R(x)\mathcal{Q}_1^{\top}J(x)) + 6(J(x)\mathcal{Q}_0R(x)\mathcal{Q}_0R(x) + R(x)\mathcal{Q}_0R(x)\mathcal{Q}_0J(x))\\ &\quad + 6(R(x)\mathcal{Q}_0J(x)\mathcal{Q}_0J(x) - J(x)\mathcal{Q}_0J(x)\mathcal{Q}_0R(x)) + 12R(x)\mathcal{Q}_0J(x)\mathcal{Q}_0R(x)\\ &\quad + 3(R(x)\mathcal{Q}_1J(x) + J(x)\mathcal{Q}_1^{\top}R(x)) + 3R(x)(\mathcal{Q}_1^{\top} - \mathcal{Q}_1)R(x)\Big),\end{aligned}$$

and the first terms for the symmetric matrix

$$
\begin{aligned}
\mathcal{R}_0 &= R(x)\\
\mathcal{R}_1 &= \frac{1}{2}\left((J(x)+R(x))\mathcal{M}_1^\top - \mathcal{M}_1(J(x)-R(x))\right) + 2\left(J(x)\mathcal{Q}_0 J(x) + R(x)\mathcal{Q}_0 R(x)\right)\\
\mathcal{R}_2 &= \frac{1}{2}\Big(J(x)\mathcal{M}_2^\top - \mathcal{M}_2 J(x) + 3(J(x)\mathcal{Q}_0 J(x)\mathcal{M}_1^\top + \mathcal{M}_1 J(x)\mathcal{Q}_0 J(x))\\
&\quad - 3(\mathcal{M}_1 R(x)\mathcal{Q}_0 J(x) - J(x)\mathcal{Q}_0 R(x)\mathcal{M}_1^\top) + 3J(x)(\mathcal{Q}_1 + \mathcal{Q}_1^\top)J(x)\\
&\quad + 12J(x)\mathcal{Q}_0 R(x)\mathcal{Q}_0 J(x) + 6(J(x)\mathcal{Q}_0 J(x)\mathcal{Q}_0 R(x) + R(x)\mathcal{Q}_0 J(x)\mathcal{Q}_0 J(x))\\
&\quad - 6(R(x)\mathcal{Q}_0 R(x)\mathcal{Q}_0 J(x) - J(x)\mathcal{Q}_0 R(x)\mathcal{Q}_0 R(x)) + R(x)\mathcal{M}_2^\top + \mathcal{M}_2 R(x)\\
&\quad - 3(\mathcal{M}_1 J(x)\mathcal{Q}_0 R(x) - R(x)\mathcal{Q}_0 J(x)\mathcal{M}_1^\top) + 3(R(x)\mathcal{Q}_0 R(x)\mathcal{M}_1^\top + \mathcal{M}_1 R(x)\mathcal{Q}_0 R(x))\\
&\quad - 3(J(x)\mathcal{Q}_1 R(x) - R(x)\mathcal{Q}_1^\top J(x)) - 6(J(x)\mathcal{Q}_0 R(x)\mathcal{Q}_0 R(x) - R(x)\mathcal{Q}_0 R(x)\mathcal{Q}_0 J(x))\\
&\quad + 6(R(x)\mathcal{Q}_0 J(x)\mathcal{Q}_0 J(x) + J(x)\mathcal{Q}_0 J(x)\mathcal{Q}_0 R(x)) + 12R(x)\mathcal{Q}_0 R(x)\mathcal{Q}_0 R(x)\\
&\quad - 3(R(x)\mathcal{Q}_1 J(x) - J(x)\mathcal{Q}_1^\top R(x)) + 3R(x)(\mathcal{Q}_1^\top + \mathcal{Q}_1)R(x)\Big),
\end{aligned}
$$

with $\mathcal{M}_i$ and $\mathcal{Q}_i$ respectively reported in Remark 7.2.3 and Remark 7.2.4. Thus, for the first terms the sampled-data port-Hamiltonian dynamics yields the form,

$$x^+ = x - \delta(\mathcal{J}_0 - \mathcal{R}_0)\bar{\nabla}H|_x^{x^+} - \frac{\delta^2}{2}(\mathcal{J}_1 - \mathcal{R}_1)\bar{\nabla}H|_x^{x^+} - \frac{\delta^3}{6}(\mathcal{J}_2 - \mathcal{R}_2)\bar{\nabla}H|_x^{x^+} + O(\delta^4).$$

Remark 7.4.4. In the case in which $J(x)$ and $R(x)$ are assumed having constant entries, say $J(x) = J$ and $R(x) = R$, the constructive matrices characterizing the series expansion in δ in (7.20) and (7.21) gets the following structure for the first terms

$$
\begin{aligned}
\mathcal{J}_0 &= J\\
\mathcal{J}_1 &= \mathbf{0}_{n\times n}\\
\mathcal{J}_2 &= \frac{1}{2}\big((J\nabla^2 H(x)J + R\nabla^2 H(x)R)\nabla^2 H(x)J\\
&\qquad + (J\nabla^2 H(x)R + R\nabla^2 H(x)J)\nabla^2 H(x)R\big),
\end{aligned}
$$

and

$$
\begin{aligned}
\mathcal{R}_0 &= R\\
\mathcal{R}_1 &= \mathbf{0}_{n\times n}\\
\mathcal{R}_2 &= \frac{1}{2}\big((J\nabla^2 H(x)J + R\nabla^2 H(x)R)\nabla^2 H(x)R\\
&\qquad + (J\nabla^2 H(x)R + R\nabla^2 H(x)J)\nabla^2 H(x)J\big).
\end{aligned}
$$

Thus, for the first terms the sampled-data port-Hamiltonian dynamics yields the form,

$$x^+ = x - \delta(\mathcal{J}_0 - \mathcal{R}_0)\bar{\nabla}H|_x^{x^+} - \frac{\delta^3}{6}(\mathcal{J}_2 - \mathcal{R}_2)\bar{\nabla}H|_x^{x^+} + O(\delta^4)$$

Remark 7.4.5. The energy-balance equality (7.15) when decoupling the $\mathcal{S}^\delta_{J-R}(\delta, f, x)$ as in (7.19), i.e. $\mathcal{S}^\delta_{J-R}(\delta, f, x) = \mathcal{J}(\delta, f, x) - \mathcal{R}(\delta, f, x)$, clearly rewrites as

$$H(x^+) - H(x) = -\delta\bar{\nabla}H|_x^{x^+\top}\mathcal{R}(\delta, f, x)\bar{\nabla}H|_x^{x^+} \leq 0.$$

Then by construction the matrix $\mathcal{R}(\delta, f, x)$ which verifies the inequality above is positive semidefinite. However, its positive semidefiniteness does not suffice to ensure that each matrix $\mathcal{R}_i$, composing the series expansion in δ of $\mathcal{R}(\delta, f, x)$ as in (7.21), is positive semidefinite.

Remark 7.4.6. The discrete gradient function Lemma 7.1.4 can be specified, in the case of port-Hamiltonian dynamics, as a series expansion in power of δ as follows

$$\begin{aligned}
\bar{\nabla}H|_x^{x+F^\delta(x)} &= \Big(I + \delta\mathcal{Q}(\delta, H, f, x)\Big)(J(x) - R(x))\nabla H(x) \\
&= \nabla H(x) + \delta\mathcal{Q}_0(J(x) - R(x))\nabla H(x) + \frac{\delta^2}{2}\mathcal{Q}_1(J(x) - R(x))\nabla H(x) + O(\delta^3) \\
&= \nabla H(x) + \frac{\delta}{2}\nabla^2 H(x)(J(x) - R(x))\nabla H(x) \\
&+ (\frac{\delta^2}{3!}\left(\frac{\partial}{\partial x}\otimes\nabla^2 H(x)\right)((J(x) - R(x))\nabla H(x)\otimes I)\,(J(x) - R(x))\nabla H(x) \\
&+ \frac{\delta^2}{2}\nabla^2 H(x)\mathrm{J}\,[(J(x) - R(x))\nabla H(x)]\,(J(x) - R(x))\nabla H(x)) + O(\delta^3).
\end{aligned}$$

7.4.1 Conservative dynamics

Conservative dynamics are dynamics related to frictionless systems, as already deeply discussed in Chapter 4. For sake of completeness, the present section contains a review of the Theorem 7.4.1 in case of zero dissipation of the continuous-time dynamics, say $R(x) = 0$.

Corollary 7.4.1. *Given a conservative port-Hamiltonian dynamics* (7.13) *with* $R(x) = 0$ $(f(x) = J(x)\nabla H(x))$*, then for any* $\delta \in]0, T^*[$*, its sampled equivalent dynamics admits the discrete conservative port-Hamiltonian structure*

$$x^+ = x + \delta \mathcal{S}_J^\delta(\delta, f, x)\bar{\nabla} H|_x^{x^+} \tag{7.22}$$

with mapping

$$\mathcal{S}_J^\delta(\delta, f, x) = \mathcal{M}(\delta, f, x)J(x)\Big(I + \delta \mathcal{Q}(\delta, H, f, x)J(x)\Big)^{-1}$$

verifying by construction the variational equality

$$H(x^+) - H(x) = \delta \bar{\nabla}^\top H|_x^{x^+} \mathcal{S}_J^\delta(\delta, f, x)\bar{\nabla} H|_x^{x^+} = 0.$$

Proof. The structure on the sampled-data matrix $\mathcal{S}_J^\delta(\delta, f, x)$ is exactly the structure given in Theorem 7.4.1 when setting $R(x) = 0$. Thus its sampled equivalent representation satisfies the lossless condition along the function $H(x)$, i.e.

$$\begin{aligned}
H(x^+) - H(x) &= \delta \bar{\nabla}^\top H|_x^{x^+} \mathcal{S}_J^\delta(\delta, f, x)\bar{\nabla} H|_x^{x^+} \\
&= e^{\delta \mathrm{L}_f} H(x) - H(x) \\
&= \int_0^\delta \nabla^\top H(x(s))J(x(s))\nabla H(x(s))ds \\
&= \delta \mathrm{L}_f H(x) + \frac{\delta^2}{2!}\mathrm{L}_f^2 H(x) + \frac{\delta^3}{3!}\mathrm{L}_f^3 H(x) + \cdots \\
&= \delta \nabla^\top H(x)J(x)\nabla H(x) + \sum_{i \geq 2} \frac{\delta^i}{i!}\mathrm{L}_f^{i-1}\left(\nabla^\top H(x)J(x)\nabla H(x)\right) + \cdots = 0.
\end{aligned}$$

□

The above result shows that the sampled-data equivalent dynamics to a conservative port-Hamiltonian system admits a sampled-data representation that preserves the property of conservation of energy which states that the total energy of the unforced system remains constant along the time. In particular, every state trajectory remains at all the sampling instants $k\delta$ on the level surface of $H(x)$ defined by its initial condition $x(0)$ $(H(x(k\delta)) = H(x(0)))$.

Remark 7.4.7. An interesting class of conservative dynamics are the ones associated with canonical Hamiltonian vector fields, of the form

$$\begin{pmatrix} \dot{q} \\ \dot{p} \end{pmatrix} = \begin{pmatrix} \mathbf{0}_{n\times n} & I \\ -I & \mathbf{0}_{n\times n} \end{pmatrix} \begin{pmatrix} \nabla_q H(q,p) \\ \nabla_q H(q,p) \end{pmatrix} \tag{7.23}$$

with $I \in \mathrm{Mat}_{\mathbb{R}}(n,n)$ and state vector $(q,p) \in \mathbb{R}^{2n}$, so that $J \in \mathrm{Sym}_{\mathbb{R}}(2n,2n)$ with by construction $R = 0$. This class of systems clearly admits an equivalent sampled-data representation of the form (7.22). According to Remark 7.4.2 the sampled-data interconnection matrix $\mathcal{S}_J^\delta(\delta, f, x)$ can be iteratively computed in series expansion in power of δ as in (7.20), with the first terms taking the form

$$\mathcal{J}_0 = \begin{pmatrix} \mathbf{0}_{n\times n} & I \\ -I & \mathbf{0}_{n\times n} \end{pmatrix}, \quad \mathcal{J}_1 = \begin{pmatrix} \mathbf{0}_{n\times n} & \mathbf{0}_{n\times n} \\ \mathbf{0}_{n\times n} & \mathbf{0}_{n\times n} \end{pmatrix}, \quad \mathcal{J}_2 = \begin{pmatrix} \mathbf{0}_{n\times n} & \phi(H) \\ -\phi(H) & \mathbf{0}_{n\times n} \end{pmatrix}$$

with

$$\phi(H) := (\nabla_p^\top \nabla_q H(q,p))^2 - \nabla_q^\top \nabla_q H(q,p) \nabla_p^\top \nabla_p H(q,p).$$

7.4.2 Dissipative dynamics

In the present section a special class of dissipative dynamics under sampling is presented. Differently from the conservative dynamics, dissipative dynamics are those whose energy dissipates along the time. In this context, dissipative dynamics are assumed of the form (7.13) but with zero interconnection matrix, say $J(x) = 0$. This dynamics is a straight generalization of the gradient dynamics already discussed. The following corollary specializes the result in Theorem 7.4.1 in case of dissipative dynamics.

Corollary 7.4.2. *Given a dissipative port-Hamiltonian dynamics* (7.13) *with* $J(x) = 0$ $(f(x) = -R(x)\nabla H(x))$*, then for any* $\delta \in]0, T^*[$*, its sampled equivalent dynamics admits the discrete conservative port-Hamiltonian structure*

$$x^+ = x - \delta \mathcal{S}_R^\delta(\delta, f, x) \bar{\nabla} H|_x^{x^+} \tag{7.24}$$

with mapping

$$\mathcal{S}_R^\delta(\delta, f, x) = \mathcal{M}(\delta, f, x)R(x)\Big(\delta\mathcal{Q}(\delta, H, f, x)R(x) - I\Big)^{-1}$$

verifying by construction the dissipation inequality

$$H(x^+) - H(x) = -\delta\bar{\nabla}^\top H|_x^{x^+}\mathcal{S}_R^\delta(\delta, f, x)\bar{\nabla}H|_x^{x^+} \leq 0.$$

Proof. The matrix $\mathcal{S}_R^\delta(\delta, f, x)$ is exactly the structure given in Theorem 7.4.1 when setting $J(x) = 0$. Thus, by construction, its sampled equivalent representation satisfies the dissipation inequality, for any δ,

$$\begin{aligned} H(x^+) - H(x) &= -\delta\bar{\nabla}^\top H|_x^{x^+}\mathcal{S}_R^\delta(\delta, f, x)\bar{\nabla}H|_x^{x^+} \\ &= e^{\delta \mathrm{L}_f}H(x) - H(x) \\ &= -\int_0^\delta \nabla^\top H(x(s))R(x(s))\nabla H(x(s))ds \leq 0. \end{aligned}$$

□

For sake of completeness, it is worth underlining that the sampled-data matrix $\mathcal{S}_{J-R}^\delta(\delta, f, x)$, given in Theorem 7.4.1, is by construction different than $\mathcal{S}_J^\delta(\delta, f, x) - \mathcal{S}_R^\delta(\delta, f, x)$, respectively arising form the conservative and dissipative case, namely

$$\mathcal{S}_{J-R}^\delta(\delta, (J-R)\nabla H, x) \neq \mathcal{S}_J^\delta(\delta, J\nabla H, x) - \mathcal{S}_R^\delta(\delta, -R\nabla H, x).$$

More in detail, the skew-symmetric and symmetric part of the matrix $\mathcal{S}_{J-R}^\delta(\delta, (J-R)\nabla H, x)$ does not recover, respectively, $\mathcal{S}_J^\delta(\delta, J\nabla H, x)$ and $\mathcal{S}_R^\delta(\delta, -R\nabla H, x)$, so that

$$\begin{aligned} &\frac{1}{2}\left(\mathcal{S}_{J-R}^\delta(\delta, (J-R)\nabla H, x) - \mathcal{S}_{J-R}^{\delta\top}(\delta, (J-R)\nabla H, x)\right) \neq \mathcal{S}_J^\delta(\delta, J\nabla H, x) \\ &\frac{1}{2}\left(\mathcal{S}_{J-R}^\delta(\delta, (J-R)\nabla H, x) + \mathcal{S}_{J-R}^{\delta\top}(\delta, (J-R)\nabla H, x)\right) \neq \mathcal{S}_R^\delta(\delta, -R\nabla H, x). \end{aligned}$$

7.5 Input-state-output port-Hamiltonian systems

In this section a generalization of port-Hamiltonian dynamics under sampling affected by external inputs are discussed. In the physical world, those dynamics are affected

by external actions u, which in practice represent for instance force, torque, angular velocity, pressure, etc.

As in Chapter 4, where a discrete-time port-Hamiltonian structure affected by the external input u has been discussed for the pure discrete-time case making reference to differential/difference representation and u-average passivity concept, the sampled-data port-Hamiltonian system can be described by the dynamics (7.14), an additional controlled part and suitably defined output map. However, differently, those discrete-time models derive from the sampling process through zero-order-holders (ZOH) of their associated continuous-time dynamics, with the input $u(t)$ assumed as a piecewise constant function over time interval of length $\delta \in]0, T^*[$ with $t \in [k\delta, (k+1)\delta[$, $T^* > 0$.

In this respect, continuous-time port-Hamiltonian systems affected by an external input u, are composed by the dynamics (7.13), with an additional input-affine controlled part and a power conjugate output map of the form

$$\dot{x} = f(x) + g(x)u = (J(x) - R(x))\nabla H(x) + g(x)u \tag{7.25a}$$

$$y = h(x) = g^\top(x)\nabla H(x) \tag{7.25b}$$

where $g(\cdot)$ is a smooth vector field over $\mathbb{R}^n$. Intuitively, by the structure itself, the port-Hamiltonian system of the form (7.25) satisfies

(i) the energy balance equation (EB) along the Hamiltonian $H(x)$, i.e.

$$H(x(t)) - H(x(0)) = -\int_0^t \nabla^\top H(x(s)R(x(s))\nabla H(x(s))ds + \int_0^t u(s)g^\top(x(s))\nabla H(x(s))ds; \tag{7.26}$$

(ii) passivity with respect to y and storage function $H(x)$, namely

$$\dot{H}(x) \leq ug^\top(x)\nabla H(x). \tag{7.27}$$

The following Theorem describes the sampled-data equivalent model to (7.25), specifying its power balance equality and expressing the sampled-data power conjugate output with respect to which passivity is guaranteed under sampling at the sampling instants thorough piecewise constant $u(t)$.

Theorem 7.5.1

Consider a continuous-time port-Hamiltonian system (7.25) and assume $u(t) = u(k\delta), \forall t \in [k\delta, (k+1)\delta[$ with $\delta \in]0, T^*[$. Then for any δ, the sampled equivalent model to (7.25) admits the discrete-time port-Hamiltonian structure

$$x^+(u) = x + \delta \mathcal{S}^\delta_{J-R}(\delta, f, x)\bar{\nabla} H|_x^{x^+} + \delta u g^\delta(x, u) \tag{7.28a}$$

$$Y^\delta_{\text{av}}(x, u) = g^{\delta\top}(x, u)\bar{\nabla} H|_{x^+}^{x^+(u)} \tag{7.28b}$$

with $\mathcal{S}^\delta_{J-R}(\delta, f, x)$ given in (7.14) and sampled input mapping

$$g^\delta(\cdot, u) = \frac{1}{\delta u}\left(e^{\delta(\mathrm{L}_f + u\mathrm{L}_g)} I_d - e^{\delta \mathrm{L}_f} I_d\right). \tag{7.29}$$

Moreover, the sampled-data system (7.28) is passive with respect to the output (7.28b) with storage function $H(x)$ and satisfies the energy balance equality

$$H(x_k) - H(x_0) = \delta \sum_{i=0}^{k-1} \bar{\nabla}^\top H|_{x_i}^{x_i^+} \mathcal{S}^\delta_{J-R}(\delta, f, x)\bar{\nabla} H|_{x_i}^{x_i^+} + \delta \sum_{i=0}^{k-1} u_i Y^\delta_{\text{av}}(x_i, u_i) \tag{7.30}$$

Proof. By definition of the sampled equivalent model in the form of a map, the sampled controlled dynamics is exactly described at the sampling instants by $x_{k+1} := x^+(u) = x + F^\delta(x, u) = e^{\delta(\mathrm{L}_f + u\mathrm{L}_g)}x$. Since the drift term is represented by the dynamics $x^+(0) = x + F^\delta(x, 0) = e^{\delta \mathrm{L}_f}x$, and given the representation provided by Theorem 7.14, one concludes that the equivalent sampled-data dynamics (7.28a) holds true with the constructive sampled-data input mapping (7.29). Computing the forward difference of $H(x)$ end exploiting the property of the discrete gradient, one gets

$$\begin{aligned} H(x^+(u)) - H(x) &= H(x^+) - H(x) + H(x^+(u)) - H(x^+) \\ &= \delta \bar{\nabla}^\top H|_x^{x^+} \mathcal{S}^\delta_{J-R}(\delta, f, x)\bar{\nabla} H|_x^{x^+} + \delta u g^{\delta\top}(x, u)\bar{\nabla} H|_{x^+}^{x^+(u)}, \end{aligned}$$

where passivity property is inferred selecting the output map (7.28b) and, consequently, the energy balance equation along the time horizon as in (7.30). □

Remark 7.5.1. The sampled-equivalent port-Hamiltonian dynamics (7.28a) admits an equivalent sampled-data Differential/Difference representation

$$x^+ = x + \delta \mathcal{S}^\delta_{J-R}(\delta, f, x)\bar{\nabla} H|_x^{x^+}, \quad x^+ = x^+(0) \tag{7.31a}$$

$$\frac{\partial x^+(u)}{\partial u} = G^\delta(x^+(u), u) \tag{7.31b}$$

$$Y^\delta(\cdot, u) = \mathrm{L}_{G^\delta(\cdot,u)} H(\cdot) \tag{7.31c}$$

with

$$G^\delta(x, u) = \int_0^\delta e^{-s \ \mathrm{ad}_{f+ug}} g(x) \mathrm{d}s \tag{7.32}$$

which verifies, due to Lemma 3.4.2,

$$\delta u g^\delta(x, u) = \left(e^{\delta(\mathrm{L}_f + u\mathrm{L}_g)} I_d - e^{\delta \mathrm{L}_f} I_d\right) = \int_0^u G^\delta(x^+(v), v) dv.$$

Note that, by construction, the dynamics (7.28a) and (7.31) are exactly equivalent.

The following corollary is deduced by the definition of u-average passivity.

Corollary 7.5.1. *Consider a continuous-time port-Hamiltonian system* (7.25) *and assume* $u(t) = u(k\delta), \forall t \in [k\delta, (k+1)\delta[$ *with* $\delta \in]0, T^*[$. *Then for any* δ, *the discrete port-Hamiltonian system* (7.31) *is u-average passive with storage function* $H(x)$ *and output map* (7.31c) *and equivalently passive with respect to the u-average output map* (7.28b).

Remark 7.5.2. As commented in Chapter 3, the output map $Y^\delta_{\mathrm{av}}(x, u)$ in (7.28b) which ensures passivity under sampling of the port-Hamiltonian system, can be expressed as a series expansion in powers of δ around the continuous-time output map as such

$$Y^\delta_{\mathrm{av}}(x, u) = \sum_{i \geq 0} \frac{\delta^i}{(i+1)!} Y^\delta_{\mathrm{av}_i}(x, u) \tag{7.33}$$

with the first terms

$$\begin{aligned}
Y^\delta_{\mathrm{av}_0}(x, u) &= h(x) = \mathrm{L}_g H(x) \\
Y^\delta_{\mathrm{av}_1}(x, u) &= (\mathrm{L}_f + u\mathrm{L}_g)\, \mathrm{L}_g H(x) + \mathrm{L}_g \mathrm{L}_f H(x) \\
Y^\delta_{\mathrm{av}_2}(x, u) &= (\mathrm{L}_f + u\mathrm{L}_g)^2\, \mathrm{L}_g H(x) + \mathrm{L}_f \mathrm{L}_g \mathrm{L}_f H(x) + u\mathrm{L}_g^2 \mathrm{L}_f H(x).
\end{aligned}$$

7.6 Comparison with the literature model

An alternative and comparable representation of port-Hamiltonian structure under sampling based on the discrete gradient function has been proposed in Aoues et al. (2017) and extensively studied and discussed in Aoues (2014). Given a continuous-time port-Hamiltonian system

$$\dot{x} = (J(x) - R(x))\nabla H(x) + g(x)u \tag{7.34a}$$
$$y = g^\top(x)\nabla H(x) \tag{7.34b}$$

the proposed model is obtained by substituting the gradient of $H(x)$ with the discrete gradient into the Euler approximate dynamics, so setting

$$x^+(u) = x + \delta(J(x) - R(x))\bar{\nabla} H|_x^{x^+(u)} + \delta g(x)u \tag{7.35a}$$
$$y_\ell = g^\top(x)\bar{\nabla} H|_x^{x^+(u)}. \tag{7.35b}$$

Again, this approximate port-Hamiltonian structure essentially differs from the sampled-data equivalent port-Hamiltonian structure in (7.28), that is

$$\begin{aligned} x^+(u) = F^\delta(x,u) &= x + \delta \mathcal{S}^\delta_{J-R}(\delta, f, x)\bar{\nabla} H|_x^{x^+} + \delta u g^\delta(x,u) \\ Y^\delta_{\text{av}}(x,u) = h^\delta(x,u) &= g^{\delta\top}(x,u)\bar{\nabla} H|_{x^+}^{x^+(u)} \end{aligned}$$

in several aspects:

- the literature model (7.35) arises with a discrete gradient $\bar{\nabla} H|_x^{x^+(u)}$ which is affected by the control variable u, while our proposed model arises with a discrete gradient of the form $\bar{\nabla} H|_x^{x^+}$;
- this reflects in an energy balance equation

$$\underbrace{H(x^+(u)) - H(x)}_{\text{stored energy}} = -\delta \underbrace{\bar{\nabla} H^\top|_x^{x^+(u)} R(x) \bar{\nabla} H|_x^{x^+(u)}}_{\text{dissipation + partial supplied}} + \delta \underbrace{u g^\top(x,u)\bar{\nabla} H|_x^{x^+(u)}}_{\text{partial supplied energy}} \tag{7.36}$$

  which does not decouple the contribution given by the external source from the internal dissipative energy;

- the literature output y_ℓ in (7.35b) associated with the port-Hamiltonian dynamics (7.35), again arises with a discrete gradient $\bar{\nabla} H|_x^{x^+(u)}$, while the proposed passive output $Y_{\text{av}}^\delta(x,u)$ arises with a discrete gradient of the form $\bar{\nabla} H|_{x^+}^{x^+(u)}$ that properly encodes the effect of u over $H(x)$;
- in case of zero input, meaning that $u = 0$, the first order approximation of the matrix $\mathcal{S}_{J-R}^\delta(\delta, f, x)$ recovers the literature representation, since

$$\mathcal{S}_{J-R}^\delta(\delta, f, x) = J(x) - R(x) + O(\delta^2).$$

7.7 Concluding remarks

In this chapter, new results for describing sampled-data equivalent models of continuous-time gradient and port-Hamiltonian dynamics have been provided. In particular, it has been shown that it is always possible to recover a suitably defined discrete-time equivalent model exhibiting a discrete-time Hamiltonian structure with respect to the same Hamiltonian function as in continuous time. In addition, the proposed approach is constructive and allows the computation of approximate models. Finally, the deduced sampled-data equivalent model preserves, beyond the structure, the same energetic properties as the continuous-time one at all sampling instants differently from the literature model given in Aoues et al. (2017). The results presented herein this chapter are given in

> *S. Monaco, D. Normand-Cyrot, M. Mattioni and A. Moreschini, "Nonlinear Hamiltonian systems under sampling", Submitted to IEEE Transactions on Automatic Control (TAC). (Under review)*

Chapter 8

Control of sampled-data port-Hamiltonian systems

Contents

8.1 Negative output feedback **187**

8.2 IDA-PBC: Input-Hamiltonian matching **189**

8.3 Concluding remarks **194**

The contents of this chapter rely on the negative output feedback stabilization and to the IDA-PBC under sampling. In particular, first, we specialize the negative output feedback design for port-Hamiltonian systems under sampling and then, approximate solutions are performed. Then we tackle the IDA-PBC problem in terms of feedback passivation under sampled-data design discussed in Chapter 3.

8.1 Negative output feedback

In many physical applications, especially in mechanical systems, damping plays an essential role since it extracts energy from the system. We have already seen that the conjugate output of the introduced discrete-time port-Hamiltonian system achieves asymptotic stabilization of the equilibrium point when a negative output feedback controller is designed for the discrete-time system. Therefore, the same result may be recast under sampling when considering the discrete-time port-Hamiltonian system

issued from sampling as an equivalent port-Hamiltonian system of the continuous-time one.

The following theorem specifies the result in Theorem 5.1.1 for the discrete-time port-Hamiltonian system issued form the sampling of a continuous-time port-Hamiltonian one.

Theorem 8.1.1: Negative output feedback under sampling

Consider a continuous-time port-Hamiltonian system

$$\dot{x} = f(x) + g(x)u = (J(x) - R(x))\nabla H(x) + g(x)u \tag{8.1a}$$
$$y = h(x) = g^\top(x)\nabla H(x) \tag{8.1b}$$

be ZSD with Hamiltonian function $H(\cdot) : \mathbb{R}^n \to \mathbb{R}$, having a minimum in $x_\star$, and assume $u(t) = u(k\delta)$, for all $t \in [k\delta, (k+1)\delta[$ with $\delta \in]0, T^*[$. Let for any δ the sampled equivalent model be

$$x^+(u) = x + \delta\mathcal{S}^\delta_{J-R}(\delta, f, x)\bar{\nabla}H|_x^{x^+} + \delta u g^\delta(x, u) \tag{8.2a}$$
$$Y^\delta_{\text{av}}(x, u) = g^{\delta\top}(x, u)\bar{\nabla}H|_{x^+}^{x^+(u)}. \tag{8.2b}$$

Then, the feedback $u = \gamma^\delta(x)$ solution to the implicit damping equality

$$\gamma^\delta(x) + \kappa g^{\delta\top}(x, u)\bar{\nabla}H|_{x^+}^{x^+(u)} = 0 \tag{8.3}$$

with gain $\kappa > 0$, achieves asymptotic stability of the closed-loop equilibrium $x_\star$.

Proof. The proof follows the lines of Theorem 5.1.1. Regarding ZSD, by construction, $Y^\delta_{\text{av}}(x, 0) = g^\top(x)\nabla H(x) + O(\delta)$ so concluding ZSD detectability of the sampled-data model for almost all δ. □

Remark 8.1.1. The digital PBC feedback solution to (8.3) is implicitly defined by the damping equality so that an exact solution might not be always computed in general. However, one can compute approximate solution to (8.3) by expressing $\gamma^\delta(x)$ as a series expansion in powers of δ, that is

$$\gamma^\delta(x) = \sum_{i\geq 0} \frac{\delta^i}{(i+1)!}\gamma_i^\delta \tag{8.4}$$

and in particular for the first term the solution to (8.3), when setting for the sake of simplicity $\kappa = 1$, yields

$$\gamma_0^\delta = -h(x) = -\mathrm{L}_g H(x)$$
$$\gamma_1^\delta = -\dot{h}(x) - \mathrm{L}_g \mathrm{L}_f H(x)$$
$$\gamma_2^\delta = -\ddot{h}(x) + \frac{1}{2}\dot{h}(x)\mathrm{L}_g^2 H(x) - \mathrm{L}_g \mathrm{L}_f \mathrm{L}_f H(x) - \mathrm{L}_f \mathrm{L}_g \mathrm{L}_f H(x) - h(x)\mathrm{L}_g \mathrm{L}_f H(x).$$

It is interesting to note that assuming quadratic Hamiltonian function $H(x) = \frac{1}{2}x^\top P x$ with $P = P^\top \succ 0$ together with the sampled-data input map $g^\delta(x) := g^\delta(x, 0)$ affine in the control variable, then the negative output feedback solution to the implicit damping equality (8.3) follows. Hence the following theorem holds and its proof follows the lines of Theorem 5.2.1.

Corollary 8.1.1. *Assume the input-affine sampled-data port-Hamiltonian system with $H(x) = \frac{1}{2}x^\top P x$ with $P = P^\top \succ 0$ in (8.2) of the form*

$$x^+(u) = x + \frac{\delta}{2}\mathcal{S}_{J-R}^\delta(\delta, f, x)P(x^+ + x) + \delta u g^\delta(x) \tag{8.5a}$$
$$Y_{av}^\delta(x, u) = g^{\delta\top}(x)Px^+ + \frac{1}{2}g^{\delta\top}(x)Pg^\delta(x)u. \tag{8.5b}$$

then $u = \gamma^\delta(x)$ with

$$\gamma^\delta(x) = -\frac{\kappa g^{\delta\top}(x)P}{1 + \frac{\kappa}{2}g^{\delta\top}(x)Pg^\delta(x)}x^+, \tag{8.6}$$

globally asymptotically stabilize with $\kappa > 0$ the closed-loop equilibrium $x_\star = 0$.

8.2 IDA-PBC: Input-Hamiltonian matching

In this section we tackle the problem of asymptotic stabilization under sampling towards a desired equilibrium in terms of feedback passivation under sampling with respect to a new Hamiltonian function which must be assigned to the closed-loop system. The discrete-time IDA-PBC has been introduced in Chapter 5 and sufficient conditions for solving the problem in assigning a desired target port-Hamiltonian structure have been given. Let us restate the DT IDA-PBC Problem 2 under a sampled-data point of view.

Problem 3 (SD IDA-PBC)**.** Given the sampled-data equivalent port-Hamiltonian system in (8.2), that is for any $\delta \in]0, T^*[$

$$x^+(u) = x + \delta \mathcal{S}^\delta_{J-R}(\delta, f, x)\bar{\nabla} H|_x^{x^+} + \delta u g^\delta(x, u) \tag{8.7a}$$

$$Y^\delta_{\text{av}}(x, u) = g^{\delta\top}(x, u)\bar{\nabla} H|_{x^+}^{x^+(u)} \tag{8.7b}$$

find $\bar{u}^\delta(x) : \mathbb{R}^n \to \mathbb{R}$, such that setting for $u = \bar{u}^\delta(x) + v$, the system is transformed into the port-Hamiltonian form

$$x^+(\bar{u}^\delta(x) + v) = x + \delta \mathcal{S}^\delta_{J_d-R_d}(\delta, f_d, x)\bar{\nabla} H_d|_x^{x^+(\bar{u}^\delta(x))} + \delta g_d(x, v)v \tag{8.8}$$

with new Hamiltonian function $H_d : \mathbb{R}^n \to \mathbb{R}_{\geq 0}$ such that $x_\star = \arg\min\{H_d(x)\}$,

$$\mathcal{S}^\delta_{J_d-R_d}(\delta, f_d, x) = \mathcal{M}(\delta, f_d, x)(J_d(x) - R_d(x))\left(I + \delta \mathcal{Q}(\delta, H_d, f_d, x)(J_d(x) - R_d(x))\right)^{-1}$$

with $f_d = (J_d(x) - R_d(x))\nabla H_d(x)$, $J_d(x) = -J_d^\top(x)$, $R_d(x) = R_d^\top(x) \succeq 0$, and $g_d(x, v)$ satisfying by construction

$$v g_d(x, v) = \bar{u}^\delta(x)(g(x, \bar{u}^\delta(x) + v) - g(x, \bar{u}^\delta(x))) + v g(x, \bar{u}^\delta(x) + v). \tag{8.9}$$

Accordingly, the closed-loop verifies the new energy balance equality

$$H_d(x_k) - H_d(x_0) = \sum_{i=0}^{k-1} v_i y_{d_i} - \sum_{i=0}^{k-1} w_{d_i}, \qquad \forall k \in \mathbb{N},$$

with dissipation $w_d \geq 0$ and new passive output

$$Y^\delta_{d_{\text{av}}}(\bar{u}^\delta)(x, v) = g_d^\top(x, v)\bar{\nabla} H_d|_{x^+(\bar{u}^\delta(x))}^{x^+(\bar{u}^\delta(x)+v)}. \tag{8.10}$$

As discussed in Chapter 5, the matching equation arising from the SD IDA-PBC Problem in the general nonlinear context takes the form

$$\mathcal{S}^\delta_{J-R}(\delta, f, x)\bar{\nabla} H|_x^{x^+} + u g^\delta(x, u) = \mathcal{S}^\delta_{J_d-R_d}(\delta, f_d, x)\bar{\nabla} H_d|_x^{x^+(u)}. \tag{8.11}$$

However, as in discrete time a general solution is tough to determine due to the implicit dependence of the control variable u into the nonlinear equation to solve, and the complexity is mainly due to the function $g^\delta(x, u)$ and $\bar{\nabla} H_d|_x^{x^+(u)}$ which are generally nonlinear in u.

In this sampled-data context we can provide a partial solution exploiting the input-Hamiltonian matching (IH$_d$M) design discussed in Section 3.5. For port-Hamiltonian systems, the result in Theorem 3.5.1 applies, so describing the sampled-data feedback $\gamma^\delta(\cdot)$ as the solution to the IH$_d$M equality

$$H_d(x^+(\gamma^\delta(x))) - H_d(x) = \int_{k\delta}^{(k+1)\delta} \mathrm{L}_{f_d} H_d(x(s))\mathrm{d}s$$

with $f_d = (J_d(x) - R_d(x))\nabla H_d(x)$. The sampled-data feedback assigns $x_\star$ and H_d as new equilibrium and storage function respectively with $H_d : \mathbb{R}^n \to \mathbb{R}_{\geq 0}$ and $x_\star = \arg\min\{H_d(x)\}$.

The involvement of the input-Hamiltonian matching is essential in this context since it avoids providing a solution to the matching equation (8.11) so reformulating the problem on the matching of the Hamiltonian function and not on the matching on the sampled-data structure of the system.

The proposition below specifies the Proposition 3.5.1 in case of continuous-time port-Hamiltonian dynamics and IDA-PBC design.

Proposition 8.2.1. *Given the continuous-time port-Hamiltonian dynamics*

$$\dot{x} = f(x) + g(x)u = f(x) = (J(x) - R(x))\nabla H(x) + g(x)u, \tag{8.12}$$

let $u = \gamma(x) + v$ be a continuous-time IDA-PBC feedback assigning the dynamics

$$\dot{x} = f_d(x) + g(x)v = (J_d(x) - R_d(x))\nabla H_d(x) + g(x)v \tag{8.13a}$$

$$y = h_d(x) = \mathrm{L}_g H_d(x). \tag{8.13b}$$

with $H_d : \mathbb{R}^n \to \mathbb{R}_{\geq 0}$ and $x_\star = \arg\,min\{H_d(x)\}$. Then, there exists $T^\star > 0$ such that for all $\delta \in [0, T^\star[$ and $t = k\delta$, $k \geq 0$, the IH$_d$M equality

$$H_d(x^+(u)) - H_d(x) = \int_{k\delta}^{(k+1)\delta} \mathrm{L}_{f_d} H_d(x(s))\mathrm{d}s \tag{8.14}$$

with $x(s) = e^{s\mathrm{L}_{f_d}} I_d|_{x_k}$ admits unique solution $u = \gamma^\delta(x)$ as a series expansion in powers of δ around $\gamma(\cdot)$; namely,

$$\gamma^\delta(x) = \gamma(x) + \sum_{i>0} \frac{\delta^i}{(i+1)!}\gamma^i(x), \tag{8.15}$$

which assigns $x_\star$ to the closed-loop system.

It is important to note that the objective to stabilize under digital feedback to the target equilibrium $x_\star$ is achieved. However, we cannot speak properly about sampled-data IDA-PBC design because the closed-loop system does not a priori exibits the target port-Hamiltonian form (8.8).

The port-Hamiltonian structure of the sampled-data system is recovered up to an error in $O(\delta^3)$ though the 1-order approximate solution. This fact is formalized below.

Theorem 8.2.1: IDA-PBC under sampling through IH_dM

Given the continuous-time port-Hamiltonian dynamics

$$\dot{x} = f(x) + g(x)u = f(x) = (J(x) - R(x))\nabla H(x) + g(x)u, \tag{8.16}$$

let $u = \gamma(x) + v$ be a continuous-time IDA-PBC feedback assigning the dynamics

$$\dot{x} = f_d(x) + g(x)v = (J_d(x) - R_d(x))\nabla H_d(x) + g(x)v \tag{8.17a}$$
$$y = h_d(x) = \mathrm{L}_g H_d(x). \tag{8.17b}$$

Setting $u = \gamma^\delta(x)$, with $\gamma^\delta(x)$ the corresponding digital solution to the IH$_d$M equality

$$H_d(x^+(\gamma^\delta(x))) - H_d(x) = \int_{k\delta}^{(k+1)\delta} \mathrm{L}_{f_d} H_d(x(s))\mathrm{d}s,$$

then its 1-order approximate feedback of (8.15),

$$\gamma^{\delta[1]}(x) = \gamma(x) + \frac{\delta}{2}\gamma^1(x), \tag{8.18}$$

with $\gamma^1(x) = \dot{\gamma}(x)$, assigns the port-Hamiltonian structure (8.8) up to $O(\delta^3)$.

Proof. The proof is constructive and is obtained by showing that the feedback (8.18) solves up to $O(\delta^3)$ the SD matching equation (8.11). According to the series

constructive terms in series of δ of the form

$$\mathcal{S}^{\delta}_{J-R}(\delta, f, x) := S(x) + \sum_{i\geq 1} \frac{\delta^i}{(i+1)!} S_i(x),$$
$$\mathcal{S}^{\delta}_{J_d-R_d}(\delta, f_d, x) := S_d(x) + \sum_{i\geq 1} \frac{\delta^i}{(i+1)!} S_{d1}(x),$$
$$\bar{\nabla} H|_x^{x^+} := \nabla H(x) + \sum_{i\geq 1} \frac{\delta^i}{(i+1)!} [H]_i(x).$$

one computes the first-order terms for $\mathcal{S}^{\delta}_{J-R}(\delta, f, x)$, $\mathcal{S}^{\delta}_{J_d-R_d}(\delta, f_d, x)$, $\bar{\nabla} H|_x^{x^+}$, $\bar{\nabla} H_d|_x^{x^+(u)}$, that are (with $S(x) = J(x) - R(x)$ and $S_d(x) = J_d(x) - R_d(x)$)

$$S_1(x) = \big(\frac{\partial f}{\partial x} - S(x)\nabla^2 H(x)\big) S(x)$$
$$[H]_1(x) = \nabla^2 H(x) S(x) \nabla H(x)$$
$$S_{d1}(x) = \big(\frac{\partial f_d}{\partial x} - S_d(x)\nabla^2 H_d(x)\big) S_d(x)$$
$$[H_d]_1(x) = \nabla^2 H_d(x) S_d(x) \nabla H_d(x).$$

Therefore, by approximating the matching equality in $O(\delta^3)$ through the constructive terms given above, and substituting $\gamma^{\delta} = \gamma_0 + \frac{\delta}{2}\gamma_1$, one ends up with one equation for each order of δ, namely

$$\delta^0 : \quad g(x)\gamma_0 = S_d(x)\nabla H_d(x) - S(x)\nabla H(x);$$
$$\delta^1 : \quad g(x)\gamma_1 = \big(S_{d1}(x) + S_d(x)\nabla^2 H_d(x) S_d(x) - (\frac{\partial f}{\partial x} + \gamma_0 \frac{\partial g}{\partial x}) S_d(x)\big)\nabla H_d(x).$$

The first equation is exactly the solution to the continuous-time IDA-PBC $\gamma_0(x) = \gamma(x)$, which is solved for $\gamma(x)$ at the sampling instants $t = k\delta$, the second equation is solved for $\gamma_1(x) = \frac{\partial \gamma_0}{\partial x}(f + g\gamma) = \frac{\partial \gamma}{\partial x} S_d(x)\nabla H_d(x) = \dot{\gamma}(x)$. Thus, one concludes that the preservation of the discrete port-Hamiltonian structure up to $O(\delta^3)$ is deduced. □

Remark 8.2.1. In the case in which $S_d(x) = J_d(x) - R_d(x)$ is assumed having constant entries, say $S_d(x) = S_d = J_d - R_d$, the port-Hamiltonian structure (8.8) up to $O(\delta^3)$ yields the form

$$x^+(u) = x + F_d^{\delta[2]}(x)$$
$$= x + \delta S_d \bar{\nabla} H_d|_x^{x + F_d^{\delta[2]}(x)}$$

with the approximate discrete gradient

$$\bar{\nabla} H_d|_x^{x+F_d^{\delta[2]}(x)} = \nabla H_d(x) + \frac{\delta}{2}\nabla^2 H_d(x) S_d \nabla H_d(x) + O(\delta^2).$$

Remark 8.2.2. From the result above, it turns out that a port-Hamiltonian structure is assigned through digital IH$_d$M feedback with an error in $O(\delta^3)$. More precisely, the 1$^{\text{st}}$-order approximate feedback

$$\gamma^{\delta[1]}(x) = \gamma(x) + \frac{\delta}{2}\mathrm{L}_{f_d}\gamma(x)$$

ensures (local) passivation through digital IDA-PBC in $O(\delta^3)$. Such a choice, naturally recovers the continuous-time counterpart as $\delta \to 0$.

8.3 Concluding remarks

Within this chapter, we discussed the stabilization problem of port-Hamiltonian systems under sampling. Notably, we provided negative output feedback computed as the solution of an implicit damping equality. We discussed that the solution is not always computable in general, though one might compute approximate solutions. Then, we discussed the IDA-PBC problem for the general nonlinear port-Hamiltonian system under sampling. As in the pure discrete-time case, the nonlinear sampled-data design solution is tough to determine and a closed-form for the sampled-data feedback is not achievable. Therefore, we partially solved the problem exploiting IH_dM, introduced in Chapter 3, to show that stabilization to the target equilibrium can be performed through matching the desired Hamiltonian behavior. The sampled-data port-Hamiltonian structure is recovered with an error in $O(\delta^3)$. The negative output feedback design and the IDA-PBC through IH_dM are respectively given in:

> *S. Monaco, D. Normand-Cyrot, M. Mattioni and A. Moreschini, "Nonlinear Hamiltonian systems under sampling", Submitted to IEEE Transactions on Automatic Control (TAC). (Under review)*
>
> *M. Mattioni, A. Moreschini, S. Monaco and D. Normand-Cyrot, On feedback passivation under sampling. 2020. Submitted to 2021 American Control Conference (ACC). (Accepted)*

Chapter 9

LTI port-Hamiltonian systems under sampling

Contents

9.1 Gradient dynamics **195**

9.2 Port-Hamiltonian systems **198**

9.3 Negative output feedback **203**

9.4 IDA-PBC: Direct discrete design **203**

9.5 Concluding remarks **205**

The aim of this chapter is to revisit and specialize the results previously presented in the nonlinear case in the linear context. We give the definition of gradient and Hamiltonian system under sampling based on the exact solution. Then, we give the expression of the negative output feedback designed for the LTI port-Hamiltonian system under sampling. Finally, due to the special structure of the LTI port-Hamiltonian systems under sampling, we revisit the result of Chapter 6, providing an IDA PBC feedback under sampling in closed-form.

9.1 Gradient dynamics

A special class of gradient dynamics given in Theorem 7.3.1, that is

$$x^+ = x - \delta \mathcal{I}(\delta, -\nabla H, x) \bar{\nabla} H|_x^{x^+},$$

with matrix

$$\mathcal{I}(\delta, -\nabla H, x) = \mathcal{M}(\delta, -\nabla H, x)(I - \delta\mathcal{Q}(\delta, H, -\nabla H, x))^{-1} \in \mathrm{Mat}_{\mathbb{R}}(n, n),$$

is the one described by the quadratic Hamiltonian function

$$H(x) = \frac{1}{2}x^\top Px$$

with symmetric and positive definite matrix P, that is $P = P^\top \succ 0$.

The results in Theorem 7.3.1 can be directly specified in this linear case.

Theorem 9.1.1: LTI gradient dynamics under sampling

Given the continuous-time gradient dynamics of the form

$$\dot{x} = -\nabla H(x) = -Px$$

with function $H(x) = \frac{1}{2}x^\top Px$ and $P = P^\top \succ 0$, then for any $\delta \in]0, T^*[$, its sampled-data equivalent dynamics admits the discrete gradient form

$$\begin{aligned} x^+ &= x - \delta\mathcal{I}(\delta, -P)\bar{\nabla}H|_x^{x^+} \\ &= x - \frac{\delta}{2}\mathcal{I}(\delta, -P)P(x^+ + x) \end{aligned} \tag{9.1}$$

with symmetric matrix

$$\mathcal{I}(\delta, -P) = \frac{2}{\delta}(I - e^{-\delta P})(I + e^{-\delta P})^{-1}P^{-1}. \tag{9.2}$$

Additionally, (9.1) it can be expressed in the explicit form as

$$x^+ = A^\delta x = e^{-\delta P}x = (I + \frac{\delta}{2}\mathcal{I}(\delta, -P)P)^{-1}(I - \frac{\delta}{2}\mathcal{I}(\delta, -P)P)x, \tag{9.3}$$

providing that the Hamiltonian function satisfies the variational equality

$$H(x^+) - H(x) = -\frac{\delta}{4}x^\top(A^\delta + I)^\top P\mathcal{I}(\delta, -P)P(A^\delta + I)x \leq 0. \tag{9.4}$$

The theorem provides linear discrete-time representation of gradient dynamics ensuring both preservation of the energetic properties and matching of the continuous-time state trajectories. The matching of the continuous-time properties are ensured

since the matrix A^δ in (9.3) is nothing else that the exact exponential representation $e^{-\delta P}$ which is explicitly computable. However, it is worth mentioning that the achieved sampled-data structure (9.2) comes with a sampled-data matrix $\mathcal{I}(\delta, -P)$ which depends on the sampling period δ and recovers the identity matrix only in first approximation in δ.

The structure of the matrix $\mathcal{I}(\delta, -P)$ describing the discrete gradient dynamics is a direct consequence of the formal definition given in (7.11). Therefore, when setting in this linear case the matrices given in Lemma 7.1.1 and Lemma 7.1.4 one gets

$$\mathcal{M}(\delta, -P) = \frac{1}{\delta}(I - e^{-\delta P})P^{-1},$$
$$\mathcal{Q}(\delta, -P) = \frac{1}{2\delta}(I - e^{-\delta P}).$$

In addition, the variational equality $H(x^+) - H(x)$ for quadratic $H(\cdot)$ can be equivalently expressed in term of integral

$$H(x^+) - H(x) = -\int_0^\delta x^\top(s)P^2x(s)ds = -\frac{\delta}{4}(x^+ + x)^\top P\mathcal{I}(\delta, -P)P(x^+ + x),$$

so that the sampled-data evolution matches at the sampling instants the continuous-time trajectory for any length of δ.

Remark 9.1.1. The matrix (9.2) can be formally defined through the series

$$\mathcal{I}(\delta, -P) = -\frac{2}{\delta}(e^{-\delta P} - I)\left(I + \sum_{p\geq 1}(-1)^p e^{-p\delta P}\right)P^{-1}. \tag{9.5}$$

Accordingly, one gets by construction the description of $\mathcal{I}(\delta, -P)$ as the series expansion in δ below

$$\mathcal{I}(\delta, -P) = \sum_{p\geq 0}\sum_{j_0\geq 0, j_1, \ldots, j_p \geq 1} \frac{(-1)^p(-\delta P)^{\sum_{i=0}^p j_i}}{2^p(j_0+1)!j_1!\ldots j_p!}, \tag{9.6}$$

which recover for the first terms

$$\mathcal{I}(\delta, -P) = I - \frac{\delta^2}{3!2}P^2 + \frac{\delta^4}{5!}P^4 + O(\delta^6).$$

The series expansion above shows that the coefficients of the odd powers in P ($(\delta P)^{2i+1}, i \geq 0$) are equal to zero in the expansion (9.6), so showing that $\mathcal{I}(\delta, -P)$ is symmetric definite.

Remark 9.1.2. The sampled-data equivalent dynamics in discrete gradient form (9.1) can be expressed as an explicit dynamics (9.3) and due to the series expansion (9.6), the closed form can be characterized for the first terms as follow

$$x^+ = \left(I + \frac{\delta}{2}P - \frac{\delta^3}{3!4}P^3 + \frac{\delta^5}{5!2}P^5 + O(\delta^6)\right)^{-1}\left(I - \frac{\delta}{2}P + \frac{\delta^3}{3!4}P^3 - \frac{\delta^5}{5!2}P^5 + O(\delta^6)\right)x.$$

It is important to note that in this linear case, the dynamics (9.1) exhibits discrete gradient form with respect to a new Hamiltonian function parametrized by the sampling period δ. This representation is given below and the proof is straightforward.

Proposition 9.1.1. *When $H(x)$ is a quadratic function, $H(x) = \frac{1}{2}x^\top Px$ with positive P, the sampled-data dynamics equivalent to $\dot{x} = -\nabla H(x) = -Px$ provides a discrete-time gradient form*

$$x^+ - x = -\delta\bar{\nabla}H^\delta|_x^{x^+} = -\frac{\delta}{2}P^\delta(x + x^+) \tag{9.7}$$

with a δ-dependent Hamiltonian function $H^\delta(x) = \frac{1}{2}x^\top P^\delta x$ with

$$P^\delta = \mathcal{I}(\delta, -P)P. \tag{9.8}$$

with $P^\delta = \mathcal{I}(\delta, -P)P$ in its series expansion

$$P^\delta = \sum_{p\geq 0}\sum_{j_0\geq 0, j_1,\ldots,j_p\geq 1}\frac{(-1)^p(-\delta P)^{\sum_{i=0}^p j_i}}{2^p(j_0+1)!j_1!\ldots j_p!}P = P - \frac{\delta^2}{3!2}P^3 + \frac{\delta^4}{5!}P^5 + O(\delta^6),$$

which is a symmetric matrix by construction.

The result presented above defines an alternative representation of the gradient dynamics. Its structure makes reference to a modified real-valued function $H^\delta(x)$ which is parameterized by the sampling period δ.

9.2 Port-Hamiltonian systems

The sampled-data structure of port-Hamiltonian dynamics is specialized, in this present section, to linear port-Hamiltonian dynamics. These particular dynamics are described in continuous-time by a quadratic Hamiltonian function along with interconnection and dissipation matrices having constant entries.

In this respect, the result in Theorem 7.3.1 can be directly specified in this case.

Theorem 9.2.1: LTI port-Hamiltonian dynamics under sampling

Given the continuous-time linear port-Hamiltonian dynamics of the form

$$\dot{x} = (J - R)\nabla H(x) = (J - R)Px$$

with function $H(x) = \frac{1}{2}x^\top Px$ and $P = P^\top \succ 0$, then for any $\delta \in]0, T^*[$, its sampled-data equivalent dynamics admits the discrete-time port-Hamiltonian structure

$$x^+ = x + \delta \mathcal{S}^\delta_{J-R} \bar{\nabla} H|_x^{x^+} \tag{9.9}$$

with $x^+ = e^{\delta(J-R)P}x$ and

$$\mathcal{S}^\delta_{J-R} = \frac{2}{\delta}(e^{\delta(J-R)P} - I)(e^{\delta(J-R)P} + I)^{-1}P^{-1}. \tag{9.10}$$

Additionally, since $(I - \frac{\delta}{2}\mathcal{S}^\delta_{J-R}P)$ is invertible for almost all δ, the port-Hamiltonian structure (9.9) can be expressed in the explicit form as

$$x^+ = A^\delta x = (I - \frac{\delta}{2}\mathcal{S}^\delta_{J-R}P)^{-1}(I + \frac{\delta}{2}\mathcal{S}^\delta_{J-R}P)x, \tag{9.11}$$

providing the Hamiltonian function satisfies the variational equality

$$H(x^+) - H(x) = \frac{\delta}{4}x^\top (A^\delta + I)^\top P \mathcal{S}^\delta_{J-R} P(A^\delta + I)x \leq 0. \tag{9.12}$$

The theorem provides linear discrete-time representation of port-Hamiltonian dynamics which preserves their structure under sampling process. The structure ensures both preservation of the energetic properties and matching of the continuous-time state trajectories. As for the LTI sampled-data gradient dynamics, the matching of the Hamiltonian and the continuous-time trajectories are ensured since the matrix A^δ in (9.11) is nothing else that the exact exponential representation $e^{\delta(J-R)P}$ which is explicitly computable and ensures a closed form. In addition the deduced sample-data matrix $\mathcal{S}^\delta_{J-R}$ depends on the sampling period δ and recovers the matrix $J - R$ only in first approximation in δ.

Remark 9.2.1. The structure of $\mathcal{S}^\delta_{J-R}$ describing the discrete LTI port-Hamiltonian dynamics is a direct consequence of Theorem 7.4.1, when specifying the matrices

$\mathcal{M}(\delta, f)$ and $\mathcal{Q}(\delta, f)$ in Lemma 7.1.1 and Lemma 7.1.4 as

$$\mathcal{M}(\delta, f) = \frac{1}{\delta}(e^{-\delta P} - I)P^{-1}(J-R)^{-1},$$
$$\mathcal{Q}(\delta, f) = \frac{1}{2\delta}P(e^{\delta(J-R)P} - I)P^{-1}(J-R)^{-1}.$$

In addition, the variational equality $H(x^+)-H(x)$ for quadratic $H(\cdot)$ can be expressed in terms of integral form

$$H(x^+) - H(x) = -\int_0^\delta x^\top(s)PRPx(s)ds = \frac{\delta}{4}(x^+ + x)^\top P\mathcal{S}^\delta_{J-R}P(x^+ + x) \leq 0, \tag{9.13}$$

with $x(s) = e^{\delta(J-R)P}x$, so that the sampled-data evolution matches at the sampling instants the continuous-time Hamiltonian behavior for any length of δ.

Remark 9.2.2. The sampled-data matrix $\mathcal{S}^\delta_{J-R}$ in (9.10) can be split as skew-symmetric and symmetric matrices respectively given by

$$\mathcal{J}^\delta = \frac{1}{2}\left[\mathcal{S}^\delta_{J-R} - \mathcal{S}^{\delta\top}_{J-R}\right] \in \mathrm{Skew}_{\mathbb{R}}(n,n)$$
$$\mathcal{R}^\delta = -\frac{1}{2}\left[\mathcal{S}^\delta_{J-R} + \mathcal{S}^{\delta\top}_{J-R}\right] \in \mathrm{Sym}_{\mathbb{R}}(n,n).$$

By virtue of the inequality (9.13) and exploiting the above decomposition one gets

$$\begin{aligned} H(x^+) - H(x) &= \frac{\delta}{4}(x^+ + x)^\top P\mathcal{S}^\delta_{J-R}P(x^+ + x) \\ &= -\frac{\delta}{4}(x^+ + x)^\top P\mathcal{R}^\delta P(x^+ + x) \leq 0, \end{aligned} \tag{9.14}$$

so showing that $\mathcal{R}^\delta \succeq 0$ due to the quadratic structure of the expression in (9.14).

Remark 9.2.3. The expression of $\mathcal{S}^\delta_{J-R}$ in (9.10) can be rewritten as

$$\mathcal{S}^\delta_{J-R} = \sum_{p\geq 0}\sum_{j_0\geq 0, j_1,\ldots,j_p\geq 1} \frac{(-1)^p(\delta(J-R)P)^{\sum_{i=0}^p j_i}}{2^p(j_0+1)!j_1!\ldots j_p!}(J-R),$$

so computing the first terms as

$$\mathcal{S}^\delta_{J-R} = \Big(I - \frac{\delta^2}{3!2}((J-R)P)^2 + \frac{\delta^4}{5!}((J-R)P)^4\Big)(J-R) + O(\delta^6).$$

Accordingly, setting $\mathcal{J}^\delta$ and $\mathcal{R}^\delta$ as a series expansion in power of δ,

$$\mathcal{J}^\delta = \sum_{i\geq 0} \frac{\delta^i}{(i+1)!}\mathcal{J}_i \tag{9.15}$$

$$\mathcal{R}^\delta = \sum_{i\geq 0} \frac{\delta^i}{(i+1)!}\mathcal{R}_i \tag{9.16}$$

one computes

$$\begin{aligned}
\mathcal{J}_0 &= J \\
\mathcal{J}_1 &= \mathbf{0}_{n\times n} \\
\mathcal{J}_2 &= \frac{1}{2}\big((JPJ+RPR)PJ + (JPR+RPJ)PR\big),
\end{aligned}$$

and

$$\begin{aligned}
\mathcal{R}_0 &= R \\
\mathcal{R}_1 &= \mathbf{0}_{n\times n} \\
\mathcal{R}_2 &= \frac{1}{2}\big((JPJ+RPR)PR + (JPR+RPJ)PJ\big).
\end{aligned}$$

Remark 9.2.4. It is worth to stress that the discrete-time linear port-Hamiltonian dynamics can be expressed explicitly as (9.11), and in its series expansion in power of δ takes the following structure

$$x^+ = \left(I - \frac{\delta}{2}(J-R)P - \frac{\delta^3}{3!2}(\mathcal{J}_2-\mathcal{R}_2)P + O(\delta^4)\right)^{-1}\left(I + \frac{\delta}{2}(J-R)P + \frac{\delta^3}{3!2}(\mathcal{J}_2-\mathcal{R}_2)P + O(\delta^4)\right)x.$$

The following Theorem introduces the sampled-data equivalent model to (7.25), specifying its power balance equality and expressing the sampled-data power conjugate output with respect to which passivity is guaranteed under sampling at the sampling instants thorough piecewise constant $u(t)$.

Theorem 9.2.2

Consider a continuous-time port-Hamiltonian system

$$\dot{x}(t) := f(x) + Bu = (J-R)Px + Bu \tag{9.17a}$$

$$y = h(x) = B^\top Px. \tag{9.17b}$$

with $J = -J^\top$, $R = R^\top \succeq 0$, and $P = P^\top \succ 0$, and assume $u(t) = u(k\delta), \forall t \in [k\delta, (k+1)\delta[$ with $\delta \in]0, T^*[$. Then for any δ, the sampled equivalent model to (9.17) admits the discrete-time port-Hamiltonian structure

$$x^+(u) = x + \delta \mathcal{S}^\delta_{J-R} \bar{\nabla} H|^{x^+}_x + \delta B^\delta u \tag{9.18}$$

$$Y^\delta_{\text{av}}(x,u) = B^{\delta\top} \bar{\nabla} H|^{x^+(u)}_{x^+} \tag{9.19}$$

with $x^+ = e^{\delta(J-R)P}x$ and $B^\delta = \frac{1}{\delta}\int_0^\delta e^{\tau(J-R)P}B d\tau$. Moreover, the sampled-data system (9.18) is passive with respect to the output (9.19) with storage function $H(x) = \frac{1}{2}x^\top P x$ and satisfies the energy balance equality

$$H(x_k) - H(x_0) = \delta \sum_{i=0}^{k-1} \bar{\nabla}^\top H|^{x_i^+}_{x_i} \mathcal{S}^\delta_{J-R} \bar{\nabla} H|^{x_i^+}_{x_i} + \delta \sum_{i=0}^{k-1} u_i Y^\delta_{\text{av}}(x_i, u_i). \tag{9.20}$$

Remark 9.2.5. The sampled-data linear port-Hamiltonian system with Hamiltonian function $H(x) = \frac{1}{2}x^\top P x$ and $P = P^\top \succ 0$ is, by construction, passive with respect to the conjugate output map (9.19) and average passive with respect to the map $Y^\delta(x) = B^{\delta\top} P x$. This is due to the fact that the conjugate output is the average output of $Y^\delta(x,u)$, i.e.

$$\begin{aligned} Y^\delta_{\text{av}}(x,u) &= \frac{1}{u}\int_0^u Y^\delta(x^+(v))\mathrm{d}v \\ &= \frac{1}{u}\int_0^u B^{\delta\top} P x^+(v)\mathrm{d}v = B^{\delta\top} P x^+ + \frac{u}{2} B^{\delta\top} P B^\delta. \end{aligned}$$

Remark 9.2.6. The output map (9.19) for the linear case can be expressed as a series expansion in powers of δ as in (7.33), that is

$$Y^\delta_{\text{av}}(x,u) = \sum_{i\geq 0} \frac{\delta^i}{(i+1)!} Y^\delta_{\text{av}_i}(x,u) \tag{9.21}$$

so obtaining for the first terms

$$\begin{aligned} Y^\delta_{\text{av}_0}(x) &= h(x) = B^\top P x \\ Y^\delta_{\text{av}_1}(x,u) &= B^\top P \left[J - 2R\right] P x + u B^\top P B \\ Y^\delta_{\text{av}_2}(x,u) &= B^\top P \left[7JPJ - 5JPR + RPJ + RPR\right] P x + u \frac{3}{2} B^\top (J-R) P^2 B. \end{aligned}$$

9.3 Negative output feedback

The same result applies to the LTI port-Hamiltonian system, but in that case provides a global result. Indeed the implicit damping equality yields a unique solution as seen for the discrete-time negative output feedback.

The following Theorem applies the result in Theorem 2.3.1 to the presented LTI sampled-data port-Hamiltonian system.

Theorem 9.3.1: LTI negative output feedback under sampling

Consider a continuous-time LTI port-Hamiltonian system

$$\dot{x} = (J - R)\nabla H(x) + Bu \tag{9.22a}$$
$$y = B^\top \nabla H(x) \tag{9.22b}$$

with quadratic Hamiltonian function $H(x) = \frac{1}{2}x^\top Px$ with $P \succ 0$ and assume $u(t) = u(k\delta), \forall t \in [k\delta, (k+1)\delta[$ with $\delta \in]0, T^*[$. Let for any δ, the sampled equivalent model to (9.22), that is

$$x^+(u) = x + \delta \mathcal{S}^\delta_{J-R} \bar{\nabla} H|_x^{x^+} + \delta B^\delta u \tag{9.23a}$$
$$Y^\delta_{\text{av}}(x, u) = B^{\delta\top} \bar{\nabla} H|_{x^+}^{x^+(u)} \tag{9.23b}$$

be ZSD with $x^+ = e^{\delta(J-R)P}x$ and $B^\delta = \frac{1}{\delta}\int_0^\delta e^{\tau(J-R)P}Bd\tau$. Then, the feedback

$$u = -\frac{\kappa B^{\delta\top} P x^+}{1 + \frac{\kappa}{2} B^{\delta\top} P B^\delta} \tag{9.24}$$

with positive gain $\kappa > 0$ achieves global asymptotic stabilization of the origin.

9.4 IDA-PBC: Direct discrete design

In Chapter 8 we tackled the IDA-PBC problem exploiting the input-Hamiltonian matching design, since in the general nonlinear case a solution to the matching equation is difficult to compute. However, since in this linear case the matching equation reduces to a linear matrix equation the IDA-PBC problem can be solved through a direct digital design which assigns the desired sampled-data closed loop structure. In

this respect, mimicking the result in discrete time, the control objective reduces to provide a state feedback

$$u = \bar{u} + v$$

which achieves the target LTI sampled-data port-Hamiltonian structure

$$\begin{aligned} x^+(\bar{u}+v) &= x + \delta(\mathcal{J}_d^\delta - \mathcal{R}_d^\delta)\bar{\nabla}H_d|_x^{x^+(\bar{u})} + \delta B^\delta v \\ &= x + \frac{\delta}{2}(\mathcal{J}_d^\delta - \mathcal{R}_d^\delta)P_d(x^+(\bar{u}) + x - 2x_\star) + \delta B^\delta v \end{aligned} \tag{9.25}$$

with respect to the desired Hamiltonian function

$$H_d(x) = \frac{1}{2}(x - x_\star)^\top P_d(x - x_\star)$$

with positive definite $P_d \in \mathrm{Sym}_{\mathbb{R}}(n,n)$, and freely chosen matrices $\mathcal{J}_d^\delta \in \mathrm{Skew}_{\mathbb{R}}(n,n)$ and positive semi-definite $\mathcal{R}_d^\delta \in \mathrm{Sym}_{\mathbb{R}}(n,n)$, solutions to the matching equation

$$\frac{1}{2}\mathcal{S}_{J-R}^\delta P(x^+ + x) + uB^\delta = \frac{1}{2}(\mathcal{J}_d^\delta - \mathcal{R}_d^\delta)P_d(x^+(\bar{u}) + x - 2x_\star). \tag{9.26}$$

Remark 9.4.1. Note that, the freely choosen matrices $\mathcal{J}_d^\delta$ and $\mathcal{R}_d^\delta$ are not the sampled-data equivalent matrices of the continuous-time system with J_d and R_d.

The following Theorem is deduced from Proposition 5.2.1 and provides a necessary and sufficient condition for solving the SD IDA-PBC problem through direct discrete design.

Theorem 9.4.1: LTI IDA-PBC under sampling: a direct discrete design

Consider the sampled equivalent port-Hamiltonian structure to (9.17) of the form

$$x^+(u) = x + \delta\mathcal{S}_{J-R}^\delta \bar{\nabla}H|_x^{x^+} + \delta B^\delta u. \tag{9.27}$$

Then, the SD IDA-PBC problem is solvable if and only if there exist $\mathcal{J}_a^\delta$, $\mathcal{R}_d^\delta$ and P_a solutions to the matching condition

$$B^{\delta\perp}(\mathcal{J}_a^\delta - \mathcal{R}_a^\delta)P + B^{\delta\perp}(\mathcal{J}_a^\delta + \mathcal{J}^\delta - \mathcal{R}_a^\delta - \mathcal{R}^\delta)P_a = 0 \tag{9.28}$$

with

$$\mathcal{J}^\delta = \frac{1}{2}\left[\mathcal{S}^\delta_{J-R} - \mathcal{S}^{\delta\top}_{J-R}\right] \in \mathrm{Skew}_{\mathbb{R}}(n,n)$$
$$\mathcal{R}^\delta = -\frac{1}{2}\left[\mathcal{S}^\delta_{J-R} + \mathcal{S}^{\delta\top}_{J-R}\right] \in \mathrm{Sym}_{\mathbb{R}}(n,n)$$

$$\mathcal{J}^\delta_d = \left[\mathcal{J}^\delta + \mathcal{J}^\delta_a\right] \in \mathrm{Skew}_{\mathbb{R}}(n,n)$$
$$\mathcal{R}^\delta_d = \left[\mathcal{R}^\delta + \mathcal{R}^\delta_a\right] \succeq 0 \in \mathrm{Sym}_{\mathbb{R}}(n,n)$$
$$P_d = \left[P + P_a\right] \succeq 0 \in \mathrm{Sym}_{\mathbb{R}}(n,n).$$

In addition, the feedback assigning the port-Hamiltonian dynamics

$$x^+(\bar{u}+v) = x + \delta(\mathcal{J}^\delta_d - \mathcal{R}^\delta_d)\bar{\nabla}H_d|^{x^+(\bar{u})}_x + \delta B^\delta v \tag{9.29}$$

is given by

$$\bar{u} = \frac{1}{2}B^{\delta\dagger}\left[(\mathcal{J}^\delta_d - \mathcal{R}^\delta_d)P_d(x^+(\bar{u}) + x - 2x_\star) - \mathcal{S}^\delta_{J-R}P(x^+ + x)\right]. \tag{9.30}$$

Equivalently, the implicit port-Hamiltonian dynamics (9.25) can be explicitly expressed in closed form as such

$$x^+(\bar{u}+v) = A^\delta_d x + A^\delta_{d,\star}x_\star + \delta B^\delta v \tag{9.31}$$

and feedback $\bar{u}$ as

$$\bar{u} = B^{\delta\dagger}(A^\delta_d - A^\delta)x + B^{\delta\dagger}A^\delta_{d,\star}x_\star, \tag{9.32}$$

with

$$A^\delta_d = \big(I - \frac{\delta}{2}(\mathcal{J}^\delta_d - \mathcal{R}^\delta_d)P_d\big)^{-1}\big(I + \frac{\delta}{2}(\mathcal{J}^\delta_d - \mathcal{R}^\delta_d)P_d\big) \tag{9.33a}$$
$$A^\delta_{d,\star} = -\left(I - \frac{\delta}{2}(\mathcal{J}^\delta_d - \mathcal{R}^\delta_d)P_d\right)^{-1}(\mathcal{J}^\delta_d - \mathcal{R}^\delta_d)P_d. \tag{9.33b}$$

9.5 Concluding remarks

This chapter specializes in the results previously presented for nonlinear gradient and port-Hamiltonian systems under sampling to the LTI case. In this respect, we recalled the definition of gradient and port-Hamiltonian systems under sampling based on

the sampled-data equivalent modeling. It is shown that discrete gradient or port-Hamiltonian representations can be recovered under exact sampling with respect to the same energy function and modified interconnection and dissipation matrices. The proposed method holds both the objectives of satisfying under sampling the energetic properties which characterize Hamiltonian dynamics and that of matching the state evolutions at the sampling instants. Finally, the stabilization problem of LTI port-Hamiltonian system is concerned. First, we apply the result in Theorem 2.3.1 to LTI systems in port-Hamiltonian representation, then we reshape the IDA-PBC solution presented in Chapter 5, since in this linear case the matching equation to be satisfied reduces to a linear matrix equation and the IDA-PBC problem can be solved with feedback control in closed form. The results presented within this chapter are reported in the following published article:

A. Moreschini, S. Monaco and D. Normand-Cyrot, Gradient and Hamiltonian dynamics under sampling, IFAC-PapersOnLine, Volume 52, Issue 16, 2019, Pages 472-477, ISSN 2405-8963, https://doi.org/10.1016/j.ifacol.2019.12.006.

A. Moreschini, M. Mattioni, S. Monaco and D. Normand-Cyrot, "Stabilization of Discrete Port-Hamiltonian Dynamics via Interconnection and Damping Assignment," in IEEE Control Systems Letters, vol. 5, no. 1, pp. 103-108, Jan. 2021, doi: 10.1109/LCSYS.2020.3000705.

Part IV

CASE STUDIES

Chapter 10

The RLC circuit

Contents

10.1 Continuous-time modeling **210**

10.2 Sampled-data modeling **211**

10.3 Digital damping feedback **218**

10.4 Discrete IDA-PBC design **225**

The most studied circuit in the literature is undoubtedly the RLC circuit. This LTI model helps to understand some of the behaviors of an electrical control system and, in the present context, how the preservation of a Hamiltonian structure under sampling has an high impact in both the design of a faithful sampled-data model and its control. For this example three aspects are illustrated:

1. Exact sampled-data port-Hamiltonian models are computed by exploiting the forms discussed in Section 9.2;

2. Based on the proposed model stabilization at the origin is achieved via exact digital negative output feedback as discussed in Section 9.3;

3. Stabilization at a desired equilibrium point is illustrated via direct discrete IDA-PBC design based on the results presented in Section 9.4.

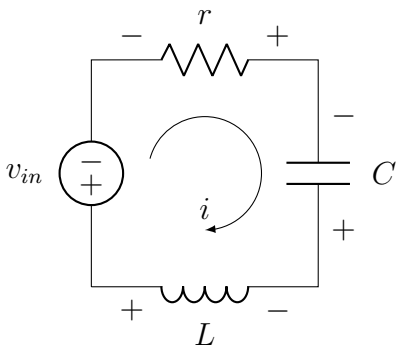

Figure 10.1: RLC circuit

10.1 Continuous-time modeling

The RLC circuit in Figure 10.1 is characterized by a voltage source v_{in} that produces volts, a resistor r, an inductor L, and a capacitor C, and a current i, as in Table 10.1. According to Kirchhoff's Law the circuit is modeled as a continuous-time port-Hamiltonian system

$$\dot{x} = \begin{pmatrix} 0 & 1 \\ -1 & -r \end{pmatrix} \nabla H(x) + \begin{pmatrix} 0 \\ 1 \end{pmatrix} u \tag{10.1a}$$

$$y = \frac{x_2}{L} \tag{10.1b}$$

setting $x_1 = Cv_C$, $x_2 = Li_L$, $v_{in} = u$, and Hamiltonian function $H(x)$, catching the energy stored in the capacitor C and in the inductor L, i.e.

$$H(x) = \frac{1}{2C}x_1^2 + \frac{1}{2L}x_2^2. \tag{10.2}$$

The continuous-time RLC dynamics represents a damped harmonic oscillator that is dissipative for zero input $u = 0$, meaning that the energy evolution satisfies the

Parameter	**Description**	**Units**
i	current	A (amperes)
v_{in}	voltage source	V (volt)
r	Resistor	Ω (ohm)
L	Inductor	H (henry)
C	Capacitor	F (farad)

Table 10.1: RLC parameters

dissipation inequality

$$\dot{H} = \nabla^\top H(x)\dot{x} = -\frac{r}{L^2}x_2^2 \leq 0,$$

behaving as a monotonically decreasing function. Invoking Lyapunov stability theory, the dissipation inequality above clearly provides asymptotic stability of the origin for $r > 0$, and marginal stability for zero resistance $r = 0$.

10.2 Sampled-data modeling

In this section we describe the sampled-data equivalent port-Hamiltonian dynamics applying the results presented in Theorem 9.2.1.

To compute the unforced sampled-data dynamics associated to the RLC system, let us first focus on the uncontrolled continuous-time dynamics

$$\begin{pmatrix} \dot{x}_1 \\ \dot{x}_2 \end{pmatrix} = \begin{pmatrix} 0 & 1 \\ -1 & -r \end{pmatrix} \nabla H(x). \tag{10.3}$$

Hereinafter, without loss of generality and for notational simplicity, we fix both the inductance L and the capacitor C as 1. Because the Hamiltonian function (10.2) is quadratic and according to Definition 2.1.1, the discrete gradient is computable as

$$\bar{\nabla} H|_x^{x^+} = \int_0^1 \nabla H|_{x+s(x^+-x)} \mathrm{d}s = \frac{1}{2}P(x^+ + x) = \frac{1}{2}P \begin{pmatrix} x_1^+ + x_1 \\ x_2^+ + x_2 \end{pmatrix}, \tag{10.4}$$

with in this case $P = I$ characterizing the Hamiltonian function, where $x := x(k\delta)$ is the state and $x^+ := x((k+1)\delta)$ is the one-step ahead of the uncontrolled evolution when $u = 0$.

Since the RLC circuit is a LTI dynamics, we can compute an exact sampled-data equivalent port-Hamiltonian representation as Theorem 9.2.1 taking the form

$$\begin{aligned} x^+ &= x + \delta \mathcal{S}_{J-R}^\delta \bar{\nabla} H|_x^{x^+} \\ &= \begin{pmatrix} x_1 \\ x_2 \end{pmatrix} + \frac{\delta}{2} \begin{pmatrix} -R_{\star 1} & J_\star \\ -J_\star & -R_{\star 2} \end{pmatrix} \begin{pmatrix} x_1^+ + x_1 \\ x_2^+ + x_2 \end{pmatrix} \end{aligned} \tag{10.5}$$

with sampled-data matrix $\mathcal{S}_{J-R}^\delta$ characterizing the dynamics given by

$$\begin{aligned} \mathcal{S}_{J-R}^\delta &= \frac{2}{\delta}(e^{\delta(J-R)} - I)(e^{\delta(J-R)} + I)^{-1} \\ &= \begin{pmatrix} -R_{\star 1} & J_\star \\ -J_\star & -R_{\star 2} \end{pmatrix}. \end{aligned}$$

Let us conduct the computations for resistance $r \geq \frac{1}{2}$. Therefore, denoting by $\alpha = -\frac{r}{2}$ and $\omega = \frac{1}{2}\sqrt{4-r^2}$, one computes the exponential matrix

$$e^{\delta(J-R)} = e^{\alpha\delta}\begin{pmatrix} \cos(\omega\delta) - \frac{\alpha}{\omega}\sin(\omega\delta) & \frac{1}{\omega}\sin(\omega\delta) \\ -\frac{1}{\omega}\sin(\omega\delta) & \cos(\omega\delta) + \frac{\alpha}{\omega}\sin(\omega\delta) \end{pmatrix}$$

and from the expression

$$\begin{aligned} \mathcal{S}^{\delta}_{J-R} &= \frac{2}{\delta}(e^{\delta(J-R)} - I)(e^{\delta(J-R)} + I)^{-1} \\ &= \begin{pmatrix} -\frac{[e^{2\alpha\delta} - 1 - 2e^{\alpha\delta}\sin(\omega\delta))]}{\delta(e^{2\alpha\delta}+1+2e^{\alpha\delta}\cos(\omega\delta))} & \frac{\frac{4}{\omega}e^{\alpha\delta}\sin(\omega\delta)}{\delta(e^{2\alpha\delta}+1+2e^{\alpha\delta}\cos(\omega\delta))} \\ -\frac{\frac{4}{\omega}e^{\alpha\delta}\sin(\omega\delta)}{\delta(e^{2\alpha\delta}+1+2e^{\alpha\delta}\cos(\omega\delta))} & -\frac{[e^{2\alpha\delta} - 1 - 2\frac{\alpha}{\omega}e^{\alpha\delta}\sin(\omega\delta)(\frac{\alpha}{\omega}e^{\alpha\delta}\sin(\omega\delta) - 1)]}{\delta(e^{2\alpha\delta}+1+2e^{\alpha\delta}\cos(\omega\delta))} \end{pmatrix} \end{aligned}$$

one obtains the exact sampled model (10.5) with the following coefficients

$$\begin{aligned} R_{\star 1} =& \frac{[e^{2\alpha\delta} - 1 - 2e^{\alpha\delta}\sin(\omega\delta))]}{\delta(e^{2\alpha\delta} + 1 + 2e^{\alpha\delta}\cos(\omega\delta))} \\ R_{\star 2} =& \frac{[e^{2\alpha\delta} - 1 - 2\frac{\alpha}{\omega}e^{\alpha\delta}\sin(\omega\delta)(\frac{\alpha}{\omega}e^{\alpha\delta}\sin(\omega\delta) - 1)]}{\delta(e^{2\alpha\delta} + 1 + 2e^{\alpha\delta}\cos(\omega\delta))} \\ J_{\star} =& \frac{\frac{4}{\omega}e^{\alpha\delta}\sin(\omega\delta)}{\delta(e^{2\alpha\delta} + 1 + 2e^{\alpha\delta}\cos(\omega\delta))}. \end{aligned}$$

Due to its structure, the sampled-data dynamics is dissipative for any $\delta > 0$, ensures a monotonically decreasing dissipation rate parameterized by δ

$$H(x^+) - H(x) = -\frac{\delta}{4}R_{\star 1}(x_1^+ + x_1)^2 - \frac{\delta}{4}R_{\star 2}(x_2^+ + x_2)^2 \leq 0.$$

As already discussed in Theorem 9.2.1, the exact sampled-data port-Hamiltonian dynamics of the form (10.5) is implicitly defined through x^+. However, due to the quadratic structure of the Hamiltonian function (10.2), the exact sampled-data port-Hamiltonian model in (10.5) can be also explicitly expressed as

$$\begin{pmatrix} x_1^+ \\ x_2^+ \end{pmatrix} = \begin{pmatrix} 1 + \frac{\delta}{2}R_{\star 1} & -\frac{\delta}{2}J_{\star} \\ \frac{\delta}{2}J_{\star} & 1 + \frac{\delta}{2}R_{\star 2} \end{pmatrix}^{-1} \begin{pmatrix} 1 - \frac{\delta}{2}R_{\star 1} & \frac{\delta}{2}J_{\star} \\ -\frac{\delta}{2}J_{\star} & 1 - \frac{\delta}{2}R_{\star 2} \end{pmatrix} \begin{pmatrix} x_1 \\ x_2 \end{pmatrix}, \tag{10.6}$$

so recovering the structure in (9.11) with state matrix

$$A^{\delta} = e^{\delta(J-R)} = \begin{pmatrix} 1 + \frac{\delta}{2}R_{\star 1} & -\frac{\delta}{2}J_{\star} \\ \frac{\delta}{2}J_{\star} & 1 + \frac{\delta}{2}R_{\star 2} \end{pmatrix}^{-1} \begin{pmatrix} 1 - \frac{\delta}{2}R_{\star 1} & \frac{\delta}{2}J_{\star} \\ -\frac{\delta}{2}J_{\star} & 1 - \frac{\delta}{2}R_{\star 2} \end{pmatrix}. \tag{10.7}$$

Accordingly, for zero dissipation (i.e. $r = 0$), the exact sampled-data Hamiltonian system (10.5) yields the following implicit sampled-data dynamics

$$\begin{aligned} x^+ &= x + \delta \mathcal{S}_J^\delta \bar{\nabla} H|_x^{x^+} \\ &= \begin{pmatrix} x_1 \\ x_2 \end{pmatrix} + \frac{\delta}{2} \begin{pmatrix} 0 & \frac{2\sin\delta}{\delta(\cos\delta+1)} \\ -\frac{2\sin\delta}{\delta(\cos\delta+1)} & 0 \end{pmatrix} \begin{pmatrix} x_1^+ + x_1 \\ x_2^+ + x_2 \end{pmatrix} \end{aligned} \tag{10.8}$$

where $\mathcal{S}_J^\delta$ is the sampled-data interconnection matrix parameterized by δ which preserves conservation of energy along the Hamiltonian function (10.2), namely

$$H(x^+) - H(x) = \delta \nabla^\top H|_x^{x^+} \mathcal{S}_J^\delta \bar{\nabla} H|_x^{x^+} = 0.$$

As discussed in Section 7.6, the model given in Yalçin et al. (2015); Aoues et al. (2017) can be compared with the proposed exact model (10.5). In fact, it reduces to the zero-order approximation of the exact sampled-data matrix $\mathcal{S}_{J-R}^\delta$, namely it is described by the implicit port-Hamiltonian model below

$$x^+ = x + \delta S_0 \bar{\nabla} H|_x^{x^+} + O(\delta^2) \tag{10.9}$$

where $S_0 = (J - R)$ verifies the following condition with respect to $\mathcal{S}_{J-R}^\delta$

$$\mathcal{S}_{J-R}^\delta = S_0 + O(\delta).$$

The so defined Euler-like model, yields a first-order dissipation rate of the form

$$H(x^+) - H(x) = -\frac{\delta}{4} r (x_2^+ + x_2)^2 + O(\delta^2),$$

which exhibits a decreasing behaviour (respectively, conservation of energy) in $O(\delta^2)$ only; it does not ensure the same dissipative behaviour (at all sampling instants) as the continuous-time dynamics as illustrated below.

Simulations

Through several simulations, the exact model (10.5) and the first-order model of the literature Yalçin et al. (2015); Aoues et al. (2017) are compared in Figure 10.2 and

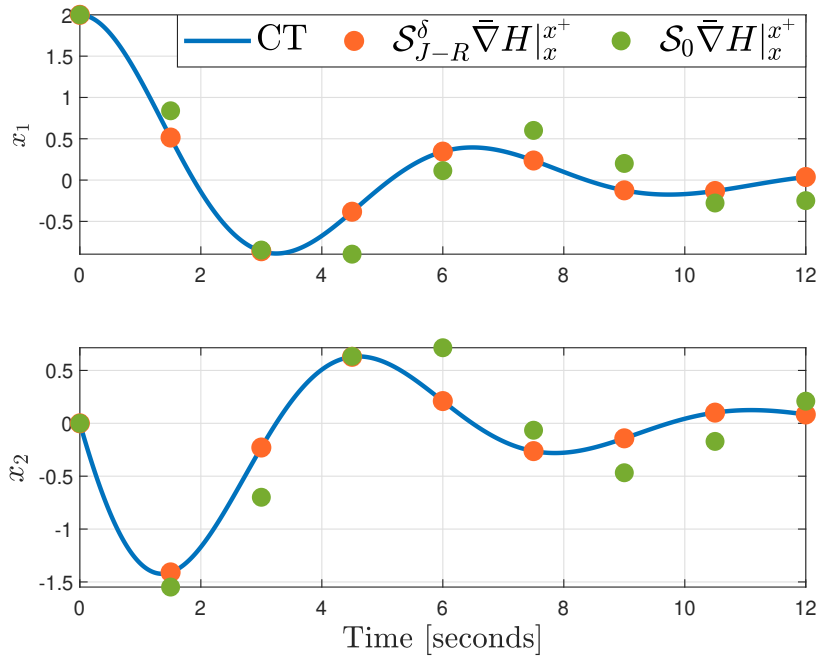

(a) State trajectories

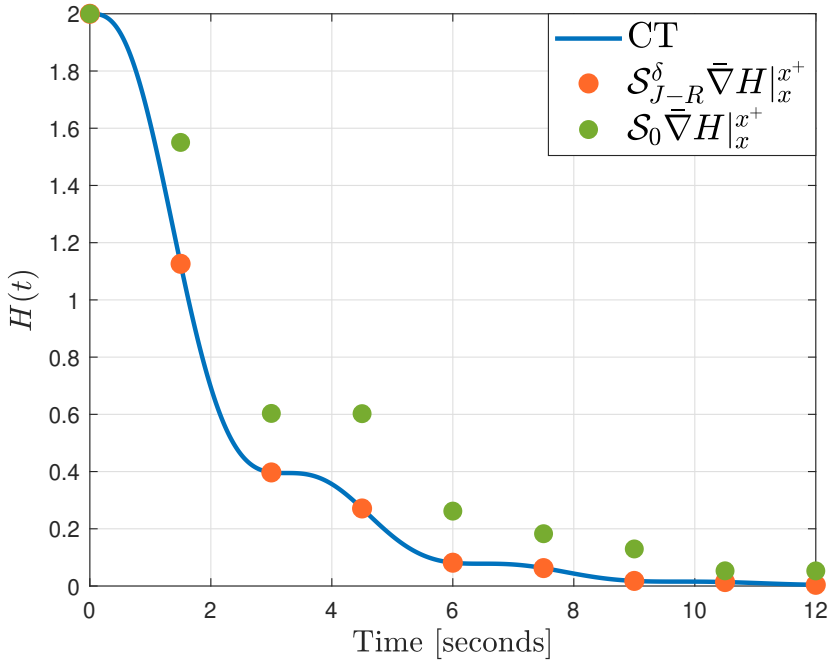

(b) Hamiltonian function

Figure 10.2: Sampled-data damped RLC model

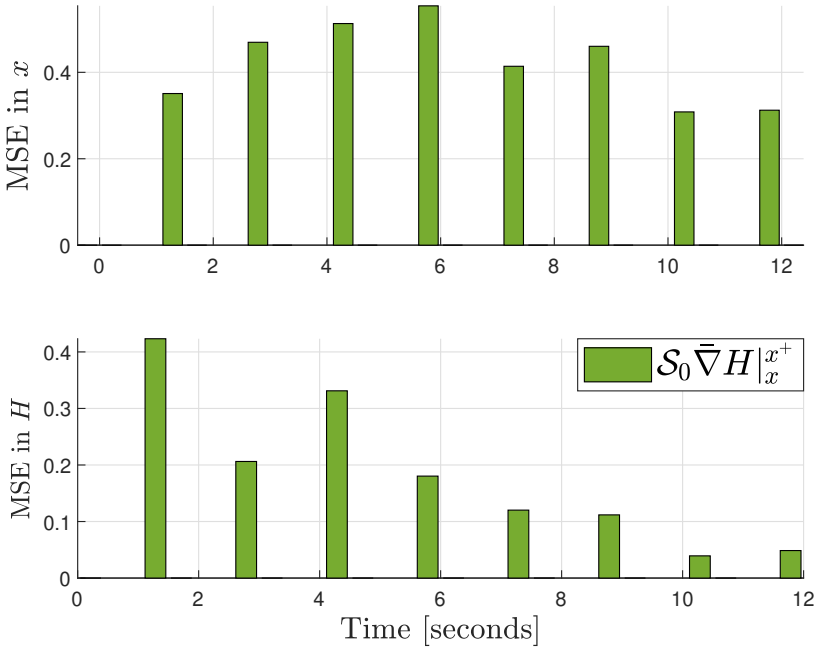

Figure 10.3: Sampled-data damped RLC model: Mean Squared Errors

Figure 10.3 illustrating for a sampling period of length $\delta = 1.5$: the time evolution of the state trajectories (a); the Hamiltonian function (b); the Mean Squared Error in Figure 10.3 for both the state x and the Hamiltonian H in the dissipative case, setting the resistance $r = 0.5$.

In Figure 10.2(a), the proposed model provides an exact matching of the continuous-time state trajectories at the sampling instants while the dynamics (10.9) is far from the continuous-time onr even though stability is preserved at any sampling instant δ. This improvement in the matching of the state is due to the higher order terms in δ contained into the exact sampled-data matrix $\mathcal{S}_{J-R}^{\delta}$. Those higher order terms improve the matching of the Hamiltonian function too as verified in Figure 10.2(b). Unlike the exact model, the Euler-like sampled-data model given in (10.9) approaches the energy behaviour of the continuous-time systems and it produces s a mismatch in both the state and Hamiltonian evolutions, as illustrated in Figure 10.3.

These comments made for the sampled-data model in the dissipative case, extend to the conservative case for zero resistance $r = 0$, as shown in Figure 10.4. Notably, the proposed sampled-data model, even in the conservative case, provides an exact matching of the continuous-time trajectories at the sampling instants. The ap-

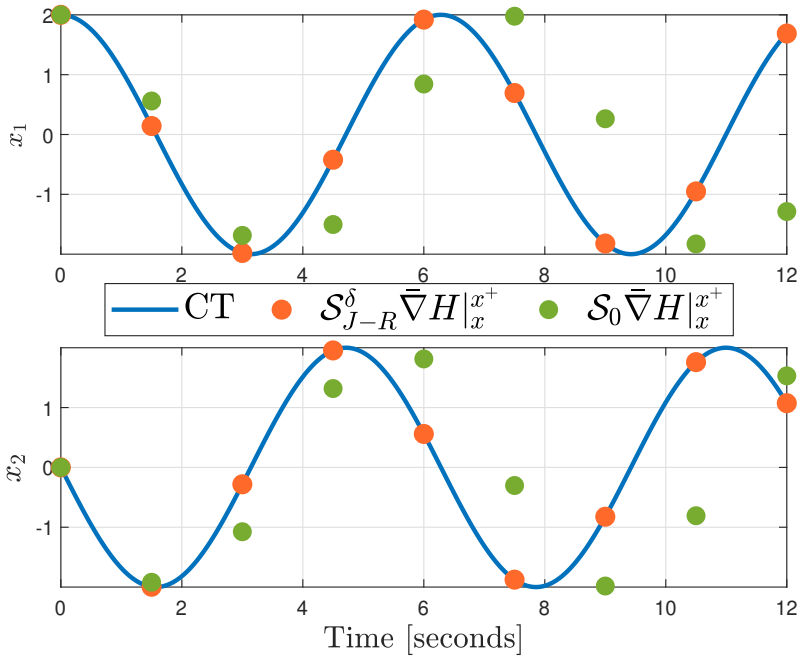

(a) State trajectories

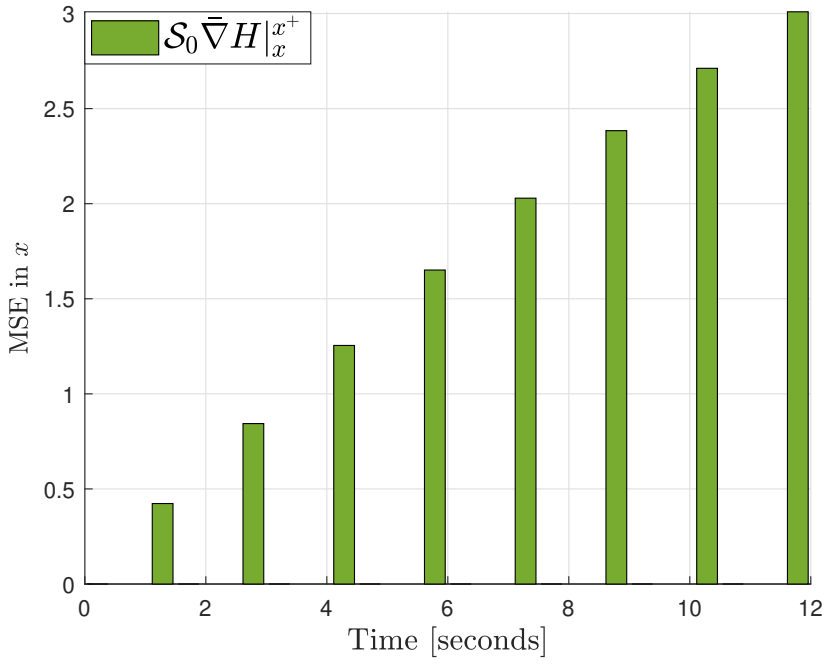

(b) Mean Squared Error of the Sampled-data RLC model

Figure 10.4: Sampled-data undamped RLC model

proximate model (10.9) provides a slower swinging than the continuous-time one, so introducing a mismatch between the sampled-data trajectories and the continuous-time ones at the sampling instants $k\delta$. This is reflected into Figure 10.4(b) where the error growth is clear for the approximate model (10.9).

Approximate solutions

Even though in the RLC circuit the discrete gradient is exactly computable, as the sampled-data dynamics might be transformed from an implicit representation (10.5) to an explicit one (10.6), it is interesting to analyze on such an example the effects of approximations on the state and Hamiltonian evolutions. Considering approximations of $\mathcal{S}^{\delta}_{J-R}$ and $\bar{\nabla}H|_x^{x^+}$ as in Remark 7.4.2, one sets

$$\mathcal{S}^{\delta}_{J-R} = \sum_{i\geq 0} \frac{\delta^i}{(i+1)!}(\mathcal{S}_{J-R})_i, \quad \bar{\nabla}H|_x^{x^+} = \sum_{i\geq 0} \frac{\delta^i}{(i+1)!}\bar{\nabla}_i H(x)$$

with by definition $\mathcal{S}^{[p]}_{J-R}$ and $\bar{\nabla}^{[p]}H(x)$ the truncations at finite order $p \geq 0$

$$\mathcal{S}^{[p]}_{J-R} = \sum_{i=0}^{p} \frac{\delta^i}{(i+1)!}(\mathcal{S}_{J-R})_i \tag{10.10a}$$

$$\bar{\nabla}^{[p]}H(x) = \sum_{i=0}^{p} \frac{\delta^i}{(i+1)!}\bar{\nabla}_i H(x). \tag{10.10b}$$

The effects of approximations of order $p_2, p_1 > 0$ on the sampled-data dynamics

$$x^+ = x + \delta S^{[p_1]}_{J-R}(x)\bar{\nabla}^{[p_2]}H(x)$$

are illustrated. For the first part and up to $p_1 = 2$, one considers the sampled-data matrix $\mathcal{S}^{\delta}_{J-R}$ approximated in $O(\delta^3)$

$$\mathcal{S}^{[0]}_{J-R} = \begin{pmatrix} 0 & 1 \\ -1 & -r \end{pmatrix}$$

$$\mathcal{S}^{[2]}_{J-R}(x) = \mathcal{S}^{[0]}_{J-R} + \frac{\delta^2}{12}\begin{pmatrix} -r & 1-r^2 \\ r^2-1 & r^3-r \end{pmatrix}$$

and for the second part up to $p_2 = 2$, one considers the discrete gradient $\bar{\nabla} H|_x^{x^+}$ with

$$\bar{\nabla}^{[0]} H(x) = \begin{pmatrix} x_1 \\ x_2 \end{pmatrix}$$
$$\bar{\nabla}^{[1]} H(x) = \bar{\nabla}^{[0]} H(x) + \frac{\delta}{2} \begin{pmatrix} x_2 \\ -(x_1 + r x_2) \end{pmatrix}$$
$$\bar{\nabla}^{[2]} H(x) = \bar{\nabla}^{[1]} H(x) + \frac{\delta^2}{4} \begin{pmatrix} -x_1 - r x_2 \\ x_2(r^2 - 1) + r x_1 \end{pmatrix}.$$

Simulations

To motivate the choice of the approximation, consider different combinations ($p_1 = \{0, 2\}$ and $p_2 = \{0, 1, 2\}$) for the matrix product $\mathcal{S}_{J-R}^{[p_1]} \bar{\nabla}^{[p_2]} H(x)$. This clearly gives a non-homogeneous sampled model in δ. Those different approximations are reported in Figure 10.6 and Figure 10.5 assuming dissipation $r = 0.3$ and sampling period $\delta = 0.9$. Figures 10.7(a), (b), (c) hint an order of approximation of both the sampled-data matrix $\mathcal{S}_{J-R}^{[p_1]}$ and discrete gradient $\bar{\nabla}^{[p_2]} H(x)$ with $p_2 > p_1$. Interestingly, the approximate sampled-data matrix $\mathcal{S}_{J-R}^{[2]}$ associated with the exact discrete gradient (10.4) provides highly comparable performances in both the state trajectories and Hamiltonian with the exact discrete model described by the exact sampled-data matrix $\mathcal{S}_{J-R}^{\delta}$.

These results (which can be compared with the exact gradient because it is explicitly computable) validate the necessity of modifying the interconnection and dissipation matrices to get better results than keeping the same interconnection matrix as the continuous-time one.

10.3 Digital damping feedback

Consider the controlled RLC circuit with control input u and internal dissipation $r = 0$ yielding a conservative sampled-data equivalent model with exact sampled-data matrix given in (10.8).

As already seen for zero dissipation, neither the continuous-time RLC system nor the sampled-data model are asymptotically stable. For digitally asymptotically stabilize the origin, one implements the digital damping feedback discussed in Theorem

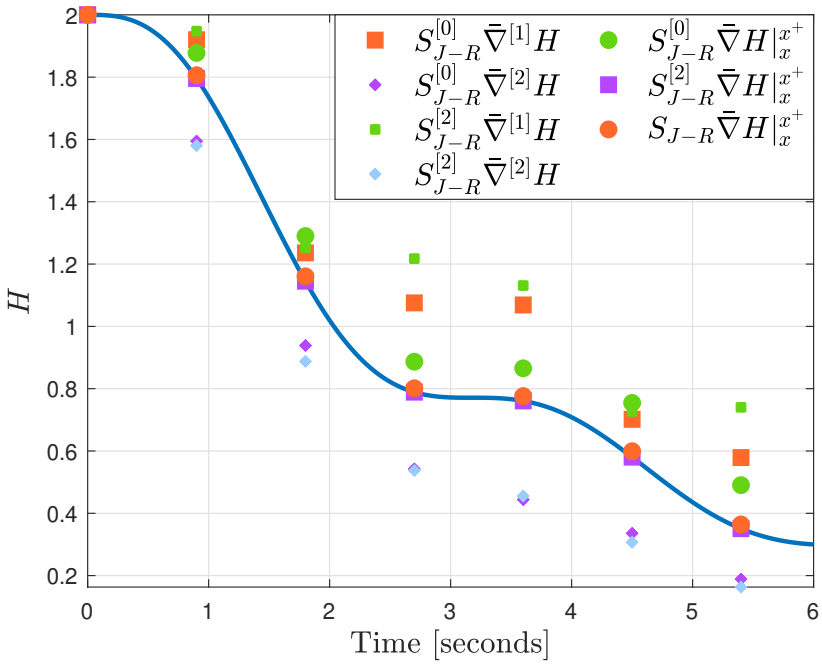

Figure 10.5: Comparison between different approximations of Sampled-data models: Hamiltonian function

9.3.1. To this end, we add the input and output ports of the system as in Theorem 9.2.2, that yields a sampled-data equivalent port-Hamiltonian system of the form

$$x^+(u) = x + \delta \mathcal{S}^\delta_{J-R}\bar{\nabla}H|_x^{x^+} + \delta B^\delta u \tag{10.11}$$

$$Y^\delta_{\text{av}}(x,u) = B^{\delta\top}\bar{\nabla}H|_{x^+}^{x^+(u)} \tag{10.12}$$

with $x^+(u) = x((k+1)\delta)$, $x = x(k\delta)$, $u = u(k\delta)$, and exact input and output mapping of the form

$$B^\delta = \begin{pmatrix} b^\delta_1 \\ b^\delta_2 \end{pmatrix} = \frac{1}{\delta}\begin{pmatrix} 1-\cos\delta \\ \sin\delta \end{pmatrix} \tag{10.13}$$

$$\begin{aligned} Y^\delta_{\text{av}}(x,u) &= B^{\delta\top}\bar{\nabla}H|_{x^+}^{x^+(u)} = B^{\delta\top}x^+ + \frac{1}{2}B^{\delta\top}B^\delta u \\ &= \frac{1}{\delta}(\cos\delta - 1)x_1 + \frac{1}{\delta}x_2\sin\delta + \frac{1}{\delta^2}(1-\cos\delta)u, \end{aligned} \tag{10.14}$$

where x^+ is the control-free dynamics given in (10.8) and admitting an explicit solution $x^+ = A^\delta x$ given in (10.7). Then the passivity-based feedback is computed as the solution to the damping feedback equation

$$u + \kappa Y^\delta_{\text{av}}(x,u) = u + \frac{\kappa}{2}B^{\delta\top}(x^+(u) + x^+) = 0,$$

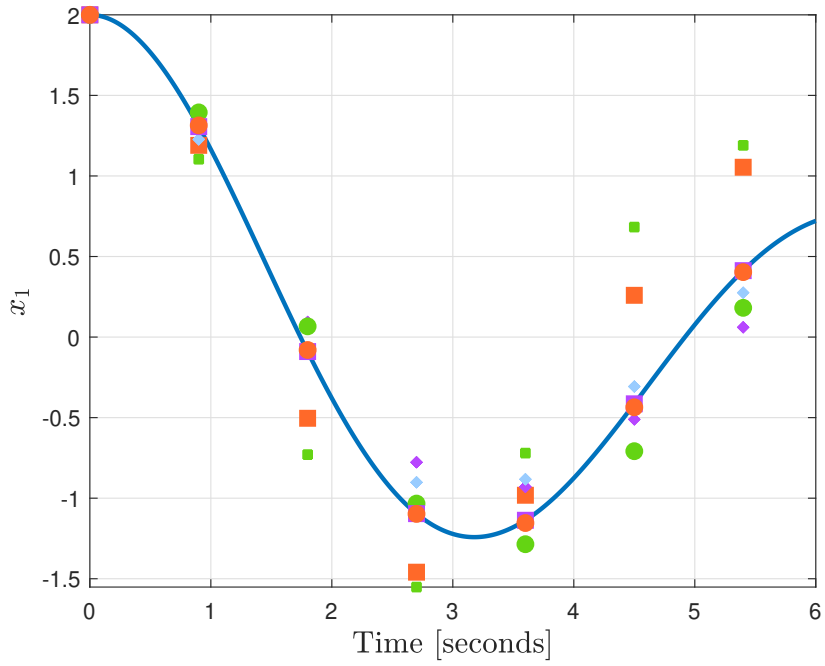

(a) Evolution of x_1

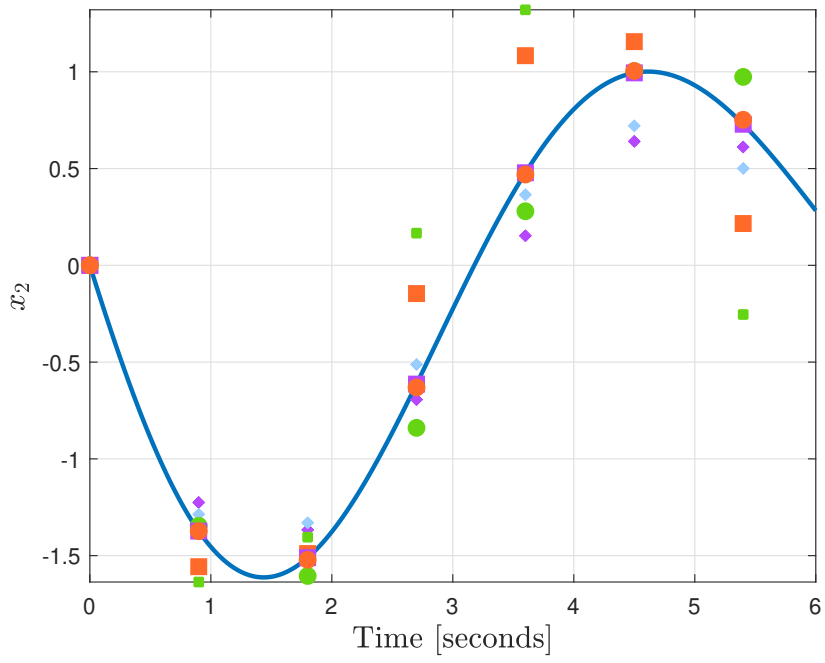

(b) Evolution of x_2

Figure 10.6: Comparison between different approximations of Sampled-data models

which specifies, in this case, as

$$u + \frac{\kappa}{\delta}(\cos\delta - 1)x_1 + \frac{\kappa}{\delta}x_2 \sin\delta + \frac{\kappa}{\delta^2}(1 - \cos\delta)u = 0. \tag{10.15}$$

Accordingly, the solution to (10.15) is given by

$$u = -\kappa \frac{x_1 \cos(\delta) - x_1 + x_2 \sin(\delta)}{\delta + \frac{\kappa}{\delta}(1 - \cos(\delta))}.$$

The feedback above makes the origin of the sampled-data RLC system (10.1) asymptotically stable in closed loop as shown in Figure 10.7, where the control effect of the proposed control has been compared with the discrete gradient-based passive control given in Aoues et al. (2017). We recall that the control provided in Aoues et al. (2017) is computed as the solution to the implicit equation

$$u = -\kappa B^\top \bar{\nabla} H|_x^{x^+(u)} = -\frac{\kappa}{2} B^\top (x^+(u) + x). \tag{10.16}$$

Simulations

The sampling period and damping gain are set as $\delta = 1.6$ and $\kappa = 0.5$. Although the control (10.16) provides satisfactory performances, the proposed feedback in (10.15) guarantees a high fidelity in in following the trajectories and the Hamiltonian of the continuous-time system controlled by the continuous-time passive feedback in van der Schaft (2000) (damping injection feeding back the continuous-time passive output (10.1b)), i.e.

$$u(t) = -\kappa B^\top \nabla H(x(t)) = -\kappa x_2(t).$$

The better performances ensured by the proposed digital control law are due to the exact modeling of the sampled-data system which involves the u-average output described in terms of the discrete gradient $\bar{\nabla} H|_{x^+}^{x^+(u)}$ between x^+ and $x^+(u)$ while in (10.16), the discrete gradient $\bar{\nabla} H|_x^{x^+(u)}$ is between x and $x^+(u)$.

Dirac structure

Because the RLC model admits an exact sampled-data model that is for any fixed δ, a discrete-time equivalent model, one can describe its associated Dirac structure representation according to Theorem 4.2.1.

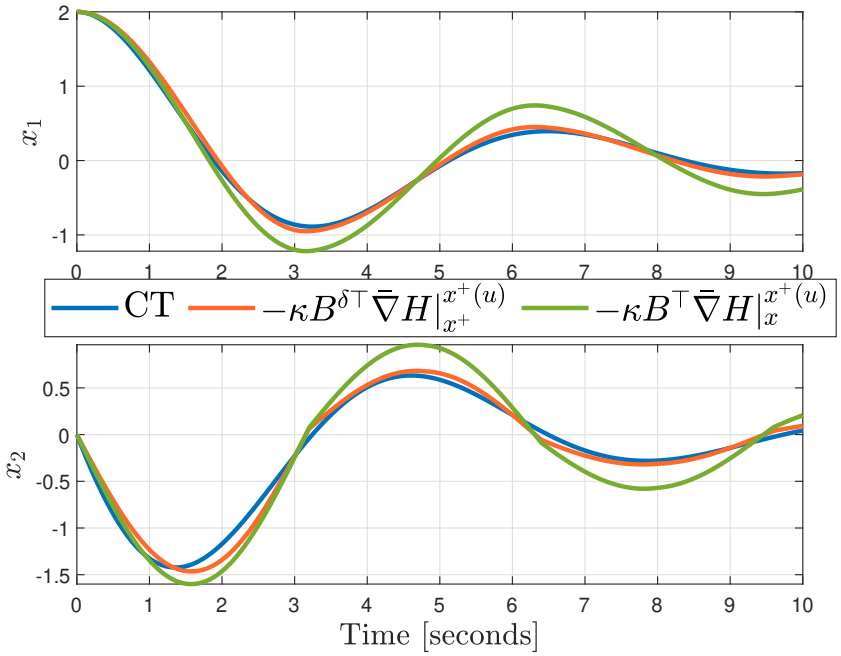

(a) State trajectories

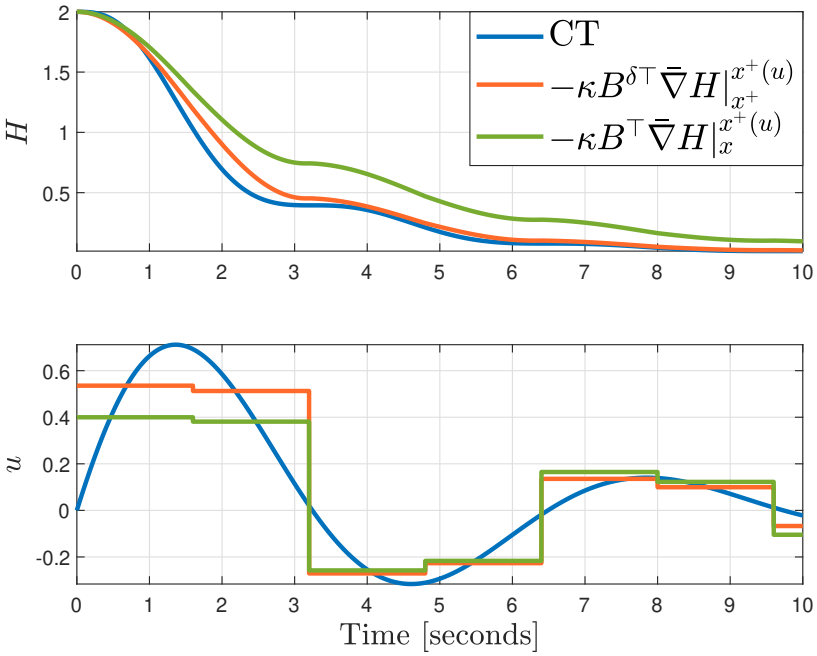

(b) Control and Hamiltonian function

Figure 10.7: Digital damping control upon the sampled-data RLC model

Setting the flows $f_S = (f_{S1}, f_{S2})$, $f_R = (f_{R1}, f_{R2})$, $f_C = (f_{C1}, f_{C2})$, and efforts $e_S = (e_{S1}, e_{S2})$, $e_R = (e_{R1}, e_{R2})$, $e_C = (e_{C1}, e_{C2})$ as

$$\begin{cases} f_{S1} &= -(x_1^+ - x_1) \\ f_{R1} &= \sqrt{R_{\star 1}}\frac{1}{2}(x_1^+ + x_1) \\ f_{C1} &= -(x_1^+(u) - x_1^+) \\ e_{S1} &= \frac{1}{2}(x_1^+ + x_1) \\ e_{R1} &= -\sqrt{R_{\star 1}}\frac{1}{2}(x_1^+ + x_1) \\ e_{C1} &= \frac{1}{2}(x_1^+(u) + x_1^+) \end{cases} \quad \begin{cases} f_{S2} &= -(x_2^+ - x_2) \\ f_{R2} &= \sqrt{R_{\star 2}}\frac{1}{2}(x_2^+ + x_2) \\ f_{C2} &= -(x_2^+(u) - x_2^+) \\ e_{S2} &= \frac{1}{2}(x_2^+ + x_2) \\ e_{R2} &= -\sqrt{R_{\star 2}}\frac{1}{2}(x_2^+ + x_2) \\ e_{C2} &= \frac{1}{2}(x_2^+(u) + x_2^+) \end{cases}$$

with $(f_I, e_I) = (Y^\delta_{\rm av}(x,u), u)$, with sampled-data output $Y^\delta_{\rm av}(x,u)$ in (10.14), one defines a Dirac structure

$$(f_S, f_R, f_C, f_I, e_S, e_R, e_C, e_I) \in \mathcal{D}$$
$$(f_R, e_R) \in \mathcal{R}$$

that yields the system in the skew symmetric graph form

$$\begin{bmatrix} f_{S1} \\ f_{S2} \\ f_{R1} \\ f_{R2} \\ f_{C1} \\ f_{C2} \\ f_I \end{bmatrix} = \begin{bmatrix} 0 & -J_\star & -\sqrt{R_{\star 1}} & 0 & 0 & 0 & 0 \\ J_\star & 0 & 0 & -\sqrt{R_{\star 2}} & 0 & 0 & 0 \\ \sqrt{R_{\star 1}} & 0 & 0 & 0 & 0 & 0 & 0 \\ 0 & \sqrt{R_{\star 2}} & 0 & 0 & 0 & 0 & 0 \\ 0 & 0 & 0 & 0 & 0 & 0 & -b_1^\delta \\ 0 & 0 & 0 & 0 & 0 & 0 & -b_2^\delta \\ 0 & 0 & 0 & 0 & b_1^\delta & b_2^\delta & 0 \end{bmatrix} \begin{bmatrix} e_{S1} \\ e_{S2} \\ e_{R1} \\ e_{R2} \\ e_{C1} \\ e_{C2} \\ e_I \end{bmatrix}, \tag{10.17}$$

with (b_1^δ, b_2^δ) in (10.13), satisfying the energy balance equality

$$e_{S1}^\top f_{S1} + e_{S2}^\top f_{S2} + e_{r1}^\top f_{R1} + e_{R2}^\top f_{R2} + e_{C1}^\top f_{C1} + e_{C2}^\top f_{C2} + e_I^\top f_I = 0.$$

Moreover, as in Theorem 5.1.2, under negative output feedback (10.15) setting the flows $f_{C_{\bar u}} = (f_{C_{\bar u}1}, f_{C_{\bar u}2})$, $f_{R_{\bar u}} = (f_{R_{\bar u}1}, f_{R_{\bar u}2})$, and efforts $e_{C_{\bar u}} = (e_{C_{\bar u}1}, e_{C_{\bar u}2})$, $e_{R_{\bar u}} = (e_{R_{\bar u}1}, e_{R_{\bar u}2})$, as

$$\begin{cases} f_{C_{\bar u}1} &= -(x_1^+(\bar u) - x_1^+) \\ f_{R_{\bar u}1} &= -\frac{\kappa}{2} b_1^\delta b_1^\delta (x_1^+(\bar u) + x_1^+) - \frac{\kappa}{2} b_1^\delta b_2^\delta (x_2^+(\bar u) + x_2^+) \\ e_{C_{\bar u}1} &= \frac{1}{2}(x_1^+(\bar u) + x_1^+) \\ e_{R_{\bar u}1} &= \frac{1}{2}(x_1^+(\bar u) + x_1^+) \end{cases}$$

$$\begin{cases} f_{C_{\bar{u}}2} & = -(x_2^+(\bar{u}) - x_2^+) \\ f_{R_{\bar{u}}2} & = -\frac{\kappa}{2} b_1^\delta b_2^\delta (x_1^+(\bar{u}) + x_1^+) - \frac{\kappa}{2} b_2^\delta b_2^\delta (x_2^+(\bar{u}) + x_2^+) \\ e_{C_{\bar{u}}2} & = \frac{1}{2}(x_2^+(\bar{u}) + x_2^+) \\ e_{R_{\bar{u}}2} & = \frac{1}{2}(x_2^+(\bar{u}) + x_2^+) \end{cases}$$

The Dirac structure (10.17) is transformed under feedback into another Dirac structure

$$\begin{bmatrix} f_{S1} \\ f_{S2} \\ f_{R1} \\ f_{R2} \\ f_{C_{\bar{u}}1} \\ f_{C_{\bar{u}}2} \\ f_{R_{\bar{u}}1} \\ f_{R_{\bar{u}}2} \end{bmatrix} = \begin{bmatrix} 0 & -J_\star & -\sqrt{R_{\star 1}} & 0 & 0 & 0 & 0 & 0 \\ J_\star & 0 & 0 & -\sqrt{R_{\star 2}} & 0 & 0 & 0 & 0 \\ \sqrt{R_{\star 1}} & 0 & 0 & 0 & 0 & 0 & 0 & 0 \\ 0 & \sqrt{R_{\star 2}} & 0 & 0 & 0 & 0 & 0 & 0 \\ 0 & 0 & 0 & 0 & 0 & 0 & \kappa b_1^\delta b_1^\delta & \kappa b_1^\delta b_2^\delta \\ 0 & 0 & 0 & 0 & 0 & 0 & \kappa b_1^\delta b_2^\delta & \kappa b_2^\delta b_2^\delta \\ 0 & 0 & 0 & 0 & -\kappa b_1^\delta b_1^\delta & -\kappa b_1^\delta b_2^\delta & 0 & 0 \\ 0 & 0 & 0 & 0 & -\kappa b_1^\delta b_1^\delta & -\kappa b_2^\delta b_2^\delta & 0 & 0 \end{bmatrix} \begin{bmatrix} e_{S1} \\ e_{S2} \\ e_{R1} \\ e_{R2} \\ e_{C_{\bar{u}}1} \\ e_{C_{\bar{u}}2} \\ e_{R_{\bar{u}}1} \\ e_{R_{\bar{u}}2} \end{bmatrix}, \tag{10.18}$$

satisfying the closed loop energy balance equality

$$e_{S1}^\top f_{S1} + e_{S2}^\top f_{S2} + e_{r1}^\top f_{R1} + e_{R2}^\top f_{R2} + e_{C_{\bar{u}}1}^\top f_{C_{\bar{u}}1} + e_{C_{\bar{u}}2}^\top f_{C_{\bar{u}}2} + e_{R_{\bar{u}}1}^\top f_{R_{\bar{u}}1} + e_{R_{\bar{u}}2}^\top f_{R_{\bar{u}}2} = 0.$$

It follows that the closed-loop sampled-data RLC system under negative output feedback (10.15) is again a sampled-data port-Hamiltonian system defined over the Dirac structure

$$(f_S, f_R, f_{C_{\bar{u}}}, f_{R_{\bar{u}}}, e_S, e_R, e_{C_{\bar{u}}}, e_{R_{\bar{u}}}) \in \mathcal{D}$$
$$(f_R, f_{R_{\bar{u}}}, e_R, e_{R_{\bar{u}}}) \in \mathcal{R},$$

associated with the graph form (10.18). Finally, as in Remark 5.1.2 the Dirac when setting $x_e = (x_f, x_c)$, with $x_f = x, x_c^+ = x^+(\bar{u}), x_c = x_f^+ = x^+(0)$ the dynamics over $\mathcal{X}_e$ adopts the augmented state-space representation of the form (4.1), that is

$$x_e^+ - x_e = (J_e(x_e) - R_e(x_e))\nabla H|_{x_e}^{x_e^+}$$

with augmented skew symmetric and resistive matrices

$$J_e(x_e) = \begin{pmatrix} 0 & J_\star & 0 & 0 \\ -J_\star & 0 & 0 & 0 \\ 0 & 0 & 0 & 0 \\ 0 & 0 & 0 & 0 \end{pmatrix}, \quad R_e(x_e) = \begin{pmatrix} R_{\star 1} & 0 & 0 & 0 \\ 0 & R_{\star 2} & 0 & 0 \\ 0 & 0 & \kappa b_1^\delta b_1^\delta & \kappa b_1^\delta b_2^\delta \\ 0 & 0 & \kappa b_1^\delta b_2^\delta & \kappa b_2^\delta b_2^\delta \end{pmatrix}$$

and augmented discrete gradient function

$$\nabla H|_{x_e}^{x_e^+} = (\bar{\nabla} H|_{x_f}^{x_f^+}, \bar{\nabla} H|_{x_c}^{x_c^+})^\top = (\bar{\nabla} H|_{x_1}^{x_1^+}, \bar{\nabla} H|_{x_2}^{x_2^+}, \bar{\nabla} H|_{x_1^+}^{x_1^+(u)}, \bar{\nabla} H|_{x_2^+}^{x_2^+(u)})^\top.$$

10.4 Discrete IDA-PBC design

As discussed in Section 9.4, a digital passivity-based feedback which stabilizes the system at a desired equilibrium point (different from the initial one) assigning a suitable Hamiltonian function $H_d(\cdot)$, can be designed. In this regards, the RLC circuit can be stabilized at the desired equilibrium point

$$x_\star = \begin{pmatrix} \bar{q} \\ 0 \end{pmatrix}$$

with desired Hamiltonian function

$$H_d(x) = \frac{1}{2}(x - x_\star)^\top P_d (x - x_\star) \tag{10.19}$$

with positive definite matrix P_d. The stabilization problem is addressed through discrete-time IDA-PBC as in Theorem 6.3.1, once properly selected the matrices $J_a^\delta, R_a^\delta, P_a$ so that the following matching condition is satisfied

$$B^{\delta\perp}[(\mathcal{J}_a^\delta - \mathcal{R}_a^\delta)P - (\mathcal{S}_J^\delta + \mathcal{J}_a^\delta - \mathcal{R}_a^\delta)P_a] = 0$$

with left-hand side annihilator $B^{\delta\perp}$ of the sampled-data input vector B^δ, that is

$$B^{\delta\perp} = \alpha \begin{pmatrix} \sin(\delta) & \cos(\delta) - 1. \end{pmatrix}$$

Assuming the sampled-data target interconnection matrix unchanged ($\mathcal{J}_a^\delta = 0$), and the target equilibrium $x_\star = \mathrm{col}(\bar{q}, 0)$, then it can be assigned to (10.11) by setting the matrices

$$P_a = \begin{pmatrix} 0 & 0 \\ 0 & \tilde{N} \end{pmatrix},$$

$$\mathcal{R}_a^\delta = \begin{pmatrix} 1 - \cos(\delta) & \sin(\delta) \\ \sin(\delta) & 1 + \cos(\delta) - \frac{\tilde{N}}{\tilde{N}+1} \end{pmatrix}$$

where $\tilde{N} \in \mathbb{R}$ is freely chosen so to guarantee $P_d \succ 0$. As seen in Theorem 6.3.1, the sampled-data IDA-PBC control is the solution to the implicit equation

$$\bar{u} = \frac{1}{2} B^{\delta\dagger} \left[(\mathcal{S}_J^\delta - \mathcal{R}_a^\delta) P_d (x^+(\bar{u}) + x - 2x_\star) - \mathcal{S}_J^\delta P (x^+ + x) \right]. \tag{10.20}$$

Equivalently, setting the state matrix

$$A^\delta = \begin{pmatrix} \cos(\delta) & \sin(\delta) \\ -\sin(\delta) & \cos(\delta) \end{pmatrix}$$

the IDA-PBC control can be explicitly described as

$$\bar{u} = B^{\delta\top} [(A_d^\delta - A^\delta) x + A_{d,\star}^\delta x_\star] \tag{10.21}$$

so getting the explicit sampled-data closed-loop system

$$x^+(\bar{u}) = x + A_d^\delta x + A_{d,\star}^\delta x_\star$$

with assigned dynamical matrices

$$\begin{aligned} A_d^\delta &= (I - \frac{1}{2}(\mathcal{S}_J^\delta - \mathcal{R}_a^\delta) P_d)^{-1} (I + \frac{1}{2}(\mathcal{S}_J^\delta - \mathcal{R}_a^\delta) P_d) \\ &= \begin{pmatrix} \frac{(\tilde{N}+4)\cos^2(\delta) + (3\tilde{N}+9)\cos(\delta) + 3}{3\tilde{N}\cos^2(\delta) + (\tilde{N}+7)\cos(\delta) + 9} & -\frac{(2+2\tilde{N})\sin(2\delta)}{3\tilde{N}\cos^2(\delta) + (\tilde{N}+7)\cos(\delta) + 9} \\ -\frac{4\sin(\delta)(\cos(\delta)+2)}{3\tilde{N}\cos^2(\delta) + (\tilde{N}+7)\cos(\delta) + 9} & \frac{(1-\tilde{N})\cos(\delta) + 3 - (3\tilde{N}+4)\cos^2(\delta)}{3\tilde{N}\cos^2(\delta) + (\tilde{N}+7)\cos(\delta) + 9} \end{pmatrix}, \end{aligned}$$

$$\begin{aligned} A_{d,\star}^\delta &= -(I - \frac{1}{2}(\mathcal{S}_J^\delta - \mathcal{R}_a^\delta) P_d)^{-1} (\mathcal{S}_J^\delta - \mathcal{R}_a^\delta) P_d \\ &= \begin{pmatrix} \frac{(2\tilde{N}-4)\cos^2(\delta) - (2\tilde{N}+2)\cos(\delta) + 6}{3\tilde{N}\cos^2(\delta) + (\tilde{N}+7)\cos(\delta) + 9} & \frac{(4+4\tilde{N})\sin(\delta)\cos(\delta)}{3\tilde{N}\cos^2(\delta) + (\tilde{N}+7)\cos(\delta) + 9} \\ \frac{4\sin(\delta)(\cos(\delta)+2)}{3\tilde{N}\cos^2(\delta) + (\tilde{N}+7)\cos(\delta) + 9} & \frac{(6\tilde{N}+4)\cos^2(\delta) + (2\tilde{N}+6)\cos(\delta) + 6}{3\tilde{N}\cos^2(\delta) + (\tilde{N}+7)\cos(\delta) + 9} \end{pmatrix}. \end{aligned}$$

Accordingly, the piece-wise feedback control in (10.20) is explicitly given, for $t \in [k\delta, (k+1)\delta[,\ k \in \mathbb{N}$, by the expression

$$\begin{aligned} u = & \frac{2(1-\cos(\delta))}{3\tilde{N}\cos^2(\delta) + (\tilde{N}+7)\cos(\delta) + 9} \Big[(4\tilde{N}\bar{q} - 4x_1 - 10\bar{q})\cos^2(\delta) - 5x_2 \sin(2\delta) \\ & + (4\tilde{N}x_1 - 2\tilde{N}\bar{q} - 4\bar{q})\cos(\delta) + 14\bar{q} + 4x_1 + 2\tilde{N}x_2 \sin^3(\delta) \\ & - (2\tilde{N}x_2 + 6x_2)\sin(\delta) - 3\tilde{N}x_2 \sin(2\delta) - (2\tilde{N}\bar{q} + 4\tilde{N}x_1)\cos^3(\delta) \Big]. \end{aligned}$$

The proposed solution is based on a direct discrete-digital design and differs from the digital solution given in Aoues et al. (2015a, 2013); Sümer and Yalçın (2011) as our digital controller requires constructive matrices $\mathcal{R}_a^\delta$ and P_a induced by the annihilator $B^{\delta\perp}$. The model proposed in Aoues et al. (2015a, 2013); Sümer and Yalçın (2011) strictly relies upon an emulated-like design which assigns the discrete-time model with the same R_d and J_d of the continuous-time design, namely u is the solution of the following equality

$$(J(x) - R(x))\bar{\nabla}H|_x^{x^+(u)} + Bu = (J_d(x) - R_d(x))\bar{\nabla}H_d|_x^{x^+(u)}. \tag{10.22}$$

The benefits of the proposed direct digital design with respect to the literature is illustrated by means of simulations.

Simulations

The comparison between the proposed control (10.21) and the one given in the literature as solution to (10.22) is given 10.8 and 10.9. Setting $\bar{q} = 2$, $\tilde{N} = 0$, and initial condition $x_0 = col(20, 10)$, Figure 10.8 shows that both the proposed control and the literature control, for $\delta = 1$, stabilize the closed-loop RLC system at the desired equilibrium point but with different performances. The literature control is much closer to the continuous-time trajectories even though the proposed model shows, in Figure 10.8(b), a faster decreasing of the Hamiltonian function. However, the improvement of the proposed controller is much evident in Figure 10.9 where a sampling period of length $\delta = 2.5$ has been considered. For a grater sampling period the literature controller induces an instability of the closed-loop system since the design is based on an approximate sampled-data model, while the proposed model still guarantees asymptotic stability of the desired equilibrium point with again much nicer energy properties.

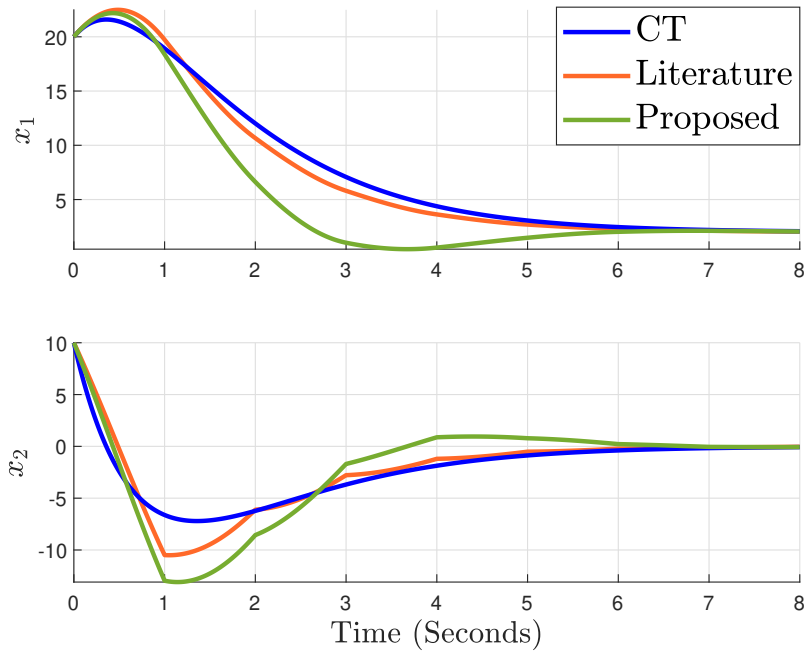

(a) State trajectories

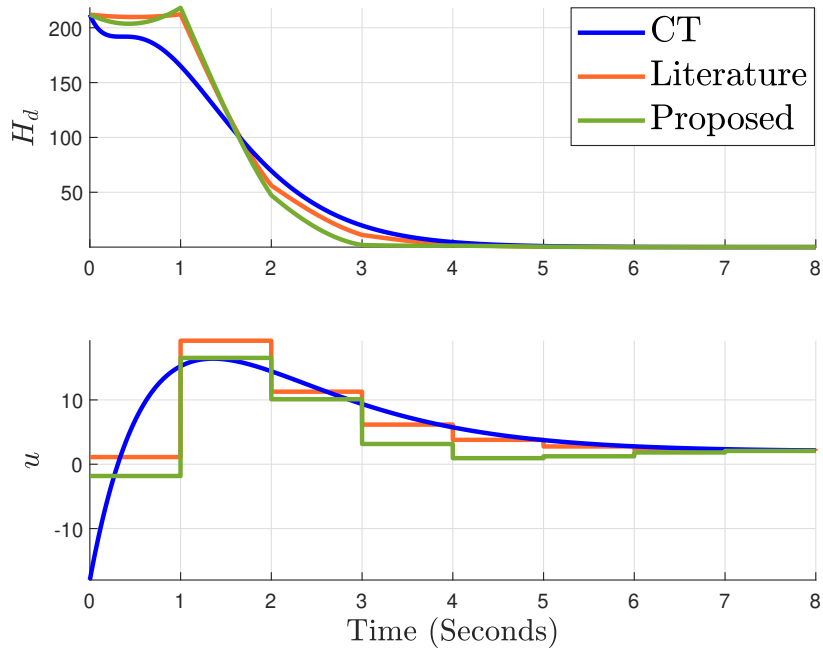

(b) Control and Hamiltonian function

Figure 10.8: Digital IDA-PBC control for the RLC model with $\delta = 1$

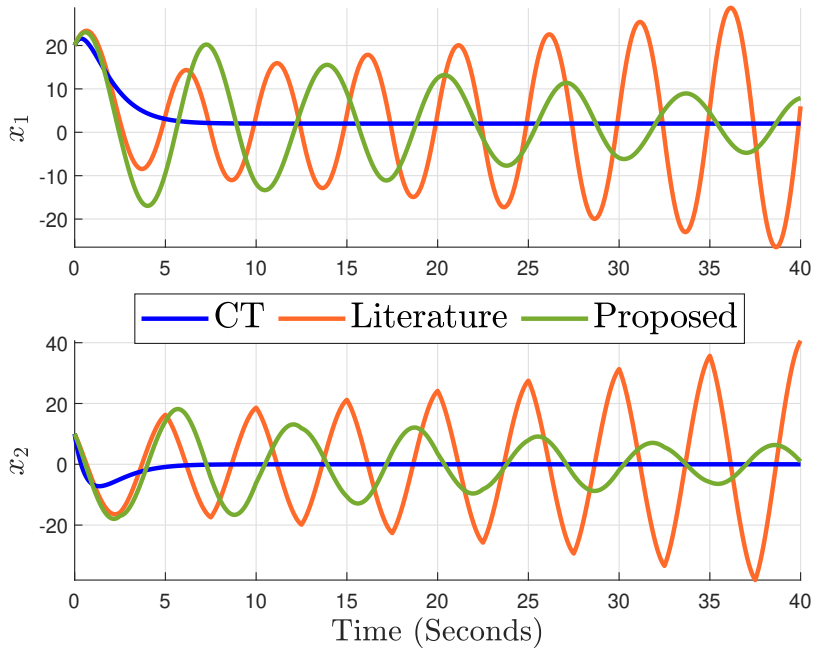

(a) State trajectories

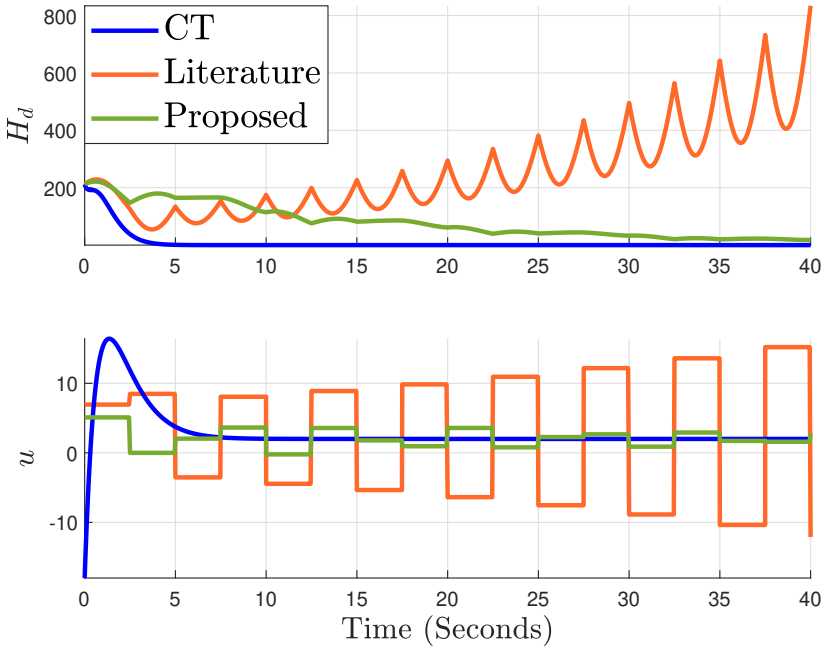

(b) Control and Hamiltonian function

Figure 10.9: Digital IDA-PBC control for the RLC model $\delta = 2.5$

Chapter 11

The Gravity Pendulum

Contents

11.1 Continuous-time modeling **232**

11.2 Sampled-data modeling **233**

11.3 Damping feedback design **242**

11.4 Energy-based digital stabilization **250**

In this case study we consider the sampled-data design and the digital stabilization of the gravity pendulum system. A sketch of its mechanical representation is given in Figure 11.1. This case study represents one of the most studied mechanical systems and is used here to illustrate how a nonlinear port-Hamiltonian system associated with a quadratic and separable Hamiltonian function can be modeled and controlled under sampling. The example is interesting because, even though the discrete gradient can be exactly computed, the nonlinearity of the dynamics makes difficult the computation of an exact sampled-data port-Hamiltonian model so that approximations are performed. More in detail, three aspects are illustrated:

1. approximate sampled-data port-Hamiltonian models are computed truncation the series expansion describing the exact solutions as detailed in Section 7.4;

2. stabilization at the origin is achieved via digital negative output feedback based on the average output discussed in Section 8.1;

3. stabilization at a desired equilibrium point is illustrated via sampled-data IDA-PBC based on input-Hamiltonian-matching (IH_dM) discussed

in Section 8.2.

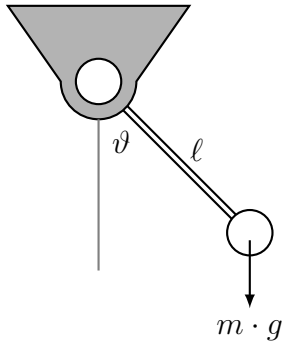

Figure 11.1: Simple Gravity Pendulum

11.1 Continuous-time modeling

The gravity pendulum system consists of a mass hanging from a string attached at a pivot so that it can swing freely. Ideally, when the mass is displaced sideways from one of its equilibrium points (one stable, and one unstable), it is affected by the gravity force which accelerates the mass with an oscillatory motion towards its stable equilibrium point. In this case study the gravity pendulum is a massless string ℓ to which a bob of mass m is attached. The position of the mass is described by the angle θ of the string makes with the vertical axis. The pendulum is affected by a downward gravitational force mg, where g denotes the acceleration due to gravity.

The Hamiltonian function catching respectively the kinetic and the potential energy of the gravity pendulum, is described by the function

Parameter	**Description**	**Units**
ϑ	Pendulum angle	rad
m	Bob mass	kg
l	String length	m
g	gravity constant	$\mathrm{m{\cdot}s^{-2}}$

Table 11.1: Gravity pendulum parameters

$$H(\vartheta, \dot{\vartheta}) = \frac{m\ell^2}{2}\dot{\vartheta}^2 + mg\ell(1 - \cos(\vartheta)). \tag{11.1}$$

Due to the Newton's second law, the dynamics of the pendulum is described by the equation of motion in its tangential direction

$$ml^2\ddot{\vartheta} + r\dot{\vartheta} + mg\ell\sin(\vartheta) = u,$$

where u is the torque injected into the dynamics, $m\ell^2$ describes the moment of inertia associated with the pendulum, and $r = b\ell^2$ defines the damping force acting onto the system with coefficient of friction b. Notably, the damping force is used to represent friction at the pivot and/or air resistance.

Setting the generalized coordinates, position and momentum, as $x_1 = \vartheta$ and $x_2 = m\ell^2\dot{\vartheta}$, the continuous-time dynamics of the gravity pendulum can be represented as a two dimensional port-Hamiltonian system of the form

$$\begin{pmatrix} \dot{x}_1 \\ \dot{x}_2 \end{pmatrix} = \begin{pmatrix} 0 & 1 \\ -1 & -r \end{pmatrix} \nabla H(x_1, x_2) + \begin{pmatrix} 0 \\ 1 \end{pmatrix} u \tag{11.2a}$$

$$y = \frac{1}{ml^2} x_2 \tag{11.2b}$$

It is clear from the model that the system (11.2a) has equilibrium points coinciding respectively with $(x_{1\star}, x_{2\star}) = (0, 0)$ and $(x_{1\star}, x_{2\star}) = (\pi, 0)$. However, applying the Lyapunov Theorem one notices that only $(0, 0)$ is a stable equilibrium point for the system in free evolution when $r > 0$. More in general, the gravity pendulum is intuitively stable in its downward position and unstable in its upward position, for all $r \geq 0$.

11.2 Sampled-data modeling

We are interested in the design of the sampled-data port-Hamiltonian representation of the gravity pendulum described by the equations (11.2a) when the control input is set as $u = 0$. For notational simplicity, in the model below the mass and the string

are assumed such that $m\ell^2 = 1$ and $mg\ell = 1$, so that the Hamiltonian function (11.1) reduces as

$$H(x_1, x_2) = \frac{1}{2}x_2^2 + (1 - \cos(x_1)). \tag{11.3}$$

The sampled-data model is based on Theorem 7.4.1. To begin with, let define the sampled equivalent dynamics as a sampled-data port-Hamiltonian dynamics of the form

$$x^+ = x + \delta \mathcal{S}^\delta_{J-R}(f, x)\bar{\nabla} H|_x^{x^+}, \tag{11.4a}$$

describing the sampled version of (11.2a) in the uncontrolled case, where $x := x(k\delta)$ is the state and $x^+ := x((k+1)\delta)$ is the one-step ahead of the uncontrolled evolution when $u = 0$. For the gravity pendulum system, the discrete gradient $\bar{\nabla} H|_x^{x^+}$ and the discrete Jacobian $\bar{J}[\nabla H]|_x^{x^+}$ can be exactly computed as

$$\bar{\nabla} H|_x^{x^+} = \begin{pmatrix} -\frac{\cos(x_1^+) - \cos(x_1)}{x_1^+ - x_1} \\ \frac{x_2^+ + x_2}{2} \end{pmatrix}, \tag{11.5a}$$

$$\bar{J}[\nabla H]|_x^{x^+} = \begin{pmatrix} \frac{\sin(x_1^+) - \sin(x_1)}{x_1^+ - x_1} & 0 \\ 0 & 1 \end{pmatrix}. \tag{11.5b}$$

The sampled-data matrix $\mathcal{S}^\delta_{J-R}(f, x)$ characterizing the port-Hamiltonian dynamics, and describing both the sampled-data interconnection and dissipation part, is given in Theorem 7.4.1 as

$$\mathcal{S}^\delta_{J-R}(f, x) = \mathcal{M}(\delta, f, x)(J(x) - R(x)) \left(I + \delta \mathcal{Q}(\delta, H, f, x)(J(x) - R(x))\right)^{-1},$$

with matrices $\mathcal{M}(\delta, f, x)$ and $\mathcal{Q}(\delta, H, f, x)$ respectively given in Lemma 7.1.1 and Lemma 7.1.4. Closed forms of the matrix $\mathcal{S}^\delta_{J-R}(f, x)$ cannot be computed in practice, however it can be characterized exploiting the corresponding series expansion in power of δ given in (7.16) as

$$\mathcal{S}^\delta_{J-R}(f, x) = \sum_{i \geq 0} \frac{\delta^i}{(i+1)!} (\mathcal{S}_{J-R})_i(x).$$

Accordingly, from the expression above and following the expression (7.18) one computes the first terms as

$$(\mathcal{S}_{J-R})_0 = \begin{pmatrix} 0 & 1 \\ -1 & -r \end{pmatrix}, \tag{11.6a}$$

$$(\mathcal{S}_{J-R})_1 = \begin{pmatrix} 0 & 0 \\ 0 & 0 \end{pmatrix}, \tag{11.6b}$$

$$(\mathcal{S}_{J-R})_2(x) = \frac{1}{2}\begin{pmatrix} -r & \cos(x_1) - r^2 \\ r^2 - \cos(x_1) & r^3 - r\cos(x_1) \end{pmatrix}, \tag{11.6c}$$

which yield the approximate sampled-data port-Hamiltonian dynamics in Theorem 7.4.1 of the form

$$x^+ = x + \delta(\mathcal{S}_{J-R})_0 \bar{\nabla} H|_x^{x^+} + \frac{\delta^3}{3!}(\mathcal{S}_{J-R})_2(x)\bar{\nabla} H|_x^{x^+} + O(\delta^4) \tag{11.7}$$

that is given precisely by,

$$\begin{pmatrix} x_1^+ \\ x_2^+ \end{pmatrix} = \begin{pmatrix} x_1 \\ x_2 \end{pmatrix} + \begin{pmatrix} -\frac{\delta^3}{3!2} r & \delta + \frac{\delta^3}{3!2}(\cos(x_1) - r^2) \\ -\delta + \frac{\delta^3}{3!2}(\cos(x_1) - r^2) & \frac{\delta^3}{3!2} r^3 - \delta r - \frac{\delta^3}{3!} r\cos(x_1) \end{pmatrix} \begin{pmatrix} \frac{\cos(x_1^+) - \cos(x_1)}{x_1 - x_1^+} \\ \frac{x_2^+ + x_2}{2} \end{pmatrix} + O(\delta^4).$$

The approximate sampled-data model above is dissipative with respect to the Hamiltonian function (11.3) through the dissipative part, $\mathcal{R}(\delta, x) = \frac{1}{2}(\mathcal{S}_{J-R}^{\delta}(f, x) + \mathcal{S}_{J-R}^{\delta\top}(f, x))$, namely

$$\mathcal{R}(\delta, x) = \begin{pmatrix} \frac{\delta^2}{3!2} r & 0 \\ 0 & r - \frac{\delta^2}{3!2} r^3 + \frac{\delta^2}{3!} r\cos(x_1) \end{pmatrix} + O(\delta^3).$$

Therefore, computing the energy variation of the Hamiltonian function along the approximate port-Hamiltonian dynamics (11.7), one gets

$$\begin{aligned} H(x^+) - H(x) =& -\delta \bar{\nabla}^\top H|_x^{x^+} \mathcal{R}(\delta, x) \bar{\nabla} H|_x^{x^+} \\ =& -\frac{\delta}{4} r (x_2^+ + x_2)^2 - \frac{\delta^3}{3!2} r \frac{(\cos(x_1^+) - \cos(x_1))^2}{(x_1 - x_1^+)^2} \\ & - \frac{\delta^3}{3!4} r (\cos(x_1) - \frac{1}{2} r^2)(x_2^+ + x_2)^2 + O(\delta^4) \leq 0. \end{aligned}$$

Alternatively, in the conservative case, namely when the pendulum is not affected by any internal friction force and the damping term is zeroed ($r = 0$), the sampled-data dissipation matrix is null, that is $\mathcal{R}(\delta, f, x) = 0$ as in Chapter 7. Accordingly, the sampled-data port-Hamiltonian dynamics is characterized by the skew-symmetric matrix $\mathcal{S}_J^\delta(f, x)$ only which can be computed through its series expansion in power of δ given in (7.16) as

$$\mathcal{S}_J^\delta(f, x) = \sum_{i \geq 0} \frac{\delta^i}{(i+1)!} (\mathcal{S}_J)_i(x)$$

with for the first terms

$$(\mathcal{S}_J)_0 = \begin{pmatrix} 0 & 1 \\ -1 & 0 \end{pmatrix}$$
$$(\mathcal{S}_J)_1 = \begin{pmatrix} 0 & 0 \\ 0 & 0 \end{pmatrix}$$
$$(\mathcal{S}_J)_2(x) = \begin{pmatrix} 0 & \frac{1}{2}\cos(x_1) \\ -\frac{1}{2}\cos(x_1) & 0 \end{pmatrix},$$

providing a conservative approximate sampled-data port-Hamiltonian dynamics with respect to the Hamiltonian function (11.3). The energy variation verifies conservation of energy $H(x^+) - H(x) = 0$ at all the sampling instants $t = k\delta$.

As already mentioned exact solutions cannot be computed. Thus approximations of the sampled-data model are defined by truncating the corresponding series expansion of $\mathcal{S}_{J-R}^\delta(f, x)$, as

$$\mathcal{S}_{J-R}^{[p]}(x) = \sum_{i=0}^{p} \frac{\delta^i}{(i+1)!} (\mathcal{S}_{J-R})_i(x) \tag{11.8}$$

at the desired order $p \geq 0$.

Remark 11.2.1. When truncating $\mathcal{S}_{J-R}^\delta(f, x)$ in $O(\delta^3)$, i.e. $p = 2$ in (11.8), we get that the energy variation is negative semidefinite if the sampling period δ verifies

$$\delta \in \left[0, \sqrt{\frac{12}{r^2 + 2}}\right].$$

Accordingly, the corresponding truncated model in $O(\delta^4)$ ensures dissipation of energy for any damping force $r > 0$.

When $p = 0$, keeping the interconnection sampled-data matrix equal to the continuous-time one, one recovers the literature model in Aoues et al. (2017) and Yalçin et al. (2015) which comes with the following sampled-data approximate representation,

$$\begin{aligned} x^+ &= x + \delta(J-R)\bar{\nabla}H|_x^{x^+} \\ &= \begin{pmatrix} x_1 \\ x_2 \end{pmatrix} + \delta \begin{pmatrix} 0 & 1 \\ -1 & -r \end{pmatrix} \begin{pmatrix} \frac{\cos(x_1^+)-\cos(x_1)}{x_1-x_1^+} \\ \frac{x_2^+ + x_2}{2} \end{pmatrix} \end{aligned} \tag{11.9}$$

that is deduced from the approximate Euler model when replacing the gradient $\nabla H(x)$ with the discrete gradient $\bar{\nabla}H|_x^{x^+}$.

Clearly, the approximate model (11.9) neglects additional terms of the series expansion defining the sampled-data matrix $(\mathcal{S}_{J-R})_i$. Those additional terms computed up to a desired order by using the methodology presented above improve the performances of the sampled-data model.

As a consequence of the approximation, even though the approximate model (11.9) is dissipative and verifies the energy variation (11.3), that is

$$H(x^+) - H(x) = -\frac{\delta}{4} r (x_2^+ + x_2)^2 \leq 0,$$

it does not match the continuous-time evolution of $H(\cdot)$.

Simulations

The implication and effectiveness of the proposed sampled-data model of the gravity pendulum system are reported in Figure 11.3, Figure 11.4 and Figure 11.2 where the approximate model at order $p = 2$ is compared with the one proposed in the literature, say $p = 0$.

Figure 11.3 and Figure 11.4 illustrate respectively the Mean Squared Error and the time evolution of the state trajectories and the Hamiltonian function of both the state x and Hamiltonian H in the damping case, with $r = 0.37$, and sampling period of length $\delta = \frac{\pi}{4}$. Clearly, the proposed model in (11.7) provides a better matching of the continuous-time trajectories and a better Hamiltonian evolution with respect to the literature model. Interestingly enough is the conservative case given in Figure 11.2 where the time evolutions of the state trajectories and the Mean Squared Error for the state x are reported. One notices that the proposed model yields a better

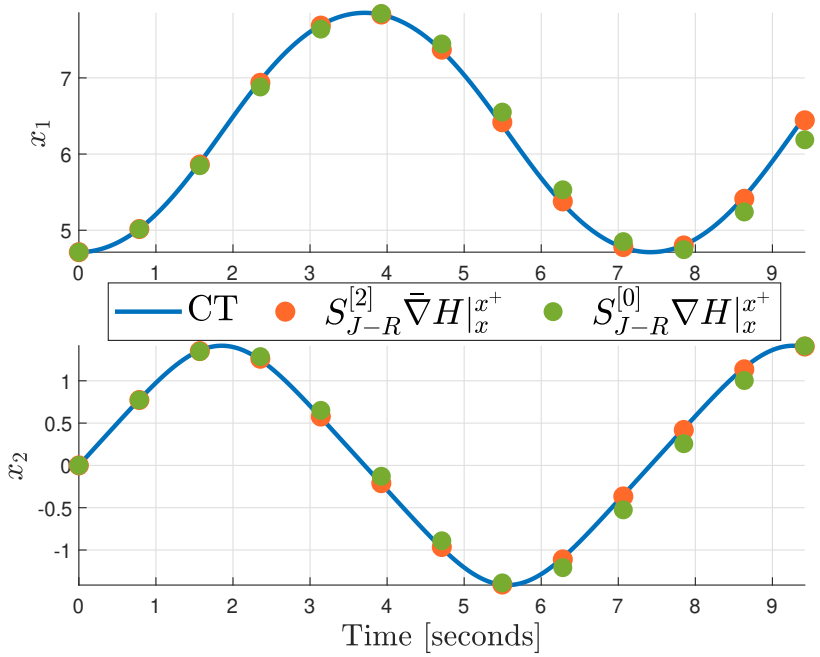

(a) State trajectories

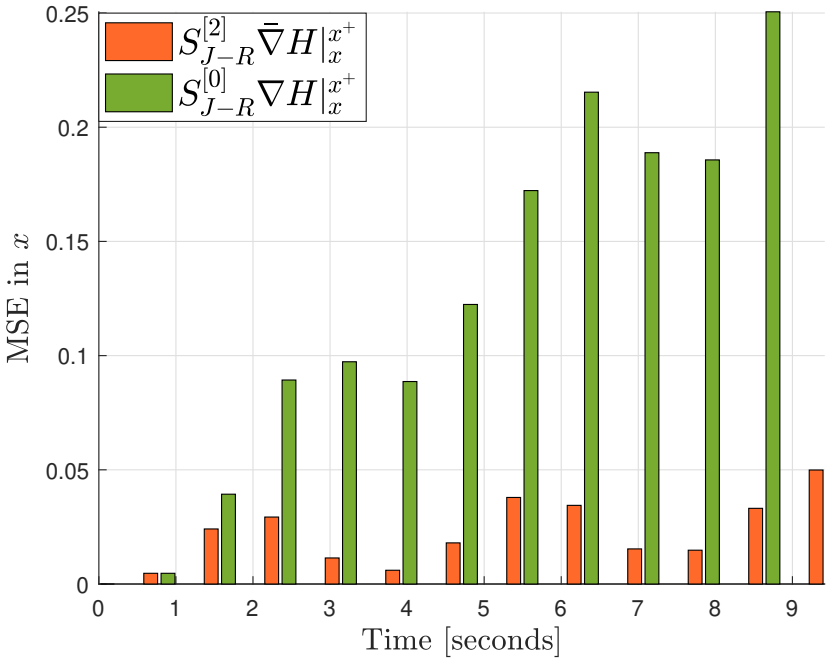

(b) Hamiltonian function

Figure 11.2: Sampled-data undamped gravity pendulum

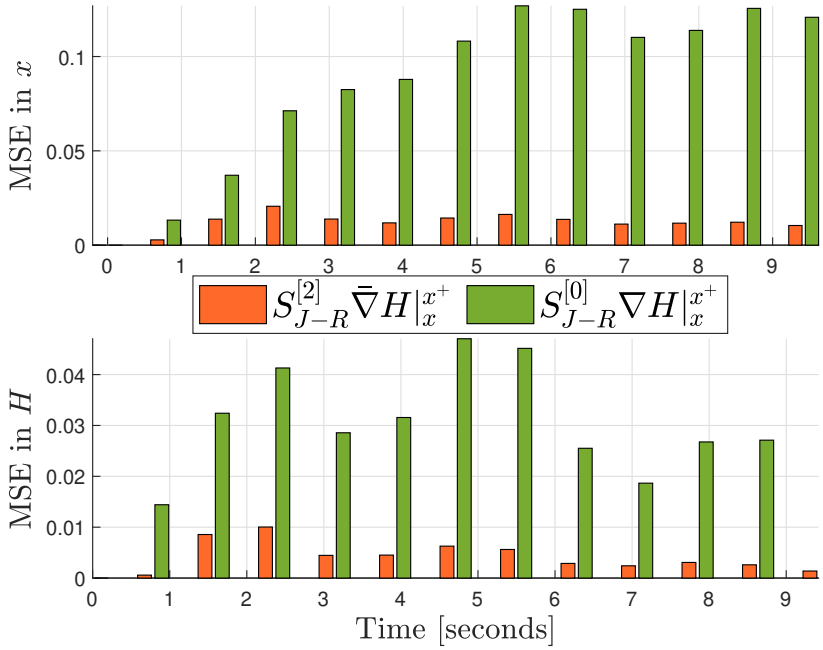

Figure 11.3: Sampled-data damped gravity pendulum: Mean Squared Error

approximation of the continuous-time system, showing preservation of the trajectories with a much small mismatch of the continuous-time trajectories than the literature model as reported in Figure 11.2. Note that, the proposed model achieves better performances than those of the literature with only one additional term into the approximate sampled-data dynamics.

Remark 11.2.2. In the simulations where the computation of an exact gradient is involved, to provide an exact solution to the implicit sampled-data port-Hamiltonian systems, both the implicit sampled-data models have been solved numerically through the numerical equation solver function *vpasolve* powered by MATLAB® and Symbolic Math Toolbox™. In particular, for both the proposed and literature models, we ask for any x to find x^+ as solution to (11.7) and (11.9) respectively.

Approximate solutions through approximate discrete gradient

In this part we provide approximate solutions of both the sampled-data matrix $\mathcal{S}^{\delta}_{J-R}(f,x)$ and the discrete gradient function $\bar{\nabla}H|^{x^+}_x$. In particular, in what follows we illustrate the relevancy of an approximation of $\mathcal{S}^{\delta}_{J-R}(f,x)$ and $\bar{\nabla}H|^{x^+}_x$ when

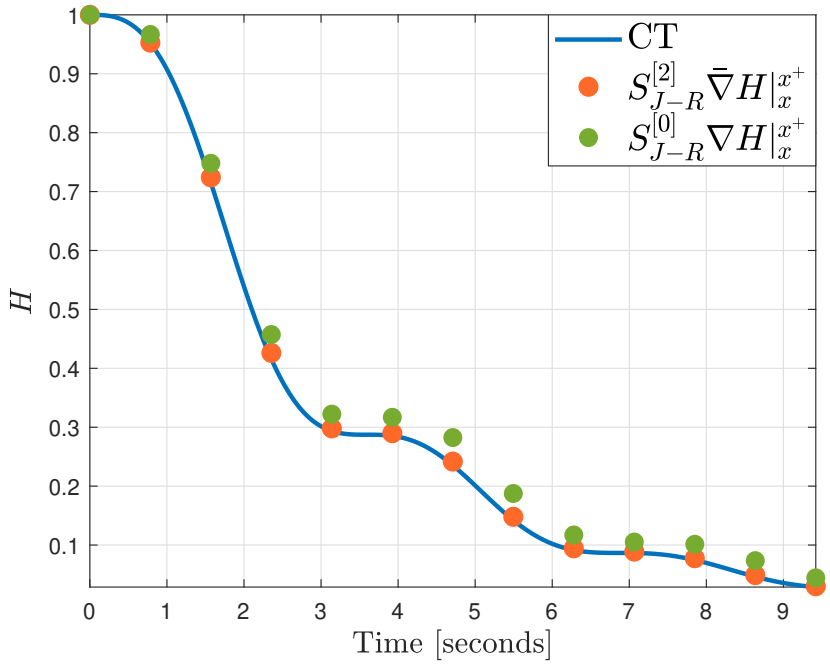

(a) Hamiltonian function

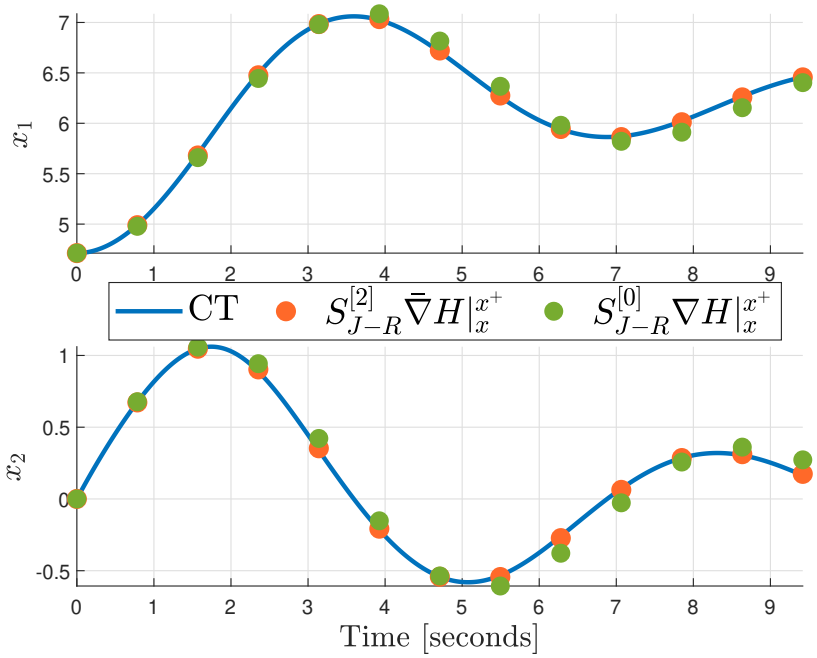

(b) State trajectories

Figure 11.4: Sampled-data damped gravity pendulum

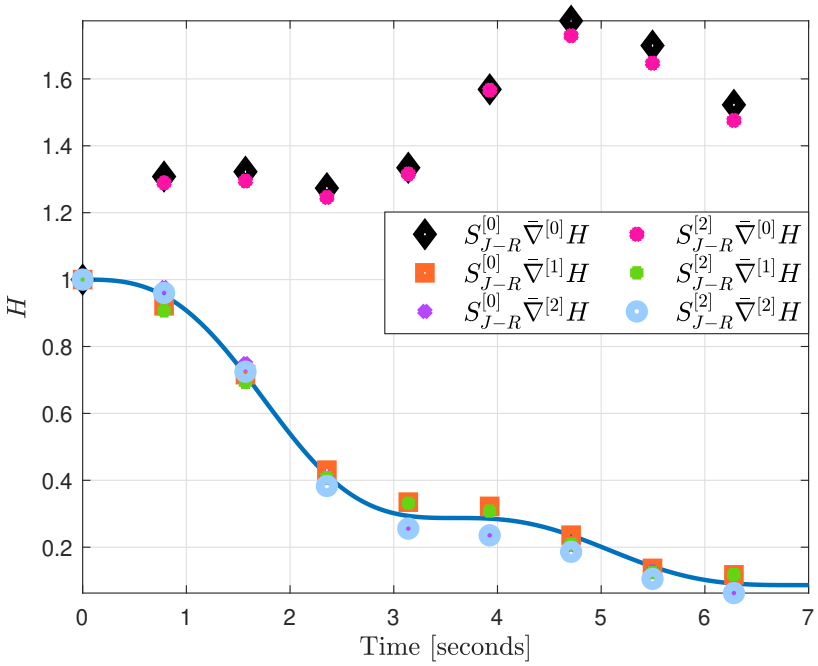

Figure 11.5: Comparison between different approximations of Sampled-data models: Hamiltonian function

computation of exact solutions are though or not feasible. Denoting by $\mathcal{S}^{[p]}_{J-R}(x)$ and $\bar{\nabla}^{[p]}H(x)$ as in (10.10), the truncation of the corresponding series expansions at any finite order, the sampled-data approximate dynamics are given by

$$x^+ = x + \delta \mathcal{S}^{[p_1]}_{J-R}(x)\bar{\nabla}^{[p_2]}H(x)$$

for $p_2, p_1 > 0$.

As already mentioned, the approximate sampled-data matrices for the gravity pendulum system are given by

$$\mathcal{S}^{[0]}_{J-R} = \begin{pmatrix} 0 & 1 \\ -1 & -r \end{pmatrix}$$

$$\mathcal{S}^{[2]}_{J-R}(x) = \mathcal{S}^{[0]}_{J-R} + \frac{\delta^2}{12}\begin{pmatrix} -r & (\cos(x_1) - r^2) \\ r^2 - \cos(x_1) & r^3 - r\cos(x_1) \end{pmatrix}$$

and approximate discrete gradient

$$\bar{\nabla}^{[0]}H = \begin{pmatrix} \sin(x_1) \\ x_2 \end{pmatrix}$$
$$\bar{\nabla}^{[1]}H = \bar{\nabla}^{[0]}H + \frac{\delta}{2}\begin{pmatrix} \cos(x_1)x_2 \\ -(\sin(x_1) + rx_2) \end{pmatrix}$$
$$\bar{\nabla}^{[2]}H = \bar{\nabla}^{[1]}H - \frac{\delta^2}{4}\begin{pmatrix} \frac{2}{3}\sin(x_1)x_2^2 + \cos(x_1)(\sin(x_1) + rx_2) \\ \cos(x_1)x_2 - r\sin(x_1) - r^2x_2 \end{pmatrix}.$$

Assuming different combinations for the approximate sampled-data model with $S_{J-R}^{[p_1]}(x)\bar{\nabla}^{[p_2]}H(x)$ for $p_1 = \{0, 2\}$ and $p_2 = \{0, 1, 2\}$, simulation are reported in Figure 11.5 and Figure 11.6 for dissipation $r = 0.37$ and sampling period $\delta = \frac{\pi}{4}$.

11.3 Damping feedback design

Let us focus the attention on the digital stabilization of the undamped gravity pendulum system. To achieve that purpose, consider the controlled gravity pendulum with input torque u and zero internal dissipation $r = 0$, yielding a conservative sampled-data equivalent model with the free-control part given by the approximate sampled-data model (11.7). In this case, the control action yields in practice a digital control which injects a piece-wise constant torque into the continuous-time gravity pendulum system, to provide asymptotic stability of the origin in case of zero internal dissipation.

According to the sampled-data port-Hamiltonian system, affected by a nonzero control action, presented in Theorem 7.28, the sampled-data equivalent model of the gravity pendulum system takes the form

$$x^+(u) = x + \delta((\mathcal{S}_{J-R})_0 + \frac{\delta^2}{2}(\mathcal{S}_{J-R})_2(x))\bar{\nabla}H|_x^{x^+} + \delta u g^\delta(x, u) \tag{11.10a}$$
$$Y_{\mathrm{av}}^\delta(x, u) = (g^\delta(x, u))^\top \bar{\nabla}H|_{x^+}^{x^+(u)} \tag{11.10b}$$

with $\mathcal{S}_0(x), \mathcal{S}_3(x)$ and $\bar{\nabla}H|_x^{x^+}$ respectively given in (11.6a) and (11.5a), controlled part

$$\delta g^\delta(x, u) = \begin{pmatrix} g_1^\delta(x) \\ g_2^\delta(x) \end{pmatrix} = \delta\begin{pmatrix} 0 \\ 1 \end{pmatrix} + \frac{\delta^2}{2}\begin{pmatrix} 1 \\ 0 \end{pmatrix} - \frac{\delta^3}{6}\begin{pmatrix} 0 \\ \cos x_1 \end{pmatrix} + O(\delta^4)$$

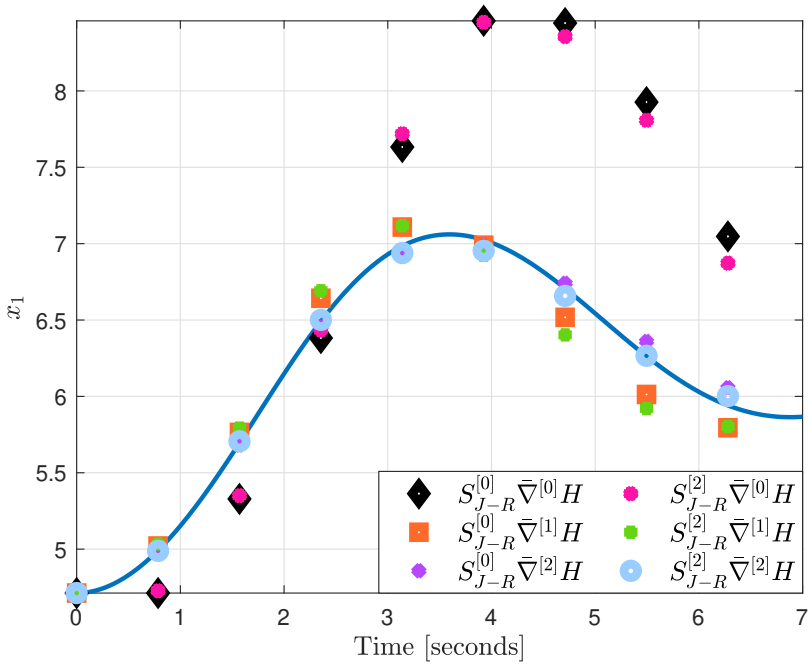

(a) Evolution of x_1

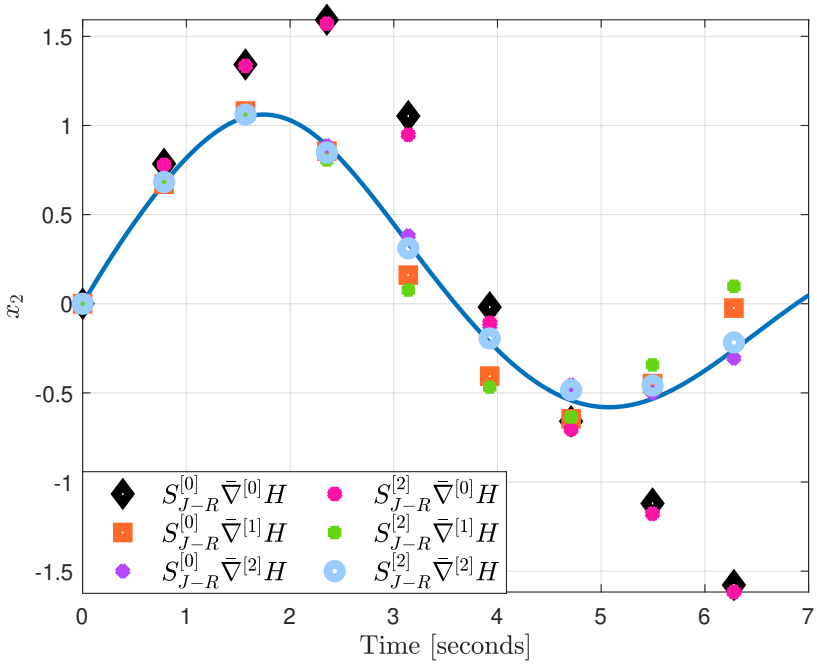

(b) Evolution of x_2

Figure 11.6: Comparison between different approximations of Sampled-data models

and exact discrete gradient between free dynamics x^+ and $x^+(u)$, that is

$$\bar{\nabla} H|_{x^+}^{x^+(u)} = \begin{pmatrix} \frac{\cos(x_1^+)-\cos(x_1^+(u))}{x_1^+(u)-x_1^+} \\ \frac{x_2^+(u)}{2} + \frac{x_2^+}{2} \end{pmatrix},$$

which yields as a series expansion in power of δ

$$\begin{aligned} \bar{\nabla} H|_{x^+}^{x^+(u)} &= \begin{pmatrix} -\frac{1}{ug_1^\delta(x,u)}(\cos(x_1^+)\cos(ug_1^\delta(x,u)) - \sin(x_1^+)\sin(ug_1^\delta(x,u)) - \cos(x_1^+)) \\ x_2^+ + \frac{1}{2}g_2^\delta(x,u)u \end{pmatrix} \\ &= \begin{pmatrix} \sin x_1 \\ x_2 \end{pmatrix} + \delta \begin{pmatrix} x_2 \cos x_1 \\ \frac{1}{2}u - \sin x_1 \end{pmatrix} + \frac{\delta^2}{2} \begin{pmatrix} -x_2^2 \sin x_1 - \cos x_1(\sin x_1 + \frac{1}{2}u) \\ -x_2 \cos x_1 \end{pmatrix} + O(\delta^3). \end{aligned}$$

Accordingly, the digital passivity-based feedback, in Theorem 8.1.1, which makes the origin asymptotically stable in closed loop, is given by the solution of the implicit damping equation

$$\begin{aligned} u &= -\kappa Y_{\text{av}}^\delta(x,u) = -\kappa(g^\delta(x,u))^\top \bar{\nabla} H|_{x^+}^{x^+(u)} \\ &= -\kappa(x_2 + \frac{\delta}{2}\sin x_1 - \frac{\delta^2}{6}x_2 \cos x_1 + \delta(\frac{1}{2}u - \sin x_1)) + O(\delta^3). \end{aligned} \tag{11.11}$$

Thus, setting the control as

$$u = \sum_{i \geq 0} \frac{\delta^i}{(i+1)!} u^i,$$

the implicit damping equality rewrites as

$$u^0 + \frac{\delta}{2}u^1 + \frac{\delta^2}{6}u^2 = -\kappa(x_2 + \frac{\delta}{2}\sin x_1 + \frac{\delta}{2}u^0 - \frac{\delta^2}{6}x_2 \cos x_1 + \frac{\delta^2}{4}u^1 - \delta \sin x_1) + O(\delta^3),$$

where one gets for the first terms

$$\begin{aligned} u^0 &= -\kappa x_2 \\ u^1 &= \kappa(\kappa x_2 + \sin x_1) \\ u^2 &= \kappa\Big(x_2 \cos(x_1) - \frac{3}{2}\kappa(\kappa x_2 + \sin x_1)\Big). \end{aligned}$$

Finally, the digital damping feedback, solution to (11.11), yields the following approximate control

$$\begin{aligned} u &= u^0 + \frac{\delta}{2}u^1 + \frac{\delta^2}{3!}u^2 + O(\delta^3) \\ &= -\kappa x_2 + \frac{\delta}{2}\kappa(\kappa x_2 + \sin x_1) + \frac{\delta^2}{6}\kappa\Big(x_2\cos(x_1) - \frac{3}{2}\kappa(\kappa x_2 + \sin x_1)\Big) + O(\delta^3) \end{aligned} \tag{11.12}$$

which makes the origin asymptotically stable in closed loop.

Simulations

The improvement achieved under digital damping performed over the proposed sampled-data port-Hamiltonian representation with respect to the usual feedback given in the literature Sümer and Yalçın (2011); Aoues et al. (2017) provided by the solution of

$$u_\ell = -\kappa B^\top \bar{\nabla} H|_x^{x^+(u_l)}$$

and approximately given by

$$u_\ell = -\kappa x_2 + \frac{\delta}{2}\kappa(\kappa x_2 + \sin(x_1)) + \frac{\delta^2}{4}\kappa\Big(x_2\cos x_1 - \kappa(\kappa x_2 + \sin x_1)\Big) + O(\delta^3),$$

are reported in Figure 11.7 with a sampling period of $\delta = \frac{\pi}{2}$ and in Figure 11.8 with $\delta = \frac{2}{3}\pi$, both with damping gain $\kappa = 1$.

The proposed feedback clearly achieves stabilization of the closed-loop system with better performances with respect to the approximate control u_ℓ of the literature. These improved performances are mainly due to the u-average output described in terms of the discrete gradient $\bar{\nabla} H|_{x^+}^{x^+(u)}$ between x^+ and $x^+(u)$.

Approximations of the implicit damping equation (11.11), can be alternatively computed numerically exploiting the exact discrete gradient and the approximate sampled-data dynamics (11.10) obtained by truncating $\mathcal{S}^\delta_{J-R}(f,x)$ and $g^\delta(x,u)$ at a desired order in δ. In particular, as suggested in the literature Sümer and Yalçın (2011); Aoues et al. (2017) one gets the approximate equation

$$u = -\kappa g^\top(x)\bar{\nabla} H|_{x^+}^{x^+(u)} = -\kappa\left(\frac{x_2^+(u)}{2} + \frac{x_2^+}{2}\right) \tag{11.13}$$

which is obtained setting $g^\delta(x,u) = col(0 \quad 1)$ and based on the deduced u-average output. The proposed control is discussed in Figure 11.9, with damping improvement

$\kappa = 1$ and sampling period of length $\delta = 2.75$ and compared with the damping output feedback proposed in the literature Aoues et al. (2017) of the form

$$u = -\kappa g^{\top}(x)\bar{\nabla}H|_{x}^{x^{+}(u)} = -\kappa\left(\frac{x_2^{+}(u)}{2} + \frac{x_2}{2}\right) \tag{11.14}$$

based on the standard literature passivating output. Both the equations (11.13) and (11.14) can be numerically solved through the numerical equation solver function *vpasolve* powered by MATLAB® and Symbolic Math Toolbox™.

Accordingly, the digital feedback laws deduced as the numerical solutions to (11.13) and (11.14) are compared by means of simulations to highlight the benefits of the proposed sampled-data port-Hamiltonian structure with respect to the one usually employed in the literature, even when solutions are not computed as series expansions in power of δ. In particular, the proposed feedback computed with the discrete gradient $\bar{\nabla}H|_{x^{+}}^{x^{+}(u)}$ in (11.13) stabilizes the closed-loop system and provides satisfactory energy evolution as shown in Figure 11.9(b), while the literature control (11.14) is not stabilizing the closed-loop system at the origin for a large sampling period of $\delta = 2.75$. This failure in the stabilization purpose is mainly due to the different discrete gradients involved in to the different sampled-data port-Hamiltonian forms employed for the design leading to the definition of two different passivating outputs.

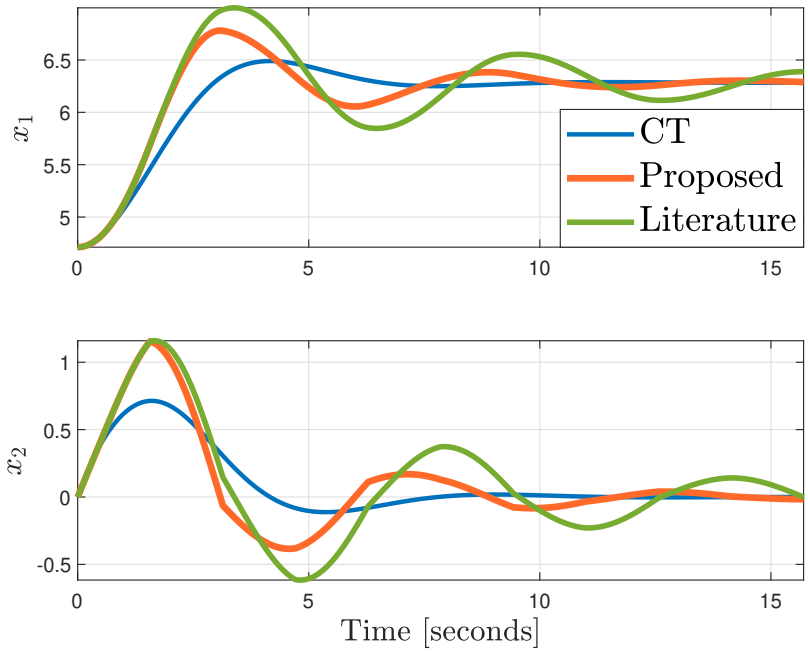

(a) State trajectories

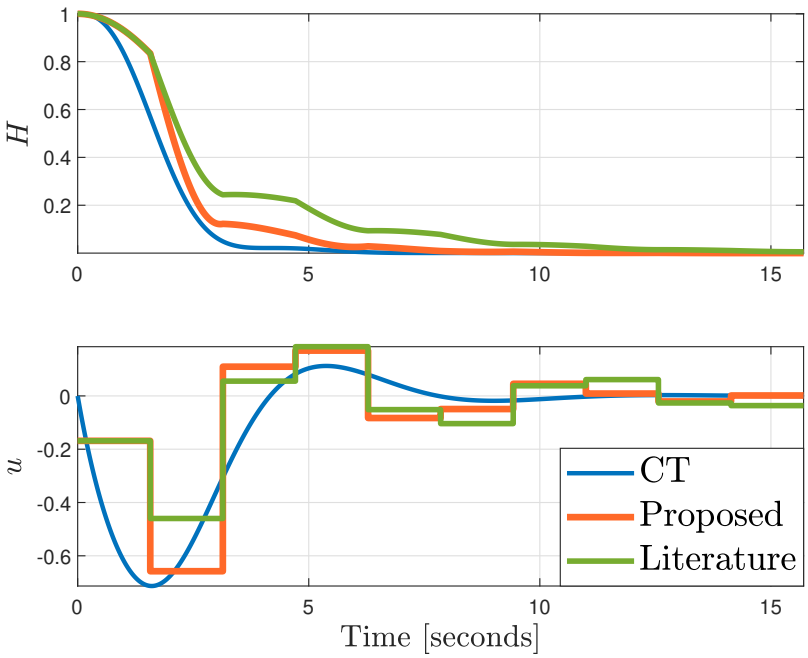

(b) Control and Hamiltonian function

Figure 11.7: Approximate digital damping control upon the sampled-data pendulum model with $\delta = \frac{\pi}{2}$

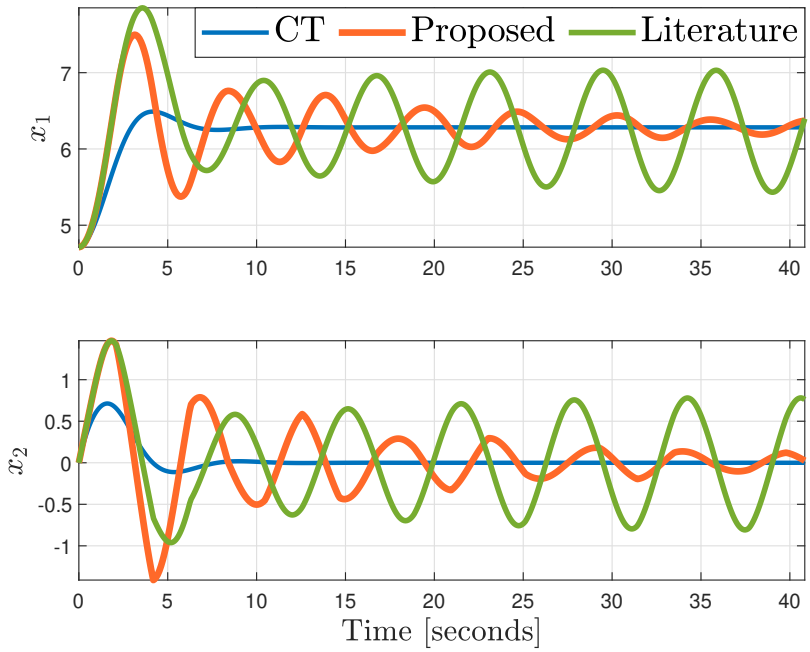

(a) State trajectories

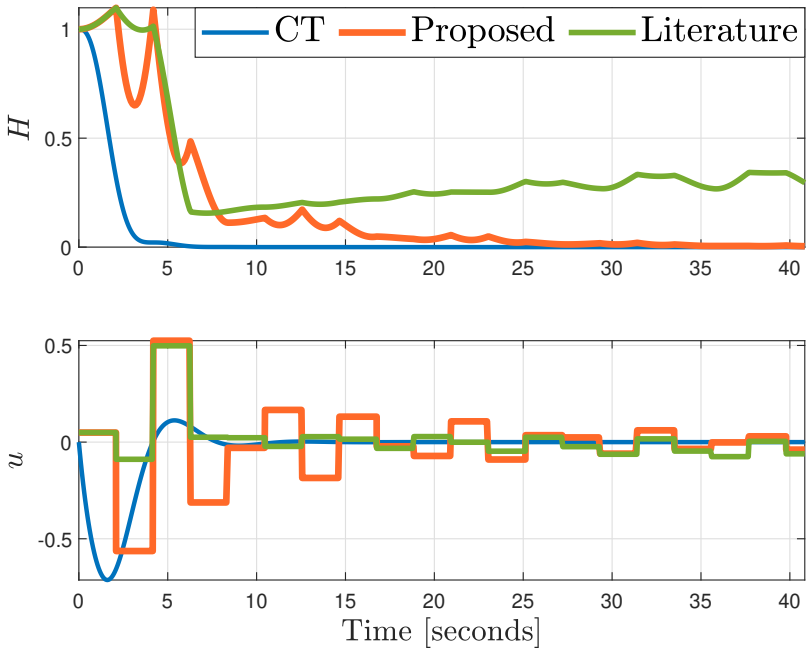

(b) Control and Hamiltonian function

Figure 11.8: Approximate digital damping control upon the sampled-data pendulum model with $\delta = \frac{2}{3}\pi$.

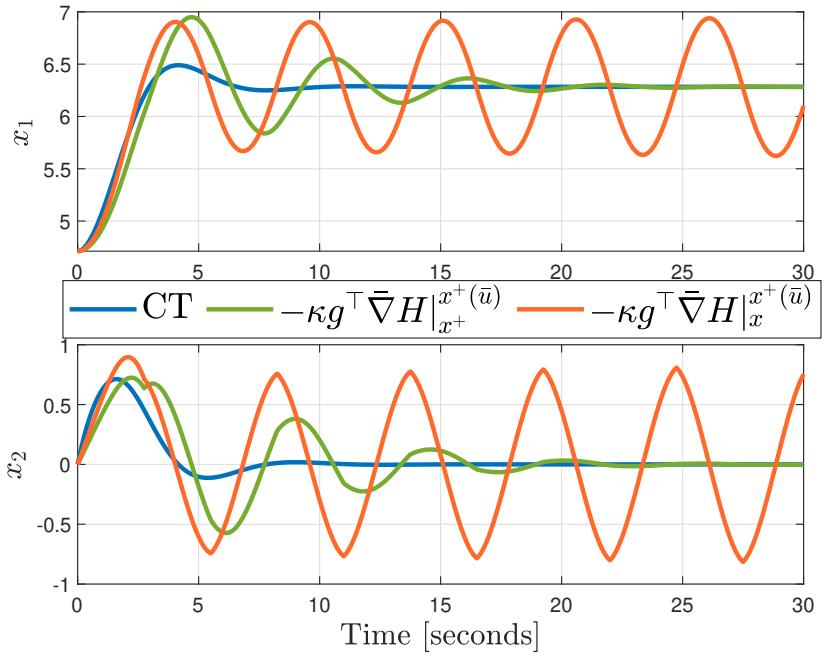

(a) State trajectories

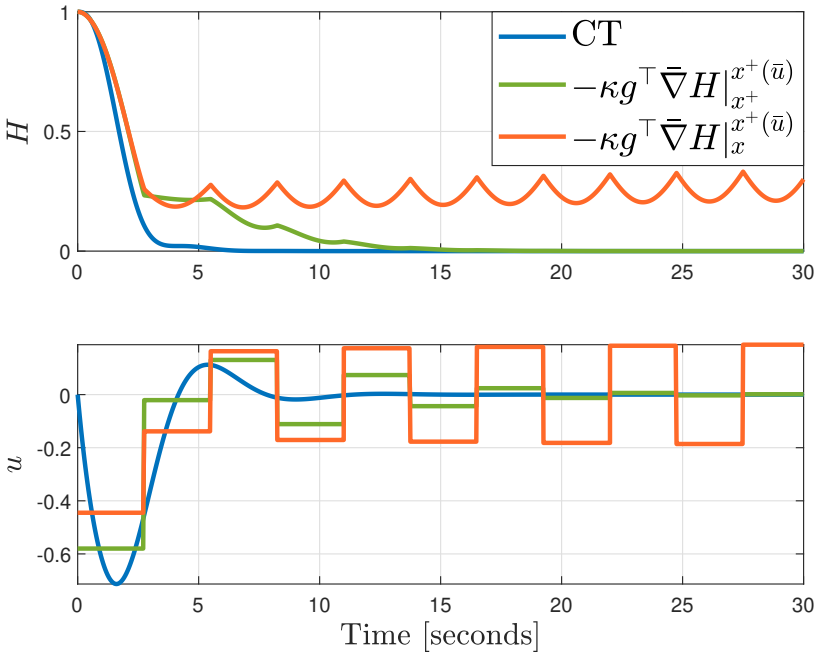

(b) Control and Hamiltonian function

Figure 11.9: Digital damping control with exact discrete gradient upon the sampled-data pendulum model

11.4 Energy-based digital stabilization

In this section the digital stabilization problem of the gravity pendulum is addressed exploiting the result in Theorem 8.2.1. The control purpose relies on the possibility of stabilizing the continuous-time gravity pendulum model (11.2a) at the desired equilibrium point, meaning at forcing the pendulum to keep a desired angular position ϑ. From the control perspective, the natural procedure to stabilize the gravity pendulum is by assigning a desired energy function, consisting of the kinetic and the potential functions, having a minimum at the desired equilibrium point. The most important step in the choice of the energy function is due to the selection of the potential energy function that should be assigned.

Continuous-time design

Consider the usual continuous-time gravity pendulum (11.2a) actuated by the torque u and assume that a desired equilibrium point

$$x_\star = col(x_{1\star}, 0)$$

is assigned to the closed-loop system. From the discussion given in Section 8.2, the continuous-time dynamics (11.2a) is feedback passive thorough the IDA-PBC feedback

$$u = \gamma(x) + v,$$

with

$$\gamma(x) = \sin(x_1) - \sin(x_1 - x_{1\star}), \tag{11.15}$$

making the closed-loop system

$$\begin{pmatrix} \dot{x}_1 \\ \dot{x}_2 \end{pmatrix} = \begin{pmatrix} 0 & 1 \\ -1 & -r \end{pmatrix} \nabla H_d + \begin{pmatrix} 0 \\ 1 \end{pmatrix} v,$$

with output $y = x_2$ passive with respect to the desired energy function

$$H_d(x) = \frac{1}{2}x_2^2 + (1 - \cos(x_1 - x_{1\star})) \tag{11.16}$$

having a minimum in $x_\star$. Thus, in the original coordinates, the new energy function $H_d(q, p)$ of the desired closed-loop system provides a shaped potential energy which

is characterized by the function $(1-\cos(\vartheta-\vartheta_\star))$ where $\vartheta_\star$ is the desired angular position of the pendulum. Furthermore, the Hamiltonian function $H_d(x)$ along the closed-loop dynamics verifies the inequality

$$\dot{H}_d(x) = -rx_2^2 + vy \leq vy.$$

Sampled-data design

As discussed in Section 3.5.2, the sampled equivalent model of the gravity pendulum (11.7) might be approximated in $O(\delta^3)$ by approximating the discrete gradient as follows

$$\bar{\nabla} H|_x^{x^+} = \begin{pmatrix} \sin(x_1) \\ x_2 \end{pmatrix} + \frac{\delta}{2} \begin{pmatrix} \cos(x_1)x_2 \\ -\sin(x_1) - rx_2 \end{pmatrix} + O(\delta^2)$$

which yields the following sampled-data dynamics in $O(\delta^3)$ given in the difference and differential representation

$$\begin{aligned} x^+ &= \begin{pmatrix} x_1 \\ x_2 \end{pmatrix} + \delta \begin{pmatrix} x_2 \\ -\sin(x_1) - rx_2 \end{pmatrix} + \frac{\delta^2}{2} \begin{pmatrix} -\sin(x_1) - rx_2 \\ r(\sin(x_1) + rx_2) - x_2\cos(x_1) \end{pmatrix} + O(\delta^3) \\ \frac{\partial x^+(u)}{\partial u} &= \delta \begin{pmatrix} 0 \\ 1 \end{pmatrix} + \frac{\delta^2}{2} \begin{pmatrix} 1 \\ -r \end{pmatrix} + O(\delta^3) \end{aligned}$$

which is equivalent to the approximate sampled-data dynamics in the form of a map

$$\begin{aligned} x^+(u) = \begin{pmatrix} x_1 \\ x_2 \end{pmatrix} &+ \delta \begin{pmatrix} x_2 \\ -\sin(x_1) - rx_2 \end{pmatrix} + \frac{\delta^2}{2} \begin{pmatrix} -\sin(x_1) - rx_2 \\ r(\sin(x_1) + rx_2) - x_2\cos(x_1) \end{pmatrix} \\ &+ \delta \begin{pmatrix} 0 \\ 1 \end{pmatrix} u + \frac{\delta^2}{2} \begin{pmatrix} 1 \\ -r \end{pmatrix} u + O(\delta^3) \end{aligned} \tag{11.17}$$

On the basis of Theorem 8.2.1, to digitally stabilize the continuous-time pendulum one computes the approximate digital control

$$u = \gamma^{\delta[1]}(x) + v, \tag{11.18}$$

with $\gamma^{\delta[1]}(x)$ in (3.45) specified as

$$\gamma^{\delta[1]}(x) = \gamma(x) + \frac{\delta}{2}\gamma^1(x) \tag{11.19}$$

and $\gamma^1(x) = \dot{\gamma}(x)$ taking the form

$$\gamma^1(x) = (\cos(x_1) - \cos(x_1 - x_{1\star}))x_2.$$

The physical interpretation of the approximate solution suggests that the digital control is a piecewise constant torque applied upon the pivot of the gravity pendulum, of the form

$$u = (\sin(\vartheta) - \sin(\vartheta - \vartheta_\star)) - \frac{\delta}{2}(\cos(\vartheta) - \cos(\vartheta - \vartheta_\star))\dot{\vartheta},$$

for all $t \in [k\delta, (k+1)\delta[$. Accordingly, the approximate sampled-data dynamics (11.17), with $v = 0$, achieves the second-order approximation of the port-Hamiltonian dynamics

$$x^+(\gamma^{\delta[1]}(x)) = x + \delta(\mathcal{S}^\delta_{J-R})_0 \bar{\nabla} H_d|_{x_k}^{x+F_d^\delta(x)} \tag{11.20}$$

along with the approximate vector field

$$F_d^{\delta[2]}(x) = \delta \begin{pmatrix} x_2 \\ -\sin(x_1 - x_{1\star}) - rx_2 \end{pmatrix} + \frac{\delta^2}{2} \begin{pmatrix} -\sin(x_1 - x_{1\star}) - rx_2 \\ r\sin(x_1 - x_{1\star}) + x_2(r^2 - \cos(x_1 - x_{1\star})) \end{pmatrix},$$

and approximated desired discrete gradient function

$$\bar{\nabla} H_d|_x^{x+F_d^{\delta[2]}(x)} = \begin{pmatrix} \sin(x_1 - x_{1\star}) \\ x_2 \end{pmatrix} + \frac{\delta}{2} \begin{pmatrix} \cos(x_1 - x_{1\star})x_2 \\ -\sin(x_1 - x_{1\star}) - rx_2 \end{pmatrix} + O(\delta^2).$$

For completeness, the sampled-data dynamics, at the sampling instants $k\delta$, is passive with storage function (11.16) and passifying output given by the expression

$$Y^\delta_{d_{\text{av}}}(\bar{u})(x, v) = x_2 + \frac{\delta}{2}(v - 2rx_2) + O(\delta^2).$$

Also in this case, the approximate passive output of the system is given physically in the original coordinates as

$$Y^\delta_{d_{\text{av}}}(\bar{u})(\vartheta, \dot{\vartheta}, v(k\delta)) = (1 - \delta r)\dot{\vartheta}((k\delta)) + \frac{\delta}{2}v((k\delta))$$

for all $t \in [k\delta, (k+1)\delta[$.

Roughly speaking, the approximate passive output in $O(\delta^2)$ is obtained by the measures of $\dot{\vartheta}(t)$ at the instant $t = k\delta$ and weighed by the proportional term $\delta(1-\delta r)$, plus the piecewise additional torque $\frac{\delta^2}{2}v(t)$. Accordingly, the closed-loop system under (11.18) verifies the dissipation inequality

$$H(x^+(u)) - H(x) \leq x_2 v + \frac{\delta}{2}(v^2 - 2rx_2 v) + O(\delta^2).$$

In addition, from Theorem 8.1.1 one computes the implicit damping equality

$$v = -\kappa x_2 - \frac{\delta}{2}(\kappa v - 2\kappa r x_2) + O(\delta^2),\ \kappa > 0$$

for all $t \in [k\delta, (k+1)\delta[$ which ensures convergence to a ball containing $x_\star$ of radius in $O(\delta^2)$. Then setting

$$v = \sum_{i\geq 0} \frac{\delta^i}{(i+1)!} v^i,$$

one obtains rewrites the implicit damping equality above as

$$v^0 + \frac{\delta}{2}v^1 = -\kappa x_2 - \frac{\delta}{2}(\kappa v^0 - 2\kappa r x_2) + O(\delta^2),\ \kappa > 0$$

so providing for the firsts terms

$$\begin{aligned} v^0 &= -\kappa x_2 \\ v^1 &= \kappa(\kappa + 2r)x_2. \end{aligned}$$

Simulations

Setting the desired equilibrium point $x_\star = col(\frac{\pi}{2}, 0)$, initial condition $x_0 = col(0, 0)$, and dissipation term $r = 0.37$, some illustrative simulations are considered in Figure 11.11, Figure 11.14, and Figure 11.12.

Figure 11.10, Figure 11.11, Figure 11.13, and Figure 11.14 compare the effect of the continuous-time feedback (11.15), the 0-order approximated feedback (that is the emulated feedback of (11.15)), namely

$$u^{\delta[0]} = \gamma^{\delta[0]} + v^{\delta[0]}$$

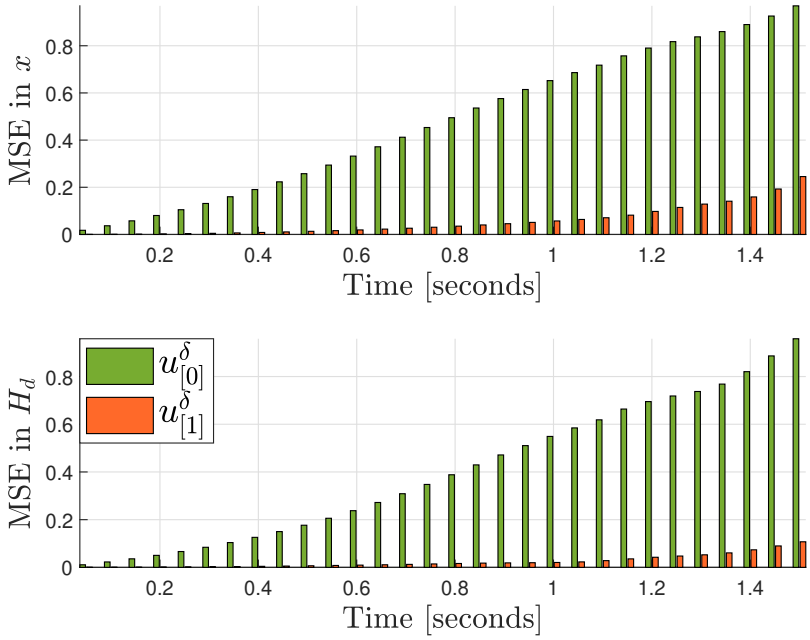

Figure 11.10: Energy-based stabilization for $\delta = 1$ and $\kappa = 0$: Mean Squared Error

and the 1st-order approximate control in (11.19)

$$u^{\delta[1]} = \gamma^{\delta[1]} + v^{\delta[1]}$$

with $v^{\delta[1]} = v^0 + \frac{\delta}{2}v^1$, applied to the pendulum system, respectively with damping injection $\kappa = 0$ and $\kappa = 0.1$. The purpose is to show their performance over the desired Hamiltonian function (11.16) and the closed-loop trajectories for a sampling interval of $\delta = 1s$. The Figure 11.11(b) highlights that the 1-order approximated feedback significantly approaches both the continuous-time trajectories and the Hamiltonian $H_d(t)$, in Figure 11.11(c), while the emulated feedback suffers the step-size of δ, so that it is not able to match neither the desired Hamiltonian nor to stabilize the desired equilibrium. This effect is better shown in Figure 11.11(a) where the Mean Squared Error with respect to both the state x and the desired Hamiltonian H_d is illustrated. The same consideration hold for a small damping improvement $\kappa = 0.1$ as depicted in Figure 11.14. Finally, Figure 11.12 compares the Root Mean Squared Error (RMSE) in the Hamiltonian matching under approximate solutions $u^{\delta[0]}$ and $u^{\delta[1]}$ for $\delta \in [0.05 : 0.05 : 1.5]$, respectively with $v = 0$, where the improvement of the proposed feedback is clear even for small values of δ.

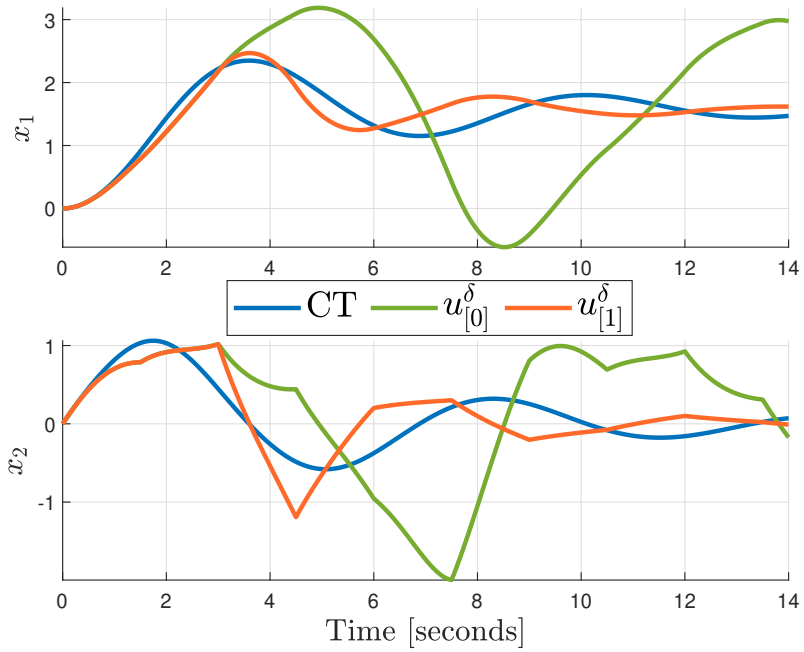

(a) State trajectories

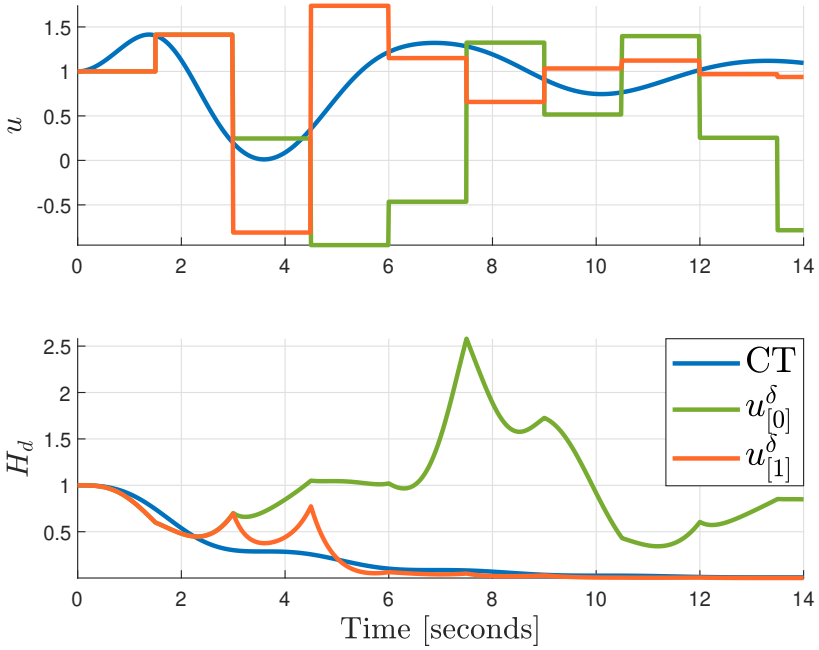

(b) Control and Hamiltonian function

Figure 11.11: Energy-based stabilization for $\delta = 1$ and $\kappa = 0$.

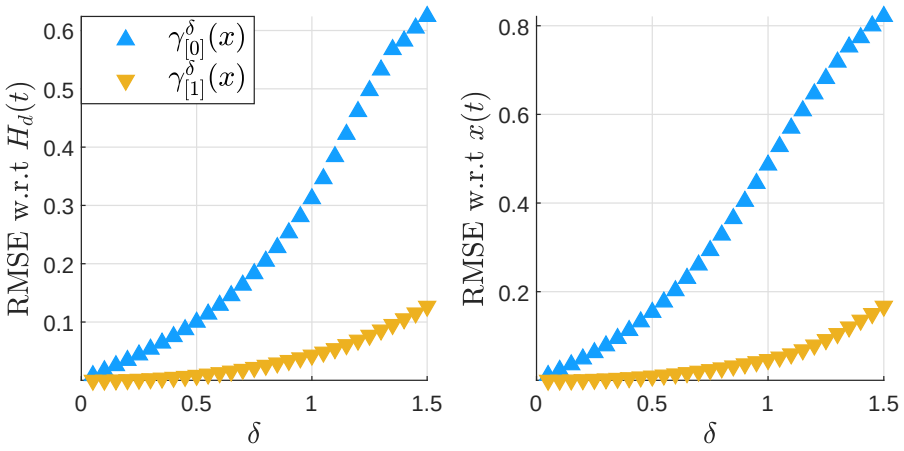

Figure 11.12: Matching error for $\delta \in [0.05, 1.5]$.

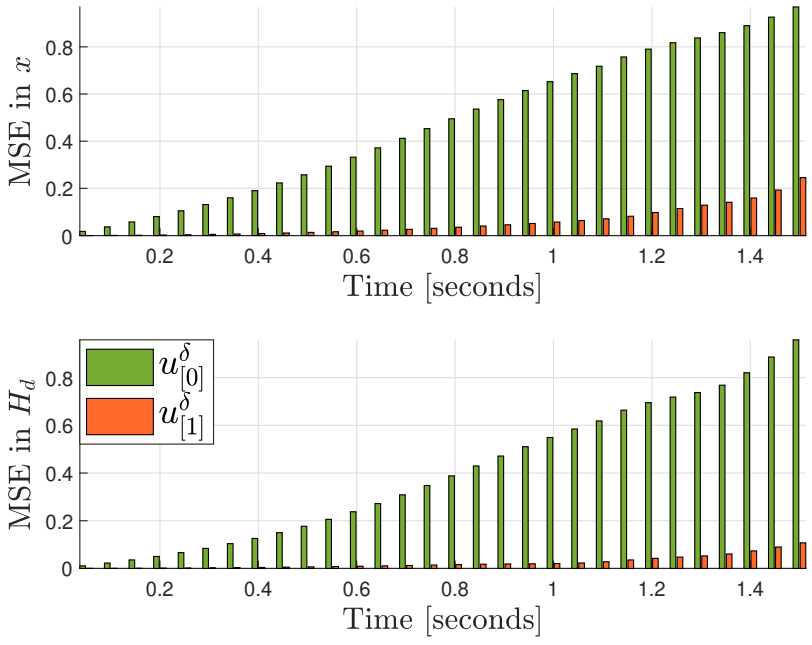

Figure 11.13: Energy-based stabilization for $\delta = 1$ and $\kappa = 0.15$: Mean Squared Error

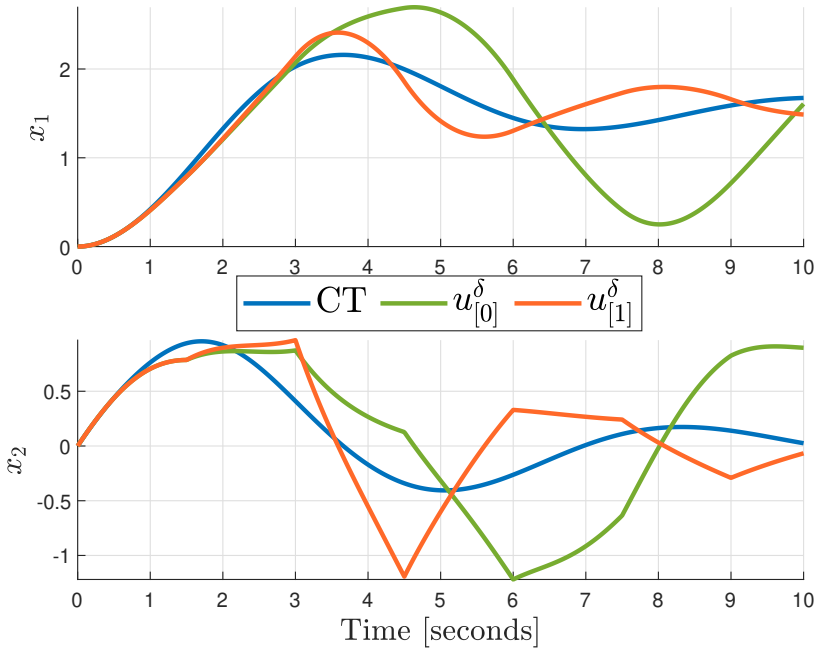

(a) State trajectories

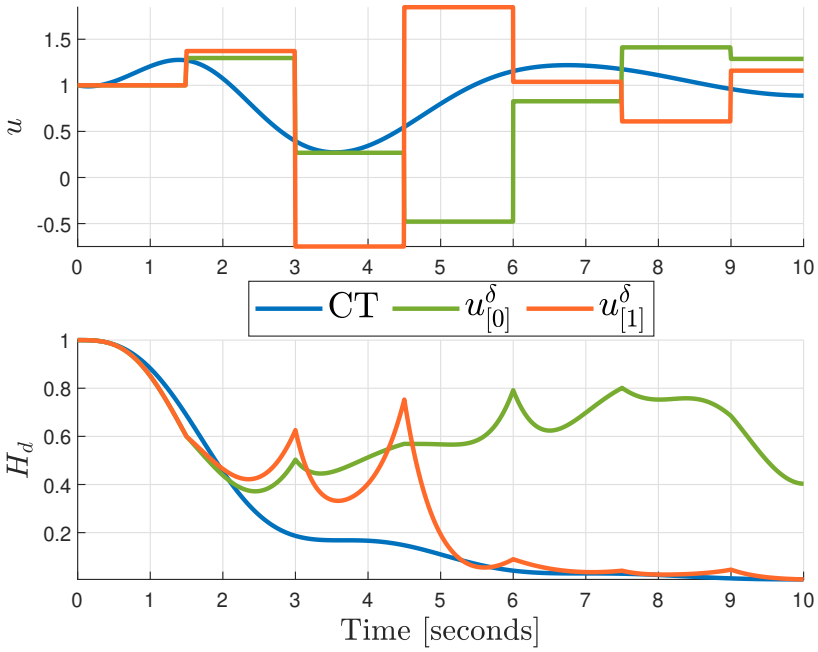

(b) Control and Hamiltonian function

Figure 11.14: Energy-based stabilization for $\delta = 1$ and $\kappa = 0.15$.

Chapter 12

The Magnetic Levitation Ball

Contents

12.1 Continuous-time modeling **260**

12.2 Sampled-data modeling **261**

12.3 Energy-based digital stabilization **271**

The Magnetic levitation system is an ubiquitous electro-mechanical system consisting of an metal ball in a vertical magnetic field created by a single electromagnet as in, as in Ortega et al. (2001); van der Schaft et al. (2014). The vertical position of the ball, in the mechanical system, can be controlled by setting the right value of the current through the electromagnet, and the current, in the electrical system, can be controlled by adjusting the voltage across the electromagnet terminals. The physical importance of this system as a case study is justified as, unlike the previous example, the magnetic levitation ball possesses a non-separable Hamiltonian function, and thus the computation of a sampled-data representation becomes much more challenging. In this case study we focus in particular on:

1. approximate sampled-data port-Hamiltonian models computed by truncating the exact series expansions as detailed in Section 7.4;

2. stabilization at a desired equilibrium point via sampled-data IDA-PBC based on IH_dM discussed as detailed in Section 8.2.

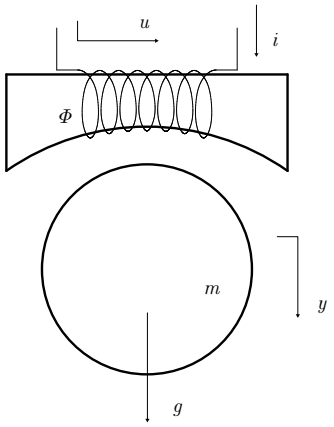

Figure 12.1: Magnetic Levitation Ball

12.1 Continuous-time modeling

The sketch of the magnetic levitation ball system is reported in Fig 12.1. The dynamical model consists of an ball in a vertical magnetic field created by a single electromagnet, as in Rodriguez et al. (2000), which comes form the Kirchoff's voltage law and Newton's second law as

$$\begin{aligned} \dot{\Phi} + ri &= u \\ m\ddot{y} &= F - mg \end{aligned}$$

with m the mass of the iron ball, r the coil resistance, i the current in the coil, F the force created by the electromagnet, u the external voltage acting on the closed-loop system, and y the ball position describing the difference between center of the ball and nominal position. Considering the standard assumption on the unsaturated flux $\Phi = L(y)i$ where $L(y)$ denotes the value of the inductance, the force created by the electromagnet is given by

$$F = \frac{1}{2}\frac{\partial L}{\partial y}(y)i^2.$$

Setting the state variable as $x = [\Phi, y, m\dot{y}]$, that is x_1 the flux, x_2 the difference between the position of the center of the ball and its nominal position (with the x_2-axis oriented downward) and x_3 the vertical momentum, the Hamiltonian representation

of the magnetic levitation system is characterized by a non-separable Hamiltonian function,

$$H(x) = mgx_2 + \frac{x_3^2}{2m} + \frac{x_1^2}{2L(x_2)}.$$

For small values of x_2, a suitable approximation of the inductance (for $-\infty < x_2 < 1$) is given by

$$L(x_2) = \frac{k}{(1 - x_2)},$$

k is a positive constant depending on the number of coil turns. Accordingly, the associated continuous-time dynamics, describing an iron ball in a vertical magnetic field created by a single electromagnet, takes the form

$$\dot{x} = \begin{pmatrix} -r & 0 & 0 \\ 0 & 0 & 1 \\ 0 & -1 & 0 \end{pmatrix} \nabla H(x) + \begin{pmatrix} 1 \\ 0 \\ 0 \end{pmatrix} u \tag{12.1a}$$

$$y = \frac{1}{k}(1 - x_2)x_1 \tag{12.1b}$$

where y denotes now the passive output of the system providing for the associated Hamiltonian function

$$\dot{H}(x) = -r\left(\frac{1}{k}(1 - x_2)x_1\right)^2 + \frac{u}{k}(1 - x_2)x_1 \leq uy.$$

12.2 Sampled-data modeling

For computing the sampled-data port-Hamiltonian model (7.14) based on the Magnetic Levitation Ball system (12.1a) let us focus on the free dynamics that is given

Parameter	**Description**	**Units**
y	ball vertical position	rad
m	Ball mass	kg
l	String length	m
g	gravity constant	$\mathrm{m{\cdot}s^{-2}}$
i	current in the coil	A (amperes)
u	voltage source	V (volt)
r	Coil resistance	Ω (ohm)

Table 12.1: Magnetic levitation ball parameters

by

$$\dot{x} = \begin{pmatrix} -r & 0 & 0 \\ 0 & 0 & 1 \\ 0 & -1 & 0 \end{pmatrix} \nabla H(x). \tag{12.2}$$

For the continuous-time dynamics given above, the sampled-data representations goes through the computations of both the discrete gradient and the discrete Jacobian function taking here the form

$$\bar{\nabla} H|_x^{x^+} = \begin{pmatrix} \frac{1}{L(x_2)}(x_1^+ + x_1) - \frac{1}{6k}(x_2^+ - x_2)(x_1 + 3x_1^+) \\ mg + \frac{1}{6k}((x_1^+)^2 + x_1^+ x_1 + x_1^2) \\ \frac{1}{2m}(x_3^+ + x_3) \end{pmatrix}$$

$$\bar{J}[\nabla H]|_x^{x^+} = \begin{pmatrix} \frac{1}{k} - \frac{1}{k}(x_2^+ + x_2) & -\frac{1}{k}(x_1^+ + x_1) & 0 \\ -\frac{1}{k}(x_1^+ + x_1) & 0 & 0 \\ 0 & 0 & \frac{1}{m} \end{pmatrix}.$$

As previously discussed, the sampled-data matrix $\mathcal{S}^{\delta}_{J-R}(f,x)$ characterizing the port-Hamiltonian dynamics, and describing both the sampled-data interconnection and dissipation part, is given in Theorem 7.4.1 as

$$\mathcal{S}^{\delta}_{J-R}(f,x) = \mathcal{M}(\delta,f,x)(J(x)-R(x))\left(I + \delta\mathcal{Q}(\delta,H,f,x)(J(x)-R(x))\right)^{-1},$$

with matrices $\mathcal{M}(\delta,f,x)$ and $\mathcal{Q}(\delta,H,f,x)$ respectively given in Lemma 7.1.1 and Lemma 7.1.4. However, since in this nonlinear case a closed form of the matrix $\mathcal{S}^{\delta}_{J-R}(f,x)$ cannot be pursued, it must be characterized exploiting the corresponding series expansion in power of δ given in (7.16) as

$$\mathcal{S}^{\delta}_{J-R}(f,x) = \sum_{i\geq 0} \frac{\delta^i}{(i+1)!}(\mathcal{S}_{J-R})_i(x).$$

Accordingly, the approximate sampled-data model of the state-space representation in Theorem 7.4.1 can be computed considering the first terms of the sampled-data matrix

$$\mathcal{S}^{\delta}_{J-R}(f,x) = (\mathcal{S}_{J-R})_0 + \frac{\delta^2}{3!}(\mathcal{S}_{J-R})_2(x) + (\mathcal{S}_{J-R})_3(x) + O(\delta^4)$$

so achieving the following sampled-data port-Hamiltonian system

$$x^+ = x + \delta(\mathcal{S}_{J-R})_0 \bar{\nabla} H|_x^{x^+} + \frac{\delta^3}{3!}(\mathcal{S}_{J-R})_2(x)\bar{\nabla} H|_x^{x^+} + \frac{\delta^4}{4!}(\mathcal{S}_{J-R})_3(x)\bar{\nabla} H|_x^{x^+}$$

where $x := x(k\delta)$ is the state and $x^+ := x((k+1)\delta)$ is the one-step ahead of the uncontrolled evolution when $u = 0$, and sampled-data matrices given by

$$(\mathcal{S}_{J-R})_0 = \begin{pmatrix} -r & 0 & 0 \\ 0 & 0 & 1 \\ 0 & -1 & 0 \end{pmatrix},$$

$$(\mathcal{S}_{J-R})_2 = \frac{rx_1}{2} \begin{pmatrix} -\frac{r^2}{x_1 L(x_2)^2} & \frac{1}{km} & \frac{r}{kL(x_2)} \\ \frac{1}{km} & 0 & 0 \\ -\frac{r}{kL(x_2)} & 0 & -\frac{1}{k^2} x_1 \end{pmatrix},$$

$$(\mathcal{S}_{J-R})_3 = r^2 x_1 \begin{pmatrix} \frac{x_1^2 - 2gkm}{2k^2 m x_1} - \frac{rx_3}{kmx_1 L(x_2)} & 0 & -\frac{2r}{kL(x_2)^2} - \frac{x_3}{k^2 m} \\ -\frac{1}{kmL(x_2)} & 0 & 0 \\ \frac{r}{kL(x_2)^2} + \frac{2x_3}{k^2 m} & 0 & \frac{x_1}{k^2 L(x_2)} \end{pmatrix}.$$

From the first of the series expansion of the sampled-data matrix $\mathcal{S}^\delta_{J-R}(f,x)$ given above, two interesting facts come to light:

- in case of zero dissipation, meaning with no resistance $r = 0$ into the electrical circuit, both the additional matrices, say $(\mathcal{S}^\delta_{J-R})_2$ and $(\mathcal{S}^\delta_{J-R})_3$, are zeroed and thus the approximate matrix $\mathcal{S}^\delta_J(f,x)$ in $O(\delta^4)$ verifies

$$\mathcal{S}^\delta_J(f,x) = \begin{pmatrix} 0 & 0 & 0 \\ 0 & 0 & 1 \\ 0 & -1 & 0 \end{pmatrix} + O(\delta^4),$$

  showing its skew-symmetry and getting energy conservation with the same interconnection matrix J as in continuous-time up to $O(\delta^4)$, that is

$$H(x^+) - H(x) = \delta \left(\bar{\nabla} H|_x^{x^+} \right)^\top \mathcal{S}^\delta_J(f,x) \bar{\nabla} H|_x^{x^+} = 0;$$

- for positive values of the resistance $r > 0$ the symmetric part of $(\mathcal{S}_{J-R})_2(x)$ and $(\mathcal{S}_{J-R})_3(x)$ is not positive definite in general. However, since the model (12.2) does hold for small values of x_2, because the approximation of the inductance $L(x)$ into $H(x)$, the approximate model still provides dissipation for δ small enough with a dissipation rate computed with the additional correcting term $(\mathcal{S}_{J-R})_2(x)$,

$$
\begin{aligned}
&H(x^+) - H(x) = \delta \left(\bar{\nabla} H|_x^{x^+}\right)^\top \left((\mathcal{S}_{J-R})_0 + \frac{\delta^2}{3!}(\mathcal{S}_{J-R})_2(x)\right) \bar{\nabla} H|_x^{x^+} + O(\delta^4) \\
&= -\delta r \left(\frac{1}{L(x_2)}(x_1^+ + x_1) - \frac{1}{6k}(x_2^+ - x_2)(x_1 + 3x_1^+)\right)^2 - \frac{\delta^3}{12}\frac{r x_1^2}{k^2 L(x_2)}\left(\frac{1}{2m}(x_3^+ + x_3)\right)^2 \\
&- \frac{\delta^3}{12}\frac{r^3}{L(x_2)^2}\left(\frac{1}{L(x_2)}(x_1^+ + x_1) - \frac{1}{6k}(x_2^+ - x_2)(x_1 + 3x_1^+)\right)^2 \\
&+ \frac{\delta^3 r x_1}{6km}\left(\frac{1}{L(x_2)}(x_1^+ + x_1)\right)\left(mg + \frac{1}{6k}((x_1^+)^2 + x_1^+ x_1 + x_1^2)\right) \\
&- \frac{\delta^3 r x_1}{6km}\left(\frac{1}{6k}(x_2^+ - x_2)(x_1 + 3x_1^+)\right)\left(mg + \frac{1}{6k}((x_1^+)^2 + x_1^+ x_1 + x_1^2)\right) + O(\delta^4).
\end{aligned}
$$

Because exact solutions cannot be computed in practice, approximations of the matrix $\mathcal{S}^\delta_{J-R}(f,x)$ are defined as the truncation of the corresponding series expansions as in Section 8.2. More in detail, approximations of the sampled-data model are defined by truncating the corresponding series expansion of $\mathcal{S}^\delta_{J-R}(f,x)$, as

$$
\mathcal{S}^{[p]}_{J-R} = \sum_{i=0}^{p} \frac{\delta^i}{(i+1)!}(\mathcal{S}_{J-R})_i(x) \tag{12.3}
$$

at the desired order $p \geq 0$. As in the Gravity pendulum system, when setting the approximation order $p = 0$ one recovers the approximate sampled-data model proposed in the literature by Sümer and Yalçın (2011); Aoues et al. (2017). More in general for higher order of p one gets

$$
\mathcal{S}^{[0]}_{J-R} = \begin{pmatrix} -r & 0 & 0 \\ 0 & 0 & 1 \\ 0 & -1 & 0 \end{pmatrix} \tag{12.4a}
$$

$$
\mathcal{S}^{[2]}_{J-R}(x) = \mathcal{S}^{[0]}_{J-R} + \frac{\delta^2 r x_1}{12}\begin{pmatrix} -\frac{r^2}{x_1 L(x_2)^2} & \frac{1}{km} & \frac{r}{kL(x_2)} \\ \frac{1}{km} & 0 & 0 \\ -\frac{r}{kL(x_2)} & 0 & -\frac{1}{k^2}x_1 \end{pmatrix} \tag{12.4b}
$$

$$
\mathcal{S}^{[3]}_{J-R}(x) = \mathcal{S}^{[2]}_{J-R}(x) + \frac{\delta^3 r^2 x_1}{24}\begin{pmatrix} \frac{x_1^2 - 2gkm}{2k^2 m x_1} - \frac{r x_3}{kmx_1 L(x_2} & 0 & -\frac{2r}{kL(x_2)^2} - \frac{x_3}{k^2 m} \\ -\frac{1}{kmL(x_2)} & 0 & 0 \\ \frac{r}{kL(x_2)^2} + \frac{2x_3}{k^2 m} & 0 & \frac{x_1}{k^2 L(x_2)} \end{pmatrix}. \tag{12.4c}
$$

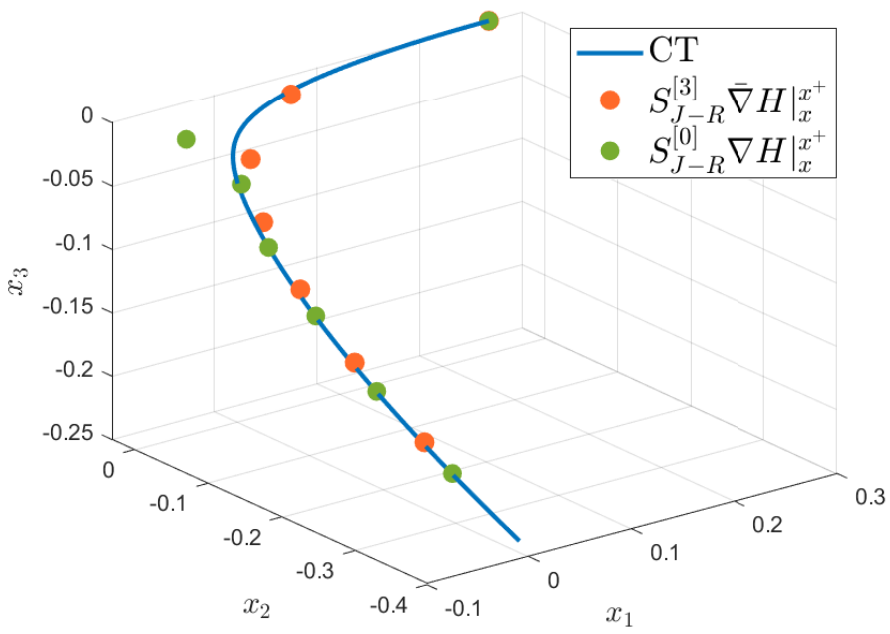

(a) Phase-portrait

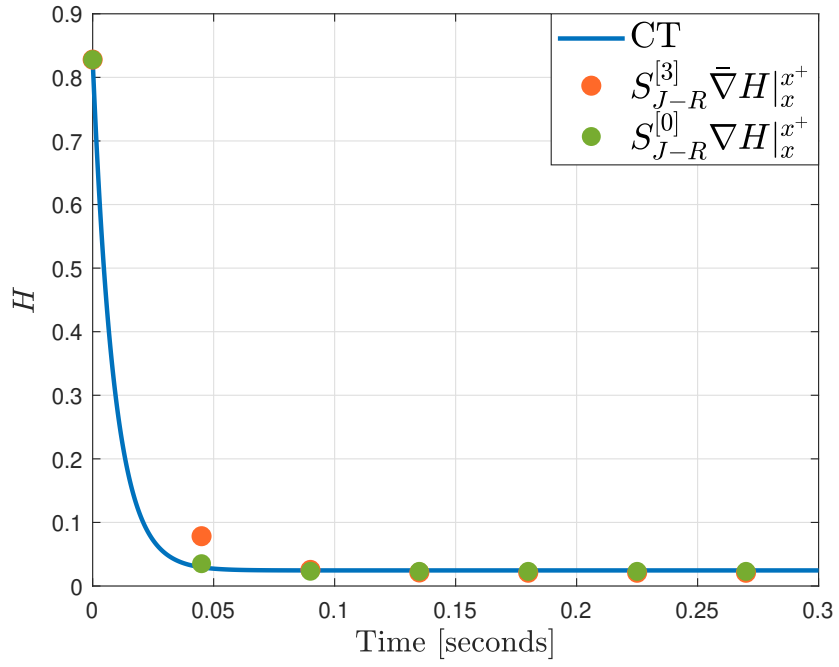

(b) Hamiltonian function

Figure 12.2: Sampled-data model of the Magnetic Levitation Ball system

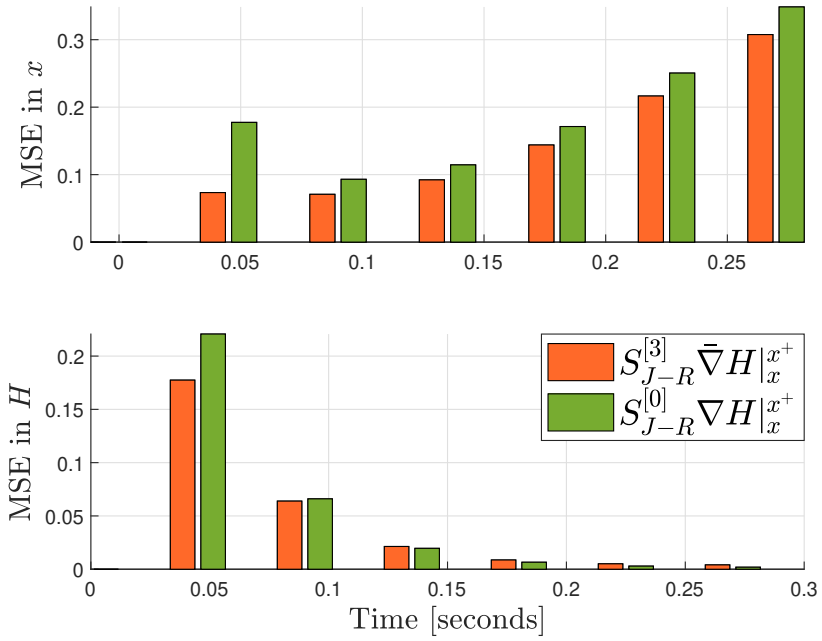

Figure 12.3: Mean Squared Error in the state x and Hamiltonian H with respect to the continuous-time of the Magnetic Levitation Ball system

Simulations

The comparison between approximate model deduced for $p = \{0, 3\}$, that are $\mathcal{S}^{[0]}_{J-R}\bar{\nabla}H|^{x^+}_x$ and $\mathcal{S}^{[3]}_{J-R}(x)\bar{\nabla}H|^{x^+}_x$ given in (12.4) has been illustrated in Figure 12.2 and Figure 12.3. The simulations are performed by setting $m = 8.44 \cdot 10^{-2}$, $k = 6.4042 \cdot \mathrm{e}^{-5}$, $r = 2.52$, $g = 9.81$, initial condition $x(0) = col(\sqrt{2kmg}, 0.3, 0)$, and a sampling period of length $\delta = 4.5 \cdot 10^{-2}$. It is clear that in this case, unlike the previous example the improvement provided by a better approximation, due to $\mathcal{S}^{[3]}_{J-R}(x)\bar{\nabla}H|^{x^+}_x$, is not much higher than the first-order approximate model $\mathcal{S}^{[0]}_{J-R}(x)\bar{\nabla}H|^{x^+}_x$, even though for in the Phase-portrait in Figure 12.2 a better matching of continuous-time trajectories is achieved. This is better seen in Figure 12.3 where the Mean Squared Error with respect to the state x and the Hamiltonian function H of the continuous-time system is reported.

Approximate solutions through approximate discrete gradient

As for the gravity pendulum system, we provide approximate solutions of both the sampled-data matrix $\mathcal{S}^{\delta}_{J-R}(f, x)$ and the discrete gradient function $\bar{\nabla}H|^{x^+}_x$. In par-

ticular, in what follows we illustrates the relevancy of approximations of $\mathcal{S}^{\delta}_{J-R}(f,x)$ and $\bar{\nabla}H|_x^{x^+}$ when computation of exact solutions are though or not feasible. In other words, in lieu of exploiting exact computation of the discrete gradient function might be interesting to analyze the effect of the non-homogeneous approximation of the sampled-data dynamics considering different approximation in δ of the sampled-data matrix $\mathcal{S}^{\delta}_{J}(f,x)$ and the discrete gradient function $\bar{\nabla}H|_x^{x^+}$. Again, denote with $\mathcal{S}^{[p]}_{J-R}(x)$ and $\bar{\nabla}^{[p]}H(x)$ the truncation of the corresponding series expansions at any finite order, then the sampled-data approximate dynamics is given by the expression

$$x^+ = x + \delta \mathcal{S}^{[p_1]}_{J-R}(x)\bar{\nabla}^{[p_2]}H(x)$$

for $p_2, p_1 > 0$. The approximate sampled-data matrices for the magnetic levitation ball are given in (12.4) whereas for the approximate discrete gradients one gets

$$\bar{\nabla}^{[0]}H = \begin{pmatrix} -\frac{x_1}{k}(x_2-1) \\ mg - \frac{x_1^2}{2k} \\ \frac{x_3}{m} \end{pmatrix}$$

$$\bar{\nabla}^{[1]}H = \bar{\nabla}^{[0]}H + \frac{\delta}{2}\begin{pmatrix} -\frac{rx_1(x_2^2-2x_2+1)}{k^2} - \frac{x_1x_3}{km} \\ -\frac{rx_1^2}{k^2}(x_2-1) \\ \frac{1}{m}(\frac{x_1^2}{2k} - mg) \end{pmatrix}$$

$$\bar{\nabla}^{[2]}H = \bar{\nabla}^{[1]}H + \frac{\delta^2 x_1}{4k^2}\begin{pmatrix} \frac{14rx_3-14rx_3x_2-3x_1^2}{6m} + \frac{18r^2x_2^2-6r^2x_2^3-18r^2x_2+6r^2+6gk^2}{6k} \\ -\frac{rx_1(5mrx_2^2-10mrx_2+5mr+3kx_3)}{3km} \\ \frac{rx_1}{m}(x_2-1) \end{pmatrix}$$

$$\bar{\nabla}^{[3]}H = \bar{\nabla}^{[2]}H - \frac{\delta^3 r}{2k^3}\begin{pmatrix} \frac{x_1(6gk^2-6gk^2x_2+2r^2x_2^4-8r^2x_2^3+12r^2x_2^2-8r^2x_2+2r^2)}{12k} \\ -\frac{rx_1^2(2gmk^2-10x_3krx_2+10x_3kr-kx_1^2-6mr^2x_2^3)}{12km} \\ -\frac{(2r^2x_1^2x_2^2-4r^2x_1^2x_2+2r^2x_1^2)m}{6rm^2} \end{pmatrix}$$
$$- \frac{\delta^3 r}{2k^3}\begin{pmatrix} \frac{x_1(10rx_2^2x_3-20rx_2x_3+10rx_3+5x_1^2x_2-5x_1^2)}{12m} + \frac{4kx_1x_3^2}{12m^2} \\ -\frac{rx_1^2(18mr^2x_2^2-18mr^2x_2+6mr^2)}{12km} \\ -\frac{krx_1^2x_3}{6rm^2} \end{pmatrix}$$

Different products $\mathcal{S}^{[p_1]}_{J-R}(x)\bar{\nabla}^{[p_2]}H(x)$ for $p_1 = \{0,2,3\}$ and $p_2 = \{0,1,2,3\}$, as in the previous case studies, produce different approximate sampled-data models with non-homogeneous discretization in δ yielding interesting behaviours at the sampling

instants $t = k\delta$. Approximate sampled-data models of the Magnetic levitation Balls system have been reported in Figure 12.4 and Figure 12.5 with sampling period of $\delta = 3.2 \cdot 10^{-2}$. Simulations empathize the suitable choice of the order approximation with respect to the discrete gradient and or the sampled-data matrices. Much clearer in 12.5, trivially better are the approximations of the discrete gradient and of the sampled-data matrix the better is the fidelity of the energetic evolution in $H(x)$, but at the same time, a better approximation of the discrete gradient has much more effect on the evolution of the system than a better approximation of the sampled-date; that is, a choice of $p_2 \geq p_1$ is preferable.

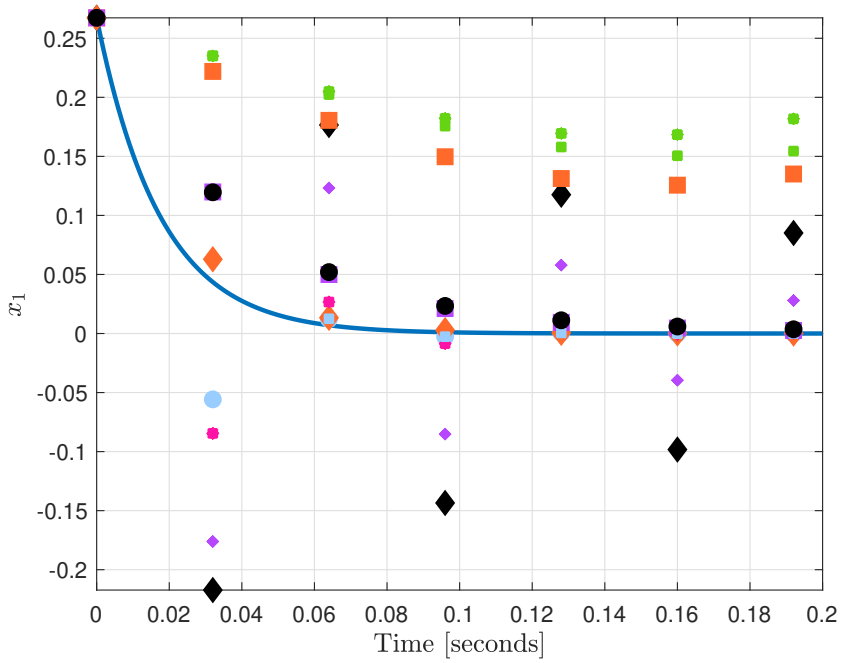

(a) State evolution x_1

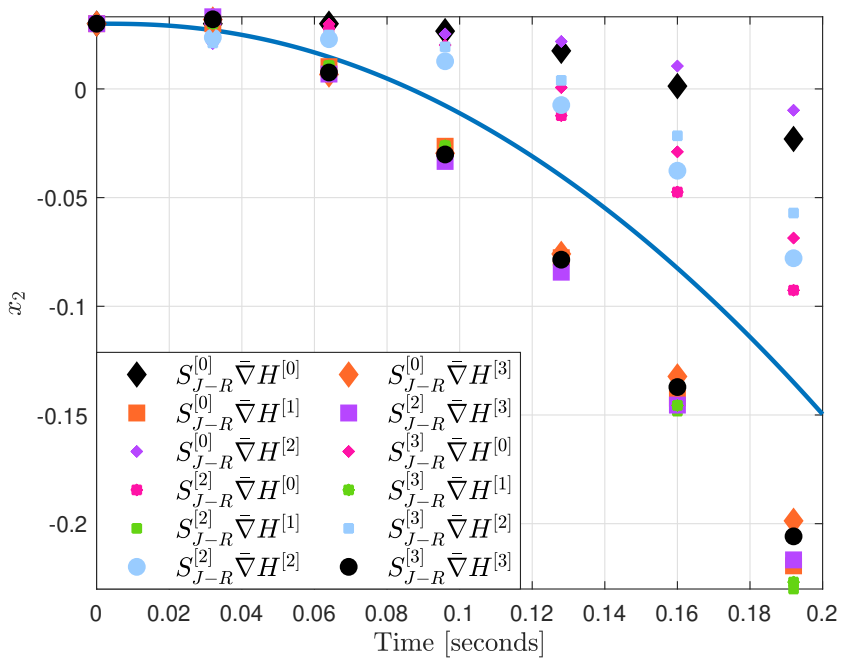

(b) State evolution x_2

Figure 12.4: Comparison between different approximate Magnetic Levitation Ball under sampling

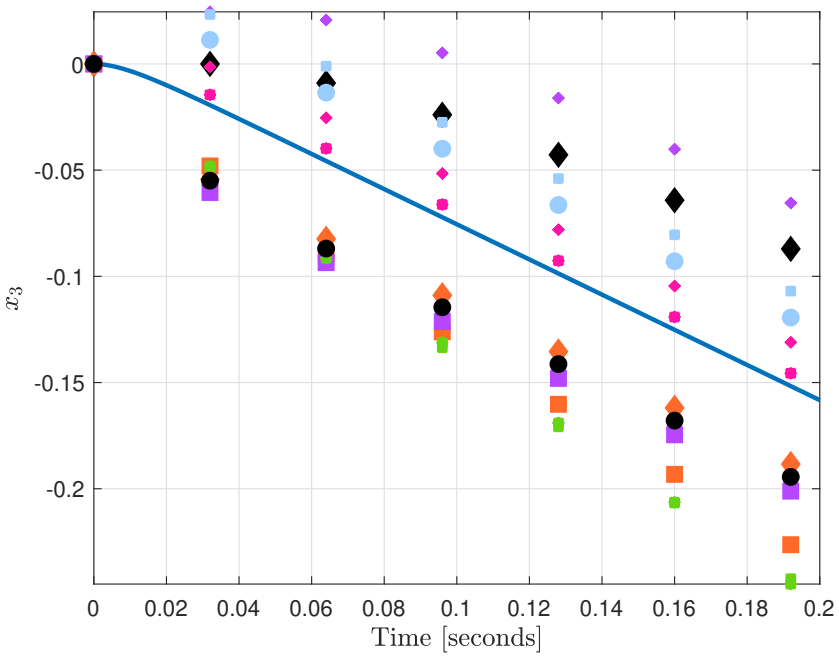

(a) State evolution x_3

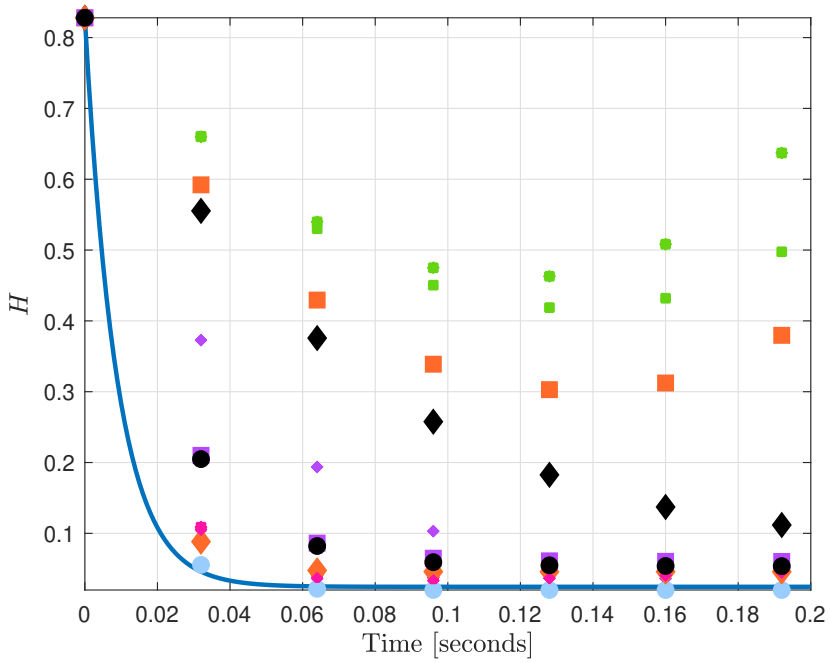

(b) Hamiltonian function H

Figure 12.5: Comparison between different approximate Magnetic Levitation Ball under sampling

12.3 Energy-based digital stabilization

After the modeling of the sampled-data representation of the Magnetic levitation Ball system, we address the problem of digitally stabilizing the system at a desired equilibrium point. In particular, the control objective is mainly to place the metal ball at a desired vertical position through a piece-wise control function injected into the continuous-time system. Precisely, due to the result in Theorem 8.2.1, let us choose a desired constant position $x_2^\star$ for the ball; the aim is to stabilize the continuous-time port-Hamiltonian dynamics (12.2) to the desired equilibrium

$$x^\star = col(\sqrt{2kmg}, x_2^\star, 0)$$

via a digital IDA-PBC strategy.

Continuous-time design

The continuous-time IDA-PBC design in Ortega et al. (2001), suggests to assign the following desired energy function

$$H_d(x) = \frac{1}{6k\alpha}x_1^3 + \frac{1}{2m}x_3^2 + mg\left(x_2 + \frac{\beta}{2}\tilde{\phi}^2 - \tilde{\phi}\right)$$

to the closed-loop system, with $\tilde{\phi} = \frac{1}{\alpha}(x_1 - x_1^\star) + (x_2 - x_2^\star)$ and $\alpha, \beta > 0$, with the corresponding IDA-PBC feedback

$$\begin{aligned}\gamma(x) =& \frac{r}{k}(1 - x_2)x_1 - \frac{\alpha}{m}x_3 - \frac{r}{\alpha}(\frac{1}{2k}x_1^2 - mg) \\ & - \frac{\beta}{r_a}((x_1 - x_1^\star) + \alpha(x_2 - x_2^\star)).\end{aligned} \tag{12.5}$$

Sampled-data design

The digital controller proposed in Theorem 8.2.1 is an approximate controller in $O(\delta^2)$ given for the Magnetic Levitation ball system by

$$\begin{aligned}\gamma^{\delta[1]}(x) &= \gamma(x) + \frac{\delta}{2}\dot{\gamma}(x) \\ &= \frac{r}{k}(1-x_2)x_1 - \frac{\alpha}{m}x_3 - \frac{r}{\alpha}(\frac{1}{2k}x_1^2 - mg) - \frac{\beta}{r_a}((x_1 - x_1^\star) + \alpha(x_2 - x_2^\star)) \\ &+ \frac{\delta}{2}(\frac{r}{k}(1-x_2) - \frac{r}{\alpha k} - \frac{\beta}{r_a})(\frac{r}{k}(1-x_2)x_1 - \frac{\alpha}{m}x_3 - \frac{r}{\alpha}(\frac{1}{2k}x_1^2 - mg) \\ &- \frac{\beta}{r_a}((x_1 - x_1^\star) + \alpha(x_2 - x_2^\star)) - r\frac{\partial H}{\partial x_1}) - \frac{\delta}{2}(\frac{r}{k}x_1 + \frac{\beta\alpha}{r_a})\frac{\partial H}{\partial x_3} + \frac{\delta}{2}\frac{\alpha}{m}\frac{\partial H}{\partial x_2}.\end{aligned} \tag{12.6}$$

Simulations

Taking advantage of the digital control purpose discussed in Section 8.2, we compare the performances of the first-order approximate control (12.6) with the emulated control

$$\begin{aligned}\gamma^{\delta[0]}(x) =& \frac{r}{k}(1-x_2)x_1 - \frac{\alpha}{m}x_3 - \frac{r}{\alpha}(\frac{1}{2k}x_1^2 - mg) \\ &- \frac{\beta}{r_a}((x_1 - x_1^\star) + \alpha(x_2 - x_2^\star)).\end{aligned} \tag{12.7}$$

The results of the closed-loop systems under the continuous-time $u_c = \gamma(x)$, the emulated $u^{\delta[0]} = \gamma^{\delta[0]}(x)$ and the improved $u^{\delta[1]} = \gamma^{\delta[1]}(x)$ are given in Figure 12.7 and Figure 12.8. Simulations are performed setting the desired vertical position $x_2^\star = 1$, the improved damping $r_a = 1$, $\alpha = 0.5$, $\beta = 0.1$, $m = 8.44 \cdot 10^{-2}$, $k = 6.4042 \cdot e^{-5}$, $r = 2.52$, $g = 9.81$, and initial condition $x_0 = col(x_1^\star, 0, 0)$ as in Ortega et al. (2001). In particular, Figure 12.7(a) highlights that both the digital controllers stabilizes the system at the desired vertical position but the improved $u^{\delta[1]}$ better matches the state trajectories obtained through u_c for a sampling period of length $\delta = 2{\cdot}10^{-2}$. However, the emulated control suffers at $t = 12$ and consequently violates the passivity condition on the desired Hamiltonian function $H_d(x)$. In Figure 12.7, a sampling period of length $\delta = 6 \cdot 10^{-2}$ as been set, showing the improved effect on the stability and the desired Hamiltonian function matching with respect to the emulated control which loose its stabilization effect on the closed-loop system, since

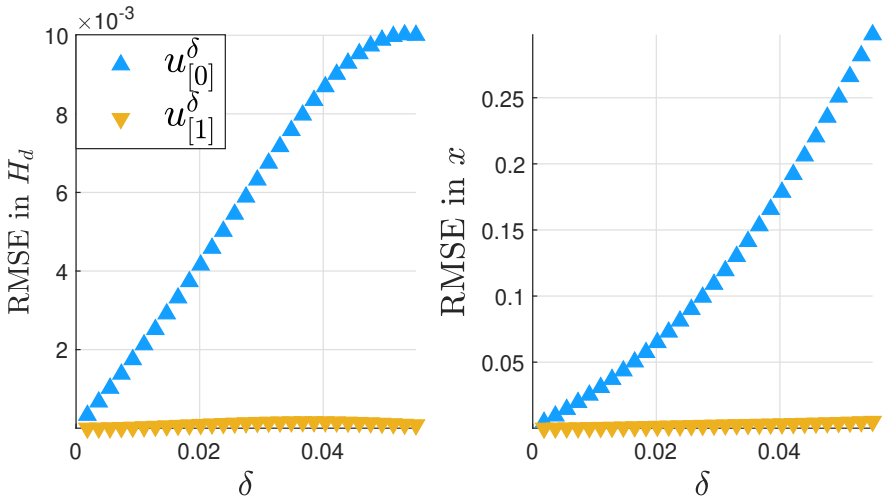

Figure 12.6: Root Mean Squared Errors

it produces instability of the closed-loop system and an unbounded growth of the desired Hamiltonian function.

The matching errors with respect to the desired Hamiltonian function $H_d(x)$ and the state trajectories x for different sampling period δ related to the emulated control $u^{\delta[0]}$ and the improved $u^{\delta[1]}$ have been reported in Figure 12.6. The Figure shows that the Root Mean Squared Error for both the $H_d(x)$ and x are clearly smaller for the improved $u^{\delta[1]}$ than the emulated $u^{\delta[0]}$, even for small value of δ, namely $\delta \in [1.8 \cdot 10^{-3}, 5.5 \cdot 10^{-2}]$.

Summarizing, even though higher order approximations of the dynamics do not improve the discretization performances of the uncontrolled system, they become fundamental in control design as notable performances are guaranteed even when including only one correcting term into the digital feedback.

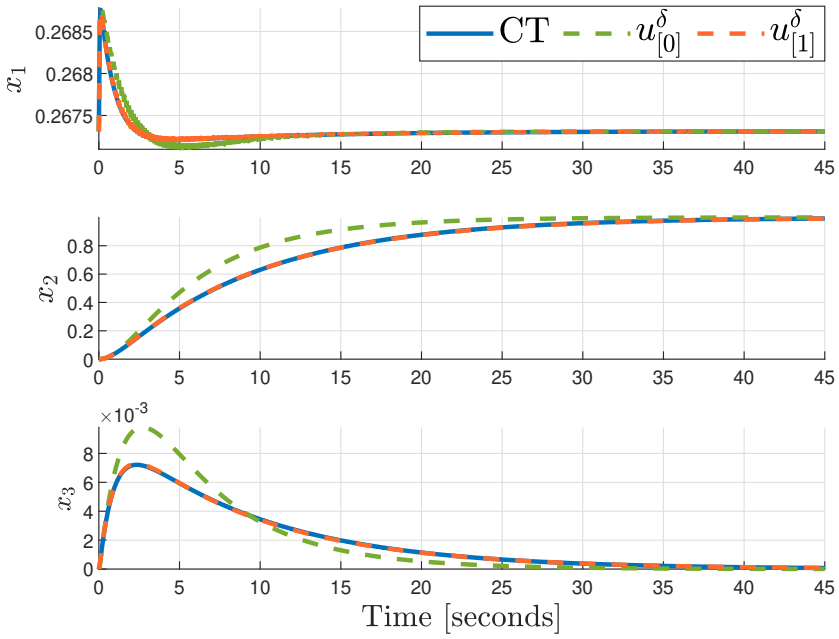

(a) State trajectories

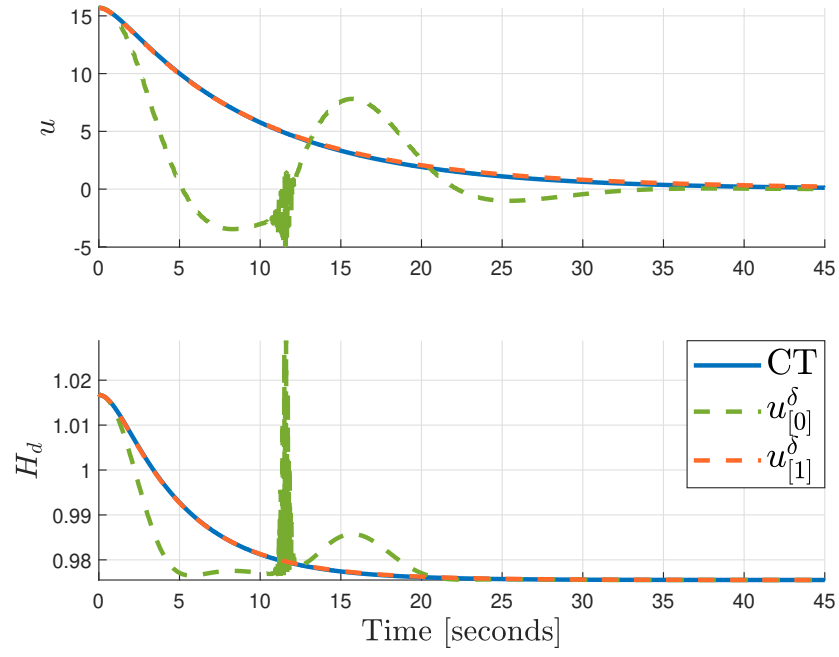

(b) Hamiltonian function and control effort

Figure 12.7: Sampled-data model of the Magnetic Levitation Ball system

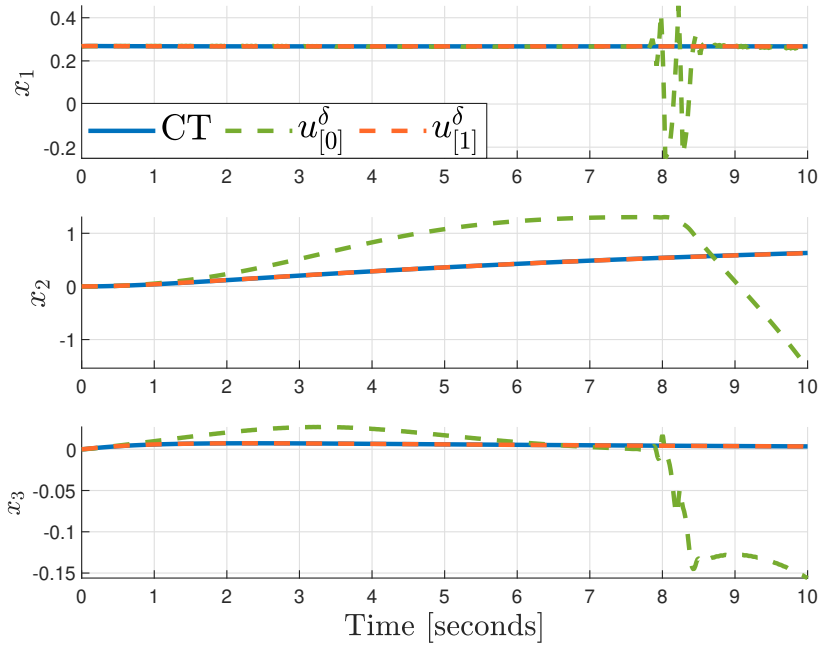

(a) State trajectories

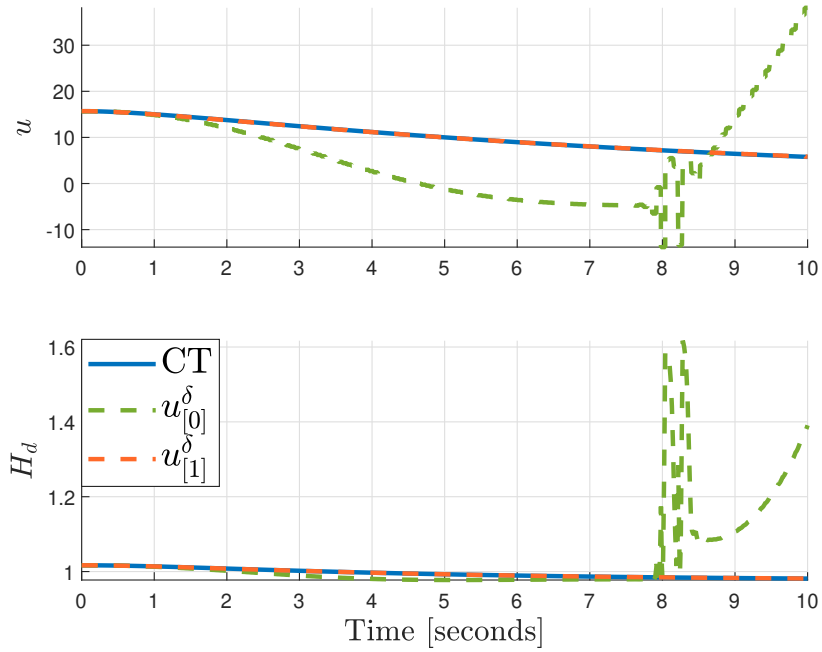

(b) Hamiltonian function and control effort

Figure 12.8: Sampled-data model of the Magnetic Levitation Ball system

Conclusions

The manuscript dealt with the modeling and control of discrete-time port-Hamiltonian systems and their characterization under sampling with the purpose of setting control methods that exploit the energy property of the system. With this in mind, the first problem which has been faced is the definition of port-Hamiltonian representations in discrete time catching the energetic structure and properties of the dynamics. To handle this issue, in Part II a novel port-Hamiltonian structure have been introduced making use of two main discrete-time concepts: Difference/Differential representation (DDR) and discrete gradient function. The definition introduced in Definition 4.1.1 provides a port-Hamiltonian system that splits into the free and controlled part the dynamics as

$$\begin{aligned} x^+ &= x + (J(x) - R(x))\bar{\nabla}H|_x^{x^+} \\ \frac{\partial x^+(u)}{\partial u} &= G(x^+(u), u) \quad \text{with} \quad x^+(0) = x^+ \\ Y(\cdot, u) &= \mathrm{L}_{G(\cdot,u)}H(\cdot) \end{aligned}$$

or equivalently achieves a structure in the form of a map as

$$\begin{aligned} x^+(u) &= x + (J(x) - R(x))\bar{\nabla}H|_x^{x^+} + g(x,u)u \\ Y_{\mathrm{av}}(x,u) &= g^\top(x,u)\bar{\nabla}H|_{x^+}^{x^+(u)}. \end{aligned}$$

From the structure of the system itself, it results that the conjugate passive output in the discrete-time context naturally arises with a u-average mapping $Y_{\mathrm{av}}(x,u)$, so recovering the concept of u-average passivity and defining an energy balance equation which clearly decouples the internal dissipated energy from the supplied one.

Similarly to the continuous-time case, a Dirac structure underlines the proposed port-Hamiltonian system. Unlike the continuous-time case, it results in Theorem

4.2.1 that the storing elements belonging to the discrete Dirac structure are decoupled in two parts: one related to the controlled dynamics, one related to the controlled-free dynamics. In addition, it has been proved in Theorem 2.4.1 that the feedback interconnection between two u-average passive systems, through the power-preserving interconnection of u-average passive outputs, results again in a passive system. This result directly applies to discrete-time port-Hamiltonian systems, in Theorem 4.2.2, proving that the power-preserving interconnection between discrete-time port-Hamiltonian systems preserves the port-Hamiltonian structure.

The introduced port-Hamiltonian system has been suitably exploited for defining energy-based controllers. As usual in a discrete time context, the major difficulty stands in the implicit dependence of the dynamics from the control variable; an aspect that makes difficult the design of any control feedback in discrete time. First in Theorem 5.1.1 the negative output feedback computed upon the output $Y_{\text{av}}(x, u)$ has been given as the solution to an implicit damping equality. Then in Theorem 5.1.2 we showed how the Dirac structure of the port-Hamiltonian system is modified under the negative output feedback, to conclude that the closed-loop system provides a port-Hamiltonian structure. Finally, in Theorem 5.2.1, the IDA-PBC stabilization problem has been investigated in the nonlinear case and sufficient conditions are given.

All the results have been specified in detail with reference to LTI dynamics in Chapter 6. In particular, we give the structure of the negative output feedback which achieves global asymptotic stabilization. Then, a necessary and sufficient condition for solving the LTI IDA-PBC problem is given along with the explicit structure of the IDA-PBC feedback.

How these results apply in the sampled-data framework? A common issue arising when a continuous-time port-Hamiltonian system is represented by a sampled-data model, for each fixed sampling period of length δ, is the loss of two fundamental properties: passivity and port-Hamiltonian structure. Therefore in Part III we tackled the problem of modeling and control port-Hamiltonian system under sampling. Namely, a novel port-Hamiltonian structure under sampling is given in Theorem 7.4.1 and with an interconnection and dissipation structure depending on the sampling period δ. The proposed structure, which is based on both the discrete gradient function and the exact solution of the associated continuous-time port-Hamiltonian system, takes

the sampled-data representation

$$\begin{aligned} x^+(u) &= x + \delta \mathcal{S}^\delta_{J-R}(\delta, f, x) \bar{\nabla} H|_x^{x^+} + \delta u g^\delta(x, u) \\ Y^\delta_{\text{av}}(x, u) &= g^{\delta\top}(x, u) \bar{\nabla} H|_{x^+}^{x^+(u)} \end{aligned}$$

The proposed model matches at the sampling instants both the trajectories and energy evolution of the continuous-time port-Hamiltonian model, so that there is no loss of information under the discretization process both in the state and energy. Moreover, the introduced sampled-data interconnection and dissipation structure $\mathcal{S}^\delta_{J-R}(\delta, f, x)$ is a matrix parameterized by δ which recovers the continuous-time matrices, say $J(x)$ and $R(x)$, in first-order approximation. The u-average output arises from the energy balance equation, presented in Theorem 7.5.1, as a conjugate variable of the supplied energy

$$H(x_k) - H(x_0) = \delta \sum_{i=0}^{k-1} \bar{\nabla}^\top H|_{x_i}^{x_i^+} \mathcal{S}^\delta_{J-R}(\delta, f, x) \bar{\nabla} H|_{x_i}^{x_i^+} + \delta \sum_{i=0}^{k-1} u_i Y^\delta_{\text{av}}(x_i, u_i)$$

which encodes all the effect of the external power without affecting the internal dissipated energy. An interesting point is that the u-average output, which comes in terms of the discrete gradient evaluated between free and controlled evolution of the sampled-data port-Hamiltonian system, is strictly reminiscent of the continuous-time counterpart. The so defined output recovers the standard passive output of the continuous-time port-Hamiltonian system when the sampling period δ approaches zero.

Similarly to the pure discrete-time case, the introduced sampled-data structure has been exploited to discuss energy-based stabilization design under sampling. First, we provide negative output feedback computed as the solution of an implicit damping equality for which approximate solutions can be performed, then we discussed the IDA-PBC problem for the general nonlinear port-Hamiltonian system under sampling. Since in the general nonlinear context a solution to the matching equality is tough to solve with an exact sampled-data control, we solved the problem exploiting in terms of feedback passivation and exploiting the IH_dM stabilization proposed in Theorem 3.5.1. In particular, we showed that a sampled-data IDA-PBC controller can be designed under sampling by matching the desired Hamiltonian function under ideal IDA-PBC feedback at all the sampling instants. This procedure avoids solving a sampled-data matching condition as the existence of the sampled-data IDA-PBC feedback is guaranteed by the solution of the continuous-time matching condition.

Also in this case modeling and control of sampled-data port-Hamiltonian systems have been detailed in the LTI case in Chapter 9. In particular, it is shown how port-Hamiltonian representations can be recovered under exact sampling along the exact solution. Then, the stabilization problem of LTI port-Hamiltonian system is concerned. First, we characterize the negative output feedback as the unique solution of the implicit damping inequality, then we give IDA-PBC feedback computed as a direct discrete design. The result reshapes the IDA-PBC solution presented in discrete time since in the LTI case, differently from the nonlinear case, the problem involves a matching equation taking the form of a linear matrix equality.

To validate the proposed methods, in Part IV, we discuss three different case studies in order to highlight computational aspects and to compare the result with the concerned literature.

First, we consider a linear-time invariant RLC system to compute an exact sampled-data port-Hamiltonian system showing preservation of the energetic property and the port-Hamiltonian structure at all the sampling instants. Further, we discuss and illustrate the digital stabilization problem. First, we stabilize the system at its zero equilibrium point through the injection of the digital negative output feedback computed over the sampled-data port-Hamiltonian model, then we assign a desired equilibrium point to the closed-loop system by designing a direct digital IDA-PBC feedback.

Then, we considered two nonlinear dynamics such as the gravity pendulum system and the magnetic levitation ball. In particular, we have seen that the sampled-data model can be performed in both the conservative and dissipative case providing a better marching of the continuous-time trajectories and energy evolution when compared with the literature model. Accordingly, for the gravity pendulum, the digital negative output feedback has been computed considering both the approximation of the discrete gradient and the exact discrete gradient by using computational software. Finally, the digital IDA-PBC stabilization through IH_dM has been designed for both the nonlinear models showing the constructive aspect and the effectiveness of the proposed methods.

Up to our knowledge the approach we propose represents a breakthrough with respect to the literature in the sense that it provides quite complete answers to basic questions:

1. The pure discrete-time modeling is validated by its associated Dirac structure.

2. The described conjugate output validates the notion of power-preserving interconnection and guarantees preservation of the port-Hamiltonian structure under feedback interconnection.

3. Hamiltonian modeling is preserved under sampling so describing novel sampled-data port-Hamiltonian forms exactly matching the continuous ones.

4. As a consequence, energy-based control design exploiting both the Hamiltonian form and average passivity can be developed addressing for the first time in discrete time or under sampling the goals of stabilization through energy management and suitable interconnection.

The main difficulties stand in the computation of the solutions in discrete time as solving nonlinear implicit algebraic equations is unavoidable. However, under sampling, these solutions always admit expansions in powers of the sampling period around the continuous-time one so making relevant their approximations. Simulated classical physical case studies illustrate these conclusions.

Perspectives

Several issues remain unsolved in the thesis work and thus a few of these open questions are mentioned below.

IDA-PBC: As already mentioned, the most interesting problem relies upon the assignment of the desired energy and desired structure to the closed-loop system. However, even though the proposed port-Hamiltonian system is suitable shaped for providing energy and structure assignment, the solution to this problem hinges on the solution $\bar{u}$ to the discrete-time nonlinear matching equation

$$(J(x) - R(x) + J_a(x) - R_a(x))(\bar{\nabla} H|_x^{x^+(\bar{u})} - \bar{\nabla} H|_x^{x^+} + \bar{\nabla} H_a|_x^{x^+(\bar{u})}) \\ = g(x, \bar{u})\bar{u} - (J_a(x) - R_a(x))\bar{\nabla} H|_x^{x^+}.$$

A general solution is tough to determine due to the implicit dependence of $\bar{u}$ into the nonlinear equation to solve, whose complexity clearly depends on the structures

of $g(x, \bar{u})$, $\bar{\nabla} H|_x^{x^+(\bar{u})}$, and $\bar{\nabla} H_a|_x^{x^+(\bar{u})}$. The problem is even more interesting under sampled-data design where the matching equation takes the form

$$\mathcal{S}^{\delta}_{J-R}(\delta, f, x)\bar{\nabla} H|_x^{x^+} + ug^{\delta}(x, u) = \mathcal{S}^{\delta}_{J_d-R_d}(\delta, f_d, x)\bar{\nabla} H_d|_x^{x^+(u)}$$

so involving matrices that depend on the sampling period. Thus, a suitable characterization of this matching equation when does not admit a closed solution $\bar{u}$ is still an open problem and might be intriguing and useful for digital stabilization purposes of physical systems.

Multi-input: Throughout the manuscript, we focused upon the single-input case and we missed the analysis upon the effect of these representations in the multi-input case, and in particular, we missed a deep understanding of energy-based stabilization through multiple input source. However, even though the results should follow the lines of the proposed methodologies, a complete understanding deserves an *ad hoc* characterization.

Dirac structure under sampling: Although we have seen how port-Hamiltonian systems in discrete time arise with an associated Dirac structure, a sampled-data Dirac structures based on the proposed sampled-data port-Hamiltonian system is missing. In particular, when a sampled-data port-Hamiltonian system is approximated at a certain order of the sampling period δ, how the associated Dirac structure changes? This question is still open and deserves a deep understanding.

Time-delay power-preserving interconnection: The analysis of power preserving interconnection introduced in Chapter 2 should be extended to time-delay feedback structures. When a delay affects the interconnection process both passivity and u-average passivity condition are lost and thus the power-preserving property. A first step in facing this issue has been investigated in Mattioni et al. (2020) referring to delayed state measurements, where we redefine a new output reduced dynamics which allows constructing a suitable output ensuring u-average passivity for the time-delay system.

Finally, the discrete-time and sampled-data modeling of port-Hamiltonian systems here addressed pave the way to a wide range of new theoretical and practical challenges in both modeling and control. A few of these attractive perspectives in modeling and control are separately mentioned below.

- The proposed sampled-data model finds application in all physical domains in which the continuous-time port-Hamiltonian systems involved in this study is applied. In addition, the pure discrete-time model proposed can be used in several contexts such as Data-Driven Control Systems, see Hou and Wang (2013), and unconstrained optimization problem, see Grimm et al. (2017).

- An attractive extension concerns distributed-parameter systems; which are models defined by considering not only the time but also space as independent parameters on which the physical quantities are defined, van der Schaft et al. (2014); van der Schaft and Maschke (2002).

- Since the proposed sampled-data port-Hamiltonian structure presents strong analogies with the port-Hamiltonian system in continuous time, it is interesting to consider hybrid interconnections of port Hamiltonian systems; namely, the interconnection between a continuous-time port-Hamiltonian system and sampled-data modeling, as it occurs in human-teleoperator systems, see Stramigioli et al. (2005).

- As studied in continuous-time the problem of reducing the state dimension of port-Hamiltonian structure is a challenging perspective. see Polyuga and Van der Schaft (2010); Ionescu and Astolfi (2013). It should be interesting to perform such a reduction analysis in the discrete time domain concerning the proposed port-Hamiltonian structure.

Bibliography

Aliyu, M. (2011). *Nonlinear H-infinity control, Hamiltonian systems and Hamilton-Jacobi equations*. CRC Press. (Cited on page 30.)

Aoues, S. (2014). *Schémas d'intégration dédiés à l'étude, l'analyse et la synthèse dans le formalisme Hamiltonien à ports*. PhD thesis, INSA de Lyon. (Cited on page 184.)

Aoues, S., Di Loreto, M., Eberard, D., and Marquis-Favre, W. (2017). Hamiltonian systems discrete-time approximation: Losslessness, passivity and composability. *Systems & Control Letters*, 110:9–14. (Cited on pages 9, 11, 12, 13, 14, 17, 110, 115, 184, 185, 213, 221, 237, 245, 246, and 264.)

Aoues, S., Eberard, D., and Marquis-Favre, W. (2013). Discrete ida-pbc design for 2d port-hamiltonian systems. *IFAC Proceedings Volumes*, 46(23):134–139. (Cited on pages 12 and 227.)

Aoues, S., Eberard, D., and Marquis-Favre, W. (2015a). Discrete ida-pbc control law for newtonian mechanical port-hamiltonian systems. In *2015 54th IEEE Conference on Decision and Control (CDC)*, pages 4388–4393. IEEE. (Cited on pages 12 and 227.)

Aoues, S., Matignon, D., and Alazard, D. (2015b). Control of a flexible spacecraft using discrete ida-pbc design. *IFAC-PapersOnLine*, 48(13):188–193. (Cited on page 12.)

Astolfi, A., Karagiannis, D., and Ortega, R. (2007). *Nonlinear and adaptive control with applications*. Springer Science & Business Media. (Cited on pages 30, 36, and 46.)

Astolfi, A. and Ortega, R. (2003). Immersion and invariance: a new tool for stabilization and adaptive control of nonlinear systems. *IEEE Transactions on Automatic control*, 48(4):590–606. (Cited on page 5.)

Astolfi, A., Ortega, R., and Sepulchre, R. (2001). Passivity-based control of non-linear systems. *Control of Complex Systems*, pages 39–75. (Cited on page 5.)

Baaiu, A., Couenne, F., Lefevre, L., Le Gorrec, Y., and Tayakout, M. (2006). Energy based discretization of an adsorption column. *IFAC Proceedings Volumes*, 39(2):753–758. (Cited on page 11.)

Barbot, J.-P., Monaco, S., and Normand-Cyrot, D. (1996). A sampled normal form for feedback linearization. *Mathematics of Control, Signals and Systems*, 9(2):162–188. (Cited on page 6.)

Barbot, J.-P., Monaco, S., and Normand-Cyrot, D. (1999). Discrete-time approximated linearization of siso systems under output feedback. *IEEE Transactions on automatic control*, 44(9):1729–1733. (Cited on page 6.)

Bassi, L., Macchelli, A., and Melchiorri, C. (2007). An algorithm to discretize one-dimensional distributed port hamiltonian systems. In *Lagrangian and Hamiltonian methods for nonlinear control 2006*, pages 61–73. Springer. (Cited on page 12.)

Battilotti, S., Lanari, L., and Ortega, R. (1997). On the role of passivity and output injection in the output feedback stabilisation problem: application to robot control. *European journal of control*, 3(2):92–103. (Cited on page 5.)

Bhatia, R. (2013). *Matrix analysis*, volume 169. Springer Science & Business Media. (Cited on page 93.)

Breedveld, P. C. (1984). Physical systems theory in terms of bond graphs. *PhD Thesis, Technische Hogeschool Twente*. (Cited on page 2.)

Brogliato, B., Lozano, R., Maschke, B., and Egeland, O. (2007). Dissipative systems analysis and control. *Theory and Applications*, 2. (Cited on pages 2, 5, 30, and 46.)

Byrnes, C. and Lin, W. (1994). Losslessness, feedback equivalence, and the global stabilization of discrete-time nonlinear systems. *IEEE Transactions on automatic control*, 39(1):83–98. (Cited on page 55.)

Byrnes, C. I., Isidori, A., Willems, J. C., et al. (1991). Passivity, feedback equivalence, and the global stabilization of minimum phase nonlinear systems. *IEEE Transactions on automatic control*, 36(11):1228–1240. (Cited on pages 5 and 34.)

Byrnes, C. I. and Lin, W. (1993). Discrete-time lossless systems, feedback equivalence and passivity. In *Proceedings of 32nd IEEE Conference on Decision and Control*, pages 1775–1781. IEEE. (Cited on page 58.)

Cardoso-Ribeiro, F. L., Matignon, D., and Lefèvre, L. (2018). A structure-preserving partitioned finite element method for the 2d wave equation. *IFAC-PapersOnLine*, 51(3):119–124. (Cited on page 12.)

Castaños, F., Michalska, H., Gromov, D., and Hayward, V. (2015). Discrete-time models for implicit port-hamiltonian systems. *arXiv preprint arXiv:1501.05097*. (Cited on page 10.)

Castaños, F., Ortega, R., van der Schaft, A., and Astolfi, A. (2009). Asymptotic stabilization via control by interconnection of port-hamiltonian systems. *Automatica*, 45(7):1611–1618. (Cited on page 45.)

Castillo, B., Di Gennaro, S., Monaco, S., and Normand-Cyrot, D. (1993). Nonlinear regulation for a class of discrete-time systems. *Systems & control letters*, 20(1):57–65. (Cited on page 6.)

Castillo, B., Di Gennaro, S., Monaco, S., and Normand-Cyrot, D. (1997). On regulation under sampling. *IEEE Transactions on Automatic Control*, 42(6):864–868. (Cited on page 6.)

Celledoni, E. and Høiseth, E. H. (2017). Energy-preserving and passivity-consistent numerical discretization of port-hamiltonian systems. *arXiv preprint arXiv:1706.08621*. (Cited on page 11.)

Chopra, N. and Spong, M. W. (2006). Passivity-based control of multi-agent systems. In *Advances in robot control*, pages 107–134. Springer. (Cited on page 5.)

Costa-Castelló, R. and Fossas, E. (2006). On preserving passivity in sampled-data linear systems. In *2006 American Control Conference*, pages 6–pp. IEEE. (Cited on page 89.)

Courant, T. J. (1990). Dirac manifolds. *Transactions of the American Mathematical Society*, 319(2):631–661. (Cited on pages 3 and 37.)

Di Gennaro, S. (2003). Passive attitude control of flexible spacecraft from quaternion measurements. *Journal of Optimization Theory and Applications*, 116(1):41–60. (Cited on page 5.)

Di Gennaro, S., Monaco, S., and Normand-Cyrot, D. (1999). Nonlinear digital scheme for attitude tracking. *Journal of guidance, control, and dynamics*, 22(3):467–477. (Cited on page 6.)

Duindam, V., Macchelli, A., Stramigioli, S., and Bruyninckx, H. (2009). *Modeling and control of complex physical systems: the port-Hamiltonian approach*. Springer Science & Business Media. (Cited on pages 4, 5, and 40.)

Eberard, D., Maschke, B., and van der Schaft, A. (2007). On the interconnection structures of discretized port hamiltonian systems. In *PAMM: Proceedings in Applied Mathematics and Mechanics*, volume 7, pages 3030005–3030006. Wiley Online Library. (Cited on page 11.)

Engø, K. and Faltinsen, S. (2001). Numerical integration of lie–poisson systems while preserving coadjoint orbits and energy. *SIAM journal on numerical analysis*, 39(1):128–145. (Cited on page 11.)

Fliess, M. and Normand-Cyrot, D. (1981). A lie-theoretic approach to nonlinear discrete-time controllability via ritt's formal differential groups. *Systems & Control Letters*, 1(3):179–183. (Cited on page 6.)

Giordano, P. R., Franchi, A., Secchi, C., and Bülthoff, H. H. (2013). A passivity-based decentralized strategy for generalized connectivity maintenance. *The International Journal of Robotics Research*, 32(3):299–323. (Cited on page 32.)

Golo, G., Talasila, V., van der Schaft, A., and Maschke, B. (2004). Hamiltonian discretization of boundary control systems. *Automatica*, 40(5):757–771. (Cited on page 11.)

Gonzalez, O. (1996). Time integration and discrete hamiltonian systems. *Journal of Nonlinear Science*, 6(5):449. (Cited on pages 11, 13, 48, and 50.)

Goodwin, G. C., Graebe, S. F., Salgado, M. E., et al. (2001). *Control system design*. Upper Saddle River, NJ: Prentice Hall,. (Cited on page 6.)

Gören-Sümer, L. and Yalçın, Y. (2008). Gradient based discrete-time modeling and control of hamiltonian systems. *IFAC Proceedings Volumes*, 41(2):212–217. (Cited on page 11.)

Greenspan, D. (1973). Discrete models. (Cited on page 48.)

Grimm, V., McLachlan, R. I., McLaren, D. I., Quispel, G., and Schönlieb, C. (2017). Discrete gradient methods for solving variational image regularisation models. *Journal of Physics A: Mathematical and Theoretical*, 50(29):295201. (Cited on page 283.)

Grizzle, J. (1985). Controlled invariance for discrete-time nonlinear systems with an application to the disturbance decoupling problems. *IEEE Transactions on Automatic Control*, 30(9):868–874. (Cited on page 6.)

Grizzle, J. and Kokotovic, P. (1988). Feedback linearization of sampled-data systems. *IEEE Transactions on Automatic Control*, 33(9):857–859. (Cited on page 6.)

Grüne, L. and Nesic, D. (2003). Optimization-based stabilization of sampled-data nonlinear systems via their approximate discrete-time models. *SIAM Journal on Control and Optimization*, 42(1):98–122. (Cited on page 6.)

Hairer, E., Lubich, C., and Wanner, G. (2006). *Geometric numerical integration: structure-preserving algorithms for ordinary differential equations*, volume 31. Springer Science & Business Media. (Cited on pages 9, 11, and 51.)

Hall, B. (2015). *Lie groups, Lie algebras, and representations: an elementary introduction*, volume 222. Springer. (Cited on page 93.)

Hamilton, W. R. (1834). Xv. on a general method in dynamics; by which the study of the motions of all free systems of attracting or repelling points is reduced to the search and differentiation of one central relation, or characteristic function. *Philosophical transactions of the Royal Society of London*, (124):247–308. (Cited on page 1.)

Hamilton, W. R. (1835). Vii. second essay on a general method in dynamics. *Philosophical Transactions of the Royal Society of London*, (125):95–144. (Cited on page 1.)

Hankins, T. L. (1980). *Sir William Rowan Hamilton*. Johns Hopkins University Press. (Cited on page 1.)

Harkort, C. and Deutscher, J. (2012). Stability and passivity preserving petrov–galerkin approximation of linear infinite-dimensional systems. *Automatica*, 48(7):1347–1352. (Cited on page 12.)

Hatanaka, T., Chopra, N., Fujita, M., and Spong, M. W. (2015). *Passivity-based control and estimation in networked robotics*. Springer. (Cited on page 32.)

Hill, D. and Moylan, P. (1976). The stability of nonlinear dissipative systems. *IEEE Transactions on Automatic Control*, 21(5):708–711. (Cited on pages 4 and 31.)

Hou, Z.-S. and Wang, Z. (2013). From model-based control to data-driven control: Survey, classification and perspective. *Information Sciences*, 235:3–35. (Cited on page 283.)

Ionescu, T. C. and Astolfi, A. (2013). Families of moment matching based, structure preserving approximations for linear port hamiltonian systems. *Automatica*, 49(8):2424–2434. (Cited on page 283.)

Isidori, A. (2013). *Nonlinear control systems*. Springer Science & Business Media. (Cited on page 25.)

Jakubczyk, B. (1980a). Existence and uniqueness of realizations of nonlinear systems. *SIAM Journal on control and optimization*, 18(4):455–471. (Cited on page 6.)

Jakubczyk, B. (1980b). Invertible realizations of nonlinear discrete time systems. In *Proc. Princeton Conf. Info. Sc. and Syst*, pages 235–239. (Cited on page 6.)

Jakubczyk, B. and Normand-Cyrot, D. (1984). Automatique théorique. orbites de pseudo-groupes de difféomorphismes et commandabilité des systèmes non linéaires en temps discret. *Comptes rendus des séances de l'Académie des sciences. Série 1, Mathématique*, 298(11):257–260. (Cited on page 6.)

Khalil, H. (2002). *Nonlinear Systems*. Pearson Education. Prentice Hall. (Cited on page 25.)

Khalil, H. (2014). *Nonlinear control*. Pearson Higher Ed. (Cited on page 102.)

Kokotovic, P. (1992). The joy of feedback: nonlinear and adaptive. *IEEE Control Systems Magazine*, 12(3):7–17. (Cited on pages 5, 102, and 105.)

Kokotovic, P., Krstic, M., and Kanellakopoulos, I. (1992). Backstepping to passivity: recursive design of adaptive systems. In *[1992] Proceedings of the 31st IEEE Conference on Decision and Control*, pages 3276–3280. IEEE. (Cited on page 5.)

Kotta, Ü. (2006). *Inversion method in the discrete-time nonlinear control systems synthesis problems*, volume 205. Springer. (Cited on pages 6 and 48.)

Kotyczka, P. (2016). Finite volume structure-preserving discretization of 1d distributed-parameter port-hamiltonian systems. *IFAC-PapersOnLine*, 49(8):298–303. (Cited on page 12.)

Kotyczka, P. and Lefèvre, L. (2019). Discrete-time port-hamiltonian systems: A definition based on symplectic integration. *Systems & Control Letters*, 133:104530. (Cited on page 11.)

Kotyczka, P. and Maschke, B. (2017). Discrete port-hamiltonian formulation and numerical approximation for systems of two conservation laws. *at-Automatisierungstechnik*, 65(5):308–322. (Cited on page 11.)

Kotyczka, P., Maschke, B., and Lefèvre, L. (2018). Weak form of stokes–dirac structures and geometric discretization of port-hamiltonian systems. *Journal of Computational Physics*, 361:442–476. (Cited on page 11.)

Krstić, M., Kanellakopoulos, I., and Kokotović, P. V. (1994). Passivity and parametric robustness of a new class of adaptive systems. *Automatica*, 30(11):1703–1716. (Cited on page 5.)

Laila, D. S. and Astolfi, A. (2004). A note on discrete-time stabilization of hamiltonian systems. *IFAC Proceedings Volumes*, 37(13):967–972. (Cited on page 6.)

Laila, D. S. and Astolfi, A. (2005). Discrete-time ida-pbc design for separable hamiltonian systems. *IFAC Proceedings Volumes*, 38(1):838–843. (Cited on page 12.)

Laila, D. S. and Astolfi, A. (2006a). Construction of discrete-time models for port-controlled hamiltonian systems with applications. *Systems & Control Letters*, 55(8):673–680. (Cited on pages 6, 8, and 10.)

Laila, D. S. and Astolfi, A. (2006b). Discrete-time ida-pbc design for underactuated hamiltonian control systems. In *2006 American Control Conference*, pages 6–pp. IEEE. (Cited on page 12.)

Laila, D. S. and Astolfi, A. (2007). Direct discrete-time design for sampled-data hamiltonian control systems. In *Lagrangian and Hamiltonian Methods for Nonlinear Control 2006*, pages 87–98. Springer. (Cited on pages 8 and 11.)

Laila, D. S. and NešIć, D. (2003). Changing supply rates for input–output to state stable discrete-time nonlinear systems with applications. *Automatica*, 39(5):821–835. (Cited on page 55.)

Laila, D. S., Nešić, D., and Astolfi, A. (2006). 3 sampled-data control of nonlinear systems. In *Advanced topics in control systems theory*, pages 91–137. Springer. (Cited on page 6.)

Leok, M. and Ohsawa, T. (2011). Variational and geometric structures of discrete dirac mechanics. *Foundations of computational mathematics*, 11(5):529–562. (Cited on page 3.)

Lin, W. and Byrnes, C. I. (1995). Passivity and absolute stabilization of a class of discrete-time nonlinear systems. *Automatica*, 31(2):263–267. (Cited on pages 55 and 58.)

Loria, A., Panteley, E., Nijmeijer, H., and Fossen, T. I. (1998). Robust adaptive control of passive systems with unknown disturbances. *IFAC Proceedings Volumes*, 31(17):841–846. 4th IFAC Symposium on Nonlinear Control Systems Design 1998 (NOLCOS'98), Enschede, The Netherlands, 1-3 July. (Cited on page 5.)

Loria, A., Panteley, E., and Nijmeijer, H. (2001). A remark on passivity-based and discontinuous control of uncertain nonlinear systems. *Automatica*, 37(9):1481–1487. (Cited on page 5.)

Maschke, B. M. and van der Schaft, A. J. (1992). Port-controlled hamiltonian systems: modelling origins and systemtheoretic properties. *IFAC Proceedings Volumes*, 25(13):359–365. (Cited on page 2.)

Maschke, B. M. and van der Schaft, A. J. (1993). Port-controlled hamiltonian systems: modelling origins and systemtheoretic properties. In *Nonlinear Control Systems Design 1992*, pages 359–365. Elsevier. (Cited on page 38.)

Maschke, B. M., van der Schaft, A. J., and Breedveld, P. C. (1992). An intrinsic hamiltonian formulation of network dynamics: Non-standard poisson structures and gyrators. *Journal of the Franklin institute*, 329(5):923–966. (Cited on pages 2 and 38.)

Mattioni, M., Monaco, S., and Normand-Cyrot, D. (2019). Feedforwarding under sampling. *IEEE Transactions on Automatic Control*, 64(11):4668–4675. (Cited on page 60.)

Mattioni, M., Moreschini, A., Monaco, S., and Normand-Cyrot, D. (2020). Reduction-based stabilization of nonlinear discrete-time systems through delayed state measurements. *IFAC-PapersOnLine*, 53(2):5851–5856. In 21th IFAC World Congress. (Cited on page 282.)

Mattioni, M., Moreschini, A., Monaco, S., and Normand-Cyrot, D. (2021). On feedback passivation under sampling. In *American control conference (ACC)*. (Cited on page 18.)

McLachlan, R. I. (1995). On the numerical integration of ordinary differential equations by symmetric composition methods. *SIAM Journal on Scientific Computing*, 16(1):151–168. (Cited on page 11.)

McLachlan, R. I., Quispel, G., and Robidoux, N. (1999). Geometric integration using discrete gradients. *Philosophical Transactions of the Royal Society of London A: Mathematical, Physical and Engineering Sciences*, 357(1754):1021–1045. (Cited on pages 9, 11, 13, 14, 17, 51, and 110.)

Mei, W. and Bullo, F. (2017). Lasalle invariance principle for discrete-time dynamical systems: A concise and self-contained tutorial. *arXiv preprint arXiv:1710.03710*. (Cited on page 49.)

Monaco, S. and Normand-Cyrot, D. (1982). Sur la subordination d'un systeme non lineaire discret a un systeme lineaire. *Developpement et Utilisation d'Outils et Mod eles Math/ ematiques en Automatique, Analyse de Syst emes et Traitement de Signal*, pages 609–623. (Cited on page 6.)

Monaco, S. and Normand-Cyrot, D. (1983). Some remarks on the invertibility of nonlinear discrete-time systems. In *1983 American Control Conference*, pages 324–328. IEEE. (Cited on page 6.)

Monaco, S. and Normand-Cyrot, D. (1984). Sur la commande non interactive des systems non lineaires en temps discret. In *Analysis and Optimization of Systems*, pages 364–377. Springer. (Cited on page 6.)

Monaco, S. and Normand-Cyrot, D. (1986). Nonlinear systems in discrete time. In *Algebraic and geometric methods in nonlinear control theory*, pages 411–430. Springer. (Cited on page 48.)

Monaco, S. and Normand-Cyrot, D. (1990). A combinatorial approach of the nonlinear sampling problem. In *Analysis and Optimization of Systems*, pages 788–797. Springer. (Cited on page 15.)

Monaco, S. and Normand-Cyrot, D. (1995). A unified representation for nonlinear discrete-time and sampled dynamics. *Journal of Mathematic, System, Estimation and Control*, 7:50–3. (Cited on pages 10, 13, 48, 53, and 54.)

Monaco, S. and Normand-Cyrot, D. (1997a). Geometric properties of a class of nonlinear discrete-time dynamics. In *1997 European Control Conference (ECC)*, pages 3176–3181. IEEE. (Cited on pages 58 and 80.)

Monaco, S. and Normand-Cyrot, D. (1997b). On the conditions of passivity and losslessness in discrete time. In *1997 European Control Conference (ECC)*, pages 3621–3625. IEEE. (Cited on page 8.)

Monaco, S. and Normand-Cyrot, D. (1998). Discrete-time state representations, a new paradigm. In *Perspectives in Control*, pages 191–203. Springer. (Cited on pages 13, 53, 54, 80, 83, 87, and 88.)

Monaco, S. and Normand-Cyrot, D. (1999). Nonlinear representations and passivity conditions in discrete time. In *Robustness in identification and control*, pages 422–433. Springer. (Cited on pages 55 and 58.)

Monaco, S. and Normand-Cyrot, D. (2001). Issues on nonlinear digital control. *European Journal of Control*, 7(2-3):160–177. (Cited on page 16.)

Monaco, S. and Normand-Cyrot, D. (2005). On the differential/difference representation of sampled dynamics. In *Decision and Control, 2005 and 2005 European Control Conference. CDC-ECC'05. 44th IEEE Conference on*, pages 6597–6602. IEEE. (Cited on pages 13, 83, and 87.)

Monaco, S. and Normand-Cyrot, D. (2006). Input-state matching under digital control. In *Proceedings of the 45th IEEE Conference on Decision and Control*, pages 1806–1811. IEEE. (Cited on page 97.)

Monaco, S. and Normand-Cyrot, D. (2007). Advanced tools for nonlinear sampled-data systems' analysis and control. *European journal of control*, 13(2-3):221–241. (Cited on page 16.)

Monaco, S. and Normand-Cyrot, D. (2011). Nonlinear average passivity and stabilizing controllers in discrete time. *Systems & Control Letters*, 60(6):431–439. (Cited on pages 6, 8, 10, 13, 14, 48, 55, 57, 58, 61, 80, 101, 134, and 138.)

Monaco, S. and Normand-Cyrot, D. (2015). On optimality of passivity based controllers in discrete-time. *Systems & Control Letters*, 75:117–123. (Cited on page 140.)

Monaco, S., Normand-Cyrot, D., and Califano, C. (2007). From chronological calculus to exponential representations of continuous and discrete-time dynamics: A lie-algebraic approach. *IEEE Transactions on Automatic Control*, 52(12):2227–2241. (Cited on pages 13, 53, 54, and 88.)

Monaco, S., Normand-Cyrot, D., Mattioni, M., and Moreschini, A. (2021). Nonlinear hamiltonian systems under sampling. In *Submitted to IEEE Transactions on Automatic Control (TAC)*. (Cited on page 20.)

Monaco, S., Normand-Cyrot, D., and Tiefensee, F. (2008). From passivity under sampling to a new discrete-time passivity concept. In *Decision and Control, 2008. CDC 2008. 47th IEEE Conference on*, pages 3157–3162. IEEE. (Cited on pages 6, 8, and 83.)

Monaco, S., Normand-Cyrot, D., and Tiefensee, F. (2009). Nonlinear port controlled hamiltonian systems under sampling. In *Proceedings of the 48h IEEE Conference on Decision and Control (CDC) held jointly with 2009 28th Chinese Control Conference*, pages 1782–1787. IEEE. (Cited on page 8.)

Monaco, S., Normand-Cyrot, D., and Tiefensee, F. (2010). Sampled-data stabilization; a pbc approach. *IEEE Transactions on Automatic Control*, 56(4):907–912. (Cited on pages 6, 16, 90, and 92.)

Moreschini, A., Mattioni, M., Monaco, S., and Normand-Cyrot, D. (2019a). Discrete port-controlled hamiltonian dynamics and average passivation. In *2019 IEEE 58th Conference on Decision and Control (CDC)*, pages 1430–1435. (Cited on page 18.)

Moreschini, A., Mattioni, M., Monaco, S., and Normand-Cyrot, D. (2019b). Interconnection through u-average passivity in discrete time. In *2019 IEEE 58th Conference on Decision and Control (CDC)*, pages 4234–4239. (Cited on page 18.)

Moreschini, A., Mattioni, M., Monaco, S., and Normand-Cyrot, D. (2021). Stabilization of discrete port-hamiltonian dynamics via interconnection and damping assignment. *IEEE Control Systems Letters*, 5(1):103–108. (Cited on page 19.)

Moreschini, A., Monaco, S., and Normand-Cyrot, D. (2019). Gradient and hamiltonian dynamics under sampling. *IFAC-PapersOnLine*, 52(16):472 – 477. 11th IFAC Symposium on Nonlinear Control Systems NOLCOS 2019. (Cited on page 20.)

Moreschini, A., Monaco, S., and Normand-Cyrot, D. (2021). Dirac structures of discrete-time port-hamiltonian systems. In *Submitted to IEEE Transactions on Automatic Control (TAC)*. (Cited on page 18.)

Moulla, R., Lefevre, L., and Maschke, B. (2011). Geometric pseudospectral method for spatial integration of dynamical systems. *Mathematical and Computer Modelling of Dynamical Systems*, 17(1):85–104. (Cited on page 12.)

Navarro-López, E. M. (2005). Several dissipativity and passivity implications in the linear discrete-time setting. *Mathematical Problems in Engineering*, 2005(6):599–616. (Cited on page 8.)

Navarro-López, E. M. and Fossas-Colet, E. (2004). Feedback passivity of nonlinear discrete-time systems with direct input–output link. *Automatica*, 40(8):1423–1428. (Cited on page 58.)

Navarro-López, E. M., Sira-Ramírez, H., and Fossas-Colet, E. (2002). Dissipativity and feedback dissipativity properties of general nonlinear discrete-time systems. *European journal of control*, 8(3):265–274. (Cited on page 55.)

Nešić, D. and Grüne, L. (2005). Lyapunov-based continuous-time nonlinear controller redesign for sampled-data implementation. *Automatica*, 41(7):1143–1156. (Cited on page 6.)

Nešić, D., Teel, A. R., and Kokotović, P. (1999). Sufficient conditions for stabilization of sampled-data nonlinear systems via discrete-time approximations. *Systems & Control Letters*, 38(4-5):259–270. (Cited on pages 87 and 101.)

Normand-Cyrot, D. (1983). Théorie et pratique des systèmes non linéaires en temps discret. *Thése d'Etat es-Sciences in Physics (Paris-XI)*. (Cited on pages 6 and 48.)

Ortega, R. and Spong, M. W. (1989). Adaptive motion control of rigid robots: A tutorial. *Automatica*, 25(6):877–888. (Cited on page 5.)

Ortega, R., Spong, M. W., Gómez-Estern, F., and Blankenstein, G. (2002a). Stabilization of a class of underactuated mechanical systems via interconnection and damping assignment. *IEEE transactions on automatic control*, 47(8):1218–1233. (Cited on pages 4, 5, and 44.)

Ortega, R., van der Schaft, A., Castanos, F., and Astolfi, A. (2008). Control by interconnection and standard passivity-based control of port-hamiltonian systems. *IEEE Transactions on Automatic Control*, 53(11):2527–2542. (Cited on pages 4 and 32.)

Ortega, R., van der Schaft, A., Maschke, B., and Escobar, G. (2002b). Interconnection and damping assignment passivity-based control of port-controlled hamiltonian systems. *Automatica*, 38(4):585–596. (Cited on pages 4, 5, 32, 42, 43, and 95.)

Ortega, R., van der Schaft, A. J., Mareels, I., and Maschke, B. (2001). Putting energy back in control. *IEEE Control Systems Magazine*, 21(2):18–33. (Cited on pages 4, 5, 32, 36, 42, 44, 46, 259, 271, and 272.)

Polyuga, R. V. and Van der Schaft, A. (2010). Structure preserving model reduction of port-hamiltonian systems by moment matching at infinity. *Automatica*, 46(4):665–672. (Cited on page 283.)

Popov, V. M. (1973). *Hyperstability of control systems*. Springer-Verlag. (Cited on page 29.)

Quispel, G. and McLaren, D. I. (2008). A new class of energy-preserving numerical integration methods. *Journal of Physics A: Mathematical and Theoretical*, 41(4):045206. (Cited on page 11.)

Ragazzini, J. R. and Franklin, G. F. (1958). Sampled-data control systems. (Cited on page 5.)

Reyes-Báez, R., van der Schaft, A., and Jayawardhana, B. (2018). Passivity based distributed tracking control of networked euler-lagrange systems. *IFAC-PapersOnLine*, 51(23):136–141. (Cited on page 32.)

Rodriguez, H., Ortega, R., and Siguerdidjane, H. (2000). Passivity-based control of magnetic levitation systems: theory and experiments. In *Proc. 14th International Symposium of Mathematical Theory of Networks and Systems (MTNS2000), Perpignan, France*. (Cited on page 260.)

Sepulchre, R., Jankovic, M., and Kokotovic, P. V. (2012). *Constructive nonlinear control*. Springer Science & Business Media. (Cited on pages 25, 30, 34, 36, 46, and 95.)

Serhani, A., Matignon, D., and Haine, G. (2018). Structure-preserving finite volume method for 2d linear and non-linear port-hamiltonian systems. *IFAC-PapersOnLine*, 51(3):131–136. (Cited on page 12.)

Serhani, A., Matignon, D., and Haine, G. (2019a). Partitioned finite element method for port-hamiltonian systems with boundary damping: anisotropic heterogeneous 2d wave equations. *IFAC-PapersOnLine*, 52(2):96–101. (Cited on page 12.)

Serhani, A., Matignon, D., and Haine, G. (2019b). A partitioned finite element method for the structure-preserving discretization of damped infinite-dimensional port-hamiltonian systems with boundary control. In *International Conference on Geometric Science of Information*, pages 549–558. Springer. (Cited on page 12.)

Šešlija, M., Scherpen, J. M., and van der Schaft, A. (2012). Port-hamiltonian systems on discrete manifolds. *IFAC Proceedings Volumes*, 45(2):774–779. (Cited on page 10.)

Slotine, J.-J. E. and Li, W. (1987). On the adaptive control of robot manipulators. *The international journal of robotics research*, 6(3):49–59. (Cited on page 5.)

Sontag, E. (1979). Realization theory of discrete-time nonlinear systems: Part i-the bounded case. *IEEE Transactions on Circuits and Systems*, 26(5):342–356. (Cited on page 6.)

Sontag, E. D. (2013). *Mathematical control theory: deterministic finite dimensional systems*, volume 6. Springer Science & Business Media. (Cited on page 48.)

Sontag, E. D. and Sussmann, H. J. (1982). Accessibility under sampling. In *1982 21st IEEE Conference on Decision and Control*, pages 727–732. IEEE. (Cited on page 6.)

Spong, M. W., Hutchinson, S., and Vidyasagar, M. (2020). *Robot modeling and control*. John Wiley & Sons. (Cited on page 5.)

Stramigioli, S. (2015). Energy-aware robotics. In *Mathematical Control Theory I*, pages 37–50. Springer. (Cited on page 5.)

Stramigioli, S., Secchi, C., van der Schaft, A. J., and Fantuzzi, C. (2002). A novel theory for sampled data system passivity. In *IEEE/RSJ International Conference on Intelligent Robots and Systems*, volume 2, pages 1936–1941. IEEE. (Cited on pages 6 and 10.)

Stramigioli, S., Secchi, C., van der Schaft, A. J., and Fantuzzi, C. (2005). Sampled data systems passivity and discrete port-hamiltonian systems. *IEEE Transactions on Robotics*, 21(4):574–587. (Cited on pages 6, 8, 10, 89, and 283.)

Sümer, L. G. and Yalçın, Y. (2011). A direct discrete-time ida-pbc design method for a class of underactuated hamiltonian systems. In *IFAC World Congress*, volume 18, pages 13456–13461. (Cited on pages 12, 227, 245, and 264.)

Takegaki, M. and Arimoto, S. (1981). A new feedback method for dynamic control of manipulators. (Cited on page 5.)

Talasila, V., Clemente-Gallardo, J., and van der Schaft, A. (2004). Geometry and hamiltonian mechanics on discrete spaces. *Journal of physics A: mathematical and general*, 37(41):9705. (Cited on page 10.)

Talasila, V., Clemente-Gallardo, J., and van der Schaft, A. (2006). Discrete port-hamiltonian systems. *Systems & Control Letters*, 55(6):478–486. (Cited on pages 8 and 10.)

Tanasa, V., Monaco, S., and Normand-Cyrot, D. (2015). Backstepping control under multi-rate sampling. *IEEE Transactions on Automatic Control*, 61(5):1208–1222. (Cited on pages 98 and 102.)

Tang, B. and Brennan, M. (2013). A comparison of two nonlinear damping mechanisms in a vibration isolator. *Journal of Sound and Vibration*, 332(3):510–520. (Cited on page 129.)

Tiefensee, F., Monaco, S., and Normand-Cyrot, D. (2010). Ida-pbc under sampling for port-controlled hamiltonian systems. In *American control conference (ACC)*, pages 1811–1816. (Cited on pages 6 and 8.)

Trenchant, V., Ramirez, H., Le Gorrec, Y., and Kotyczka, P. (2017). Structure preserving spatial discretization of 2d hyperbolic systems using staggered grids finite difference. In *2017 American Control Conference (ACC)*, pages 2491–2496. IEEE. (Cited on page 12.)

Trenchant, V., Ramirez, H., Le Gorrec, Y., and Kotyczka, P. (2018). Finite differences on staggered grids preserving the port-hamiltonian structure with application to an acoustic duct. *Journal of Computational Physics*, 373:673–697. (Cited on page 12.)

van der Schaft, A., Jeltsema, D., et al. (2014). Port-hamiltonian systems theory: An introductory overview. *Foundations and Trends® in Systems and Control*, 1(2-3):173–378. (Cited on pages 2, 4, 5, 25, 37, 46, 259, and 283.)

van der Schaft, A. and Maschke, B. (2013). Port-hamiltonian systems on graphs. *SIAM Journal on Control and Optimization*, 51(2):906–937. (Cited on page 38.)

van der Schaft, A. and Maschke, B. (2018). Geometry of thermodynamic processes. *Entropy*, 20(12):925. (Cited on page 3.)

van der Schaft, A. and Maschke, B. (2020). Dirac and lagrange algebraic constraints in nonlinear port-hamiltonian systems. *Vietnam Journal of Mathematics*, 48(4):929–939. (Cited on page 3.)

van der Schaft, A. and Maschke, B. M. (2002). Hamiltonian formulation of distributed-parameter systems with boundary energy flow. *Journal of Geometry and physics*, 42(1-2):166–194. (Cited on page 283.)

van der Schaft, A. J. (2000). *L2-gain and passivity techniques in nonlinear control*, volume 2. Springer. (Cited on pages 2, 4, 25, 30, 32, 37, 38, 40, 44, 46, 123, and 221.)

Vidyasagar, M. (2002). *Nonlinear systems analysis*, volume 42. Siam. (Cited on page 30.)

Vu, N. M. T., Lefevre, L., Nouailletas, R., and Brémond, S. (2017). Symplectic spatial integration schemes for systems of balance equations. *Journal of Process Control*, 51:1–17. (Cited on page 12.)

Wiggins, S. (2003). *Introduction to applied nonlinear dynamical systems and chaos*, volume 2. Springer Science & Business Media. (Cited on pages 2, 25, and 27.)

Willems, J. C. (1972a). Dissipative dynamical systems part i: General theory. *Archive for rational mechanics and analysis*, 45(5):321–351. (Cited on page 4.)

Willems, J. C. (1972b). Dissipative dynamical systems part i: General theory. *Archive for rational mechanics and analysis*, 45(5):321–351. (Cited on pages 29 and 30.)

Willems, J. C. (1972c). Dissipative dynamical systems part ii: Linear systems with quadratic supply rates. *Archive for rational mechanics and analysis*, 45(5):352–393. (Cited on pages 29 and 30.)

Willems, J. C. (2007). The behavioral approach to open and interconnected systems. *IEEE Control Systems Magazine*, 27(6):46–99. (Cited on page 32.)

Wu, Y., Hamroun, B., Le Gorrec, Y., and Maschke, B. (2015). Power preserving model reduction of 2d vibro-acoustic system: a port hamiltonian approach. *IFAC-PapersOnLine*, 48(13):206–211. (Cited on page 12.)

Yalçin, Y., Sümer, L. G., and Kurtulan, S. (2015). Discrete-time modeling of hamiltonian systems. *Turkish Journal of Electrical Engineering & Computer Sciences*, 23(1):149–170. (Cited on pages 9, 11, 13, 14, 17, 110, 213, and 237.)

Yao, J., Guan, Z.-H., and Hill, D. J. (2009). Passivity-based control and synchronization of general complex dynamical networks. *Automatica*, 45(9):2107–2113. (Cited on page 32.)

Yuz, J. I. and Goodwin, G. C. (2005). On sampled-data models for nonlinear systems. *IEEE transactions on automatic control*, 50(10):1477–1489. (Cited on page 6.)

ÉCOLE DOCTORALE
Sciences et technologies de l'information et de la communication (STIC)

Titre : Modélisation et commande des systèmes Hamiltoniens à ports en temps discret et sous échantillonnage

Mots clés : systèmes Hamiltoniens à ports, systèmes échantillonnés, commande basée sur la passivité

Résumé : Les systèmes Hamiltoniens ont été largement étudiés dans la littérature en temps continu comme des éléments essentiels pour la modélisation de systèmes physiques complexes et en réseaux. Les schémas de commande étant nécessairement implantés au moyen de dispositifs numériques, il est primordial de disposer de modèles et de stratégies de commande échantillonnés afin de s'affranchir d'un impact négatif de la discrétisation sur les performances de contrôle. Cette thèse s'intéresse à la description de nouvelles structures Hamiltoniennes à la fois en temps discret pur et dans le contexte échantillonné. A partir de ces formes, des stratégies de stabilisation basées sur la gestion de l'énergie sont développées en temps discret et sous échantillonnage. Concernant la modélisation, la représentation par espace d'état proposée fait référence au concept de representation Différentielle et aux Différences (DDR) de dynamiques discrètes et à la notion de fonction gradient en temps discret. Les modèles proposés admettent une représentation sous forme de structure de Dirac définissant ainsi précisément les différents éléments de stockage, resistance et interaction avec l'extérieur qui constituent le système Hamiltonien. Concernant la stabilisation, la notion de passivité en u-moyenne est essentielle pour décrire des stratégies de commande par bouclage exploitant cette passivité au service d'approches de type amortissement (PBC) ou affectation de structures cibles (IDA-PBC), ceci en temps discret et sous échantillonnage. Trois examples classiques issus des domaines physiques sont développés afin d'illustrer les aspects de calcul liés à la modélisation et à la commande et valider les nouvelles stratégies proposées en illustrant leurs performances par des simulations.

Title : Modeling and control of discrete-time and sampled-data port-Hamiltonian systems

Keywords : port-Hamiltonian systems, sampled-data systems, passivity-based control

Abstract : Modeling and control of port-Hamiltonian systems are extensively studied in the continuous-time literature as powerful tools for network modeling and control of complex physical systems. Since controllers are unavoidably implemented through digital devices, accurate sampled-data models and control strategies are highly recommended to prevent a negative impact on the closed-loop performances under digital control. This thesis contributes to the description of new port-Hamiltonian structures both in a purely discrete-time and sampled-data framework. Then, on these bases, stabilizing and energy-based digital feedback strategies are developed. Regarding modeling, the proposed state-space forms make use of the concepts of Difference and Differential Representation (DDR) of discrete-time dynamics and the discrete gradient function. The proposed models exhibit a Dirac structure that properly defines the storing, resistive and external elements of the concerned port-Hamiltonian system. For stabilization purposes, the u-average passivity property has been essential for properly discussing passivity-based-control (PBC) strategies such as damping output feedback and Interconnection and Damping Assignment (IDA-PBC) both in discrete time and under sampling. Three case studies from different physical domains aim to illustrate the computational aspects related to the modeling and control design and further we validate their performances by means of simulations.